New roles for ancient interactions: functional analysis of the conserved interactions between the clathrin heavy and light chains and calmodulin

Virginia Robles Garcia

New roles for ancient interactions: functional analysis of the conserved interactions between the clathrin heavy and light chains and calmodulin

Memoria presentada por Virginia Robles García para optar al grado de Doctora
por la Universidad de Barcelona

Universidad de Barcelona
Facultad de Farmacia
Departamento de Bioquímica y Biología Molecular
Programa de Doctorado de Biomedicina

Instituto de Biología Molecular de Barcelona (IBMB-CSIC)

Doctoranda:

Virginia Robles García

Directora y Tutora:

María Isabel Geli Fernández-Peñaflor

"La ciencia se compone de errores, que a su vez, son los pasos hacia la verdad".

Julio Verne

A mis padres, a mi hermano, y a Óscar.

Agradecimientos

A Maribel, capitana del barco, por guiarme, confiar en mí y darme esta oportunidad.

A mis compañeros de batallas de laboratorio y sesiones tupper-periodísticas (en especial, Fátima, Isa, Jon, Mar, Adrian, Helen, Miriams). Saber que estaríais ahí para leerme el horóscopo cada día, no tiene precio.

A mi familia, en especial a mis padres y a mi hermano, por estar siempre a mi lado y cuidar de mí, aunque sea en la distancia.

A mis "monas" por hacer que cada vez que os vea parezca que no haya pasado el tiempo.

A mis "catalufos y extranjeros", en especial a "Pauki", porque habéis sido los humanos de referencia durante la dura escritura de tesis.

A mis compañeras de aventuras varias, Paula, Irene y Mariajo, porque sois unas máquinas, y no dejaré de aprender de vosotras.

A Óscar, compañero de viaje y copiloto. Si hemos superado dos tesis simultáneas, podremos con casi todo.

Index

aa	amino acid
ADP	adenosine 5’-diphosphate
Amp^R	ampicillin resistance gene
ATP	adenosine 5’-triphosphate
DMSO	dimethyl sulfoxide
DNA	deoxyribonucleic acid
cDNA	complementary deoxyribonucleic acid
GFP	green fluorescent protein
GST	glutathione-S-transferase
GTP	guanosine 5’-triphosphate
HA	human influenza hemagglutinin
SDS-PAGE	sodium dodecyl sulfate polyacrylamide gel electrophoresis
HEPES	N-[2-Hydroxyethyl]piperazine-N’-[2-ethanesulfonic acid]
kDa	kilodalton
Leu	leucine
mRFP	monomeric red fluorescent protein
NPA	nucleation promoting activity
NPF	nucleation promoting factor
OD_{600}	optical density at 600 nm
ORF	open reading frame
PCR	polymerase chain reaction
PMSF	phenylmethanesulfonyl fluoride
RT	room temperature
SDC	synthetic dextrose complete medium
ts	temperature-sensitive
His	histidine
Trp	tryptophan
Ura	uracil
Leu	leucine
WT	wild-type
YPD	yeast peptone dextrose medium
CME	clathrin mediated endocytosis
PM	plasma membrane
CCP	clathrin coated pits
CCV	clathrin coated vesicles
MVB	multi-vesicular body
TGN	trans-Golgi network
ILV	intra-lumenal vesicles
LL	late endosome
EE	early endosome
PtdIns(4,5)P_2	Phosphatidylinositol 4,5-bisphosphate
PtdIns(4)P	Phosphatidylinositol 4-phosphate
PtdIns(3)P	Phosphatidylinositol 3-phosphate
PtdIns(3,5)P_2	Phosphatidylinositol 3,3-biphosphate
PtdIns(3,4,5)P_3	Phosphatidylinositol 3,4,5-triphosphate

1. INTRODUCTION

Clathrin is an evolutionary conserved molecule that coats membranes endocytosed from the plasma membrane (PM) and those that move between the trans-Golgi network (TGN) and endosomes of eukaryotic cells. It also plays roles in early stages of mitosis, cytokinesis, chromosome alignment and in certain phagocytic events (Brodsky, 2012; Chen *et al*., 2013; Royle, 2012; Traub, 2005). At the cellular level, clathrin is required for major regulated secretory and endocytic pathways, which transport proteins, lipids, soluble factors, and extracellular ligands between the PM and the intracellular compartments. In multicellular organisms clathrin is involved in numerous specialized pathways of physiological relevance, such as the production of morphogen gradients, the formation of secretory granule, antigen presentation by the immune system, virus maturation, the control of glucose homeostasis, or synaptic vesicle generation.

Many proteins that interact with clathrin have been identified. In some cases the functional relevance of these molecular interactions remains unknown. Among those, the clathrin-calmodulin interaction is probably one of the most striking examples, since it involves two evolutionary conserved proteins and it was detected decades ago. The calcium sensor calmodulin plays an important role regulating a wide variety of proteins and important signaling pathways in all eukaryotes. It modulates the activity of key regulatory enzymes, ion pumps and proteins implicated in motility and it has essential roles in mitosis. Importantly, it has also been found to be implicated in endocytosis, membrane traffic and endosome fusion. Nevertheless, most calmodulin targets and the mechanisms by which calmodulin regulates specific membrane transport events are mainly unknown.

S. cerevisiae has proven to be an extremely versatile organism for studying many cellular processes, because of the ease of combining biochemical analyses with genetic studies and live imaging in this organism, and the evolutionary conservation of most essential eukaryotic cellular processes and proteins involved (Sherman, 2002). In particular, clathrin-mediated pathways are highly conserved in yeast and mammals. Components of the mammalian machinery have homologues in yeast, showing a high degree of homology to their counterparts in mammals (Shaw *et al.*, 2001). In addition, the analysis of essential multifunctional proteins such as actin or calmodulin was facilitated in this model system by the generation

and characterization of complementation groups of mutants that specifically alter binding to essential cellular targets (Munn *et al.*, 1991; Ohya & Botstein, 1994a; Robinson *et al.*, 1988). Discoveries in *S.cerevisiae* were found to parallel or anticipate others in mammalian systems (Girao *et al.*, 2008; Shaw *et al.*, 2001), supporting the use of budding yeast as a model for studying clathrin and calmodulin function and regulation.

This introduction has been divided into two main sections: the first part is focused on clathrin and the second part on calmodulin, describing for each protein their general structural and molecular organization and the conserved cellular and physiological functions, with special attention to the endosomal traffic in *S. cerevisiae*, which is the subject of this Thesis.

1.1. Clathrin

1.1.1. Historical perspective

Coated vesicles were discovered 50 years ago by Roth and Porter while they were studying the uptake of yolk protein by insect oocytes (Roth & Potter, 1964). Using electron microscopy (EM), they found that during the time that cells were actively taking up yolk, PM invaginations and vesicles that seemed to pinch-off in the cytosol from the PM were covered by representative bristle coats. Deeper in the cell, they also observed uncoated vesicles. Later on, Friend and Farqhuar described other population of coated vesicles in the Golgi of rat cells (Friend & Farquhar, 1967), showing that they had similar morphology to the bristle coats found in insect oocytes. They proposed that at least one function of the Golgi coated vesicles was to transport hydrolytic enzymes to lysosomes. Then, tangential EM sections from guinea pig brain revealed that the basic bristle-like coat was composed of a polygonal lattice that surrounded the bilayer vesicle (Kanaseki & Kadota, 1969). Isolated vesicles appeared to have similar external coat with a polygonal architecture, resembling the geometry of a football seam (Crowther *et al*., 1976; Kadota & Kadota, 1973). From these observations, it was proposed that membranous vesicles were included in a basket that could drive deformation of the membrane into a pit and vesicle, being responsible for taking up extracellular material in many types of cells. Pearse was the first to perform the biochemical

analysis of purified coats and coated vesicles from bovine brain identifying the major protein component, the clathrin heavy chain (named clathrin in reference to the cage-like structure that it forms), that appeared as a band of 180-190 kDa when analyzed by sodium dodecyl sulfate-polyacrylamide gel electrophoresis (SDS-PAGE) (Pearse, 1975). Clathrin was subsequently purified from coated vesicle extracts by gel filtration and was shown to be the only component necessary to reconstitute basket structures resembling vesicle coats *in vitro* (Crowther & Pearse, 1981; Keen *et al.*, 1979). Analysis of purified clathrin from calf brain showed that in its native form, in addition to the heavy chain, clathrin consisted of two other classes of clathrin light chains (LCa and LCb) of 33-36 kDa. Clathrin was found to assemble in a trimeric structure of three heavy chains each one associated with a light chain, the triskelion, which is the basic assembly unit of the clathrin coat (Kirchhausen & Harrison, 1981; Ungewickell & Branton, 1981).

The function of clathrin coated vesicles was also established through studies with the low density lipoprotein (LDL) transmembrane receptors, whose internalization by receptor-mediated endocytosis was impaired mutating an internalization site on the cytoplasmic side of the membrane, being unable to localize in coated pits (Anderson *et al.* 1977; Brown & Goldstein, 1977). Thus, after various studies with other PM proteins, it was concluded that receptors that carry ligands into cells by receptor-mediated endocytosis are clustered over the newly formed coated pits. Similarly, clathrin-coated pits (CCP) within the TGN were shown to transport lysosomal enzymes bound to specific receptors to the correct intracellular destination (Brown & Farquhar, 1984; Griffiths *et al.*, 1988; Lemansky *et al*., 1987). It was then found that the lattice was held onto the membrane by multisubunit protein complexes or adaptors (Pearse, 1988).

1.1.2. Structure and molecular organization

1.1.2.1. Diversity of genes and proteins

1.1.2.1.1. Clathrin heavy chain

The clathrin heavy chain is present and ubiquitously expressed in all eukaryotic cells analyzed (Wakeham *et al*., 2005). The first amino acid sequence for a clathrin heavy chain (1675 residues) was obtained from molecular clones of rat brain cDNAs (Kirchhausen *et al.*, 1987). Then the clathrin heavy chain sequences from

Saccharomyces cerevisiae (Payne & Schekman, 1985), *Dictyostelium discoideum* (O'Halloran & Anderson, 1992), *Drosophila melanogaster* (Bazinet *et al*., 1993) as well as those for *Caenorhabditis elegans*, certain plants, and various mammals (from the genome project) were obtained.

Most organisms contain a single copy of the heavy chain gene. In humans, however, there are two isoforms encoded by genes *CLTC* and *CLTC1* at genomic loci 17q23.2 for Chc17 (Dodge *et al.*, 1991) and 22q11.21 for Chc22 (Sirotkin *et al*., 1996) (Table 1). Chc17 is a ubiquitous 1675-residue protein expressed in vertebrate tissues, having a functional orthologue present in all eukaryotic organisms analyzed. Chc17 is mainly involved in membrane traffic and mitosis. The Chc22 isoform is a 1640-residue protein highly expressed in human skeletal muscle, being concentrated at neuromuscular and myotendinous junctions, with a low level detected in other tissues. It is not involved in endocytosis, but may play a role in membrane organization (Liu *et al*., 2001; Sirotkin *et al.*, 1996; Towler et al., 2004). Despite their differences in function, both isoforms are 85% similar at amino acid level (Liu *et al.*, 2001). It has been suggested that the two human genes for clathrin heavy chain were the result of a duplication which occurred between 510 and 600 million years ago in our evolution, as revealed in a comparative analysis of clathrin genes from genomes of different species (Wakeham *et al.,* 2005).

The yeast 1653-residue clathrin heavy chain (Chc1) is encoded by one single gene, *CHC1,* located in chromosome VII (Payne & Schekman, 1985) (Table 1). Clathrin heavy chain sequences are greatly conserved. For example, the yeast clathrin heavy chain shares 50% amino acid identity with the rat heavy chain, 45% amino acid identity with the one from *Dictyostelium* and 70% amino acid identity with the human Chc17.

1.1.2.1.2. Clathrin light chain

Vertebrates have two clathrin light chains, LCa (248 amino acids) and LCb (228 amino acids), expressed at characteristically different levels in different tissues, with LCa being dominant in lymphoid tissue and LCb, in brain (reviewed in (Brodsky, 2012)). They also are heterogeneously distributed in clathrin triskelia (Kirchhausen *et al*., 1983). In neuronal cells, they both have additional isoforms

arising from specific alternative splicing differences (inserting 30 or 18 amino acids) (Kirchhausen *et al*., 1987), which may be associated with the high degree of specialization involved in membrane reuptake in synapses. In humans, they are encoded on separate human chromosomes by genes *CLTA* and *CLTB*, at 9p13.3 and 5q35.2 locus, respectively (Table 1). They share similar functions and bind and regulate Chc17 but do not functionally interact with Chc22 (Liu *et al.*, 2001). Invertebrates and yeast have a single light chain gene (Wakeham *et al.,* 2005), CLC1 in yeast (Table 1), that encodes the 233 amino acid protein Clc1 (Silveira *et al.*, 1990)), which apparently partners with the Chc17 functional orthologue in these species. The predicted molecular weights from the cDNAs of all light chains are in the range of 23–26 kDa. However, the N-terminal 90 residues rich in Pro (proline) and Gly (glycine) causes anomalous electrophoretic mobility in SDS-PAGE, which has led to estimated molecular masses of 32–36 kDa (Scarmato & Kirchhausen, 1990).

Contrary to the heavy chain, the clathrin light chains have much more divergent sequences. For example, LCa and LCb share only 60% amino acid identity, despite their similar functionality. Yeast Clc1 is only 18% identical to mammalian LCb, but conserved regions in mammalians light chains are also found in yeast Clc1, suggesting that they both share similar functions (Brodsky *et al.* 1991).

Protein	**Gene name**	**Chromosome location**
Human clathrin heavy chain 17 (Chc17)	*CLTC*	17q.23.2
Human clathrin heavy chain 22 (Chc22)	*CLTC1*	22q11.21
Human clathrin light chain A (CLa)	*CLTA*	9p.13.3 8p.22 (pseudogene) 12p.13.31 (pseudogene)
Human clathrin light chain B (CLb)	*CLTB*	5q.35.2
Yeast clathrin heavy chain (Chc1)	*CHC1*	ChrVII: 107504 to 102543
Yeast clathrin light chain (Clc1)	*CLC1*	ChrVII: 832456 to 833157

Table 1: **Chromosomal locations and gene names of human and yeast clathrin subunits.**

1.1.2.2. Structure and biochemistry

1.1.2.2.1. Clathrin heavy chain structure and domain organization

Clathrin heavy chains are divided into various domains (Figure 1A): The N-terminal domain (residues 1-330), followed by the linker (aa 331 to 483 in mammals and 331 to 550 in yeast), the ankle and distal leg (aa 483 to 1073 in mammals and aa 551-1052 in yeast), a knee (aa 1074 to 1197 in mammals), a proximal leg (aa 1198-1575 in mammals and 1063-1522 in yeast) and a trimerization domain (aa 1576-1675 in mammals and 1150-1580 in yeast) (Chen *et al.*, 2002; Fotin *et al.*, 2004; Pishvaee *et al.*, 1997). The combination of the knee, proximal leg, and trimerization domain constitutes the hub, a fragment that self-assembles *in vitro* (Liu *et al.*, 1995). A 2.9 Å resolution structure of the heavy chain revealed seven 145 amino acid repeats (CHCR1 to CHCR7), each one composed each of 10 α-helixes of 10–12 residues, connected by loops (Ybe *et al*., 1999), which constitute a long α-solenoid region that forms the ankle, distal leg, and proximal leg segments (Figure 1A and 1C). The C-terminal is involved in trimerization. It also comprises a helical tripod that projects inward from the vertex of each three-legged clathrin triskelion (Fotin *et al*., 2004), and interacts with the uncoating ATPase Hsc70 (which mediates the ATP-dependent disassembly of the clathrin coat, together with its co-factor auxilin) through the motif QLMLT (Rapoport *et al.*,2008; Xing *et al*., 2010) (Figure 2C and 3A). The proximal domain comprises a region for light chain binding (Chen *et al.*, 2002; Kirchhausen *et al*., 1983; Liu *et al*., 1995). Besides, binding of the yeast clathrin light chain to heavy chain depends on additional residues in the yeast heavy chain trimerization domain (Pishvaee *et al*., 1997). The terminal domain (TD) is folded into a seven-bladed β-propeller (Haar *et al.* 1998) (Figure 1C) connected to CHCR1 of the ankle by a linker region. It is the region of the outer triskelion, positioned closest to the membrane surface in the assembled coat (Fotin *et al*., 2004). The TD binds accessory proteins and adaptors such as AP-1, AP-2, the Ggas or AP180, which simultaneously bind to clathrin and to transmembrane proteins, and/or phospholipids and which might also bind to other components of the clathrin coated vesicle (CCV) machinery (Lemmon & Traub, 2012; Owen, 2004; Owen *et al.*, 2004). An additional binding site for adaptors is localized between CHCR1 and CHCR2, in the ankle domain (Knuehl *et al*., 2006). Accessory proteins bear clathrin binding motifs, which interact with different sites on the terminal domain (Figure 1C). One of this consensus TD binding motifs

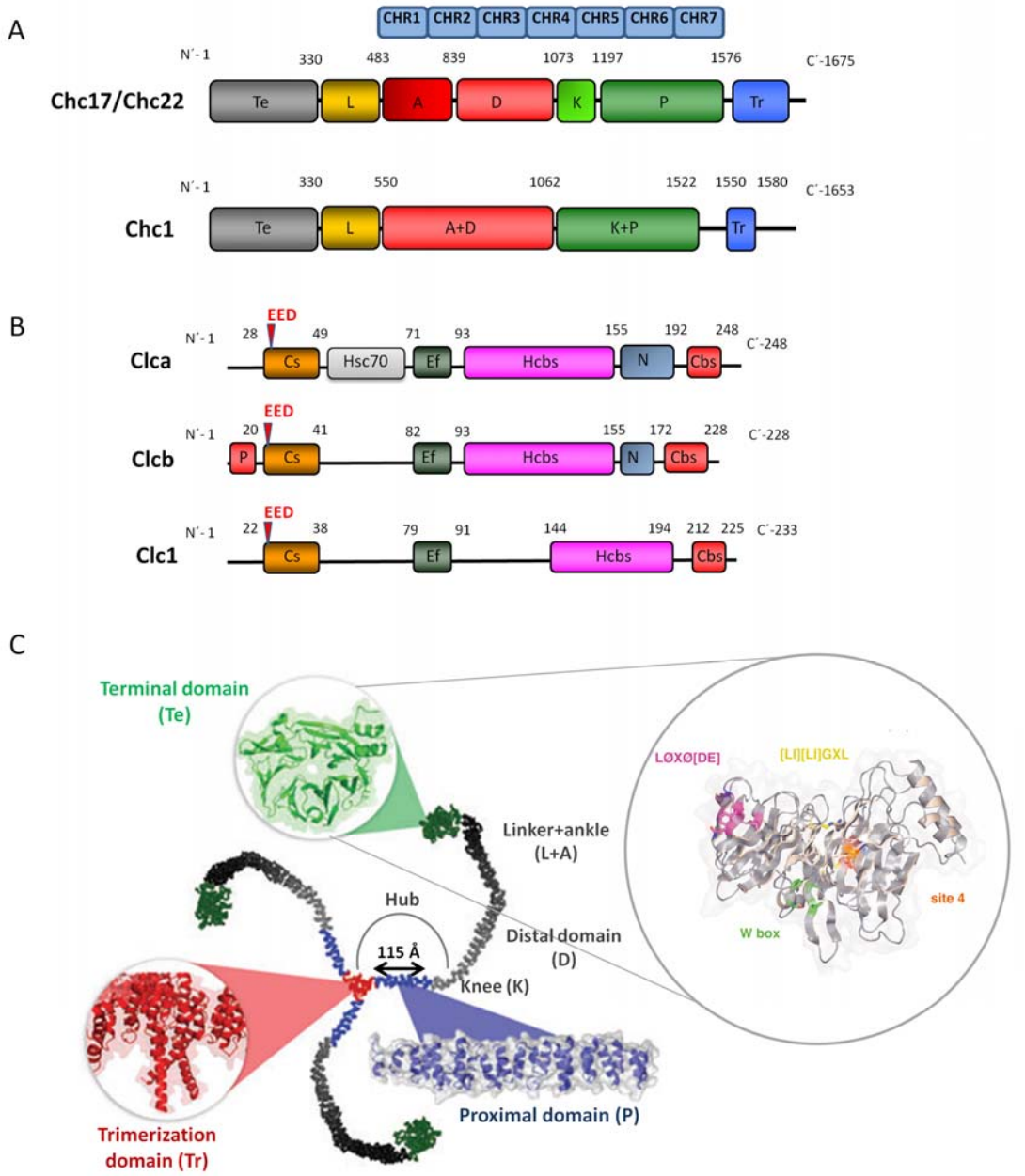

Figure 1. Structure and domain organization of yeast and human clathin heavy and light chains. A) Aligned domain organization and amino acid boundaries of human Chc17 and Chc22 and yeast Chc1, indicating above the relative location of the of the seven clathrin heavy chain repeats (CHCR 1–7). B) Aligned domain organization and amino acid boundaries of human CLa and LCb and yeast Clc1. C) Structure of a heavy chain triskelion, indicating the domain organization of each chain and a ampliated ribbon diagram of the terminal domain in a lateral view defining the four different sites for interaction with different clathrin-binding motifs (see also Table 2). N: N-terminal doain, P: phosphorilation site region; Cs: 22-residue consensus sequence. EED: three negatively charged amino acids; Hsc70: Hsc70 binding region; Ef: EF-hand (calcium binding region); Hcbs: heavy chain binding site; N: neuronally expressed inserts; Cbs: calmodulin binding site. Adapted from (Brodsky, 2012; Lemmon & Traub, 2012).

is known as a clathrin box (LØXØ[DE]) (single letter amino acid code, where Ø represents a hydrophobic residue; alternative residues are in brackets) (Lemmon & Traub, 2012). Other sites that independently bind to the TD have been found in vertebrate proteins, such as the W-box site (PWXXW) (Miele *et al*., 2004) (see Table 2 for a review of the clathrin box TD-interacting motifs). There are many other proteins that physically bind clathrin, but not all interaction motifs have precisely been mapped. For example, the clathrin heavy chain has been shown to bind calmodulin *in vitro* (Merisko *et al.* 1988), but whether they interact *in vivo* and the interaction motifs implicated have not been clarified yet.

	Adaptor motif	**Clathrin HC location**[a]	**Key clathrin HC residues**	**Examples**	**Sequence motif**
TD site 1: clathrin-box motif	LØXØ[DE]	TD groove between blades 1 & 2	I80 T87 Q89 F91 K96 K98	Amphiphysin β-arrestin 1 AP-2 β2 subunit *S.c*. Ent1/2 *S.c*. yAP1802 *S.c*. Apl2 (AP-1 β1)	LLDLD LIEFE LLNLD LIDL[c] LIDM[c] LLDLD
TD site 2: W-box motif	PWXXW	Top of β-propeller	F27 Q152 I154 I170	Amphiphysin SNX9	PWDLW PWSAW
TD site 3: β-arrestin 1L site	[LI][LI]GXL	TD groove between blades 4 & 5	R188 Q192	β-arrestin 1L AP-2 β2 subunit	LLGDL LLGDL
TD site 4	Unknown	TD exposed surface of blade 7	E11	Unknown	Not available
Ankle	Unknown, non linear?	CHC1R1/2	C682 G710	Gga1	Thr613+ Asn622

Table 2. The clathrin heavy chain (HC) terminal domain (TD)-binding motifs. Single letter amino acid code; Ø represents a hydrophobic residue; alternative residues are in brackets; X represents any amino acid. *S.c. Saccharomyces cerevisiae. a*. See Figure 1C for the relative positioning of the four TD interaction surfaces. c. The extreme C-terminus of the protein.

1.1.2.2.2. Clathrin light chain structure and domain organization

The primary structures and a variety of experimental approaches have correlated the structural domains of the light chains with various functions. The combined results show that the clathrin light chains are linear arrays of functionally distinct domains. Despite the strong sequence divergence between mammals and yeast clathrin light chains, the regions found in mammalian cells are also conserved in yeast Clc1 (Silveira *et al.*, 1990), suggesting that they share similar functions (Figure 1B).

The N-termini of the light chains bears a very conserved sequence (aa 22-38 in yeast Clc1; aa 28-49 in mammalian LCa and aa 20-41 in mammalian LCb), whose first three residues are negatively charged (EED). A number of studies have revealed that this light chain N-terminal acidic region interacts with the central coiled-coil dimerization domain of the Hip1/Hip1R/Sla2 family of proteins (Chen & Brodsky, 2005; Newpher *et al.*, 2006) and this interaction regulates assembly of triskelions into cages (see section 1.1.2.2.3.).

The clathrin light chains are unstructured until they bind to the heavy chains (Brodsky, 2012). The central region of all light chains contains 10 heptad repeats that form α-helical coiled-coils, and this central region is necessary and sufficient for the light-chain binding to the heavy chain (Scarmato & Kirchhausen, 1990). Mutational analysis indicates that three tryptophan residues within this region (mammalian 93-155 residues and yeast 144-194 residues) play a key role in the clathrin heavy and light chain interaction (Chen *et al*., 2002). As commented before, the light chains bind along the proximal domain of the heavy chain, through CHCR7 (Scarmato & Kirchhausen, 1990), although the C-termini of the heavy chain subunit also contributes to the interaction (Ybe *et al*., 2007) and the yeast Clc1 binding also depends on additional residues on the trimerization domain of Chc1 (Pishvaee *et al*., 1997).

LCa also has an unique region that binds the chaperone Hsc70 and stimulates its activity *in vitro* (DeLuca-Flaherty *et al*., 1990), and LCb also includes a unique target site for serine phosphorylation near the N-terminus (Bar-zvis & Branton, 1986; Sites *et al*., 1988). These differences indicate a potential for distinct functions. Besides, the clathrin light chains bind calcium *in vitro* with low affinity,

through residues 71-93/82-93 in mammals and 79-91 in yeast. This residues form a calcium chelating loop similar to the EF-hand loop characteristic of other calcium-binding proteins (Mooibroek *et al*.,1987; Näthke *et al.*, 1990; Silveira *et al*., 1990). Importantly, this calcium-binding site is situated between the Hsc70 binding site and the heavy chain binding site (Brodsky, 1990), so it may have a role in regulating clathrin assembly, consistent with the observation that the *in vitro* self-assembling of clathrin coats requires calcium (Ungewickell & Ungewickell, 1991).

Similar to purified clathrin heavy chains, vesicles and coats, mammalian and yeast clathrin light chains bind calmodulin through a region in their C-terminus (mammalian residues 192-248/209-228, and yeast Clc1 residues 212-225) (Pley, 1995; Silveira *et al*., 1990), but its functional role has not been assessed yet. The regions close to the C-terminal domains of mammalian light chains can have inserted sequences resulting from alternative splicing of light chain RNAs in neurons. The neuron-specific light chains have been shown to interact more efficiently with calmodulin (Pley, 1995), which may suggest a specific role for the clathrin-calmodulin interaction in the synapses.

1.1.2.2.3. Clathrin triskelions, lattices and coats: structure, assembly and disassembly

The basic assembly unit of the clathrin lattice is the triskelion, with three heavy chains, each one associated with one light chain (Crowther & Pearse, 1981; Ungewickell & Branton, 1981)(Figure 2A and 2B). The trimerization domain forming the vertex of the trimer comprises a helical tripod that extends from CHCR7 below the triskelion vertex toward the cell membrane (Fotin *et al.*, 2004). The vertex is puckered, which gives the triskelion a characteristic orientation (Figure 2B).

Light chains are stable subunits of the triskelion, and there is no evidence that they actively detach from heavy chains in the cell (Brodsky, 2012)**.** Clathrin light chains have two different conformations when bound to heavy chains, one that extends from the trimerization domain to the bend in the knee, and the other retracted from the knee (Wilbur *et al*., 2010). The extended clathrin light chain is associated with a “straighter” knee that is not compatible with formation of high affinity salt bridges between residues of the heavy chains (Ybe *et al*., 1998) and lattice

assembly, whereas the bent knee is compatible with lattice assembly (Wilbur et al., 2010) (Figure 2C). The clathrin light chain undergoes a conformational change during pH-induced assembly, with a pH-sensitive salt bridge that mediates the light chain-knee interaction. At physiological pH, the assembly inhibition by the light chains is suppressed by adaptor binding ((Ybe *et al.*, 1998) and references therein), which possibly change the local environment to induce a conformational chain of the light chains (Brodsky, 2012).

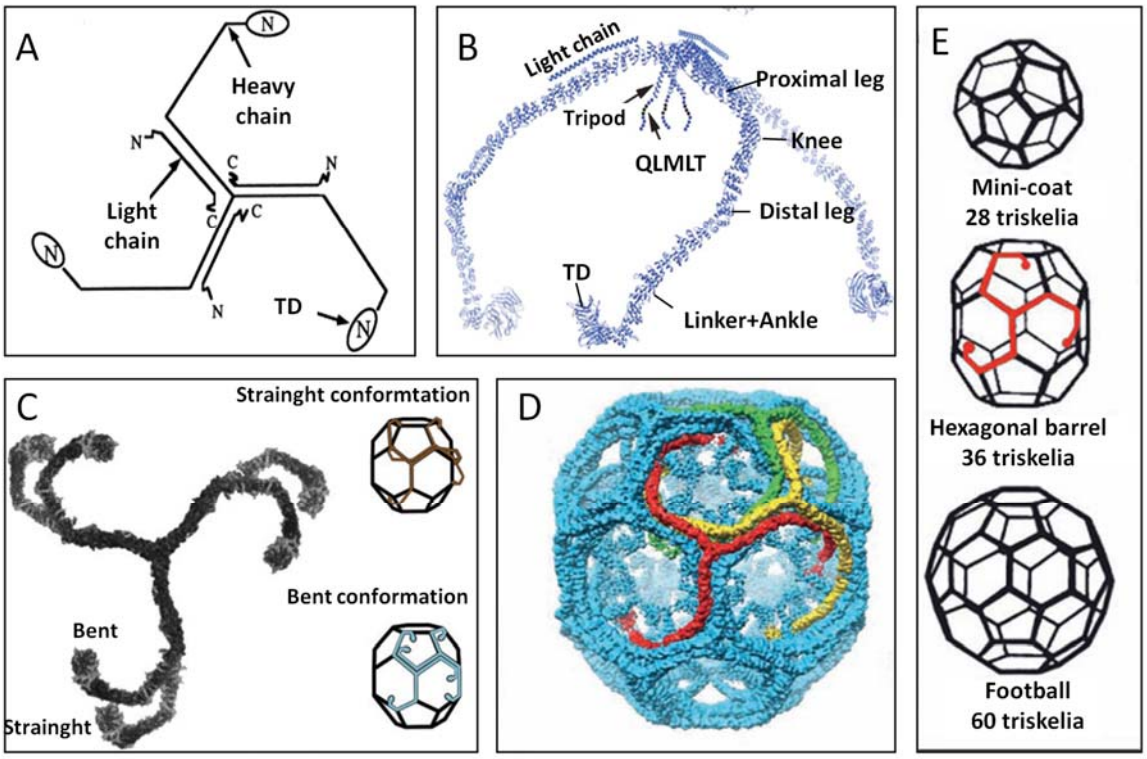

Figure 2. Structures of clathrin triskelions, lattices and coats. A) Schematic representation of a clatrhin heavy and light chains triskelion (taken from (Hirst *et al.,* 1998). B) Side view of a clathrin triskelion showing its three-dimensional shape as deduced from the cryoEM reconstruction of a D6 barrel coat (adapted from (Kirchhausen, 2000). C) Representation of the structure of triskelions with all bent or all straight heavy chain knees. Representations on the right show how the straight knee conformation is incompatible with the dimensions of the clathrin lattice, whereas the bent knee resulting from conformational change of light chains is compatible with lattice assembly (taken from (Brodsky, 2006). D) Clathrin hexagonal barrel at 7.9 Å. Three triskelions are highlighted to show how triskelia interact in the cage (taken form (Royle, 2006). E) Three examples of clathrin cages with different geometry (taken form (Royle, 2006).

Hence, clathrin light chains may act to prevent premature triskelion association *in vivo*, assuring productive clathrin assemblies only at sites that contain cargo and adaptors. This is consistent with the fact that the clathrin light chains inhibit spontaneous triskelion self-assembly *in vitro* at physiological pH (at low pH clathrin triskelions are able to self-assemble (Brodsky, 1988)) in the absence of regulatory factors such as adaptors or calcium (Liu *et al.*, 1995; Ungewickell & Ungewickell, 1991). Also, biochemical studies have shown that the C-terminal domains of the light chains interact with the trimerization domain of the heavy chains, being important for stabilization of the mammalian triskelion hub assembly *in vitro* at low pH (Ybe et al., 2007). Experimental evidence also indicates an essential role for the light chain in the trimerization of the heavy chain in yeast, since heavy chain mutations that weakened light chain binding, as well as light chain knockouts, resulted in heavy chain detrimerization (Huang *et al.*, 1997). In a cell, the pucker of the trimer could be altered by changes in the light chain, at the trimerization domain and/or knees, or by cargo interaction with adaptors beneath the clathrin TD (Brodsky, 2012).

Clathrin triskelions are packaged into a lattice (Figure 2D) around coated pits and vesicles during clathrin-mediated budding events. When clathrin assembles in the lattice, the center of a triskelion is associated with each lattice point in a vertex and the knees and TD are situated below the vertex of another triskelion (Fotin *et al*., 2004) (Figure 2D). The proximal leg of a heavy chain in a triskelion locates beside a proximal leg of the triskelion centered on the adjacent vertex, and the leg then curves around, so that its distal segment lies just beneath the proximal segment of a second leg from the adjacent triskelion (Figure 2D). It is believed that this proximal-distal contacts might make a principal contribution to coat assembly and stability (Kirchhausen *et al.* 2014; Kirchhausen, 2000). In the triskelion, each heavy chain projects inward as a long α-helix, followed by the less-ordered, carboxy-terminal segment (Fotin *et al*., 2004). The three long helices (one from each heavy chain) form a tripod-like structure that holds the trimer together and links it non-covalently to more distal parts of other trimers beneath it (Fotin *et al*., 2004). The TD emerges inward from the clathrin lattice and represents the region of the outer triskelion positioned closest to the membrane surface in the assembled coat, free to contact adaptors and other membrane-interacting components (Haar *et al*., 1998).

Assembly of purified clathrin heavy and light chains into a polyhedral basket is triggered *in vitro* by low pH or addition of calcium, both, non-physiological conditions, or by interaction with adaptors (Crowther & Pearse, 1981; Liu *et al*., 1995; Ungewickell & Ungewickell, 1991; Ybe *et al.*, 1998). During propagation of the clathrin lattice *in vivo*, the clathrin-adaptor nucleus can recruit further untethered clathrin from the cytosolic pool and adaptors from either the cytosol or the membrane (Kirchhausen *et al*., 2014) that would stabilize coated pit. The rate of adaptors recruitment, relative to clathrin, diminishes substantially during subsequent phases of coat assembly (Loerke *et al.,* 2011). The formation of the coat is a continuous process, and a clathrin coat should not be considered as a static structure but as a dynamic network in which there is a constant exchange of interacting partners.

Early studies on isolated clathrin coated pits demonstrated that the coat consisted of at least 12 pentagons, which introduce curvature, and a variable number of hexagons (Crowther & Pearse, 1981). The ability of clathrin to self-assemble into pentagons and hexagons and its ability to generate curvature *in vitro* in a cell-free system with purified components, suggested that it was clathrin that forced membrane curvature, but the alternative view in which the formation of pentagons into the lattice is a consequence of membrane curvature cannot be ruled out, as initial bending of PM during coat formation in yeast can occur in the absence of clathrin (Idrissi *et al.,* 2012). Thus, in yeast clathrin does not play an essential structural role to define the morphology or size of the endocytic coat, as it seems for mammals (Duncan & Payne, 2005; Hinrichsen *et al.*, 2006) but rather, it might have a regulatory role (Boettner *et al*., 2011; Idrissi *et al*., 2012; Kaksonen *et al.*, 2005; Newpher *et al*., 2006). The contour of a clathrin leg in a lattice reaches nearly three edges. When legs associate to form coats or cages, they incorporate pentagonal openings as well as hexagonal ones (Crowther & Pearse, 1981). 12 pentagons are required to form a closed shell, if all the other openings are hexagons. If all the openings were hexagonal, the lattice would be a flat array. The number of hexagonal openings and the distribution of pentagonal openings among them, define the size and shape of the overall structure (Crowther & Pearse, 1981; Fotin *et al.,* 2006; Kirchhausen *et al*., 2014; Pearse & Crowther, 1987) (Figure 2E). *In vitro*, these properties are determined by the presence or absence of an AP (adaptor) core and the equilibrium pucker of clathrin triskelions (Kirchhausen,

2000). Besides, the characteristics of the cargo could also influence the size and shape of a vesicle (Jackson *et al.*, 2010; Kirchhausen, 2000). The barrel-like coat structure with D6 symmetry is particularly regular (Figure 2E, hexagonal barrel). Coated vesicles isolated from cells or tissues are found to be more heterogeneous in size and shape than the coats assembled for cryo-EM studies. Tomographic reconstructions of individual coated vesicles have shown the variety of lattices present in a preparation from bovine brain (Cheng *et al.* 2007). Most of these coated vesicles probably represent intermediates in pre-synaptic membrane uptake. Clathrin coats are typically > 90 nm in diameter and contain about 35–40 triskelions, whereas coats derived from the Golgi apparatus or those in the synaptic terminal are 75-100 nm in diameter. They enclose a spherical vesicle whose size can vary according to the size of the coat. In contrast, the coat thickness remains relatively constant at ∼22 nm (Pearse & Crowther, 1987). The gap between the coat and the vesicle can accommodate not only the various adaptors, but also the many other regulatory proteins that participate in cargo sorting, budding, and uncoating (Kirchhausen *et al.*, 2014).

Some cell types in culture (for example, HeLa cells) are also found to create abundant, relatively long-lived clathrin arrays at the interface with the substrate on which they are growing. When studied by EM, these flat clathrin arrays correspond to extended clathrin lattices, which can be of substantially greater diameter and have very different dynamics than the sharply invaginated canonical coated pits (Saffarian *et al.,* 2009). These large non-canonical structures, now termed “coated plaques,” can cover membranes and sequester cargo such as the transferrin receptor. Nucleation of branched actin microfilaments probably drives plaque movement into the cell, contrary to what was observed for mammalian spherical coats budding (Saffarian *et al.,* 2009). EM studies have shown that coated plaques have a high concentration of lattice defects that may be consequence of the resistance of the underlying support to curve, so that lattice defects will lead to a patchwork of hexagons unable to curve (Reviewed in (Traub, 2009)).

Clathrin has also been found to constitute a flat bilayered structure characterized by EM in mammalian early endosomes (EE) maturing to multivesicular bodies (MVB) and in MVB (Sachse *et al.,*2002) , distinct from the “canonical” PM and TGN

clathrin coats. These flat clathrin arrays form a lattice with no evidence of rounded bud production, and have an unusual EM morphology that is not seen at PM plaques. They are not associated with actin and are dependent on the presence of PtdIns(3)P ((Sachse *et al.,*2002) and references therein), but also bind adaptors, such as Hrs (ESCRT-III) (Raiborg *et al*., 2001), and operate by sequestering cargo for targeting to lysosomes (Raiborg *et al.*, 2006). The unusual appearance of bilayered clathrin coats could indicate inclusion of structural components that preclude lattice curvature (Traub, 2009).

The clathrin heavy chain legs are found on the outer surface of the clathrin lattice, providing the structural backbone, while the clathrin light chains are exposed to the cytoplasmic face of coated vesicles and pits, potentially facilitating their interaction with cytoplasmic regulatory elements as calcium, calmodulin or Hsc70, and exhibiting properties that suggest that it plays a role in regulating clathrin dynamics. The N-terminal light chain acidic region interacts with Hip1/Hip1R/Sla2, which also regulates clathrin dynamics (Boettner *et al.*, 2011; Chen & Brodsky, 2005; Wilbur *et al*., 2008). Biochemical studies firstly showed that the light chains inhibit spontaneous triskelion self-assembly at physiological pH *in vitro* (Liu *et al*., 1995) but neutralizing the light chain acidic residues suppresses clathrin assembly inhibition (Ybe *et al*., 1998). Subsequently, it was shown that Hip1/Hip1R/Sla2 binding to the N-terminus of the light chain releases the clathrin light chain N-terminal negative regulation on the assembly of the clathrin lattice (Chen & Brodsky, 2005) and induces a conformational change in HIP1/HIP1R/Sla2 that reduces its affinity for actin (Chen & Brodsky, 2005; Wilbur *et al*., 2008). The evidence suggests a model whereby HIP1 related proteins are recruited to clathrin-coated membranes via the clathrin light chain, then dissociate from the light chain and bind membranes through clathrin light chain-independent interactions, which allow them to influence actin dynamics and vesicle scission (Boettner *et al*., 2011; Newpher *et al*., 2006; Newpher & Lemmon, 2006a).

Uncoating a clathrin lattice under physiological conditions *in vitro* or within a cell requires ATP hydrolysis. This reaction is carried out in mammals by the Hsc70 chaperon, also called the uncoating ATPase (Rapoport *et al.*, 2008; Xing *et al*., 2010), and it is facilitated by the DNAJ-domain-containing co-chaperons auxilin1 (neuronal-specific) and auxilin2/GAK (Cyclin G-associated kinase, ubiquitous expressed) (Lee *et al*., 2006; Yim *et al*., 2010) (Figure 3A and section 1.1.3.3.). They

are recruited to a coated vesicle immediately after it has pinched off from the membrane and function to present substrate to Hsc70 (Lee *et al.*, 2006). Biochemical and cryoelectron microscopy studies of purified auxilin and Hsc70 bound to purified clathrin, localize auxilin binding to the coat region underneath the vertex (Xing *et al.*, 2010)(Figure 3B). Hsc70 interacts with a C-terminal peptide of clathrin heavy chain (QLMLT), next to the trimerization domain (Rapoport *et al*., 2008b; Xing *et al.*, 2010) (Figure 3A). It has been proposed that Hsc70 is recruited to a position close to its target by the auxilin J-domain. Auxilin binding to clathrin heavy chain may destabilize the clathrin lattice, allowing Hsc70 to bind to the released C-terminus where it would split ATP (Ungewickell *et al.*, 1997; Ungewickell *et al*., 1995). ATP hydrolysis by Hsc70 bound in this region may then potentially alter the triskelion pucker and put strain. Accumulation of local tension imposed at multiple vertices can then lead to disassembly of the coat (Xing *et al.,* 2010), with its components returning to the cytosol to be recruited and reused in another round of CCV formation. Disassembling of endosomal flat bilayered clathrin coats is thought to be carried out in mammals by RME-8 and Hsc70 (McGough & Cullen, 2013; Shi *et al.*, 2009). RME8 is an endosomal specific auxilin-like protein, that also contains a DNA J-domain that interacts with Hsc70 stimulating its ATPase activity (Chang *et al.*, 2004; Girard *et al*., 2005; Shi *et al.,* 2009).

Calcium binding in a region next to the Hsc70 binding site and the heavy chain interaction domain of the clathrin light chain LCa has been suggested to also have the potential to regulate clathrin assembly and disassembly. *In vitro*, calcium suppresses the triskelions self-assembly inhibition by the light chains (Ungewickell & Ungewickell, 1991), by maybe neutralizing the negative regulatory sequences in light chains. *In vivo* though, the physiological calcium concentration and the low calcium affinity of the light chains are not sufficient to enhance clathrin assembly. Therefore, it has been suggested that at physiological calcium concentrations, low affinity calcium binding to the E-F hand motif may instead act to signal clathrin uncoating by revealing a binding site for Hsc70. It has been suggested that Hsc70 binding to LCa in a calcium-dependent manner may induce a conformational change that facilitates Hsc70-mediated coat disassembly (DeLuca-Flaherty *et al.*, 1990). Besides, it has been recently suggested a role for light chains in contributing to clathrin disassembly by improving the efficiency with which auxilin facilitates

disassembly. Hsc70 binding to the clathrin cage may induce a clathrin light chain conformational change that would facilitate auxilin dissociation after clathrin uncoating. In the absence of light chains,auxilin would no longer dissociate effectively from the released clathrin triskelion (A. Young et al., 2013).

Yeast also has an auxilin (Swa2) and the Hsc70 ortholgues, Ssa1, Ssa2, Ssa3 and Ssa4 (see also section 1.1.3.3.). Swa2 and Ssa1 also bind clathrin and are able to uncoat mammalian and yeast clathrin coats *in vitro* (Krantz *et al.*, 2013), but their exact roles in uncoating yeast clathrin coated vesicles *in vivo* have not been elucidated yet.

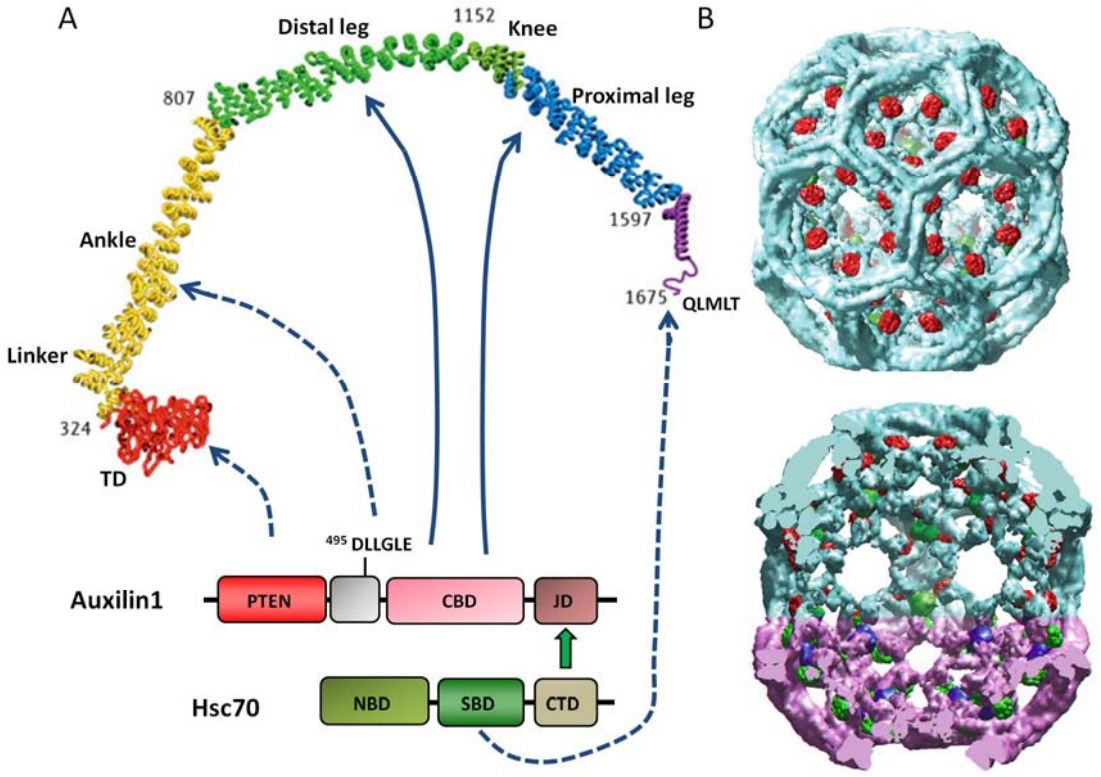

Figure 3. Hsc70 and auxilin binding to clathrin heavy chain dirive clathrin coat disassembly. A) Representation of the molecular strucure of a mammalian clathrin heavy chain with the different domains differentially coloured. The potential Hsc70 binding motif (QLMLT) is labelled near the C-terminus of the protein. Bellow are represented linear diagrams of the domain organization of mammalian auxilin1 (PTEN: phosphatase-and-tensin-homologue domain; CBD: clathrin-binding domain; JD: J domain) and Hsc70 (NBD: nucleotide-binding domain; SBD: substrate-binding domain; CTD: C-terminal domain) indicating their interactions and the position of a clathrin-box motif in auxilin1. Biochemically defined interactions are shown using solid lines, whereas proposed interactions are shown using dashed lines (adapted from (Edeling *et al.*, 2006)). B) Outside view (above) and cutaway view (below) of the complete coat. Clathrin is in blue, auxilin1 is in red and Hsc70 is in green (taken from (Xing *et al.*, 2010).

1.1.3. Clathrin binding partners in *S.cerevisiae*

1.1.3.1. Clathrin adaptors to cargo

A clathrin adaptor is a protein that links clathrin to the protein or lipid components of a cellular membrane and defines the type of cargo that will accumulate in the clathrin coated pit. Clathrin adaptors bind to clathrin TD and to three classes of targeting signals in the membrane associated proteins destined to clathrin coated vesicles: 1) short, linear motifs; 2) post-translational modifications such as ubiquitination and phosphorylation; and 3) folded, structural motifs (Kelly & Owen, 2011).

AP-2

AP-2 is a tetrameric adaptor involved in CME (Hinrichsen *et al.*, 2003). The four subunits of the AP-2 complex contains two large α2 and β2 subunits of 110-120 kDa (Apl3 and Apl1 in yeast, respectively), a medium subunit of approximately 50 kDa, μ2 (Amp4 in yeast), and a small 15-20 kDa subunit, σ2 (Asp2 in yeast) (Figure 4). The large subunits can be divided into an N-terminal trunk domain of 60–70 kDa and a C-terminal appendage domain of 15–30 kDa. The trunk is joined to its appendage by an unstructured hinge linker of between 50 and 200 amino acids that binds the clathrin TD. The C-terminal appendage domain of the large subunits constitutes binding platforms for accessory proteins that participate in coat assembly and vesicle formation, including other adaptors. The N-terminal regions of β2 and α2 subunits together with the medium and small subunits constitute the core complex, which binds to PtdIns(4,5)P_2, which is enriched in PM, and sorting signals in the cytoplasmic domains of cargo proteins. The subunits of the yeast AP-2 complex exhibit 26-49% of amino acid sequence identity with the corresponding regions of the human homologue, extending the homology throughout the length of the Apl3 (26% identity), Amp4 (32% identity) and Asp2 (49% identity) subunits. The Apl1 subunit exhibit similarity only to the core region human β2 (32% identity) and it is considerably a shorter protein. Importantly, the yeast hinge of subunit Apl1 does not bind clathrin (Yeung *et al.*,1999), unlike its human counterpart (Edeling *et al.,* 2006; Thieman *et al.*, 2009; Willox & Royle, 2012). Despite these differences, yeast AP-2 appears to be functionally homologous to its mammalian homologue having a role in endocytosis, albeit with different relevance (Carroll *et*

al., 2009; Huang *et al.*, 1999; Yeun *et al.*, 1999b). At the moment, only one cargo has been defined for the yeast AP-2 (Carroll *et al.*, 2009).

AP-1

AP-1 has been implicated in the formation of CCV vesicles at the TGN and in the retrograde transport from endosomes to the TGN and to the PM (Ohno, 2006; Valdivia *et al.,* 2002). AP-1 contains four subunits with the same general molecular and structural organization of AP-2: one small σ1 subunit (Asp1 in yeast), one medium μ1 subunit (Apm1 in yeast), and two large subunits, β1 and γ1 (Apl2 and Apl4 in yeast, respectively) (Figure 4). The core complex of AP-1 binds to the Golgi-localized PtdIns(4)P, playing a significant role in recruiting AP-1 to the Golgi membrane (Wang *et al.*, 2003). AP-1 recruitment involves also a direct interaction with the small GTPases Arf1 (Austin *et al*., 2000). Active GTP-bound Arf1 recruits the Golgi-associated adaptor AP-1 to the TGN. Thus, TGN targeting of AP-1 is achieved by interaction with both the Golgi-enriched PtdIns(4)P and the active

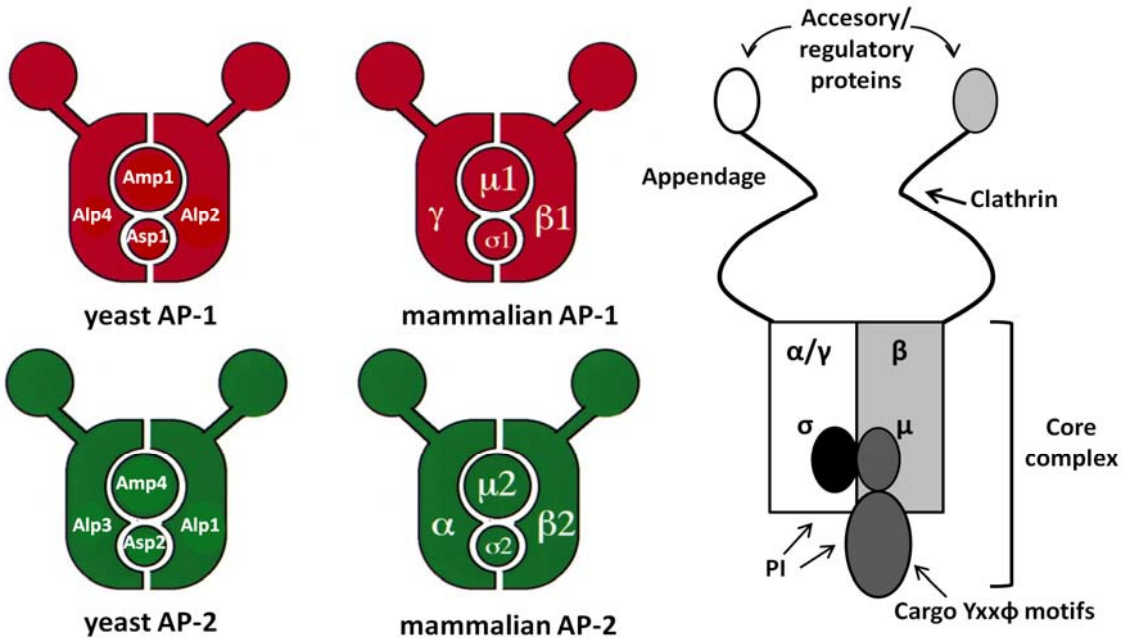

Figure 4. Schematic representation of the structure and domain organization of the yeast and mammalian AP-1 and AP-2 multimeric complexes showing the different interacting partners. PI: phosphoinositides. (Illustration adapted from (Owen *et al.,* 2004b; Hirst Robinson 1998)).

Arf1. AP-1 also binds clathrin and it has been found as a component of clathrin coated vesicles (Phan *et al.*, 1994). Yeast AP-1 subunits share 31%-54% amino acid sequence identity with mammalian AP-1. Interestingly, yeast Apl2 and Apl1 subunits are only 26% identical, whereas mammalian β1/ β2 subunits identity is 83%, suggesting that yeast β subunits functions in AP-1 and AP-2 have diverged.

AP-1 has roles in the anterograde and retrograde recycling from TGN to endosomes in yeast and mammals (Ohno, 2006; Owen *et al.*, 2004; Valdivia *et al.,* 2002) (see sections 1.1.4.1.2.1. and 1.1.4.1.2.2.. for further details).

Syp1 (FCHo1)

Syp1 is a member of the muniscin family, homologous to human FCHo1 and FCHo2 (Reider *et al.*, 2009) involved in endocytic uptake. It contains an N-terminal F-BAR (Bin, Amphiphysin, Rvs) that is able to induce membrane curvature, a central proline-rich domain, and a C-terminal μ homology domain (μHD) similar to the cargo binding domain in the C-terminus of the mamalian μ subunit of AP-2 (Figure 5). Syp1 binds to Ede1 at endocytic sites (Reider *et al.*, 2009; Stimpson *et al.,* 2009). It is suggested to have a role in localization of endocytic sites (Stimpson et al., 2009), in constricting the invagination neck and in regulating the nucleation promoting activity (NPA) of the yeast WASP Las17 (Idrissi *et al*., 2012; Reider *et al.,* 2009; Wendland *et al.*, 2009) (see section 1.1.4.1.1.1. for further details). It also appears to act as an specific adaptor for uptake of the PM stress sensor Mid2 (Reider *et al.*, 2009).

yAP1801 and yAP1802 (AP1080/CALM)

yAP1801 and yAP1802 are yeast homologues of the mammalian monomeric adaptors AP180/CALM. Their N-terminus contains a PtdIns(4,5)P_2 binding domain and a ANTH (AP180 N-terminal Homology) domain, which is similar to a ENTH (Epsin N-terminal homology) domain but it does not generate membrane curvature. The C-terminal region includes a variable number of NPF (asparagine-proline-phenylalanine) motifs that bind to EH (Eps15 homology) domains and a clathrin box (Ford *et al*., 2001) (Figure 5). It is likely that there is also specialization during cargo recognition, appearing yAP1081/2 to act as selective adaptors for the v-SNARE Snc1 (Burston *et al*., 2009).

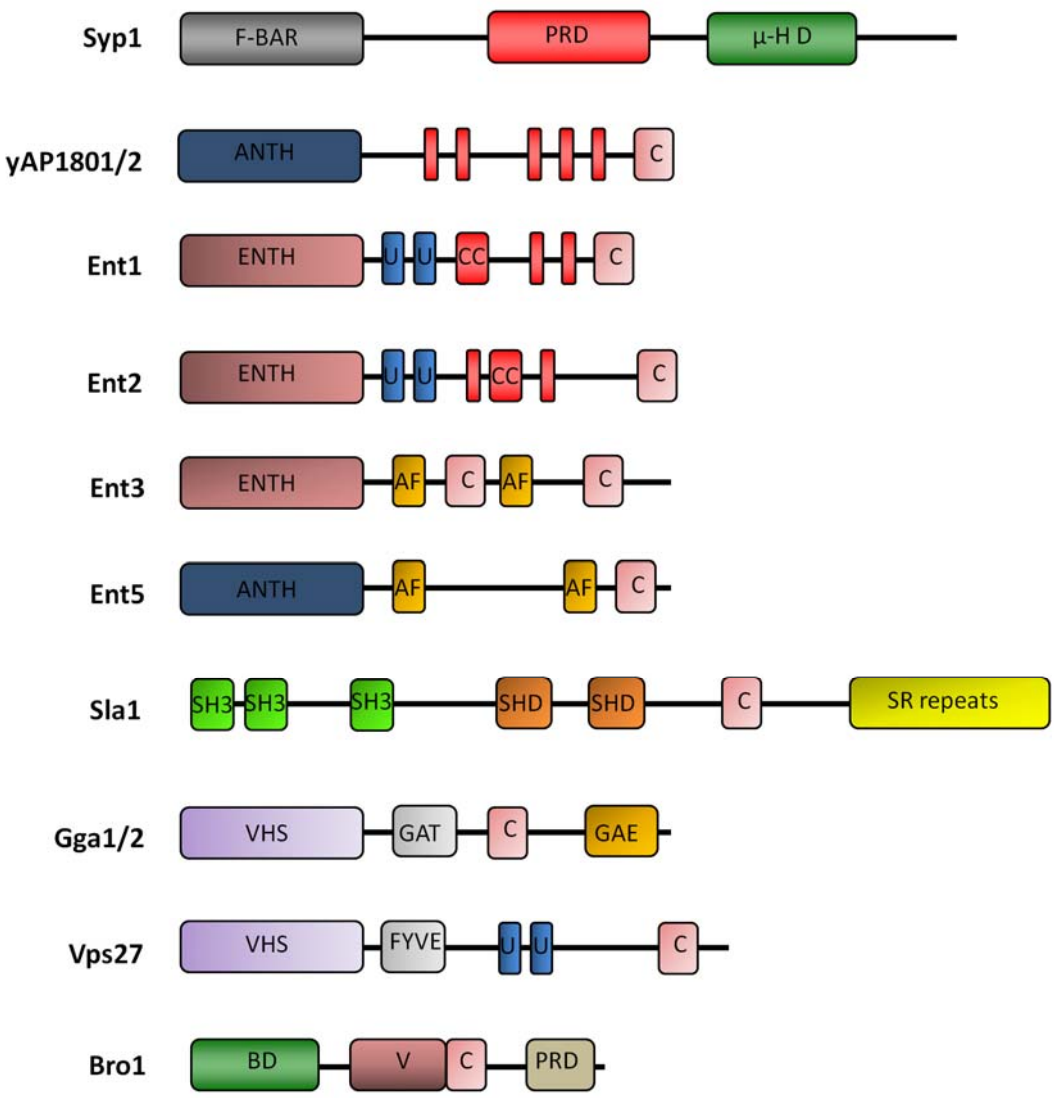

Figure 5. Domain organization of yeast monomeric clathrin adaptors to cargo. Several domains involved in protein-membrane interactions are shown. ANTH: AP180 N-terminal homology. ENTH: Epsin N-terminal homology. F-BAR: Fes/CIP4 homology-Bin/Amphiphysin/Rvs domain; FYVE: Fab1, YOTB, Vac1 and EEA1 domain. A number of protein-protein interaction domains are also represented. Red bars: asparagine-proline-phenylalanine-rich regions (NPF motifs). PRD: proline-rich domain, they bind to SH3 domains. SH3: Src homology 3 domain. CC: coiled-coil domain. U: ubiquitin associated domain, or UBA domain. C: clathrin box domain, also involved in clathrin binding. µ-HD: µ-adaptin homology domain, it is involved in cargo sorting and/or Ede1 binding. Other domains depicted are: SHD: Sla1 homology domain; SR repeats: serine-arginine-rich regions; AF: Acidic phenylalanine GAE binding sequence; VHS: Vps27, Hrs, STAM domain; GAT: GGA and Tom1 domain; GAE: C-terminal γ-adaptin ear domain; BD: Bro1 domain; V: V domain; PRD: proline-rich domain.

Ent1, Ent2, Ent3 and Ent5 (Epsins)

These adaptors contain an N-terminal ENTH (Epsin N-terminal homology) domain in the case of Ent1, Ent2 and Ent3, that is able to insert into the lipid bilayer through an amphipathic helix inducing membrane curvature, and an ANTH (AP180 N-terminal homology) domain in the case of Ent5, that does not generate membrane curvature. Ent1 and Ent2 also contain two ubiquitin interacting motifs (UIM) and two NPF motifs. Ent3 and Ent5, on the contrary, have a region containing an acidic phenylalanine GAE (Gamma Adaptin Ear) binding sequence. All them contain clathrin box motifs that bind to clathrin ((Aguilar *et al*., 2003) and references therein) (Figure 5).

Ent1 and Ent2 are homologues of the mammalian endocytic adaptors epsins which bind to PtdIns(4,5)P_2 (enriched at the PM). Their UIMs are required for their recruitment to cellular membranes and to bind ubiquitin (Aguilar *et al.,* 2003), the best characterized internalization signal in yeast for binding endocytic cargo proteins. On the contrary, Ent3 and Ent5 co-localize with clathrin at the TGN (Duncan *et al.*, 2003). Surprisingly, their lipid binding domains bind preferentially PtsIns(3)P and PtdIns(3,5)P_2 *in vitro* (phosphoinositides associated with endosomes (Eugster *et al.*, 2004; Friant *et al.,* 2003)), whereas the TGN is enriched at PtdIns(4)P (reviewed in (De Matteis & Godi, 2004)). Taking into account the weak affinities of Ent3 and Ent5 for PtdIns(4)P, these results suggested that *in vivo*, lipid binding is not a primary determinant for membrane recruitment, but instead, specific protein-protein interactions determine the assembly site (Myers & Payne, 2013). Consistently, Ent3 interacts with Gga2, which binds TGN membranes specifically and Ent5 requires AP-1 binding for its recruitment to the TGN (Daboussi *et al.*, 2012).

In mammals, a single epsin-related protein involved in TGN-endosome traffic has been identified, EpsinR, which binds PtdIns(4)P and localizes to the TGN (Hirst *et al*., 2003; Saint-Pol *et al*., 2004). EpsinR binds AP-1 and clathrin and contains an N-terminal ENTH domain that interacts with some SNAREs (Hirst *et al.,* 2004).

Sla1 (Intersectin-like)

The adaptor protein Sla1 consist of three N-terminal polyprolin binding SH3 (Src Homoly 3) domains, two central SHD (Sla1 Homology Domains) domains, a variant

of the consensus clathrin box and finally an unstructured C-terminus (Figure 5). The SHD2 domain of Sla1 binds to the variant clathrin box providing intramolecular inhibiton of clathrin binding. There is not a clear homologue in mammals, although organization similarities have been found with intersectin (Howard *et al.*, 2002) or CIN85 (Dikic, 2002), that are associated with clathrin-mediated endocytosis and interact with actin and clathrin based machineries.

Sla1 is an endocytic adaptor for PM cargo containing the NPxFD endocytic sorting motif in their cytoplasmic domains (Howard *et al*., 2002). Also, Sla1 might function as a regulator of actin dynamics (Rodal *et al.*, 2003) (see section 1.1.4.1.1.2.).

Gga1 and Gga2

Gga (Golgi-localized gamma ear-containing, Arf-binding) proteins are localized in the TGN and endosomes (Costaguta *et al.*, 2001; Daboussi *et al.,* 2012; Traub, 2005). Mammals have three GGA proteins, whereas only two are found in yeast, Gga1 and Gga2, which share 60% homology and being Gga2 expressed 5-10 fold the levels of Gga1 (Costaguta *et al.*, 2001). They contain an N-terminal VHS (Vps27, Hrs, STAM) domain that binds to PtdIns(4)P (Demmel *et al.*, 2008) and to Pik1 PtdIns(4)-kinase (Daboussi *et al.*, 2012) (Figure 5). In mammals the Gga VHS domain binds to acidic dileucin sorting motifs with the consensus DxxL, but these key residues that contact the sorting motifs are not conserved in yeast ((Myers & Payne, 2013) and references therein). However, it has recently been shown that the yeast cargo Kex2 binds specifically the Gga2 VHS domain thought a GBS (Gga Binding Site) in its C-tail, facilitating its transport from the TGN to the prevacuolar compartment (PVC) (De *et al*., 2012). Following the VHS domain, there is a GAT (GGA and Tom1) domain that binds to the GTP-activated form of Arf1 (Boman *et al.*, 2002) and ubiquitin, being the latter interaction important for the efficient sorting of some membrane proteins from the TGN to the ILV (Intra Luminal Vesicles) of the MVB (Deng *et al*., 2009). C-terminal to the GAT domain, there is a flexible region that contains clathrin box motifs that directly bind clathrin. However, they might be able to bind clathrin through other binding sequences or through indirect interactions because deletion of those clathrin box motifs do not significantly alter their functionality (Mullins *et al*., 2001). They also have a C-terminal γ-adaptin ear (GAE) domain, homologous to the appendage domain of the AP-1 γ subunit, that serves as binding platform for interaction with other

clathrin associated proteins, such as Ent3 and Ent5 (Duncan *et al*., 2003), although this domain does not seem to be essential for Gga function (Mullins & Bonifacino, 2001), suggesting alternative binding interactions that might recruit Ent3 and Ent5 to membranes.

Vps27 (Hrs)

Vps27, homologue of mammalian Hrs, forms the ESCRT-0 complex together with Hse1 (mammalian STAM). ESCRT-0 is involved in ubiquitinated protein sorting into the ILV of the MVB (Hurley, 2010). Both Vps27 and Hrs possess an 8-helix VHS domain at their N-termini similar to Ggas (Mao *et al*., 2000), and contain ubiquitin interacting motifs (UIMs) that are essential for the function of ESCRT-0 in MVB sorting (Shih *et al.*, 2002). Vps27 also binds PtdIns(3)P via its FYVE (Fab1, YOTB, Vac1 and EEA1) domain (Misra & Hurley, 1999), and the ESCRT-I protein Vps23 via the PTAP-like motifs in the C-terminal region (Bilodeau *et al.,* 2003). It also contains clathrin-binding motifs that interact with clathrin *in vivo* and *in vitro* (Bilodeau *et al.*, 2003; Raiborg *et al.*, 2002), and a predicted helical region of around 100 amino acids through which Vps27/Hrs binds to Hse1/STAM (Asao *et al.*, 1997) (Figure 5). Thus, Vps27 would associate with ubiquitinated cargo and with the membrane via PtdIns(3)P and recruit ESCRT-I to MVB, triggering ESCRT-mediated MVB sorting (see section 1.1.4.1.2.3. for further details).

Bro1 (ALIX)

Yeast Bro1, homologue of the mammalian ALIX, is a protein required for promoting the recruitment of the deubiquitinating enzyme Doa4 to the assembling ESCRT-III complex (reviewed in (Hurley, 2010)), although it has recently been suggested to function in parallel with ESCRT-0 to recognize and sort ubiquitinated cargos in the MVB (Pashkova *et al.*, 2013). It has a N-terminal banana-shaped Bro1 domain which binds to the C-terminal region of Snf7 (SCRT-III), and a central V domain, which binds ubiquitin and clathrin, possibly through a conserved clathrin binding box motif within an unstructured loop at V domain vertex, although other motifs may also be sufficient for clathrin association ((Pashkova *et al.*, 2013) and references therein). Finally, it also has a flexible C-terminal proline-rich domain (PRD) that binds Doa4 (Richter *et al.*, 2007) (Figure 5).

1.1.3.2. Proteins linking clathrin to the actin cytoskeleton

Some proteins act as a linker between clathrin coats and the actin cytoskeleton, an important interaction that is required for vesicle invagination and fission in yeast.

Sla2 (Hip1R)

Sla2 is the yeast homologue of mammalian HIP1 and HIP1R. It binds PtdIns(4,5)P_2 through its N-terminal ANTH (AP180 N-terminal homology) domain and to F-actin through its C-terminal talin-like domain (Raig, 1997; Sun *et al*., 2005) (Figure 6). In addition, Sla2 contains a coiled-coil domain that mediates Sla2 dimerization and interacts with endocytic proteins including the actin NPF (nucleation-promoting factor) Pan1, negatively regulating its nucleation promoting activity *in vitro* (Toshima *et al.*, 2007), and Clc1, which seems to spatially regulate the actin-binding activity of Sla2 (Boettner *et al.*, 2011) (see section 1.1.2.2.3.). Thus, Sla2 serves *in vivo* as a linker between endocytic sites at the PM and the actin cytoskeleton. Besides, mammalian HIP1R appears to coordinate actin assembly with clathrin budding also at the TGN for trafficking to the lysosome (Carreno *et al*., 2004a).

In yeast, Ent1 has also been shown to cooperate with Sla2 in PM-actin cytoskeleton coupling. The ANTH domain of Sla2 and the ENTH domain of Ent1 bind each other in a ligand-dependent manner to provide critical anchoring of both proteins to the membrane. The C-terminal parts of Ent1 and Sla2 bind redundantly to actin filaments, constituying a molecular linker that transmits the force generated by the actin cytoskeleton to the PM, leading to membrane invagination and vesicle budding (Skruzny *et al*., 2012). Mammalian epsin has also been found to directly interact with actin, suggesting that epsin might also have a role in helping actin interact with the CCPs and generating the force required for a pit to develop into a vesicle (Messa *et al*., 2014).

1.1.3.3. Clathrin binding proteins involved in clathrin-coated vesicle scission and uncoating

Rvs167 (Amphiphysins and endophilins)

Rvs167 is a N-BAR-domain-containing protein related to the mammalian amphiphysins and endophilins, that recognize and stabilize highly curved membranes and contribute to membrane scission (reviewed in (Boettner *et al*., 2011)) (Figure 6). They have an amphipathic helix preceding the BAR domain (N-BAR domain proteins), that folds and inserts into membranes (Gallop *et al*., 2006). An unstructured linker has binding sites for AP-2 appendages and clathrin and connects the BAR domain to a carboxy-terminal SH3 domain, which binds the proline-rich, carboxy-terminal regions of two membrane-directed enzymes, the dynamin GTPase and the synaptojanin lipid phosphatase, recruiting them to CCPs (David *et al.*, 1996; Verstreken *et al.,* 2003).

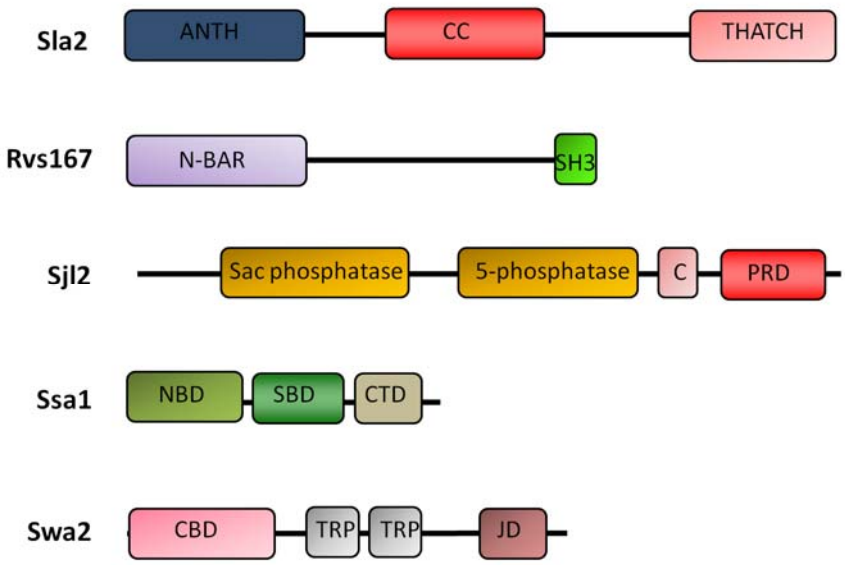

Figure 6. Schematic representation of the structure and domain organization of yeast clathrin binding partners Sla2, Rvs167, Sjl2, Ssa1 and Swa2. Domain organization clathrin binding partners that link clathrin to the actin cytoskeleton (Sla2), and that are involved in scission and uncoating (Rvs167, Sjl2, Ssa1 and Swa2). ANTH: AP180 N-terminal homology; CC: coiled-coil domain; THATCH: talin- HIP1R/Sla2 actin-tethering C-terminal homology domain, it mediates interaction with actin filaments; ENTH: N-BAR: N-terminal amphipathic helix-Bin/Amphiphysin/Rvs domain; SH3: Src homology 3 domain, it binds to proline-rich regions; 5-phosphatase: PtdIns(4,5)P_2-5-phosphatase domain; Sac phosphatase: PtdIns(4)P-phosphatase region; C: clathrin box motifs; PRD: proline-rich domain, it binds to SH3 domain-containing proteins; PTEN: phosphatase-and-tensin-homologue domain; CBD: clathrin-binding domain; JD: J domain; TRP: tetratricopeptide repeats; JD: J domain.

Sjl1, Sjl2 and Sjl3 (Synaptojanins)

Sjl1, Sjl2 and Sjl3 encode the yeast synaptojanins, which are inositol phosphatases (McPherson *et al.,* 1996). They have two separate phosphatase domains, one of which dephosphorylates PtdIns(4,5)P_2 or PtdIns(3,4,5) P_3 at the 5´ position of the inositol ring (5´ phosphatase domain) and one that dephosphrylates PtdIns(3)P or PtdIns(4)P (Sac phosphatase domain) ((Stefan *et al*., 2002) and references therein). A proline-rich, carboxy-terminal tail binds the SH3 domain of the amphiphysins and the endophilins (Verstreken *et al.*, 2003). They also have clathrin and AP-2-binding motifs, distal to the proline-rich segment (reviewed in (Kirchhausen *et al.,* 2014) (Figure 6).

Sjl2 functions at endocytic sites hydrolyzing PtdIns(4,5)P_2 to form PtdIns(4)P contributing to clathrin coat disassembling (Stefan *et al*., 2002; Stefan *et al*., 2005) (See section 1.1.4.1.1.5.). Sjl3 on the contrary, function with AP-1 and clathrin in the TGN to EE pathway (Ha *et al.*, 2003).

Ssa1 (Hsc70)

Ssa1 is the yeast orthologe of Hsc70 (70-kDa heat-shock cognate protein (Hsc70) chaperone)(Werner-washburne *et al*., 1987), which is an ATP-dependent "disassembly enzyme" for many subcellular structures, including CCV (see section 1.1.2.2.3. and Figure 3). It contains a nucleotide-binding domain (NBD), a substrate-binding domain (SBD) that binds to the C-terminal part of clathrin heavy chain, and a C-terminal domain (CTD) which binds the J-domain of auxilin (Edeling *et al*., 2006; Xing *et al.*, 2010) (Figure 3 and 6).

Ssa1 physically interacts with Chc1 and Clc1 but its role in yeast clathrin uncoating *in vivo* has not been investigated ((Krantz *et al*., 2013) and references therein).

Swa2 (Auxilin)

Swa2 is the ortholog of the mammalian auxilin 1. Mammalian cells express a brain-specific auxilin1 and a ubiquitous auxilin2 that function as Hsc70 co-chaperons necessary for clathrin uncoting of CCV of both PM and TGN origin (Greener *et al.,* 2000; Umeda *et al*., 2000) (see section 1.1.2.2.3.). Auxilin 2, also called cyclin G-associated kinase (GAK) is also a member of the Ark1/Prk1 family of kinases. Auxilins have a PTEN-like domain composed of a phosphatase-like (PD) and C2

subdomains, a central segment with binding sites for dynamin, AP-2, and clathrin, and a C-terminal J-domain that recruits Hsc70 (Edeling *et al*., 2006; Rapoport *et al.,* 2008; Xing *et al.,* 2010) (Figure 3). In addition, GAK has an N-terminal Ser/Thr kinase domain of unknown *in vivo* function.

In yeast, Swa2 also binds clathrin but its function *in vivo* is not very clear (Gall *et al*., 2000; Toret *et al.*, 2008) (see section 1.1.2.2.3). It contains a clathrin binding domain in its N-terminus, a tetratricopeptide repeat (TPR), as well as a J- domain in its C-terminus (Gall *et al*., 2000) (Figure 6). In yeast, Ark1 and Prk1 kinases phosphorylate various clathrin coat components contributing to coat disassembling (Cope *et al.*, 1999; Toret et al., 2008; Zeng, Yu, & Cai, 2001) (see section 1.1.4.1.1.5.), but do not have J-domains and do not act as co-chaperones.

1.1.3.4. Calmodulin

Calmodulin is a calcium sensor with important roles in regulating many proteins and signalling pathways in all eukaryotes in response to calcium. It comprises two homologous globular domains containing each one two calcium- binding EF-hands. Both domains are connected by a central flexible linker (see section 1.2.2.2.).

Mammalian and yeast purified clathrin components, such as triskelions and coated vesicles, bind to calmodulin *in vitro* (Lisanti *et al*., 1982; Pley, 1995*;* Linden *et al*., 1981). Purified yeast and mammalian clathrin light chains interact with calmodulin *in vitro* through its C-terminal domain (Pley, 1995; Silveira *et al*., 1990), and the mammalian clathrin heavy chain has also been shown to bind calmodulin *in vitro* when purified and immobilized on nitrocellulose membranes (Merisko *et al.* 1988). It is not clear though whether clathrin and calmodulin interact *in vivo* and what is the functional significance of this interaction.

1.1.4. Conserved cellular functions of clathrin: from yeast to mammals

In higher eukaryotes, clathrin is essential for viability (Bazinet *et al.*, 1993), whereas in yeast clathrin knock outs are viable or not, depending on the strain background (Lemmon & Jones, 1987; Payne *et al*., 1987; Silveira *et al.,* 1990). Yeast cells that survive in the absence of the clathrin heavy and light chains have allowed to thoroughly studying their function. *chc1Δ* and *clc1Δ* cells grow slowly, become polyploid and exhibit membrane trafficking defects (Huang *et al.*, 1997; Lemmon

et al., 1990; Payne *et al*., 1988; Silveira *et al.*, 1990), which can partially be bypassed in yeast by other transport routes. In the next sections, we will discuss the major cellular functions of clathrin in endocytic uptake, endosomal and TGN trafficking, and in cell division in yeast.

1.1.4.1. Clathrin-mediated membrane traffic pathways

Membrane traffic between structurally and functionally different compartments is essential to maintain the cellular homeostasis. Transport intermediates loaded with selected cargo are continuously generated from distinct organelles and, after travelling through a packed cytosol, fuse with the target membrane in a highly regulated manner, which involves the function of the Rab GTPases, tethering and SNARE complexes. Membrane traffic is roughly organized in the secretory and the endocytic pathways (Figure 7). The secretory pathway mainly delivers newly synthesized proteins translocated to the endoplasmic reticulum, through the Golgi complex and to the PM. In addition, transport intermediates derived from the Golgi can deliver material to other organelles, including the endosomal compartments. The endocytic pathway internalizes material from the PM, mostly targeted for degradation. Transport carriers from the PM fuse with the early endosomal compartments, which will mature to late endosomes (LE) and fuse with the hydrolytic organelles: the lysosomes in animal cells and the vacuoles, in plants and yeast. In order to maintain the organelle integrity, forward transport through the secretory and endocytic pathways requires part of the proteins and lipids to be transported back to the membrane of origin via the retrograde routes. For instance, receptors recognizing hydrolytic enzymes destined to the vacuole and to the lysosome are recycled back to the TGN, for further rounds of transport, once they have delivered their cargo. Seemingly, an important portion of the material internalized from the PM is recycled back to the cell surface. Importantly, v-SNAREs that label the origin and destination of transport intermediates need to be rapidly transported back to the original compartment to avoid loss of the compartment identity.

Traffic between the organelles of the endocytic and secretory pathways is generally mediated by tubular or vesicular carriers. In most cases, formation of these carriers implies assembly of a proteinaceous coat on the cytoplasmic face of the donor compartment membrane. Coats that sequester cargo and impose

curvature to the lipid bilayer include clathrin, COPI, COPII and the retromer complexes (Figure 7). COPI forms coated vesicles which travel from the Golgi to the endoplasmic reticulum (ER) and between Golgi subcompartments ((Orci *et al.*, 1997) and references therein), and COPII generates vesicles that travel from the ER to the *cis* face of the Golgi complex (Barlowe *et al.*, 1994; Salama *et al.*, 1993) (Figure 7). On the contrary, retromer assembly on endosomes creates membrane domains and tubules for retrograde transport from the endosomes to the TGN in

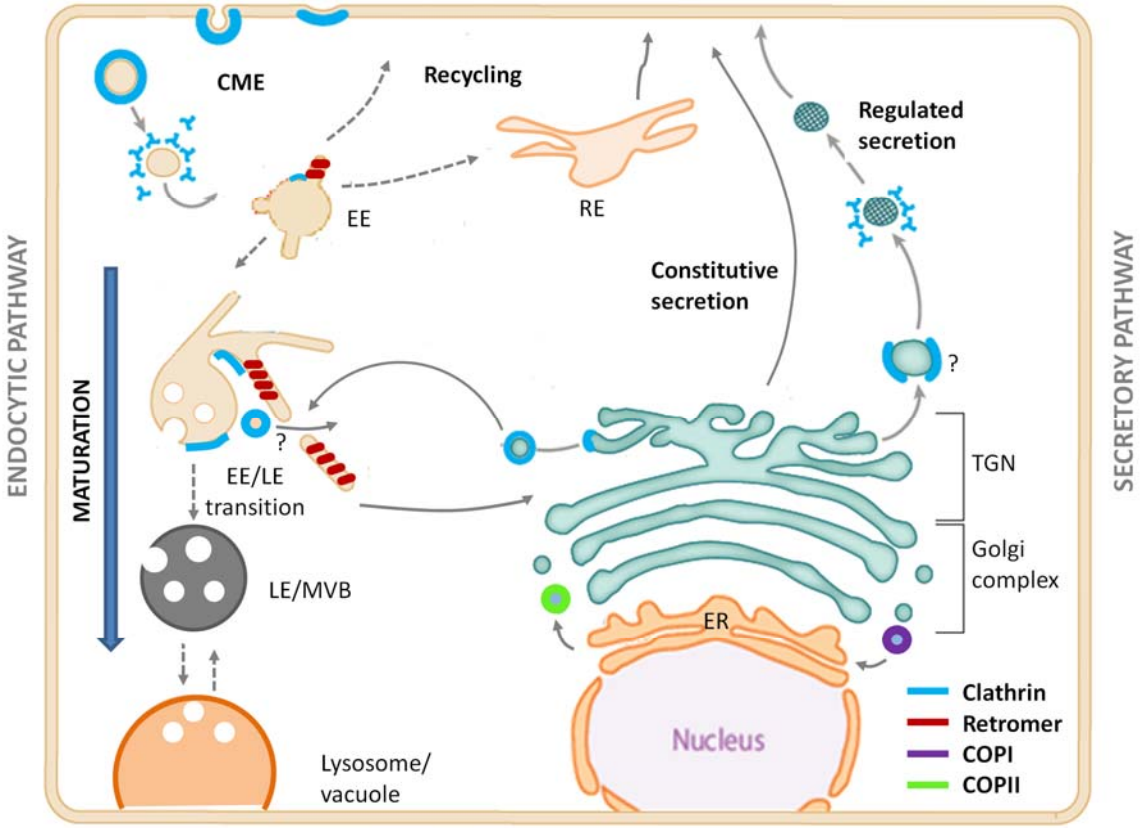

Figure 7. **Intracellular membrane trafficking pathways.** Schematic representation of the location of the different coats covering membranes (clathrin, retromer, COPI and COPII) and their role in the different cellular trafficking pathways. Solid arrows and spheres indicate trafficking events mediated by vesicle transport, whereas dashed lines show events mediated by direct fusion or fission of organelles. Clathrin forms several types of structures on the cytoplasmic face of cellular membranes. At the PM, these include CCPs and budded coated vesicles as well flat lattices (sometimes called "plaques") in the case of human cells. On the TGN, clathrin coats are observed at the ends of emanating tubules and also on CCVs. On early endosomal membranes, clathrin forms coated regions adjacent to retromer-coated regions. On late endosomal membranes, clathrin also forms a sorting patch with a bilayered appearance that initiates ESCRT component recruitment and assembly. CME: clathrin mediated endocytosis; EE: early endosome; LE: late endosome; RE: recycling endosome; MVB: multivesicular body; TGN: trans-Golgi network; ER: endoplasmic reticulum. (Figure adapted from (Brodsky, 2012; Owen *et al,.* 2004; Lemmon, 2000)).

yeast (Seaman *et al*., 1998) and mammals and also to PM in higher eukaryotes ((Burd & Cullen, 2014) and references therein) (Figure 7). Clathrin coats are the most abundant and participate in the formation of vesicles that transit from the PM to the endosomes and in the formation of CCVs that function in the anterograde and retrograde transport between the TGN and the endosomes ((Brodsky, 2012) and references therein) (Figure 7). In mammals, clathrin has also been found to cooperate in the retromer-dependent retrograde transport to the TGN (Popoff *et al.*, 2007) but whether it participates forming bona fide CCVs or even generating curvature is uncertain.

In addition to the vesicular membrane traffic, clathrin has also been implicated as a flat lattice in the ESCRT-dependent degradative pathway that brings ubiquitinated membrane proteins to the ILV of the MVB (Raiborg *et al*., 2006; Sachse *et al*., 2002) (Figure 7). The ESCRT complexes recruit ubiquitinated membrane proteins destined for degradation at the surface of EE and pack them in vesicles that bud into the lumen of the compartment (reviewed in (Hurley, 2010)), opposite to clathrin, COPI, COPII and retromer transport intermediates, which bud off from the donor compartment into the cytosol. As the EE matures to the LE via the adquisition and retrieval of material to and from its limiting membrane, the ILV accumulate and will finally be delivered to the lumen of the vacuole and the lysosome by a mechanism that probably implies the transient fusion with the LE (Huotari & Helenius, 2011). Within this pathway, clathrin does not generate vesicles but rather form membrane subdomains that accumulate ubiquitinated membrane proteins (Raiborg et al., 2006). A similar role has been proposed for clathrin in the retromer pathway (Popoff *et al.*, 2007).

Multiple specific adaptors recruit clathrin to different cellular membranes and determine the location of clathrin assembly and the type of cargo that is accumulated in the transport intermediates (Kirchhausen, 2002). The clathrin-mediated transport pathways and its molecular components have been conserved from yeast to mammals. Given its genetic amenability, *Saccharomyces cerevisiae* has proven to be an excellent model system to study of the molecular aspects of membrane traffic, providing the basis for elucidating such mechanisms in more complex organisms. In this section, the conserved roles of clathrin and adaptor proteins in the membrane traffic pathways in the yeast *S. cerevisiae* outlined before will be discussed, indicating some important mechanistic or functional

differences with higher eukaryotes. We will focus in describing the generation of transport intermediates and the roles of clathrin in protein sorting and membrane budding, most relevant to this work. A detailed description of the tethering and fusion machinery in the secretory and endocytic pathways can be found in (Bishop, 2003; Bowers & Stevens, 2005; S K Lemmon & Traub, 2000). In the last sections, specific roles of clathrin in higher eukaryotes and their relevance in human disease will be briefly discussed.

1.1.4.1.1. Clathrin-mediated endocytosis (CME) from the plasma membrane in yeast.

Endocytosis is the process whereby cells internalize part of their own PM together with samples of the extracellular material. Material destined for internalization is delivered to early endosomal compartments, from where it can either be recycled back to the PM or be transported to the late endosomal and lysosomal compartments for degradation. In mammals, endocytic cargo molecules can be internalized from the cell surface using different endocytic pathways (reviewed in (Doherty & McMahon, 2009)), but CME is the major route for selective receptor internalization. Indeed, it is the best studied and characterized membrane budding event *in vivo*.

Clathrin knockouts have been generated in various organisms, revealing a universal requirement for clathrin in endocytosis. However, considering the relatively strong evolutionary conservation of the clathrin heavy chain, it was surprising that some yeast strains harboring the deletion of *CHC1* were viable (Lemmon & Jones, 1987; Payne *et al.*, 1987), and could still endocytose, even though at a slower rate (Payne *et al*., 1988). It was hypothesized then that clathrin might not be essential for the budding step, but might play a regulatory role in yeast, or that an alternative actin-dependent, clathrin-independent internalization pathway might overcome the uptake defects in clathrin-deficient cells. Indeed, a novel clathrin-independent actin-dependent endocytic pathway was recently described (Prosser *et al.,* 2011), but its relative contribution to fluid-phase and to receptor-mediated endocytosis has not been characterized yet.

In yeast, clathrin appears to promote or stabilize the initial recruitment of endocytic coat proteins and maybe couple adaptor loading to the initiation of actin

polymerization (Kaksonen *et al*., 2005; Newpher & Lemmon, 2006; Newpher *et al.*, 2005). However, endocytic coats in cells lacking Chc1 (*chc1Δ*) can still form at reduced levels and in such situation, endocytic vesicle formation can proceed (Kaksonen *et al*., 2005; Newpher & Lemmon, 2006; Newpher *et al.*, 2005), consistent with the partial defect in endocytosis in *chc1Δ* cells (Payne *et al.*,1988). Strikingly also, the shape and the organization of the endocytic coat does not seem to change in the absence of Chc1 (Idrissi *et al.*, 2012).

Yeast lacking the clathrin light chain displays slow growth and endocytosis defects comparable to *chc1Δ* cells (Chu *et al.*, 1996; Huang *et al.*, 1997; Silveira *et al.,* 1990). In *clc1Δ* cells, Chc1 levels are reduced to 10-25% of wild type levels, and the residual Chc1 is predominantly monomeric (Chu *et al.,* 1996; Huang *et al*., 1997), revealing a role for Clc1 in the trimerization of the clathrin heavy chain, and suggesting that phenotypes exhibited by *clc1Δ* cells may result indirectly from the loss of Chc1. Overexpression of Chc1 in the *clc1Δ* increases the level of Chc1 trimers and partially improves growth and sorting defects in the late secretory and endosomal pathways but it cannot rescue the endocytic defect (Chu *et al.,* 1996; Huang *et al.*, 1997). Strikingly, overexpression of Clc1 in *chc1Δ* cells partially rescues the endocytic uptake defects but not the TGN endosomal trafficking (Huang *et al.*, 1997; Newpher *et al*., 2006), indicating that at least in yeast, the Clc1 can provide some of the clathrin function in the absence of triskelions. Specifically, overexpressing the N-terminal part of Clc1, which binds Sla2, suppresses the endocytic phenotypes of clathrin heavy chain null mutant, including progression of stalled Sla2-containing endocytic patches (Boettner *et al.*, 2011; Newpher *et al.*, 2006). In the same way, overexpression of the HIP1 (Sla2 homologue) protein-binding region of clathrin light chain causes an alteration in actin cytoskeleton structure in mammalian cells (Chen & Brodsky, 2005). These results supports the regulatory role of clathrin in endocytosis (see section 1.1.2.2.3.) (Boettner *et al.*, 2011; Chen & Brodsky, 2005; Newpher *et al.*, 2006; Wilbur *et al.*, 2008).

By contrast, in the context of multicellular organisms, clathrin seems essential (Bazinet *et al.*, 1993). siRNA has been used in some mammalian cell types to deplete the heavy chain, resulting in decreased endocytosis (Hinrichsen *et al.*, 2003; Huang *et al.*, 2004), and AP-2 membrane domains failing to curve, as assessed by EM (Hinrichsen *et al*., 2006). The data clearly suggests a structural role for clathrin in endocytic budding. Surprisingly, knocking down the clathrin light

chain in mammalian cells does not alter endocytosis (Huang *et al*., 2004). This can be due to the ability of mammalian heavy chain to trimerize in the absence of light chain (Liu *et al*., 1995), or to a non mandatory role of actin in CME in some mammalian cells where the role of the light chains coupling actin to clathrin coats might not be essential neither.

Genetic analysis of endocytic uptake in yeast has lead to the identification of more than 50 genes involved in CME (reviewed in (Boettner *et al.,* 2011)). The core components of the mammalian CME machinery have homologues in yeast and indeed, their discovery in *S. cerevisiae* anticipated their study in mammalian cells (i.e. Rvs167/endophilin, Myo5/myosin I, or Las17/WASP) (Table 3). Simultaneous live-cell two-color imaging and total internal reflection microscopy (TIRF) techniques have been particularly valuable to establish the spatio-temporal order of arrival and dissociation of the different endocytic proteins in yeast, and pioneered similar studies in mammals that showed remarkable similarities between the two cell types ((Boettner *et al.*, 2011; Merrifield & Kaksonen, 2014; Perrais & Merrifield, 2005)and references therein).

Endocytic proteins are transiently recruited in an invariable, sequential and partially overlapping manner at the cortical sites where an endocytic vesicle is being produced ((Weinberg & Drubin, 2011) and references therein). Based on differences in protein function and their dynamics at endocytic sites, the endocytic proteins have been assigned into different functional modules: the early module, the coat module (early, intermediate and late), the Wasp/Myosin module, the actin module, the scission module, and the uncoating module (Kaksonen *et al*., 2005; Stimpson *et al.*, 2009) (Table 3 and Figure 9).

Despite these similarities, significant differences have been noted. The relative importance of clathrin, specific clathrin adaptors, actin, myosin and dynamin in cargo recruitment, membrane deformation and vesicle scission differ between mammals and yeast, maybe reflecting differences in the membrane composition, the cargo internalized and/or the exposure to osmotic pressure.

Recently, the study of yeast endocytosis employing time resolved electron microscopy techniques has further define the nature of the primary endocytic profile at the PM and has provided high resolution, dynamic information about the

organization of the molecular complexes that deform the PM, not available for other budding processes in a cellular context (Idrissi *et al.*, 2008, 2012; Kaksonen *et al.*, 2005; Kukulski *et al.*, 2012). These experiments have revealed that endocytic invaginations are wide-necked (30–50 nm) tubules covered by BAR-domain proteins, surrounded by an actin matrix, and coated at the tip with a clathrin hemisphere, which moves into the cytosol as the tubular profile elongates and mature up to 200 nm in length (Idrissi et al., 2008; 2012) (Figure 8). Interestingly and contrary to yeast, mammalian cells display round, clathrin-coated budding profiles that are attached to the membrane by narrow necks (Conibear, 2010). Whether structural differences between the yeast and human clathrin are responsible for these differences is currently unknown, although recent studies suggest that a differential involvement of dynamin (GTPase that drives the pinching off of endocytic-coated vesicles at the PM in higher eukaryotes) in the process could be responsible for these morphological differences (Ferguson *et al.*, 2010).

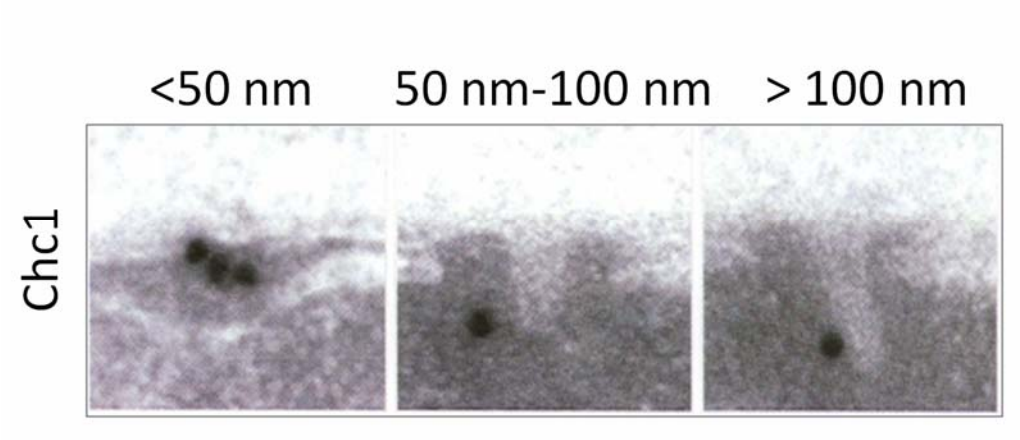

Figure 8. **Primary endocytic profiles of budding yeast**. Electron micrographs of ultrathin sections from *S. cerevisiae* showing PM-associated invaginations shorter than 50 nm, between 50 nm and 100 nm, and longer that 100 nm, decorated with immunogold particles against Chc1. (Reproduced from (Idrissi *et al*., 2008)).

The next sections will explain the current model of clathrin- and actin-dependent endocytic budding in *S. cerevisiae,* separated in five main steps: nucleation of clathrin cages, assembly of the endocytic coat, actin-driven membrane deformation, vesicle scission and coat dissociation (see Figure 9 for a scheme of the spatiotemporal and modular organization of proteins during the endocytic pathway in yeast). Similarities and differences with mammalian cells will be underlined.

Module	**Protein or complex**	**Functionally related proteins**	**Function**
Early	Ede1	Eps15	Scaffold protein
	Syp1	FCHo1/2	Endocytic adaptor Membrane curvature sensing/bending (F-BAR protein)
Early coat	Chc1/Clc1	Clathrin	Formation of clathrin cage Possible regulatory function
	yAP1801/2	AP180	Endocytic adaptor Scaffold protein that links the endocytic coat to the PM
	Pal1	-	Not known
	AP2	AP2	Endocytic adaptor
Intermediate coat	Sla2	HIP1R	Scaffold protein that links the endocytic coat to the the PM Regulation of actin dynamics (inhibits Pan1 NPA) (ANTH protein)
	Ent1/2	Epsin	Scaffold protein that links the endocytic coat to the PM (ENTH protein)
Late coat	End3	-	Scaffold protein
	Pan1	Intersectin	NPF Scaffold protein
	Sla1	Intersectin/ CIN85	Endocytic adaptor Regulation of actin dynamics (inhibits Las17 NPA)
WASP/Myosin	Las17	WASP	NPF Recruits Vrp1 to the endocytic patch

	Vrp1		Regulation of actin dynamics (co-activator of Myo5 NPA)
	Bzz1	Syndapin	Regulation of actin dynamics (relieves Sla1 inhibition on Las17) F-BAR protein
	Myo5	Myosin-I	Motor protein; NPF (requires Vrp1)
	Bbc1	-	Regulation of actin dynamics (inhibits Myo5 and Las17 NPA)
Actin	Arp2/3	Arp2/3	Actin nucleator Promotes actin filament branching
	Abp1	ABP1	NPF Regulation of actin dynamics (inhibits Las17 NPA, recruits Ark1/Prk1 kinases, and Sjl2)
	Sac6	Fimbrin	Actin filament bundling
	Scp1	Transgelin	Actin filament bundling
	Cap1/2	Capping protein	Actin filament capping at barbed ends
Amphiphysin	Rvs161/167	Amphiphysin	Membrane curvature sensing/bending Promotes vesicle scission (N-BAR protein)
	Vps1	Dynamin	Might help to promote vesicle scission
Uncoating/Disassembly	Ark1/Prk1	AAK1	Pan1 and Sla1 phosphorylation Regulation of actin dynamics (inhibits Pan1 NPA) Vesicle uncoating
	Sjl2	Synaptojanin-1	PtdIns(4,5)P_2 dephosphorylation
	Cof1	Cofilin	Regulation of actin dynamics (filament severing/disassembly)
	Aip1	Aip1	Regulation of actin dynamics (filament severing/disassembly)
	Crn1	Coronin	Regulation of actin dynamics (filament severing/disassembly)

Table 3. *Saccharomyces cerevisiae* proteins involved in CME. List of endocytic proteins functioning in CME, grouped in functional modules and including the name of their mammalian homologues or functionally related proteins and a general overview of their main molecular functions in endocytosis. NPA: nucleation promoting activity. NPF: nucleation promoting factor See text for further details.

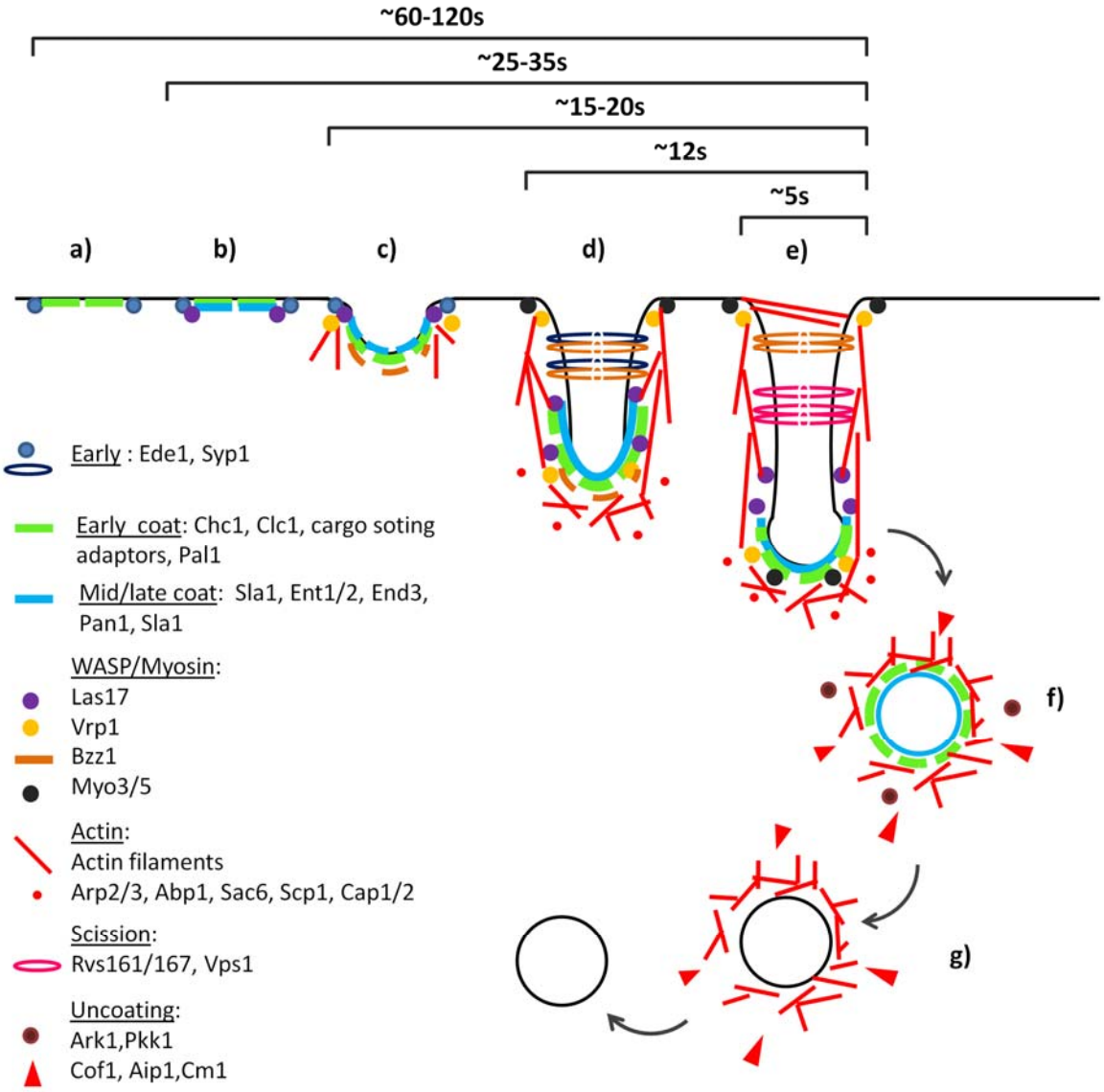

Figure 9. Model for the spatiotemporal and modular organization of proteins during the endocytic uptake from the PM in yeast. (a,b) Early factors (Syp1 and Ede1) and the early coat components (clathrin, yAP1801/2, Pal1, AP-2) are recruited to the PM during the immobile phase (a), which is followed by the ordered assembly of the mid/late coat ((b); Sla2, Ent1/2, Pan1 , End3 and Sla1). Las17 is also recruited around this time. (c,d) Shortly before the mobile phase, arrives the WASP/myosin module components (Vrp1, Bzz1) coinciding with emergence of membrane curvature(c) and initiation of the corralled movement. Then the tubular invagination elongates coincident with the accumulation of myosin-I at the base of primary endocytic profiles and with massive actin polymerization (d). (e) Once the extended tubule forms, the scission module (Rvs161/167) narrows the neck of the vesicle to promote scission together with other redundant scission mechanisms. (f) After release, the nascent vesicle is immediately uncoated by the synaptojanin and Prk1/Ark1 activities. (g) The vesicle then moves rapidly inwards, followed by disassembly of the actin cap through the action of Cof1, Aip1 and Crn1. See text for further details. (Illustration adapted from (Boettner *et al.,* 2012; Weinberg & Drubin, 2012; Idrissi *et a*l., 2012; Idrissi, 2014))

1.1.4.1.1.1. Nucleation of clathrin cages: Early module and clathrin

To date, there is no clear consensus about how endocytic sites are initiated in particular regions of the PM. In yeast, clathrin patches are assembled at the PM simultaneously with the components of the early module, composed of the Eps15 related protein Ede1 and the FCHo1 homologue Syp1, a member of the BAR domain containing protein family (Stimpson *et al.*, 2009) (see section 1.1.3.1.). Cargo adaptors then progressively concentrate on the endocytic patch (Boettner *et al.,* 2009; Stimpson *et al.,* 2009). Yeast deficient in Ede1 display defects in both fluid phase and receptor mediated endocytosis (Gagny *et al.*, 2000), contain few endocytic patches, and fail to recruit Ent1 (Stimpson *et al.*, 2009), which support Ede1 as a initiator of endocytosis and recruiter of other adaptors. Ede1 is not considered a bona fide endocytic coat component since it disappears from endocytic sites prior to clathrin and does not move inward with the vesicle that invaginates. Syp1 binds to Ede1, and deletion of *SYP1* causes a defect in the polarized distribution of endocytic patches, rather than in the overall number, indicating a role in localization instead of in initiation of endocytic sites (Stimpson et al., 2009). In addition, Syp1 has a role in the constriction of the invagination neck (Idrissi *et al.,* 2012). Besides, it appears to act as an specific adaptor for uptake of the PM stress sensor Mid2 (Reider *et al.*, 2009).

What defines recruitment of clathrin and the early module at specific sites is unknown and it might imply the interaction with certain cellular structures such as the septin ring (Stimpson *et al.*, 2009), the cortical ER (Stradalova *et al.*, 2012) or the eisosomes (structured PM subdomains involved in signaling) (Walther *et al.*, 2006), a high concentration of cargo (Carroll *et al.*, 2012) or the local production of certain lipid species such as PtdIns(4,5)P_2 (Antonescu *et al*., 2011; Boucrot *et al.,* 2009). In mammals, clathrin patches are also assembled at the PM together or slightly after the FCHo1 family members (Cocucci *et al.,* 2012; Henne *et al.*, 2010). However, knocking down FCHo1 proteins does reduce the number of clathrin coated pits, so they do have a role in initiation of coat assembly (Henne *et al*., 2010). The clathrin patches seem to have a transient nature unless they coalesce with cargo and adaptor clusters that diffuse in the plane of the PM (Ehrlich *et al.*, 2004). PtdIns(4,5)P_2 binding to clathrin adaptors at the PM is essential for adaptor recruitment and cargo interaction (Antonescu *et al.,* 2011).

1.1.4.1.1.2. Assembly of the endocytic coat: cargo clathrin adaptors and linkers to the actin cytoskeleton

Immediately after Ede1, Syp1 and clathrin, arrive the cargo adaptors AP-2 and yAP180 proteins (see section 1.1.3.1.) and Pal1, whose function remains unknown (Carroll *et al.*, 2012). Yeast lacking both AP180 homologues do not display obvious endocytic defects (Huang *et al.*, 1999), suggesting functional redundancy possibly with adaptors Ent1/2 (Maldonado-Báez *et al.*, 2008). However, yAP1081/2 also seem to play unique roles in the recruitment of certain cargo such as the v-SNARE Snc1 (Burston *et al*., 2009). Similarly, mutations in yeast AP-2 subunits do not have a detectable defect on the α-factor induced uptake of the GPCR (G-protein coupled receptor)Ste2 or the fluid phase endocytic marker Lucifer yellow (Huang *et al*., 1999; Yeung *et al*.,1999b), but it has a unique role recruiting specific cargo (Carroll *et al.*, 2009).

Cargo is proposed to have a role in regulating the transition point of endocytic sites from the early stages to later stages of the vesicle formation, so that the process is paused until cargo loading is completed (Carroll *et al*., 2012). Although clathrin has classically been considered as a scaffold for cargo adaptors and a driving force for membrane invagination, in *S. cerevisiae*, clathrin might rather have a regulatory role as discussed, being initial membrane bending independent of clathrin recruitment but presumably dependent on membrane-sculpting BAR and ENTH domains held by some scaffolding proteins, such as Ede1 or Sla1 (Idrissi *et al.*, 2012), or by lateral interactions among the adaptors (Skruzny *et al.*, 2012).

After clathrin and the early adaptors, arrives the intermediate coat module, which comprises the proteins Sla2 (HIP1R) (see section 1.1.3.2.) and the yeast epsins Ent1 and Ent2 (Carroll *et al.*, 2012; Kaksonen *et al.*, 2003; Toret *et al*., 2008) (see section 1.1.3.1.). Both Sla2 and Ent1/2 bind PtdIns(4,5)P_2 through their ANTH and ENTH domains, respectively, being thought to act as linkers between endocytic proteins and the lipid bilayer (Aguilar *et al.*, 2003; Sun *et al.*, 2005). Sla2 and Ent1 also bind actin filaments and its actin binding activity is regulated by phosphoinositides and clathrin (Boettner *et al.,* 2011; Skruzny *et al.*, 2012), indicating that they might be essential regulators of the actin polymerization at endocytic sites by controlling the recruitment an anchorage of short actin filament seeds, needed for Arp2/3 dependent actin polymerization (Skruzny *et al*., 2012)(see section 1.1.2.2.3.). A

role for the N-terminal domain of clathrin regulating HIP1R binding to actin has also been demonstrated in mammalian cells (Wilbur *et al.*, 2008). Yeast *ent1Δ ent2Δ* are inviable, due to an independent role for the ENTH domain in cell polarity (Aguilar *et al.*, 2006), and *ent1Δ ent2Δ* cells expressing just the ENTH domain are endocytically competent, consistent with their functionally redundancy with yAP1081/2 adaptors (Maldonado-Baez *et al.*, 2008).

Subsequent to the intermediate coat recruitment, the late coat module composed of End3, Pan1, and Sla1 arrives (Carroll *et al*., 2012; Kaksonen *et al.,* 2003; Kaksonen et al., 2005; Toret *et al.*, 2008). The late coat module is thought to act as a complex to adapt, scaffold and regulate actin at endocytic sites, similar to intersectin in mammals (Qualmann & Kessels, 2002). End3 is essential for endocytosis (Benedetti *et al.,* 1994; Raths *et al.,*1993), and via its two EH domains might interact with cargo adaptors and other endocytic proteins (Howard *et al.,* 2002; Suzuki *et al.*, 2012). Actually, mutation of the End3 EH domains causes a defect in coat maturation and endocytic internalization (Suzuki *et al*., 2012). Pan1 has actin NPF activity (Duncan *et al.,* 2001) but its most important role may be to serve as a scaffold to recruit other proteins to endocytic sites (Miliaras *et al.,* 2004). Similarly, Sla1 is a multifunctional cargo-sorting adaptor/scaffold that also functions as a regulator of actin dynamics at the endocytic patch (see section 1.1.3.1. and next section 1.1.4.1.1.3.). Cells lacking Sla1 are impaired of NPxFD-mediated endocytosis of α-factor receptor (Howard *et al.*, 2002). It has been proposed that the NPxFD/Sla1 system is specialized for proteins that constitutively recycle between the cell surface and internal compartments, since all Sla1-specific cargo cycle between the PM, the endosomes and the TGN (Piao *et al.*,2007). The stability of the Pan1/End3/Sla1 complex is regulated by the Ark1/Prk1 kinases (AAK1), which phosphorylate the complex, promoting disassembly (Toret *et al*., 2008; Zeng *et al.,* 2001).

1.1.4.1.1.3. Actin-driven membrane deformation

Together with the coat component, Las17 (homologue of mammalian WASP) is recruited to the PM (Kaksonen *et al.*, 2003) but its NPF activity is inhibited by the earlier arriving proteins Syp1 and Sla1 (Boettner *et al.,* 2009; Rodal *et al.*, 2003), that co-localize with Las17 at the ultrastructural level at this initial phase (Idrissi *et al.*, 2008; 2012). Vrp1 (WIP) and Bzz1 (a syndapin related protein) arrive to the

endocytic patch about 10 seconds after Las17 recruitment (Sun *et al.,* 2006). Their arrival is coincident with the initiation of an actin-dependent corralled movement of the endocytic coat (Kim et al., 2006; Y. Sun et al., 2006) and with the initial bending of the PM (Idrissi *et al.*, 2012), thus indicating that the early and the coat modules remain flat until this stage, and that initiation of actin polymerization is tightly coupled to the emergence of membrane curvature (Idrissi *et al.*, 2012; Kukulski *et al.*, 2012). Whether actin is required for initial membrane bending is still controversial but it certainly contributes to its stabilization and to the elongation of the endocytic invaginations (Idrissi *et al.*, 2012; Idrissi & Geli, 2014; Kukulski *et al.*, 2012). Bzz1 bears an F-BAR domain, which is predicted to recognize membrane curvature, and it has been shown to release the Sla1 inhibition on Las17 (Sun *et al.*, 2006). Thus, it has been suggested that initial membrane curvature might recruit Vrp1 and Bzz1, which then will initiate actin polymerization at sites of endocytic budding (Idrissi *et al.,* 2012). Las17 and Pan1 initially localize on the endocytic coat, which covers the tip of the endocytic invaginations (Idrissi *et al.*, 2008), and they are thought to initiate actin polymerization at endocytic sites (Galletta & Cooper, 2009; Sun *et al.*, 2006) to form an actin cap (Idrissi et al., 2012; Sun *et al.*, 2006) crosslinked by the the Arp2/3 complex (Svitkina & Borisy, 1999), Abp1 (which stabilizes Arp2/3 dependent branching, similar to the mammalian cortactin) (Goode *et al*.,2001) and the yeast fimbrin Sac6 (Idrissi *et al.,* 2012). Together with the transgelin homologue Scp1 (actin filament bundling and crosslinking proteins) (Gheorghe *et al.*, 2008), and capping proteins Cap1/Cap2 (which block the actin filament barbed ends, preventing further elongation of actin filaments) (Loisel *et al.*,1999) the Arp2/3 complex, Sac6 and Abp1 compose the endocytic actin module (Kaksonen *et al*., 2005). Mutations on components of this module do not affect actin assembly, but impair productive internalization of the coat, indicating that the formation of a properly built actin network is essential for driving membrane bending and vesicle scission (Kaksonen *et al*., 2005).

The type-I myosin Myo5, an actin-dependent molecular motor (Sun *et al.,* 2006) and potent NPF (Geli *et al.,* 2000; Lechler *et al*., 2001; Sun *et al.*, 2006) similar to Las17 (Rodal *et al.,* 2003) , is recruited to the endocytic site about 10 seconds after Vrp1 and Bzz1, coinciding with the burst of massive actin polymerization that drives the growth of the endocytic tubular profiles from 70 to about 200 nm before fission (Idrissi *et al.,* 2008, 2012; Sun *et al.*, 2006, Kaksonen 2003). Both, the

motor and nucleation promoting activities of Myo5 are strongly required for the elongation of the tubular endocytic invaginations (Galletta *et al.,* 2008; Idrissi *et al.*, 2012; Sun *et al*., 2006). Myo5 colocalizes at the base of invaginations longer than 70 nm (Idrissi *et al.,* 2008) and together with the WIP homologue Vrp1, is thought to promote the appearance of actin filaments with barbed ends facing the PM, which can be pushed away, off from the PM, by its motor activity (Idrissi et al., 2008, 2012; Sun *et al.*, 2006). Pushing away the endocytic actin cap, firmly attached to the endocytic coat by Ent1 and Sla2, is thought to drive elongation of the endocytic invaginations (Idrissi & Geli, 2014).

Thus, actin assembly is essential for yeast endocytosis under normal growth conditions, providing the force necessary for membrane deformation (Idrissi *et al*., 2012; Kaksonen *et al.*, 2003) and probably also for scission (Kishimoto *et al.,* 2011) and for moving the newly formed vesicles away from the PM (Kim *et al.*, 2006). By contrast, different studies suggest that actin is not absolutely required for budding of CCVs in mammalian cells under osmotic support (Saffarian *et al*., 2009; Yarar *et al.,* 2005). The relative contribution of actin in CME seems to vary depending on the tension applied to the membrane (Boulant *et al.,* 2011). Consistently also, providing osmotic support to the yeast cells relaxes the actin dependency for endocytosis (Aghamohammadzadeh & Ayscough, 2009).

1.1.4.1.1.4. Vesicle scission

A few seconds before the endocytic invaginations reach their maximal length, the yeast amphiphysins Rvs161 and Rvs167 arrive. TREM (Time Resolved Electron *Microscopy)* has demonstrated that fission occurs half way during the 10 second life span of Rvs167 (Kukulski *et al.*, 2011). Rvs161 and Rvs167 bear N-Bar domains, which are predicted to recognize and stabilize highly curved membranes (Frost *et al.,* 2009) (see section 1.1.3.3.). They localize at the invaginations neck (Idrissi *et al*., 2008) where they may contribute to narrow it (Kishimoto *et al.,* 2011). However, genetic and fluorescence microscopy experiments suggest that the yeast amphiphysins are not the only molecules involved in fission, as null mutations of *RVS161* or *RVS167* causes a defect in vesicle scission only in 25% of the endocytic patches (Kaksonen *et al.*, 2005; Kishimoto *et al.,* 2011). In higher eukaryotes, the GTPase dynamin is required for the scission of CCPs from the PM (Ungewickell & Hinrichsen, 2007; van der Bliek & Meyerowitz, 1991). In yeast, the dynamin-like

protein Vps1, is also recruited to endocytic patches (Smaczynska-de Rooij *et al*., 2010) but its deletion only cause limited effects on vesicle scission from the PM, most likely due to functional redundancy with other scission machineries (Mishram *et al.,* 2011; Nannapaneni *et al.*, 2010; Smaczynska-de Rooij *et al*., 2010, 2012). Experimental evidence suggest that actin polymerization, the type I myosins and the hydrolysis of PtdIns(4,5)P_2 by the synaptojanins also contribute to membrane scission (Ferguson *et al.*, 2010; Jonsdottir & Li, 2004; Kishimoto *et al.*, 2011; Singer-krüger *et al.*, 1998; Stefan *et al.*, 2005). In addittion, theoretical studies have led to the proposal that generation of a lipid phase boundary between the PtdIns(4,5)P_2 protected by the BAR-domain proteins and PtdIns generated by PtdIns(4,5)P_2-5-phosphatase Sjl2 (yeast synaptojanin) (see section 1.1.4.1.1.4.) might also contribute to squeeze the endocytic profile (Liu *et al.*, 2009).

1.1.4.1.1.5. Coat dissociation

Once having pinched off from the PM, the internalized vesicle undergoes coat and actin disassembly. Abp1 recruits coat disassembly factors such as the PtdIns(4,5)P_2 phosphatase Slj2 and the Ser/Thr protein kinases Ark1/Prk1 (Cope *et al.*, 1999; Stefan *et al.,* 2005) (see section 1.1.3.3.). The Sjl2 activity hydrolyzes PtdIns(4,5)P_2, reducing the affinity of coat components that have PtdIns(4,5)P_2-binding domains such as Sla2, yAP1801/1802 or Ent1/2 for the membrane (Sun *et al.*, 2007; Toret *et al.*, 2008). In addition, Ark1/Prk1-mediated phosphorylation of the coat proteins Sla1 and Pan1 disrupts their interaction, leading to their disassembly from the vesicle (Toret *et al.*, 2008; Zeng *et al*., 2001). Prk1 phosphorylation may also negatively regulate actin assembly by deactivating Pan1 at the end of internalization. In fact, inhibition of Ark1/Prk1 activity results in an accumulation of Sla1- and actin-labeled endocytic vesicles (Sekiya-Kawasaki *et al*., 2003). On the contrary, the major mammalian homologue of Ark1/Prk1, AAK1, promotes endocytosis by phosphorylating the μ-subunit of AP-2, increasing the adaptor's affinity for membranes and cargo-sorting motifs (Ricotta *et al.,* 2002). The related kinase GAK, also phosphorylates AP-2 μ-chains, but it functions in the uncoating of clathrin coats during endocytosis through its auxilin domain (Lee *et al.*, 2006). Yeast also has an auxilin, Swa2, but it does not seem to be essential for endocytosis (Toret *et al.*, 2008) (see section 1.1.2.2.3. and 1.1.2.3.).

Other factors involved in actin disassembly, such as cofilin, Aip1 and coronin are also recruited about this time (Lin *et al.*, 2010). Cofilin severs ADP-bound actin filament (Moon *et al.*, 1993) and Aip1 caps the barbed ends generated by cofilin to prevent its further elongation and/or filament re-anealing (Balcer *et al.*, 2003). Coronin is an actin bundling protein that synergizes with Cof1 and Aip1 to disassemble the endocytic actin network (Gandhi *et al*., 2010). The signals that turn on or recruit uncoating factors are unclear, but membrane curvature, actin filaments and lipid composition are likely candidates.

1.1.4.1.2. Intracellular clathrin-dependent endocytic pathways

As already commented, clathrin coats are also involved in the anterograde and retrograde transport between TGN and endosomes and between endosomes and vacuoles/lysosomes ((Lemmon & Traub, 2000) and references therein). However, these pathways in general and the role of clathrin plays in them in particular, have not been so well characterized as CME from the PM. So, in some cases the molecular function of clathrin is uncertain

Clathrin has a role in TGN-endosome traffic of the α-factor processing enzymes Kex2 (Chu *et al*. , 1996; Huang *et al.,* 1997; Payne & Schekman, 1989; Seeger & Payne, 1992) and dipeptidyl aminopeptidase A (DPAP A, also known as Ste13) (Deloche *et al*., 2002; Seeger & Payne, 1992) (Figure 10). The α-factor is the matting pheromone secreted by *Mat***α** cells, which is recognized by the GPCR Ste2 expressed in cells of the opposite matting type (*Mat***a**) (Bardwell *et al*. , 1994). The α-factor is synthesized as a large peptide that is glycosylated as it moves through the Golgi apparatus, and it is cleaved to its mature form by the Kex2 TGN protease (Julius *et al.*, 1983; Julius *et al.*, 1984). Kex2 is maintained through an efficient clathrin-dependent cycling between the TGN and endosomes (Payne & Schekman, 1989; Seeger & Payne, 1992). Once processed, the α-factor is secreted to the media and causes the matting response in *Mat***a** cells ((Bardwell *et al.*, 1994) and references therein). Defects in Kex2 localization can be observed indirectly in assays that test the maturation of secreted α-factor or by the vacuolar degradation of Kex2 or its miss-targeting to the PM (Payne & Schekman, 1989; Seeger & Payne, 1992).

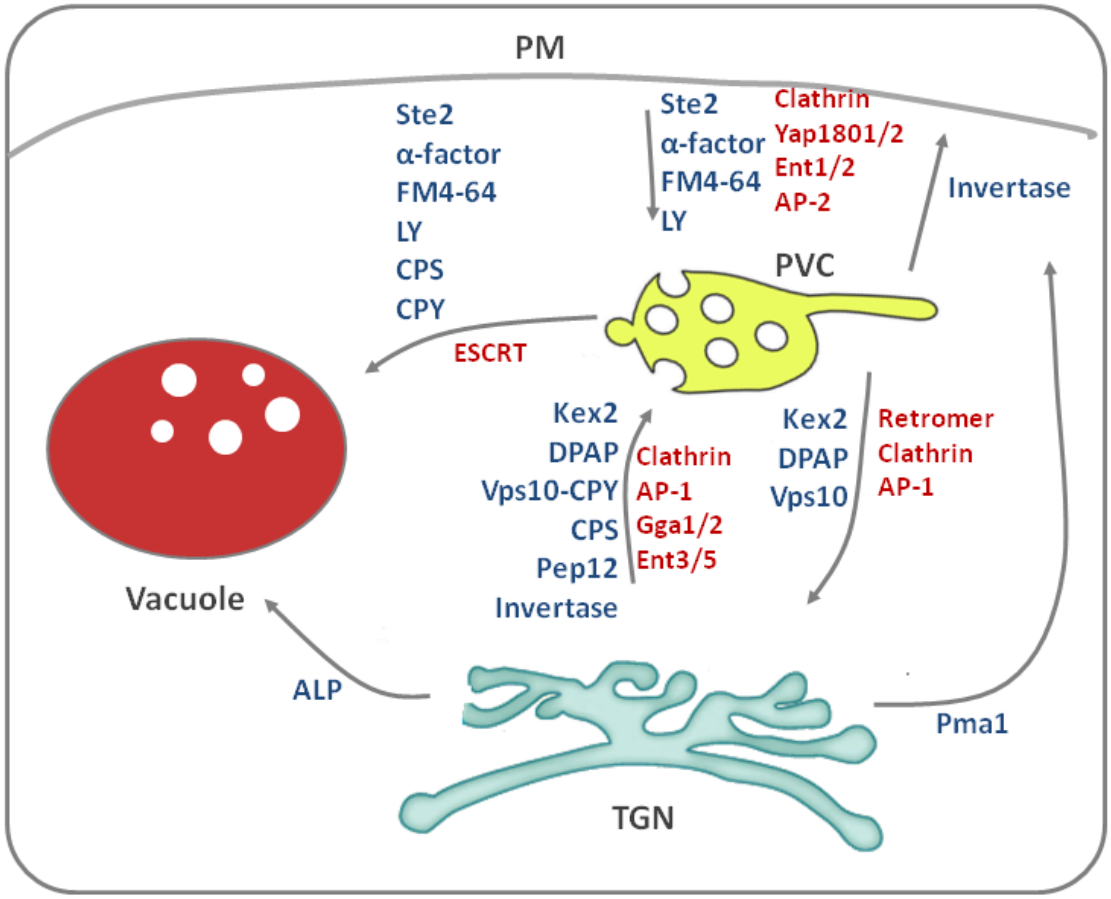

Figure 10. **Cargo travelling through the endosomal and secretory system in *Saccharomyces cerevisiae* and some molecular machinery implicated**. The cargo travelling through the distinct compartments is colored in blue and some representative sorting membrane budding machinery working in each pathway is colored in red..The early and late endosomes are shown together as the prevacuolar compartment (PVC) for simplicity. PM: plasma membrane; TGN: trans-Golgi network; ESCRT: Endosomal Sorting Complexes Required for Transport; ALP: alkaline phosphatase; CPS: carboxypeptidase S; CPY: carboxypeptidase Y, FM4-64: N-(3-triethylammoniumpropyl)-4-(p-diethylaminophenyl-hexatrienyl) pyridinium dibromide, marker used for the PM and internalized lipids; LY: Lucifer Yellow, marker for fluid phase endocytosis.

chc1Δ and *clc1Δ* cells secrete an immature inactive form of the α-factor pheromone (Chu *et al*., 1996; Huang *et al.,* 1997; Payne & Schekman, 1989; Seeger & Payne, 1992), and Kex2 is secreted to the cell surface in clathrin mutants (Payne & Schekman, 1989; Mary Seeger & Payne, 1992) consistent with a role of clathrin in TGN-endosome trafficking. The observation that overexpression of Chc1 in *clc1Δ* cells partially improved TGN retention of Kex2, whereas overexpression of Clc1 in

chc1Δ cells does not (Huang *et al.,* 1997), indicates that, unlike for the endocytic uptake, clathrin plays an structural role the TGN endosomal trafficking pathways.

Care must be taken when analyzing the trafficking defects of clathrin null cells. CPY (carboxypeptidase Y) is a vacuolar hydrolase synthesized as a precursor and delivered to the TGN, where it binds its receptor Vps10 (analogous to the M6P-R in mammalian cells) to be transported in CCV to endosomes (Marcusson *et al.*, 1994). Upon dissociation from Vps10 in the acidic endosomal compartment, CPY continuous its travel to the vacuole to be proteolytically cleaved and activated, whereas Vps10 goes back to the TGN (Cooper & Stevens, 1996; Marcusson *et al*., 1994) (Figure 10). Surprisingly, maturation of newly synthesized vacuolar CPY appeared normal in *chc1Δ* and *clc1Δ* cells (Payne *et al.*, 1988). However, CPY was secreted by a thermosensitive clathrin mutant *chc1-521,* immediately after shift to non-permisive temperature, indicative of a defect in TGN sorting. After sustained incubation of the *chc1-521* strain at restrictive temperature, cells got adapted to the lack of clathrin, being able to process CPY in the vacuole (Mary Seeger & Payne, 1992). This was found to be a consequence of the Vps10 receptor being missorted to the PM, from where it can be recycled to the TGN and endosomes by endocytosis, indicating that some of the retrograde pathways and the endocytic uptake are not completely impaired (Deloche & Schekman, 2002). These results supported though a role for clathrin in sorting proteins between the TGN and endosomes, which is conserved in mammalian cells (Traub, 2005).

1.1.4.1.2.1. Gga1/2, Ent3/5 and AP-1- dependent forward traffic from TGN to the endosomes

The TGN has an important role in protein sorting. Newly synthesized proteins, cargo receptors and SNAREs travel through ER and Golgi via to COPI and COPII coated vesicles ((Brandizzi & Barlowe, 2013) and references therein). Once they reach the TGN, proteins can travel in different membrane-enclosed carriers to several possible destinations: the extracellular space, regulated secretory vesicles, endosomes and vacuoles (Gu *et al*., 2006). Direct secretion from the TGN to the cell surface, or direct transport to the vacuole, does not involve clathrin (Payne *et al.*, 1987; Seeger & Payne, 1992). The latest pathway, is named the ALP pathway in yeast because of its most studied cargo protein, the alkaline phosphatase, which require the AP-3 adaptor complex but not clathrin (Cowles *et al.*, 1997; Stepp *et*

al., 1997). By contrast, clathrin is involved, together with adaptors AP-1, Gga1/2 and Ent3/5 and the dynamin-like GTP-ase Vps1, in the anterograde transport from TGN to EE or LE of different cargo ((Lemmon & Traub, 2000) and references therein)(Figure 10).

Deleting the *GGA* genes or the dynamin-like protein Vps1, results in most of the CPY being secreted to the extracellular media in the pseudomature form (Finken-Eigen *et al*., 1997; Hirst *et al*., 2000; Rothman & Stevens, 1986). Consistent also with a role in TGN to endosome trafficking of the Gga1/2 proteins and Vps1, cells bearing mutations in the genes encoding these proteins secrete α-factor as an inactive precursor form, and Kex2 is missorted to the cell surface from where it reaches the vacuole via the endocytic pathway (De *et al.*, 2013; Mullins & Bonifacino, 2001; Nothwehr *et al.,* 1995). Further, Pep12, a t-SNARE required for vesicular intermediates traveling between the Golgi apparatus and the vacuole, through LE (Figure 10), is missorted to an EE and do not progress to the LE in cells lacking *GGA1* and *GGA2* (M. W. Black & Pelham, 2000).

Deletions of the yeast AP-1 subunits, individually or combined with each other, result in no growth, endocytosis or α-factor maturation defects. However, in combination with the *chc1-521* or *chc1Δ* mutations, deletion of the AP-1 subunits specifically exacerbated the α-factor maturation defects without further affecting endocytosis (Phan *et al*., 1994). Deletion mutants of AP-1 subunits also aggravated the growth and trafficking phenotypes of *gga1/2* TGN adaptors mutants, suggesting that AP-1 and Gga1/2 proteins may control parallel pathways out of the late Golgi (Costaguta *et al*., 2001; Hirst *et al*., 2001).

Yeast deletion mutants on *ENT3* or *ENT5* genes do not cause trafficking defects on their own, but the simultaneous deletion of both genes decreases clathrin localization to the TGN and leads to defects on α-factor and CPY maturation (Duncan *et al.* , 2003), consistent with a redundant role of these proteins in TGN to endosome traffic. Some evidence also suggests a role for Ent3 in cargo selection for Gga-mediated transport pathway (Chidambaram *et al.,* 2004). Ent3 is able to recognize multiple SNAREs involved in fusion at LE, supporting its function as an adaptor that direct SNARE into Gga-containing CCV for transport to LE (Chidambaram *et al.,* 2004).

As already described, transport from the late Golgi to endosomes requires clathrin and the clathrin adaptors AP-1, Gga1/2 and Ent3/5. However, how they relate to each other at the molecular level in TGN CCV formation has not been clearly defined. Given the differential transport defects on different cargos upon impairing Ggas or AP-1 functions, it was proposed that Ggas and AP-1 function in distinct parallel pathways, or that they had different cargo selectivity working together to form one vesicle type in the TGN-endosome pathway (Boman, 2001). However live-cell imaging experiments support a model whereby two sequential waves of clathrin originate at the TGN with different adaptors that are separated in time and space (Daboussi *et al.*, 2012) (Figure 11). Gga2 assembles first together with Arf1 at the TGN membrane, recruiting Ent3 and a minor population of Ent5, constituting the first wave (Daboussi *et al*., 2012). Ent3 binds SNAREs involved in targeting/fusion to LE, thereby specifying the destination of Gga-enriched CCVs (Chidambaram *et al.,* 2004). Arf1 Gga-enriched coats stimulates Pik1 activity and increases PtdIns(4)P synthesis at the TGN (Audhya *et al.*, 2000), promoting assembly of AP-1/Ent5 coats, recruited in the second wave (Daboussi *et al*., 2012). AP-1 enriched CCVs would mediate TGN-to-EE transport, whereas Ggas and Ent3 would mediate traffic to the late endosomal compartments (Daboussi *et al.*, 2012). Thus, these results suggest that clathrin coats forming at the TGN consisting of one or other type of adaptor, would be enriched with specific cargo and based on incorporation of targeting/fusion proteins will fuse with different donor membranes (Daboussi *et al.,* 2012). It has been proposed that Gga enriched CCV would transport proteins from the TGN directly to LE, whereas AP-1 enriched CCV would act to transport proteins from the TGN to EE and/or to retrieve proteins back to the TGN ((Daboussi *et al*., 2012) and references therein).

Coated vesicle scission from TGN for the CPY and ALP pathways is carried out by the dynamin-like GTPase Vps1 (Finken-Eigen *et al.*, 1997; Rothman & Stevens, 1986; Wilsbach & Paynel, 1993). Cells lacking Vps1 however, are able to transport proteins to the vacuole through the PM (Nothwehr *et al.,* 1995).

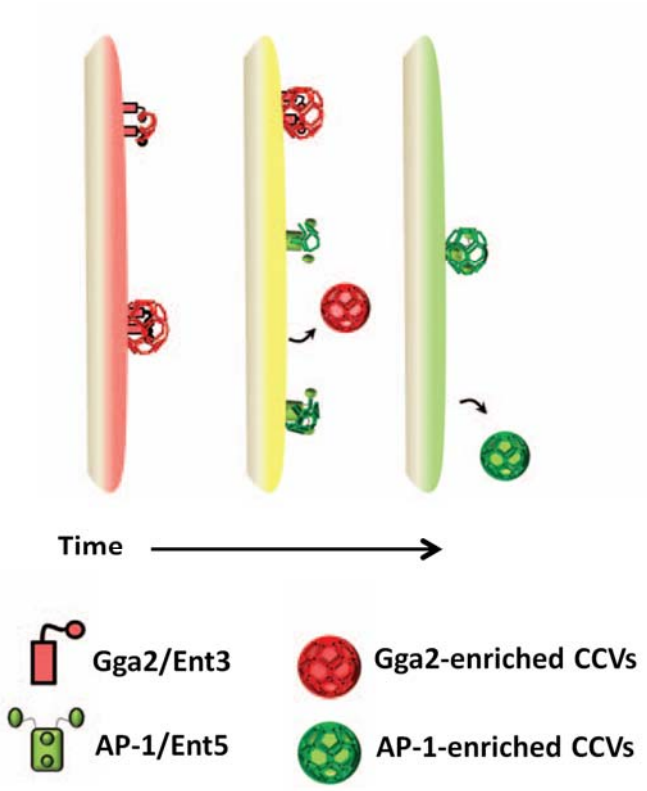

Figure 11. Model for the sequential adaptor-enriched clathrin-coated vesicle formation at the TGN. Initially, low PtdIns(4)P concentrations produced by Pik1 (previously recruited by Arf1 and Frq1 favor recruitment of Gga/Ent3 proteins and assembly of Gga-enriched CCV without significant AP-1 recruitment. As PtdIns(4)P levels increase by further recruitment of Pik1, Gga CCVs mature and concomitantly AP-1/Ent5 is recruited, initiating formation of distinct AP-1-enriched CCV (Figure taken from (Daboussi *et al*., 2012)).

1.1.4.1.2.2. Endosome-TGN retrograde transport

As discussed, the most accepted model for transport along the endocytic pathway postulates that once the incoming vesicles from the PM fuse with each other and with preformed EEs, the compartment starts maturing to progressively acquire the characteristics of the LE (Huotari & Helenius, 2011). The LE will then fuse with the vacuoles or the lysosome and deliver its luminal content for degradation, including the ILV (Huotari and Helenius, 2011). Endosomal maturation is accompanied by the loss or Rab5/Vps21 GTPases enriched subdomains and the progressive acquisition of Rab7/Ypt7, by the conversion of the CORVET to the HOPS tethering complexes and by the loss or acquisition of different t-SNAREs (Pep12 in LE in

yeast and Vam3 in vacuolar membranes), which altogether define the subset of organelles and transport intermediates that can fuse with the maturing compartment ((Balderhaar & Ungermann, 2013; Huotari & Helenius, 2011) and references therein). Endosomal maturation is also accompanied by the acidification of the lumen of the organelle from approximately pH6 to 5, a change in morphology that implies the loss of tubular extension and the accumulation of ILV, the conversion of PtdIns(3)P to PtdIns(3,5)P_2 and the activation of certain ion transporters, including calcium channels (reviewed in (Balderhaar & Ungermann, 2013; Huotari & Helenius, 2011)).

Endosomal maturation requires the retrieval of material from the limiting membrane of the endosomes, either by retrograde routes to the PM and the TGN or via the formation of ILV by the ESCRT-0, I, II and III complexes (Huotari & Helenius, 2011). In mammals, recycling to the PM can use a fast pathway controlled by the Rab4 GTPase that involves retromer and WASH-induced Arp2/3-dependent actin polymerization and which might also require clathrin (Temkin *et al.*, 2011). In addition, proteins can be diverted to a slower recycling pathway controlled by Rab11, which involves transport to the recycling endosomes ((Grant & Donaldson, 2011) and references therein). No Rab4 or Rab11 homologues have been described in yeast and consistently, the main retrograde transport route to the PM seems to imply the retrograde traffic to the TGN (Pelham, 2002). It is known that retrograde traffic from the endosomes to the TGN in yeast and mammals is dependent on retromer, AP-1 and clathrin, but how clathrin and retromer relate to each other at this point is really not understood (Bonifacino & Rojas, 2006) (Table 5). AP-1 and clathrin either form bona fide CCV that carry certain cargo to the TGN previous to retromer budding or in parallel pathways and/or they form platforms to concentrate cargo for retromer transport carriers (Bonifacino & Rojas, 2006). In addition, bilayered clathrin plaques associated to the ESCRT-0 complex have been observed on endosomes in mammalian cells (Sachse *et al.*, 2002). The bilayered clathrin plaques are thought to generate membrane subdomains implicated in the recruitment of ubiquitinated membrane proteins destined for internalization (Raiborg *et al*., 2006; Sachse *et al*., 2002). Even though clathrin plaques have not been visualized in yeast, the ESCRT-0-clathrin interaction seems to be conserved (Bilodeau *et al*., 2003). In the next sections the role of

clathrin in endosomal retrograde traffic to the TGN and in the degradative pathway will be discussed.

1.1.4.1.2.2.1. AP-1 dependent retrograde traffic from the endosomes to the TGN.

AP-1 and clathrin have a clear role in retrograde transport. In mammals, AP-1 and clathrin are required to retrieve CI-M6PR (cation-independent mannose 6-phosphate receptor) (Meyer *et al*., 2000), and clathrin, epsinR and dynamin are needed for retrieval of Shiga toxin (Lauvrak *et al.*, 2004). Indeed, mice knockouts of either the μ1 or γ1 genes of AP-1 result in embryonic lethality, but mutant fibroblasts from μ1A-/- mice are viable and exhibits defects of the CI-MPR traffic from endosome to TGN (Meyer *et al*., 2000).

In yeast, AP-1 and clathrin are required for the transport of the t-SNARE Tgl1 (t-SNARE affecting a late Golgi compartment), the chitin synthase 3(Chs3) and DPAP-A form EE to the TGN (Valdivia *et al.*, 2002). These findings imply that AP-1 can assemble on different membranes (TGN or endosomes) to sort specific cargo, presumably into CCV, and send them to different destinations (endosomes or TGN). Recruitment of cargo into CCV at different sites could depend on the affinity of sorting signals for AP-1 or on the participation of different auxiliary proteins.

1.1.4.1.2.2.2. Clathrin in the retromer pathways

The retromer was first identified in yeast, and functions in retrieval to TGN of cargo such as the CPY receptor Vps10 (Seaman *et al.*, 1997; Seaman *et al.,* 1998). It comprises five subunits organized in two subcomplexes: 1) The cargo-selective subcomplex formed by Vps26, Vps29 and Vps35, which recruits cargo via an interaction between Vps35 and a sorting motif in the cytoplasmic tail of cargo such as Vps10 and 2) the tubulating SNXs (sortin nexins) Vps5 and Vps17, which dimerize via interactions in their C-terminus (Seaman *et al*., 1998) (Figure 12). The mammalian retromer, which functions in retrograde transport of acid-hydrolase receptors (such as the M6PR), comprises an orthologous first subcomplex, formed by two isoforms of Vps26, Vps29 and Vps35 and a second subcomplex that comprises Snx1, Snx2 (both orthologous to Vps5) and Snx5 and Snx6 (orthologous to Vps17) (Seaman *et al.*, 2013). All the SNXs belong to the SNX-BAR subfamily capable of sensing and driving membrane curvature forming membrane tubules (van Weering *et al.*, 2010). The SNXs comprise an N-terminal phosphoinositide-

binding domain that interacts the early endosomal PtdIns(3)P, so that they can couple cargo recognition with membrane deformation (reviewed in (van Weering *et al.*, 2010)). PtdIns(3)P is synthesized in yeast by the PI3K (phosphatidylinositol 3-kinase) complex II, which consists of Vps15, Vps34 (Herman *et al.*, 1992), and the associated proteins Vps30 and Vps38 (Kihara *et al.*, 2001). In addition, it has been found that yeast retromer function depends on its interaction with the Rab7-GTPase-like Ytp7 (Balderhaar *et al.*, 2010; Liu *et al.*, 2012) and the sorting nexins Vps5 and Vps17, which retrieve Vps10 (Stack *et al.*, 1993) along with another sorting nexin such as Mvp1 (Chi *et al.*, 2014) or the sorting nexins Snx4, Snx41 and Snx42, which are involved in Snc1 retrieval from early endosome (Hettema *et al.*, 2003) (Table 4). Similar to mammals, mutations of any of the retromer subunits, prevent Vps10 retrieval to the TGN, leading to its degradation in the vacuole, and as a consequence, missorting of pro-CPY (Seaman *et al.*, 1997).

EM analysis in mammalian cells has shown that the retromer is associated with vacuolar/tubular endosomes that correspond to intermediates in the maturation from EE to LE (Arighi *et al.*, 2004), where it can co-localize with clathrin and AP-1 (Popoff *et al.*, 2007). Some data has indicated that the Chc22 clathrin heavy chain isoform functions in endosomal protein sorting, but it is not known if this is in concert with retromer (Esk *et al*., 2010). It has recently been suggested that clathrin and AP-1 adaptors act together with retromer, rather than in separate retrograde pathways, as a platform to enrich a subset of cargos within subdomains in the endosome (Popoff *et al.*, 2007). A recent model suggests that clathrin enriches cargo on a subset of SNX-BAR-retromer-decorated endosomes prior to membrane deformation, possibly through the recruitment of cargo adaptors and/or by spatially confining cargo within an endosomal subdomain (McGough & Cullen, 2013). Then clathrin is removed, and the retromer is capable of deforming the membrane to generate tubular structures that carry the concentrated cargo (McGough & Cullen, 2013). However, the way clathrin dynamics is regulated to allow the formation or processing of these retromer carriers needs to be better investigated.

In mammalian cells, WASH, a member of WASP family, is thought to be a key regulator of retromer-dependent tubule formation and/or scission (Derivery *et al.*, 2009; Gomez & Billadeau, 2010). No homologue of WASH exists in yeast, but the *S. cerevisiae* N-WASP Las17 is required for LE motility (Chang *et al*., 2005), suggesting

that actin polymerization on endosomal compartments also occurs in yeast. Whether it is or not required for retromer dependent tubule formation or fission is not known. Besides, it has recently been shown that fission of retromer SNX-BAR coated tubules from yeast endosomes is promoted by the dynamin-related protein Vps1 (Chi *et al*., 2014).

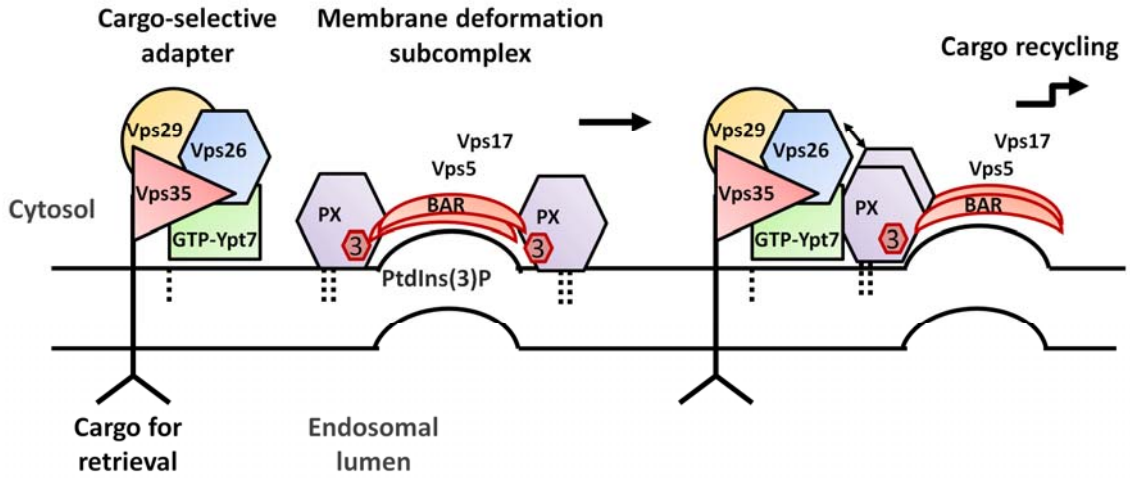

Figure 12. The yeast retromer complex and its interactions. In yeast, the Vps5/17 sorting nexin subcomplex recruits the Vps26/29/35 subcomplex to the endosome, where it functions as a retrograde cargo receptor. Vps35 interacts with Vps26 through its N-terminus and with Vps29 through its C-terminus. Vps35 also interacts with cargo such as Vps10. Vps5 and Vps17 dimerize through their C-terminal (BAR) domains, and have PX domains that can bind to PtdIns(3)P. Vps5 alone interacts with the Vps26/29/35 subcomplex through the N-terminal regions of both Vps26 and Vps5. On the endosome, activated Ypt7 promotes export of cargo from the endosome via tubular/vesicular domains decorated by retromer (adapted from (Seaman, 2005)).

1.1.4.1.2.3. Clathrin in the MVB pathway

The ESCRT (Endosomal Sorting Complexes Required for Transport) complexes drive membrane deformation with opposite curvature as compared to the clathrin and the COPI and COPII coats. They are required for a number of important cellular functions including autophagy, budding of enveloped viruses from the PM, and the membrane abscission step in cytokinesis and the generation of ILVs in the endosomes that carry ubiquitinated membrane proteins destined for degradation within the lumen of the vacuole (cellular functions of ESCRT complexes reviewed

Protein	Mutant *vps* gene class	Comments
Vps5, Vps17	*Class B* (fragmented vacuoles: more than 20 small, vacuole-like compartments.)	Retromer component; sorting nexins
Vps26	*Class F (*one large vacuole surrounded by a number of fragmented vacuolar structures)	Retromer component; predicted arrestin fold
Vps29	*Class A* (wild-type: 3–10 spherical vacuoles that cluster in one area of the cytoplasm. In dividing cells, the vacuole extends from mother to daughter cell along the cell axis)	Retromer component; predicted phosphoesterase fold
Vps35	*Class A*	Retromer component; cargo-binding activity
Grd19	-	Sorting nexin that is involved in retrieving the t-SNARE Pep12
Snx4, Snx41, Snx42	-	Sorting nexins that are involved in retrieving the v-SNARE Snc1
Vps34	*Class D* (single, large vacuole that fails to extend into daughter cell buds)	PtdIns(3)P -kinase that is involved in retromer recruitment to membranes
Vps15	*Class D*	Serine/threonine kinase that activates Vps34
Vps30, Vps38	*Class A*	These proteins form a complex with Vps15 and Vps34 and target them to endosomes
AP-1, clathrin	-	Components of TGN and endosomal clathrin coats

Table 4. Proteins that are involved in budding and cargo selection at endosomes in *Saccharomyces cerevisiae*. AP-1: adaptor protein-1; SNARE: soluble N-ethylmaleimide-sensitive fusion protein (NSF) attachment protein receptor; Snc1: suppressor of the full allele of CAD-1; Snx/SNX: sorting nexin; TGN: trans-Golgi network; t-SNARE: target-membrane SNARE; v-SNARE: vesicle-membrane SNARE; Vps: vacuolar protein sorting.

in (Hurley, 2011; Slagsvold *et al*. , 2006)). The evolutionary conserved machinery of the ESCRT complexes consist of a subset of 17 VPS proteins that were firstly identified in yeast, belonging to the class E VPS proteins, and that assemble into five different subcomplexes ESCRT-0, ESCRT-I, ESCRT-II, ESCRT-III and the Vps4 complex (Table 5 and Figure 13) (Hurley, 2011; Slagsvold *et al*. , 2006).

In yeast, mutations in any of the components of the ESCRT complexes cause the appearance of a large, aberrant prevacuolar MVB called "class E compartment", which by EM appears as a structure with aberrant stacks of flattened endosomal cisternae (Raymond *et al.*, 1992). These mutants are unable to sort proteins into ILVs, and thus, the aberrant compartment accumulates endocytosed cargo and late Golgi proteins, with a generalized failure in endosomal sorting, but no defect in PM endocytic uptake (Babst *et al*., 2002; Babst *et al*., 2002; Katzmann *et al.*, 2001; Katzmann *et al.*, 2003). In mammalian cells, siRNA-mediated knockdown of different ESCRTs components lead to different morphologies that ranged from enlarged MVB that fold into cisternae or tubulated vacuolar domains of EE or enlarged MVB with fewer ILVs (Bache *et al.,* 2006; Doyotte *et al.,* 2005; Malerød *et al.,* 2007; Razi & Futter, 2006).

Clathrin has been found to constitute a flat bilayered structure characterized by EM in mammalian MVB (Sachse *et al.*, 2002), distinct from the "canonical" PM and TGN clathrin coats. These clathrin flat coats are recruited on endosomes by an interaction with Vps27/Hrs (Raiborg *et al.*, 2001) and form restricted microdomains (Raiborg *et al*., 2002). The cooperative coassembly of ESCRT-0 and clathrin facilitates cargo concentration and ESCRT complex recruitment, thus enabling their efficient sorting into the degradative pathway (Raiborg *et al.*, 2006). Since clathrin has not been detected inside intraluminal vesicles by EM (Sachse *et al*., 2002), the flat coat might dissociate before endosomal invagination or alternatively, invagination might occur at sites adjacent to the coat.

Core complexes	MVB sorting proteins	Mutant *vps* gene class	Comments
Vps27 complex	Vps27 Hse1	Class E	Cargo and PtdIns(3)P interaction Interaction with Hua1 and Rsp5
ESCRT-I	Vps23 Vps28 Vps37 Mvb12	*Class E* *Class E* *Class E* *Class E*	Cargo and Vps27 interaction Assembly with ESCRT-II (Vps36)
ESCRT-II	Vps22 Vps25 Vps36	*Class E* *Class E* *Class E*	Assembly with ESCRT-III (Vps20) Cargo and PtdIns(3)P interaction; assembly with ESCRT-I (Vps28)
ESCRT-III	Vps20 Vps32/Snf7 Vps2/Did4 Vps24	*Class E* *Class E* *Class E* *Class E*	Assembly with ESCRT-II (Vps25) Membrane deformation; vesicle invagination
Vps4 complex Modulators/ adaptors	Vps4 Vps31/Bro1 Vps60/Mos10 Vps46/Did2 Vta1	*Class E* *Class E* *Class E* *Class E* -	ESCRT disassembly and recycling Doa4 recruitment, ESCRT-III interaction ESCRT-III-like protein Positive regulator of Vps4
Regulatory kinases	Hua1 Rup1 Vps34 Vps15	- - *Class D* *Class D*	Links Rsp5 to Hse1 Complex with Rsp5 and Ubp2 PtdIns(3)P synthesis
Ubiquitin ligase	Rsp5	-	Cargo ubiquitination
Deubiquitinating enzymes	Doa4 Ubp7	- -	Cargo deubiquitination Cargo deubiquitination

Table 5. Components of the ESCRT machinery involved in sorting cargo to vacuoles via the MVB in *Saccharomyces cerevisiae*.

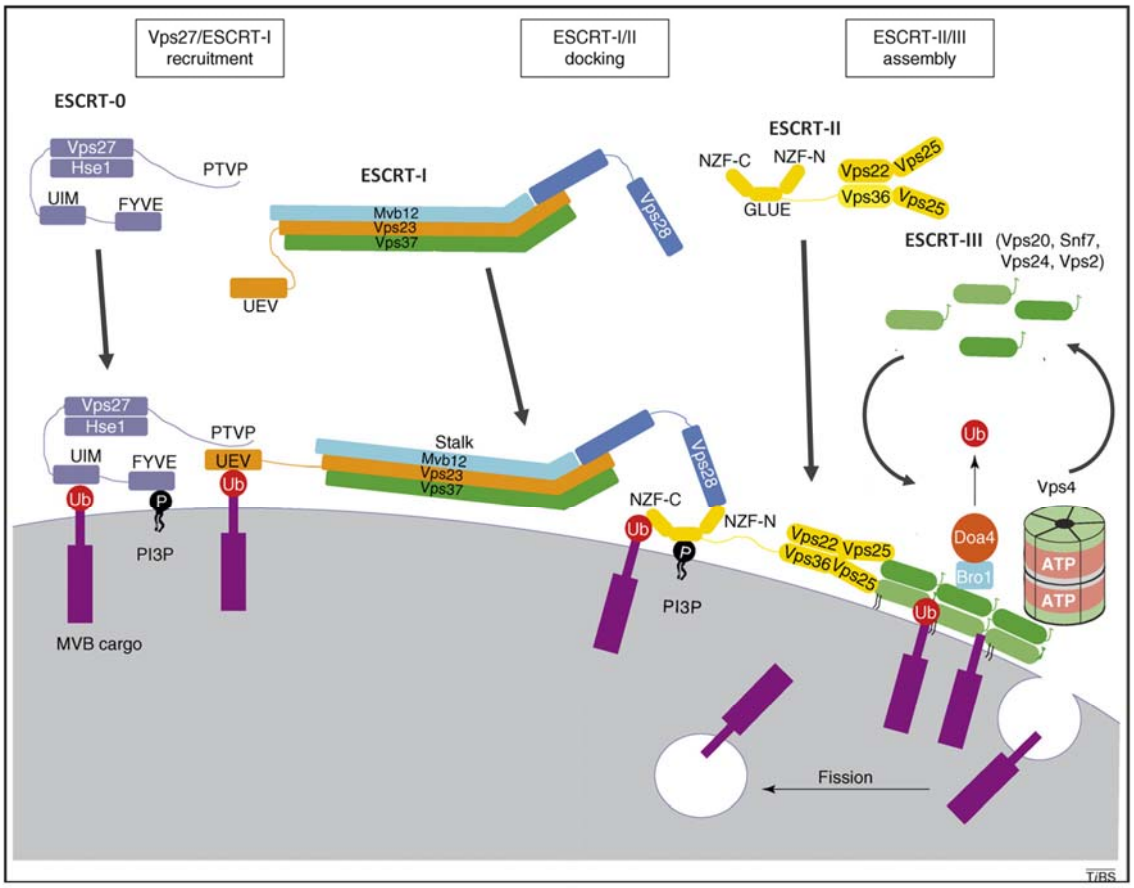

Figure 13. Schematic representation of the ESCRT machinery involved in sorting cargo to vacuoles via MVBs in yeast. The four ESCRTs are recruited to endosomes by their interactions with membranes, clathrin, ubiquitin (Ub) and with each other. The FYVE domain of Vps27 binds PtdIns(3)P (PI3P) on the endosomal membrane resulting in membrane docking of the Vps27-Hse1 complex. The UIM domains of Vps27 and Hse1 recognize and bind ubiquitylated cargo for sorting into MVB vesicles. Vps27–Hse1 complex recruits the ESCRT-I complex to the membrane via interactions with Vps23. Membrane-bound ESCRT-I binds ubiquitylated cargo via the ubiquitin-conjugating enzyme E2 variant (UEV) domain of Vps23 and recruits ESCRT-II to the membrane via interactions between Vps28 and Vps36 (ESCRT-II). ESCRT-II binds endosomal PI3P and ubiquitylated cargo via the GRAM-like ubiquitin-binding in EAP45 (GLUE) domain of Vps36. Membrane-bound ESCRT-II recruits the downstream ESCRT-III complex via interactions between Vps25 and Vps20. ESCRT-III orchestrates the last steps in the pathway in which ubiquitin is removed by a deubiquitinase (Degradation of alpha-4 (Doa4)), and the complexes are disassembled by the AAA+ ATPase Vps4 following cargo sorting into MVB vesicles. Budding away from the cytosol is facilitated by a curvature-inducing factor that could flex the membrane by being localized to the neck of the budding vesicle that might be recruited by the ESCRT machinery. Ub: ubiquitin. (Figure taken from (Saksena *et al.*, 2007).

The existence of the flat bilayered clathrin in the yeast MVB has not been demonstrated yet. Therefore, although clathrin is assumed to have a role in the yeast MVB pathway the extent of its involvement is unclear. Clathrin have been shown to co-localize at a certain extent with the ESCRT-III component Snf7 (Newpher et al., 2005), which suggest that clathrin may mediate some function at the MVB in yeast. Besides, yeast Vps27 binds clathrin *in vivo* and *in vitro* (Bilodeau *et al.,* 2003), and shares function with mammalian Hrs. However, mutations of the Vps27 clathrin box motifs have no effect on loading of some cargo into the MVB (Bilodeau *et al.,* 2003). A possible explanation for this lack of effect, is the recent finding of another component of the ESCRT complex, Bro1, that also binds clathrin, and functions as a second ubiquitin-sorting receptor early in the MBV pathway (Pashkova *et al.*, 2013)). However, direct evidence demonstrating the existence of a flat endosomal clathrin coat in the yeast MVB is still missing.

1.1.4.1.2.4. Other possible clathrin roles in endosomal trafficking pathways in mammalian cells

In mammals, clathrin has been involved in recycling of transferrin to the PM, as the so-called "G-clathrin" (as it was detected as gyrating signals of GPF-Clca in the vicinity of endosomes) (Zhao & Keen, 2008). However, the role of clathrin in recycling from the endosome to the PM is still a matter of debate.

In the TGN, apart from having roles in sorting of lysosomal/vacuolar enzymes, some studies implicate clathrin in the maturation of secretory granules by removing constitutively expressed proteins (Molinete *et al.*, 2001). In addition, it may have a role in maintaining the Golgi complex integrity (Radulescu & Shields, 2012; Radulescu *et al.*, 2007)since clathrin-mediated membrane traffic might be required to deliver proteins that promote Golgi-complex assembly.

1.1.4.2. Clathrin interaction with microtubules and its role in cell cycle

In mammals, Chc17 localizes and concentrates at the mitotic spindle during mitosis, when formation of CCV is shut down since membrane trafficking is only taking place during interphase (Okamoto *et al*., 2000). This clathrin is directly associated to the spindle by the N-terminal domain of clathrin heavy chain and is not interacting with membranes. It forms a complex with two spindle proteins, TACC33 (Transforming Acidic Coiled-Coil protein 3) and ch-TOG (colonic hepatic

Tumour Overexpressed Gene), which have roles in microtubule growth and stabilization (Booth *et al.*, 2011; Hood *et al*., 2013). The TACC3-ch-TOG-Chc17 complex contributes to centrosome integrity during early mitosis and to stabilize kinetochore fibres to aid segregation of chromosomes (Booth *et al.,* 2011; Royle *et al*., 2005). It has been proposed that clathrin act to physically crosslink adjacent microtubules (MTs) comprising the kinetochore fibres (K-fibres) (Booth *et al.,* 2011).

Clathrin has been observed on spindles of human, rat, mouse, pig, frog, and plant cells, but it is unclear whether the mitotic function of clathrin is conserved in *Saccharomyces cerevisiae*. TACC3 and ch-TOG are less conserved than clathrin between species. Indeed, in yeast there is not a clear homologue of TACC3 (reviewed in (Royle, 2012)). Thus, the microtubule stabilization role for Chc17 might have emerged by recent evolution. Interestingly, *S. cerevisiae* has a single MT that acts as a 'K-fibre', so no clathrin inter-MT crosslinking would be required (Royle, 2012).

Interestingly, a role of the ESCRT machinery in the membrane abscission step of cytokinesis has been suggested. ESCRTs complexes localize to midbodies (Jez G Carlton & Martin-Serrano, 2007), the structure connecting two daughter cells just prior to the completion of cell division in the final step of cytokinesis. ESCRT mutants in human cells, *Arabidopsis* and *S. pombe* have impairments in cell division, but curiously, ESCRT genes have not been reported as cell division mutants in *S.cerevisiae* (reviewed in (Hurley, 2010; Slagsvold *et al.*, 2006)). Localization of ESCRTs to the midbody requires the presence of the centrosomal and midbody protein CEP55, which recruits ESCRT-I and subsequently ESCRT-III, leading to cleavage of the membrane neck by the same mechanism as in MVB biogenesis (Jez G Carlton & Martin-Serrano, 2007).

Membrane trafficking has also multiple roles in cytokinesis. Indeed, Chc17 has been shown to play a role during mitotic cell expansion and completion of the abscission step, a process in which Chc22, α-adaptin, epsin, eps15, endophilin II, syndapin II and the GTPase dynamin II are implicated as well, suggesting that their function in this process is membrane traffic-dependent (Smith & Chircop, 2012). Thus, given the characterized interaction between ESCRT-III complexes and clathrin (Raiborg *et al.*, 2002) and that both have been shown to function in

cytokinesis, it could be suggested a cooperative function of both proteins in this process.

1.1.5. Physiological functions of clathrin in multicellular organisms and involvement in disease

Clathrin-mediated trafficking pathways are implicated in many key physiological functions. For example, CME controls the lipid and protein composition of the PM and therefore regulates how cells interact with their environments. In high eukaryotes, it controls constitutive and stimulated internalization of many receptors such as those carrying metabolites as cholesterol or iron (Brown & Goldstein, 1977; Pearse, 1982), or receptors Tyr kinases (RTKs) (such as EGFR) and GPCRs (as β2 adrenergic receptor)(Huang *et al*., 2004). By influencing the surface composition of cells, clathrin-mediated pathways regulate signal transduction, for example, by controlling the cell surface exposure of the receptor and therefore, its accessibility to the signal, or by terminating signaling via the specific down-regulation of ligand-bound receptors. In addition, clathrin-dependent trafficking pathways can control the activity of ion channels transporters (van de Graaf *et al.*, 2008). Therefore it is not surprising that clathrin plays important roles in cell differentiation and development, or in very specialized physiological function such as the regeneration of synaptic vesicles of antigen presentation by the immune system (reviewed in (McMahon & Boucrot, 2011)). In addition, CME is used by toxins (i.e. anthrax, botulinium, tetanus, shiga and diphtheria) pathogenic bacteria and funghi (i. e. *Listeria monocytogenes*, *Staphylococcus aureus*, the uropathogenic *Escherichia coli* (UPEC) and *Candida albicans*) and a number of virus (i. e. the rhinovirus, Semliki forest virus, hepatitis C, poliovirus, reovirus , influenza virus and maybe HIV-1) to enter the cell (reviewed in (Brodsky, 2012; McMahon & Boucrot, 2011; Myers & Payne, 2013).

Apart from the role of CME in infectious diseases, perturbations of clathrin-dependent trafficking pathways have also been associated with a range of human diseases. Loss of function in central components of these pathways, such as clathrin, AP-2, epsin and dynamin, results in embryonic lethality, so no human diseases are associated with genetic defects on these core components. However, several perturbations of clathrin-mediated trafficking pathways have been reported in numerous human affections, such as cancer, myopathies,

neuropathies, metabolic and genetic syndromes, autoimmune diseases and psychiatric and neurodegenerative diseases ((McMahon & Boucrot, 2011; Puertollano, 2006) and references therein) (for a more detailed description of clathrin-mediated trafficking defects associated with human diseases, see table 6).

Disease cathegory	Defective protein	Disorder
Cancer	Chc	Large B-cell lymphoma Renal cancer Breast cancer
	Eps15	Lung cancer
	HIP1	Lung cancer Breast cancer
	CALM	Acute myeloid leukaemia Acute lymphoblastic leukaemia
Psychiatric diseases	Amphiphysin	Schizophrenia
	Endophilin	Schizophrenia
	Dynamin	Schizophrenia
	Synaptojanin	Bipolar disorder
Neurodegenerative diseases	CALM	Alzheimer
	Amphiphysin	Alzheimer
Genetic syndromes	Synaptojanin	Down syndrome
	Intersectin	Down syndrome
Neuropathies & myopathies	Amphiphysin	Autosomal dominant centronuclear myopathy
	Dynamin	Dominant intermediate Charcot-Marie-Tooth disease (CMT)
	Rab7	CMT
Autoinmune diseases	Amphiphysin	Stiffman desease (autoinmune disease against amphiphysin)

Table 6. Disorders associated with components of clathrin-mediated trafficking pathways (McMahon & Boucrot, 2011; Puertollano, 2006).

1.2. Calmodulin

1.2.1. Historical perspective

Calmodulin (CALcium MODULated proteIN; Cmd) is an essential, ubiquitous, calcium-binding protein found in all eukaryotic organisms examined. It is one of the major intracellular calcium (Ca^{2+}) sensors mediating cellular responses to the Ca^{2+} fluxes generated by certain hormones and mitogenic agents, stress and pathogenesis (Carafoli, 1988; Carafoli *et al.,* 2001; Mendozas *et al*., 1994; Withee *et al.,* 1997). It also senses the action of Ca^{2+} pumps activated throughout the cell cycle (Lu & Means, 1993). It can bind to and regulate many different targets in a Ca^{2+}-dependent or Ca^{2+}-independent way (Tidow & Nissen, 2013). Many of the proteins that bind Cmd are unable to bind Ca^{2+} themselves, so they use Cmd as a Ca^{2+} sensor and signal transducer in a variety of cellular processes including the organisation of cytoskeleton, cell proliferation (Chin & Means, 2000; Lu & Means, 1993 and membrane trafficking (Apodaca *et al*., 1994; Lladó *et al.*, 2004, 2008; Peters & Mayer, 1998; Tebar *et al.*, 2002; Wu *et al.*, 2009). Cmd is expressed in many cell types and can have different subcellular locations, including the cytoplasm, the spindle body or centrosome, or the PM or other organelle membranes (Luby-Phelps *et al*., 1995; Moser *et al.*, 1997; Spang *et al.*, 1996). Cmd plays a multitude of cellular functions in different cell types, having roles in important physiological processes, such as inflammation, metabolism, apoptosis or muscle contraction, among others (Martin W Berchtold & Villalobo, 2014; Racioppi & Means, 2012; M. P. Walsh, 1994).

In spite of the central importance of Cmd in Ca^{2+}-mediated signal transduction pathways in all eukaryotes, many Cmd-protein interactions and their functional relevance remain to be identified and characterized, possibly because the multiple functions of Cmd hinders identification of mutations that specifically alters those interactions. The analysis of essential multifunctional proteins such as Cmd has been facilitated in *Saccharomyces cerevisiae* by the generation and characterization of complementation groups of mutants that specifically alter binding to essential cellular targets (Ohya & Botstein, 1994a). The high degree of conservation of Cmd and the easy yeast genetics makes *S. cerevisiae* a suitable model system to study these essential and multifunctional protein.

Cmd was discovered in 1970 independently by S. Kakiuchi and W. Y. Cheung. Kakiuchi revealed the Ca^{2+}-dependent activation of phosphodiesterase (Kakiuchi *et al.*, 1970), and Cheung showed that Cmd was a Ca^{2+}-binding protein (Cheung, 1970). Five years before, S. Ebashi discovered other Ca^{2+}-binding protein in the striated muscle cell, troponin (Ebashi & Kodama, 1965), which functions as the regulator of muscle contraction by receiving intracellular Ca^{2+}. Ebashi used EGTA to preferentially chelate Ca^{2+} over K^{+}, Na^{+}, and Mg^{2+}, revealing that Ca^{2+} is indispensable to this particular process. This approach was later on used by Kakiuchi to investigate the Ca^{2+} role in Cmd function. Later, it was found that Cmd and troponin were both regulating the skeletal muscle contraction by activating enzymes such as the myosin kinases (Yagi *et al.*, 1978).

1.2.2. Structure and molecular organization

1.2.2.1. Diversity of calmodulin genes and proteins

The essential and conserved protein Cmd is found in all eukaryotes, including animals, plants and fungi. In mammals it is encoded by three non-allelic genes, *CALM1*, *CALM2* and *CALM3,* that are dispersed throughout the genome. In humans, they are located on the chromosome loci 14q24-q3, 2p21.1-p21.3 and 19q13.2-q13.3, respectively (Berchtold *et al.,* 1993). Although their coding sequences differ, they encode an identical protein of 148 amino acids and 17 kDa. Yeast Cmd (Cmd1), however is encoded by an unique gene that is required for viability, *CMD1* (Davis *et al.*, 1986), located in chromosome II (ChrII:458362 to 457919). The Cmd amino acid sequences from animal, plant, and protist kingdoms share 85% identity, but yeast Cmd1 however is only 60% identical to the primary structure of other Cmds and it can poorly activate some of the target enzymes of vertebrate origin (Luan *et al.*, 1987). Nevertheless, it shares many physical and functional properties with Cmds from higher organisms (Ohya *et al.*, 1987), and can be replaced by vertebrate Cmds (Davis & Thorner, 1989).

1.2.2.2. Structure and biochemistry

Cmd is composed of 8 α-helices, and comprises two homologous globular domains connected by a central flexible linker (Babu *et al.*, 1985; 1988; Barbato *et al.*, 1992; Kretsinger *et al.*, 1986; Kuboniwa *et al.,* 1995). Each domain contains two Ca^{2+}-binding motifs called EF-hands, each bind one Ca^{2+} ion (Figure 14A). An EF-

hand has 30 residues organized in a N-terminal α-helix (the E helix) immediately followed by a centrally located Ca^{2+}- binding loop and a C-terminal α-helix (the F helix) (Babu *et al.*, 1988) (Figure 14B). Cmd affinity for Ca^{2+} (Kd=5 x 10^{-7} M to 5 x 10^{-6} M) fits with the range of intracellular Ca^{2+} concentrations within most cells (10^{-7} M to 10^{-6} M) (D. Chin & Means, 2000). The C-terminal EF-hands have a 3 to 5 fold higher affinity for Ca^{2+} than the N-terminal sites (Andersson *et al.*, 1983; Linse *et al*. 1991; Anderson *et al*., 1982) and each domain adopts different conformations in the presence (holo-Cmd) or absence (apo-Cmd) of Ca^{2+} (Zhang *et al.,* 1995). In the absence of Ca^{2+}, the N-terminal domain has a "closed" conformation where the helices of the EF-hands are packed together. On the contrary, the C-terminal domain of apo-Cmd has still a "semiopen" conformation with the hydrophobic

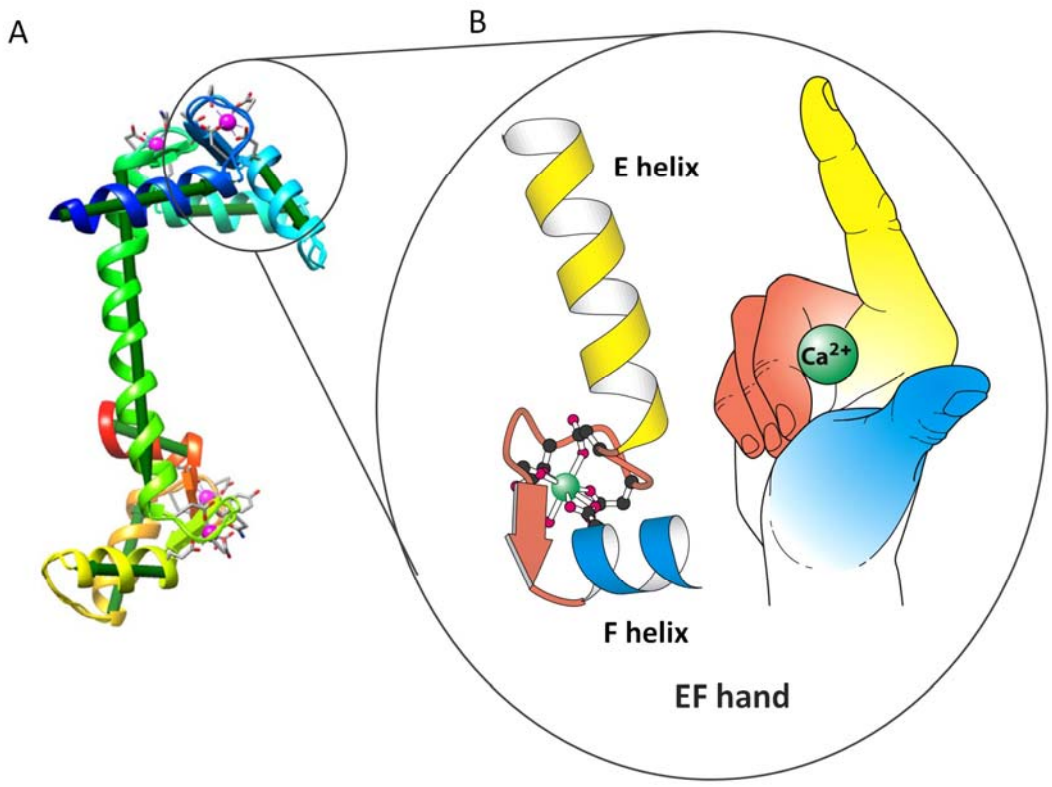

Figure 14. Structure of calmodulin and EF-hand Ca^{2+} binding motifs. A) Ribbon representation of an extended calmodulin. The four calcium ions in the EF hands are depicted as magenta spheres. The cartoon is colored from blue (N terminus) to red (C terminus). B) 3D structure and cartoon ilustration of the canonical EF-hand Ca^{2+}-binding motif. The EF-hand motif contains about 30 residue helix-loop-helix topology, resembling the spread thumb and forefinger of the human hand. Ca^{2+} is coordinated by ligands within the 12-residue loop, including seven oxygen atoms from the sidechain carboxyl or hydroxyl groups, a main chain carbonyl group, and a bridged water (figure adapted from (Kursula, 2014).

sites partially exposed and accessible, allowing this domain to interact with some target at resting levels of intracellular Ca^{2+} (Swindells & Ikura, 1996). When Ca^{2+} concentrations arise, Ca^{2+} ions bind to each Ca^{2+}-binding loop in the EF-hands by seven primarily carboxylate ligands, leading to alterations in the interhelical angles and changing the conformation of the two domains from a "closed" to an "open" conformation ((Hoeflich & Ikura, 2002) and references therein) (Figure 15). As a consequence, the hydrophobic residues in the methionine-rich hydrophobic pockets (existing between helices 2 and 3 as well as between helices 5 and 6) are exposed providing a soft, flexible site for embedding a hydrophobic side chain present in the Cmd-binding domain of the target protein ((Hoeflich & Ikura, 2002) and references therein). This conformational change releases free energy, and this ability to convert the Ca^{2+} binding into biochemical energy is the basis of the Cmd ability to transduce Ca^{2+} signals (D. Chin & Means, 2000).

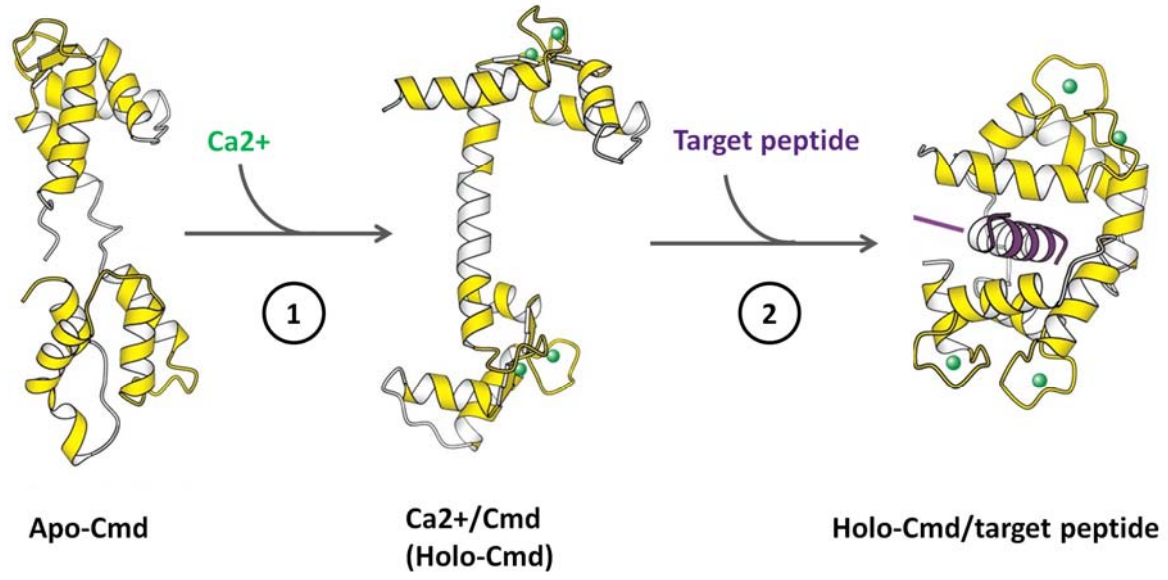

Figure 15. Ribbon presentation of apo-calmodulin, extended holo-calmodulin, and collapsed holo-calmodulin bound to a target peptide. 1) Ca^{2+} binding at the Cmd EF-hands produces large changes in the helices in both domains, resulting in a conformation change that exposses several hydrophobic residues for target peptides binding. 2) The two Cmd lobes come together and bury the target peptide between them in a collapsed globular conformation. Cmd is coloured in yellow, Ca^{2+} ions in green, and target peptide in purple. The N-terminal lobe of Cmd is orientated to the top, the C-terminal lobe to the bottom of the figures. (Figure adapted from (Vetter & Leclerc, 2003)).

The primary structure of *S. cerevisiae* Cmd1 is similar to its vertebrate counterpart, although there are some structural differences. Vertebrate Cmd binds four molecules of Ca^{2+} per molecule of Cmd, whereas yeast Cmd1 only binds three (Luan *et al.,* 1987; Starovasnik, *et al*., 1993). This is the consequence of a deletion of one residue in the Ca^{2+} binding loop and the substitution of a highly conserved glutamate at position 12 for glutamine, in the most C-terminal EF-hand (Luan *et al*., 1987; Starovasnik et al., 1993; Yazawa *et al.*, 1999). In adittion, yeast Cmd1 bound to Ca^{2+} has a more compact comformation due to interactions between the N- and C-terminal domains (Lee & Klevit, 2000; Yoshino *et al.*, 1996). Despite these differences in biochemical properties, vertebrate Cmd is able to complement the essential function of Cmd in yeast (Davis & Thorner, 1989), thus its basic functions appear to be conserved.

1.2.2.3. Structural aspects of the calmodulin interaction with target proteins

Calmodulin-binding proteins (CmdBPs) can be classified into three cathegories based upon their Ca^{2+} ion requirement for Cmd binding: Ca^{2+}-dependent, Ca^{2+}-independent and Ca^{2+}-inhibited. CmdBPs do not have a conserved amino acid sequence for Cmd binding. Many Ca^{2+}-dependent CmdBPs have one or more Cmd-binding domains of approximately 20 amino acids in length that are characterized by a basic amphipathic α-helix with two suitably spaced and oriented hydrophobic anchors, which insert into the methionine-rich pockets in Cmd ((Kursula, 2014; Tidow & Nissen, 2013) and references therein). The positively charged residues in the target form salt bridges to Cmd and may determine the binding orientation of the target peptide ((Kursula, 2014; Tidow & Nissen, 2013) and references therein). Based on the separation of hydrophobic anchor residues in the target peptides, different recognition modes have been identified (Tidow & Nissen, 2013) (Figure 16). The most common are 1-10 and 1-14, where each residue interacts with one hydrophobic cavity of the C-terminal or N-terminal domain of Cmd. However, modes 1-12, 1-16, 1-17 and subclasses 1-8-14 and 1-5-10 (where two hydrophobic residues from the peptide lie in the same pocket of Cmd) have also been identified in crystal structures (reviewed in (Kursula, 2014; Tidow & Nissen, 2013)). Interactions between Ca^{2+}-free Cmd and targets have also been characterized, which involve the IQ motifs in target proteins, identified on the basis of the consensus sequence [I,L,V]-QxxxR[G,x]xxx[R,K] (where x is any amino acid) (reviewed in (Kursula, 2014; Tidow & Nissen, 2013)). In addition, there is also a

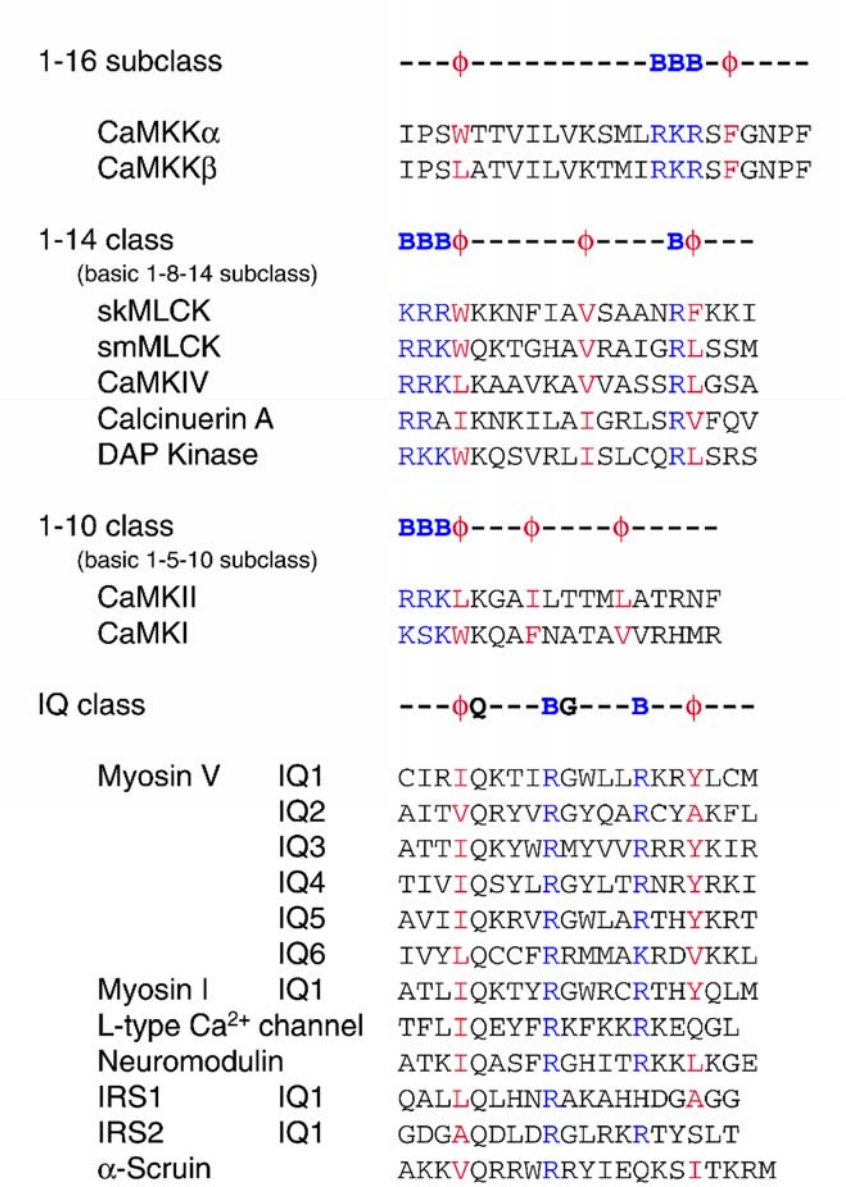

Figure 16. Amino acid sequence alignment of several examples of Cmd-binding motifs. There are three major classes and several subclasses of Cmd-binding motifs already characterized. The 1-14 class comprises the 1-14, 1-8-14, basic 1-8-14 and 1-5-8-14 subclasses, where each number represents the presence of a hydrophobic residue; for the basic 1-8-14 motif, three basic residues precede the first hydrophobic residue. The 1-10 class consists of the 1-10, 1-5-10, basic 1-5-10 and hydrophilic 1-4-10 subclasses. The latter motif has three hydrophilic residues following the hydrophobic residue at the tenth position. The IQ class consists of both complete and incomplete IQ motifs, the latter so-called for the absence of the second basic residue. Single letter code. ϕ in the consensus sequence indicates an hydrophobic residue, B indicates a basic residue. CaMKKα/β: rat Ca^{2+}-calmodulin-dependent kinase kinase isoform α or β; skMLCK: rabbit skeletal muscle myosin light chain kinase; smMLCK: rabbit smooth muscle myosin light chain kinase; CaMKIV: mouse Ca^{2+}-calmodulin-dependent kinase IV; DAP kinase I: human death-associated protein (DAP) kinase I; CaMKI/II: rat Ca^{2+}-calmodulin-dependent kinase I/II; Myosin V: mouse dilute non-muscle myosin V heavy chain (all six tandem IQ motif repeats shown); Myosin I: bovine (brush border) myosin I heavy chain-like protein (first of two IQ motifs shown); IRS1/2: mouse insulin receptor substrate 1/2 (first of two IQ motifs shown). (Figure obtained from (Yap et al., 2000)).

limited number of Ca^{2+}-inhibited CmdBPs that only bind to Cmd in the absence of Ca^{2+} (Kursula, 2014; Tidow & Nissen, 2013). Given the diversity in function of known CmdBPs, it is not surprising that the Cmd binding motifs varies between one protein and other. Generally, proteins that share similar functionality often exhibit similar domain layouts (Yap *et al.,* 2000).

Other classifications of CmdBPs have been done based on their regulation by intracellular Ca^{2+} concentrations (D. Chin & Means, 2000). Briefly, class A effectors bind irreversibly to Cmd irrespective of the presence of Ca^{2+}. Class B bind to Cmd in the absence of Ca^{2+} but dissociate reversibly in the presence of Ca^{2+}. Class C effectors form low-affinity, inactive complexes with Cmd at low concentrations of Ca^{2+}. At higher concentrations they engage in a high-affinity complex and are activated by Cmd. Class D effectors bind to Cmd in the presence of Ca^{2+}, but Cmd inhibits their function. Class E are activated by Ca^{2+}-bound Cmd. Finally, for class F effectors, Cmd binding promote their regulation (specifically via phosphorylation) indirectly by another Cmd-regulated kinase. In spite of the proposed classifications, the actual binding mechanisms that function between Cmd and its targets are not well understood.

It has been shown that the α-helical conformation of the central Cmd linker is consequence of crystal packing, but in solution, the central linker region is very flexible and unstructured (Barbato *et al*., 1992; Kuboniwa *et al.*, 1995; Wall *et al*., 1997). Consequently, the N- and C-terminal lobes do not adopt a defined orientation relative to each other in solution, but display a tumbling motion, being held together by the central linker (Barbato *et al*. 1992; Kuboniwa *et al.*, 1995; Wall *et al.*, 1997), suggesting an equilibrium between different conformational states ((Kursula, 2014) and references therein). The classical structure of Cmd bound to its ligand in a Ca^{2+}-dependent way, involves the disruption of the long central helix, allowing the two lobes to come together and bury the target peptide between them, in a collapsed globular conformation (Ikura *et al*., 1992; Meador *et al*., 1992)(Figure 15). However, other non-canonical conformations have been observed, for example in the crystal structures of a Cmd-calcineruin 2:2 complex, in which Cmd remains extended and two peptides bind between the two Cmd molecules with only a very slight opening of the lobes without unfolding of the central α-helix (Ye *et al.*, 2006; 2008). However, it is not clear if it is a physiologically relevant conformation, or if it is a crystallization artifact (Kursula,

2014). The conformation of Cmd when binding in its apo-Cmd form, is often dictated by the C-terminal lobe, which has a dominant role in these complexes, while the conformation of the N-terminal lobe varies (Black & Persechini, 2011). In fact, most structures of the IQ domain-Cmd complexes involve at least partially charged Ca^{2+}-Cmd, presenting a rather canonical collapsed conformation. When the C-lobe is Ca^{2+}-free, it directs the N-lobe to a binding site within the IQ domain, and to interact productively with this site the N-lobe must be Ca^{2+}-free. When the C-lobe is Ca^{2+}-bound, it directs the N-lobe to a site upstream of the consensus sequence, and it appears that the N-lobe must be Ca^{2+}-bound to interact productively with this site. Thus, Ca^{2+}-dependent changes in the conformation of the bound C-lobe appear to be responsible for directed N-lobe binding (Black & Persechini, 2011).

It has been recently shown that target proteins can change the conformation of Cmd and either increase or decrease its affinity for Ca^{2+} (Miao Zhang *et al.*, 2012). The dissociation of Cmd from its target protein has been suggested to be iniciated by the loss of Ca^{2+} ions from the from the N-terminal, likely followed by loss of Ca^{2+} from the C-terminal lobe and subsequently followed by rapid loss of the peptide (Brown *et al.,* 1997).

The presence of the two globular domains are required for binding and activation of Ca^{2+}-dependent target proteins, since experiments done with Cmd fragments containing 2 or 3 Ca^{2+} binding domains showed that none of these fragments are effective, at least for a set of particular targets (Hanley *et al.*, 1990; Minowa *et al.*, 1988). On the contrary, mutations in the central linker abolish binding and activation of only a specific subset of Cmd interacting proteins (Persechini *et al.*, 1991), indicating that, depending on the target, the long helix can serve as either a flexible tether or properly orient the 2 globular ends that contain the Ca^{2+} binding sites. Experiments of site-directed mutagenesis or chemical modifications to introduce diverse amino acid changes into Cmd purified from bacteria, and subsequent analysis of its activation properties on a variety of enzymes *in vitro*, showed that each amino acid change differentially affected binding and activation of a number of different enzymes. Thus, it was proposed that Cmd must bind to each target enzyme in a distinct manner and that both hydrophobic and hydrophilic interactions must be involved (Strynadka & James, 1990).

1.2.3. Cellular functions of calmodulin: from yeast to humans

1.2.3.1. Genetic analysis of calmodulin function

Despite the biochemical differences between the mammalian and the yeast *Saccharomyces cerevisiae* Cmds, their functions are highly conserved, and all known Cmd targets in *S. cerevisiae* have a functional homologue or orthologue in higher eukaryotes. The ease of the genetic analysis in yeast has been extremely valuable to the understanding of the Cmd regulatory roles, by helping identifying physiologically relevant targets of Cmd and by establishing the functional significance of both Ca^{2+}-bound and Ca^{2+}-free Cmd *in vivo* (Geiser *et al*., 1991). In particular, the generation and characterization of a collection of yeast Cmd1 conditional mutants that specifically alter binding to essential cellular targets facilitated the analysis of this multifunctional protein and identified many of its essential functions (Ohya & Botstein, 1994a, 1994b).

The first essential role desscribed for Cmd1 was in nuclear division. Original articles demonstrated that two temperature-sensitive *cmd1* mutants (*cmd1-1,* which contains two amino acid substitutions, isoleucine 100 to asparagine and glutamic acid 104 to valine, and *cmd1-101* which corresponds the C-terminal part of Cmd1 under the control of the *GAL1* promoter) accumulated DNA and showed abnormalities in the mitotic spindle morphology (Davis, 1992; Sun *et al*., 1992).

Further genetic analysis by Ohya and Botstein established that Cmd1 had other additional essential functions (Ohya & Botstein, 1994). They generated a collection of point mutations in the yeast Cmd1 by changing conserved phenylalanine residues (which were predicted to strongly contribute to the interaction of Cmd1 with its targets ((Ikura *et al.*, 1992) and references therein) to alanines to eliminate hydrophobic interactions with minimal disturbance of the main chain conformation (Table 7) (Ohya & Botstein, 1994b). The strains expressing the *cmd1* mutants as the only source of Cmd1 were screened for temperature sensitivity and they were subjected to complementation analysis to define those mutants that alter binding to the same target or target subsets. Cmd1 mutations that when expressed within the same cell do not complement for the growth defect are likely to affect the interaction with at least one and the same essential cellular target (even though the interaction with other essential or non-essential targets might be

affected by these mutations to differential extents). In contrast, mutants belonging to different complementation groups are thought to alter the interaction with a different set of essential targets and thus, support growth when expressed within the same cell. The *cmd1* mutants were classified into four intragenic complementation groups (A, B, C and D) for the temperature sensitive growth defect, each bearing distinct, major phenotypic defects (Table 7 and Figure 17): (A) actin cytoskeleton disorganization, (B) Cmd1 delocalization, (C) nuclear division and (D) budding defects, respectively (Ohya & Botstein, 1994). Further, two other *cmd1* mutants (*cmd1-242* and *cmd1-247*) that did not complement any other of the Cmd1 mutations for their growth defect were identified and defined as dominant for this phenotype. Interestingly, mutants from intragenic complementation groups A and B are both negative for endocytic uptake at the

Intragenic complementation group	**Mutant**	**Residue mutated**	**Uptake**	**Phenotype**
A Actin cytoskeleton disorganization	*cmd1-226*	F92	-	ts
B Calmodulin delocalozation	*cmd1-228*	F12,16,19	-	ts
C	*cmd1-239*	F65,	+	ts
Nuclear division defects	*cmd1-250*	F12,65,68	+	ts
D	*cmd1-231*	F12,89	+	ts
Budding defects	*cmd2-233*	F12,140	+	ts
Dominant	*cmd1-242*	F65,140	+	ts
	cmd1-247	F89,140	-	ts

Table 7. Intragenic complementation groups for the Ohya and Botstein´s yeast calmodulin mutants, based on their termosensitive growth defects. Table representing the yeast Cmd1 point mutants generated by Y. Ohya and D. Botstein (Ohya & Botstein, 1994a,b) indicating the location of the different phenylalanine residues mutated to alanine in each mutant and classified into intragenic complementation groups specifying the different phenotypes displayed by each one. F: Phenylalanine; ts: thermosensitive.

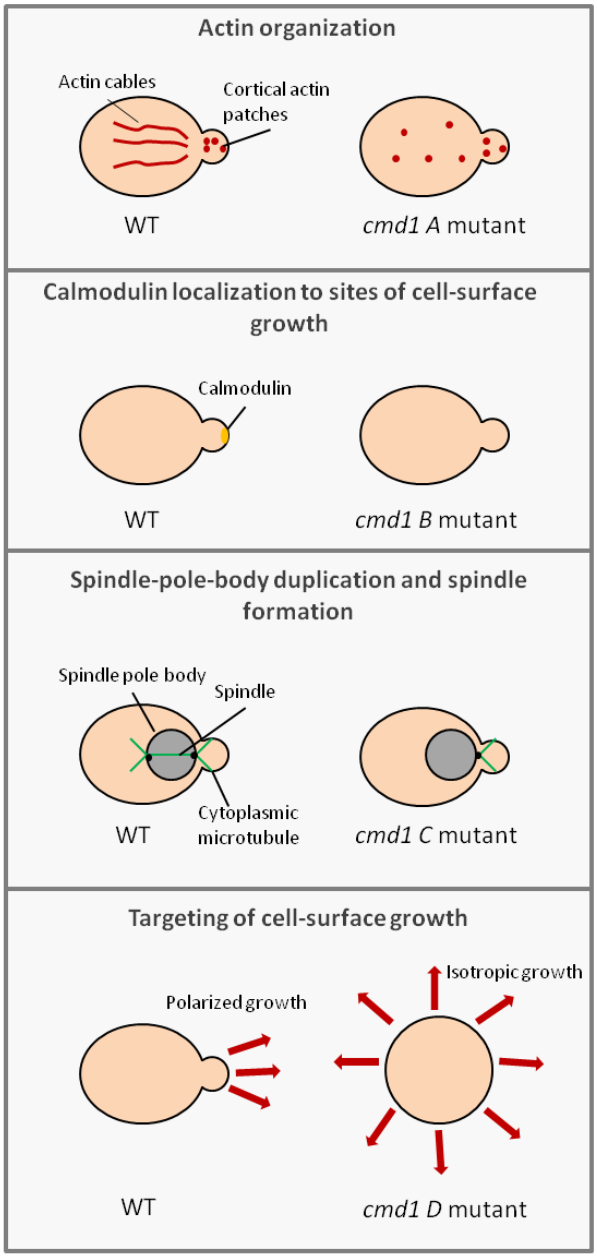

Figure 17. Aberrant phenotypes of the intragenic complementation groups. Ilustration representating the diverese phenotypes displayed by the different yeast *cmd1* mutant complementation groups.

restrictive temperature, even though they still complemented each other the misfunction in endocytic uptake, indicating the mutations affect binding to different endocytic targets (Geli *et al.*, 1998). Mutants from intragenic complementation groups C and D show WT uptake kinetics (Geli *et al.*, 1998). Interestingly, the *cmd1-242* was not defective whereas de *cmd1-247* was defective

and it was complemented for its endocytic defect by a mutant in the group B (*cmd1-228*) but not a mutant group A (*cmd1-226*) indicating that definition of the complementation groups depends on the cellular process under analysis.

As the role of Cmd1 as an intracellular Ca^{2+} sensor was well established, it was expected that its function *in vivo* would depend on its ability to bind Ca^{2+}. However, some yeast *cmd1* Ca^{2+}-binding-defective alleles in which Ca^{2+} binding loops were altered by site-directed mutagenesis were found to display neither significative disruptions in growth and morphology nor changes in intracellular Cmd1 localization (Geiser *et al.*, 1991). Thus, in *S. cerevisiae* the essential functions of Cmd1 do not seem to depend on its ability to be regulated by Ca^{2+}. Strikingly also, the Cmd1 mutant unable to interact with Ca^{2+} was also not defective in endocytic internalization (Kübler *et al.,* 1994). An unsolved caveat in these articles though is wheather the mutations introduced mimicked the constitutively Apo or Holo-Cmd1.

1.2.3.2. Calmodulin targets and cellular functions

Yeast Cmd1 has been shown to bind and regulate many different targets in a Ca^{2+}-dependent or Ca^{2+}-independent way, with important roles in different cellular processes (Table 8).

1.2.3.2.1. Ca^{2+}-independent calmodulin functions in *S.cerevisiae*

1.2.3.2.1.1. Role in mitosis

Cmd1 localizes to the spindle pole body (SPB) (Geiser *et al.,* 1993; Muller *et al.,* 2005; Spang *et al.,* 1996; Stirling *et al.* 1994), which corresponds to the microtubule organizing center (MTOC) or centrosome in mammalian cells. The SPB is responsible for nucleating nuclear and cytoplasmic microtubules throughout the cell cycle (Lim *et al.,* 2009). Nuf1/Spc110 is a component of the SPB and was identified by genetic analysis as the essential target of Cmd1 in mitosis (Geier *et al*., 1996; Stirling *et al*., 1994). The C-terminal part of Nuf1 binds Cmd1 *in vitro* and *in vivo* (Geiser *et al.,* 1993; Stirling *et al*., 1994). In addition, Cmd1 was found to bind Nuf1 at the central plaque of the SPB (Spang *et al*., 1996), which also contains the additional SPB components Spc29 and Spc42 (reviewed in (Helfant, 2002)). This interaction seems to anchor Nuf1 to the spindle pole during mitosis.

Protein	Essential	Cmd1 binding site; aa location	Function	Localization	Mammalian homologues
Nuf1/ Spc110	Yes	I; 897-917	Anchors MTs to SPB	SPB	Kendrin
Myo2	Yes	I; IQ motifs: 790-940	Polarized growth, vacuole inheritance	Bud tip, bud neck	Class V myosins: Dilute P190
Myo4	No	Putative	mRNA localization	Cytosolic	Class V myosins
Myo5	No	I; IQ motifs: 725-753	Endocytosis	Actin patches	Class I myosins
Myo3	No	Putative	Endocytosis	Actin patches	Class I myosins
Arc35	Yes	Dc; ND	Endocytosis, spindle assembly	Actin patches	Subunit 2 of Arp2/3 complex
Calcineurin	No	D:;453-476	Signaling, stress response, Ca2+ homeostasis, G2/M	Cytosolic	Calcineurin
Cmk1, Cmk2	No	D; Cmk1p: 313-340 Cmk2p: 323-350	Signaling, stress responses	Cytosolic	CaM Kinase II
Iqg1p	Yes	D; ND	Cytokinesis	Actomyosin ring	IQGAPs
Gad1	No	D; ND	Oxidative stress		Glutamate decarboxylase
Dst1/ Ppr2	No	D; ND	Transcription	Nucleus	TFIIS

Table 8. Calmodulin targets of *Saccharomyces cerevisiae*. ND: not determined; I: Ca^{2+} -independent; D: Ca^{2+} -dependent; MT: microtubules; SPB: spindle pole body.

Cmd1 binding to Nuf1 is essential for the connection between the microtubules and the SPB, since disruption of Nuf1-Cmd1 binding causes defective spindle formation and a loss of microtubule attachment to the SPB (Kilmartin & Goh, 1996; Sundberg *et al.,* 1996).

However, *NUF1* alleles that encode a C-terminally truncated protein completely lacking the Cmd1-binding site are dominant suppressors of *cmd1-1* (Geiser *et al.*, 1993). It was suggested that Cmd1 binding to Nuf1 releases the intramolecular inhibition in Nuf1, allowing its binding to Scp29 and thus to the SPB, since Nuf1 binds Scp29 only when bound to Cmd1 (Elliott *et al.,* 1999).

Cmd also localizes to the vertebrate MTOC and binds to the centrosome component kendrin, structurally related to Nuf1, in a similar manner ((Flory *et al.,* 2000) and references therein). Kendrin is involved in the maintenance of centrosome cohesion (Matsuo *et al.,* 2010).

1.2.3.2.1.2. Role in polarized growth and vacuole inheritance

MYO2 is an essential gene encoding for the heavy chain of one of the non-muscle class V myosins, which are associated with Griscelli syndrome and deafness in humans. Type V myosins have been implicated in vesicle and mRNA trafficking and some of them have been found to bind Cmd (reviewed in (Reck-peterson *et al.,* 2000)). Myo2 is required for polarized secretion and vacuole inheritance in yeast (Hill et al., 1996; Johnston *et al.* 1991). Myo2 binds the Ca^{2+}-free form of Cmd1 through six tandemly repeated IQ sites in its neck region *in vitro* and *in vivo* (Brockerhoff et al., 1994; Sekiya-Kawasaki et al., 1998). Deletion of IQ sites does not affect yeast viability suggesting that Cmd1 binding to Myo2 is not essential (Stevens & Davis, 1998). However it does affect the motility of transported vesicles indicating that Cmd1 works as a myosin light chain that confers stiffness to its lever arm (Schott *et al.*, 2002). Some mutations in the C-terminal tail of Myo2 selectively disrupt either polarized secretion or vacuole inheritance, indicating that distinct regions within this domain mediate Myo2 attachment to different cargoes (Catlett *et al*., 2000). Myo2 and Cmd1 both localize at the bud tip and bud neck of yeast cells (zones of cell surface growth and polarized secretion) (Brockerhoff *et al.*, 1994) and Cmd1 localization to these sites depends on its binding to Myo2 (Stevens & Davis, 1998). Genetic interactions between *CMD1* and *MYO2* are also

consistent with the biochemical experiments indicating that their interaction is Ca^{2+}-independent (Brockerhoff *et al.,* 1994; Sekiya-Kawasaki *et al.*, 1998)

Myo4 is another non-essential yeast class V myosin involved in transport/localization of specific mRNAs (Bobola *et al.*, 1996; Jansen *et al.*, 1996; Long, 1997; Takizawa *et al.,* 1997) which contains also six IQ sites predicted to bind Cmd1 and/or Cmd1 related light chains (Haarer *et al.*, 1994). Although the interaction of Cmd1 and Myo4 has not been carefuly demonstrated, cells lacking the Myo2 IQ sites delocalized Cmd1 even further when *MYO4* was deleted, suggesting Cmd1 and Myo4 actually interact (Stevens & Davis, 1998).

1.2.3.2.1.3. Role in endocytosis

Cmd1 was proposed to have a Ca^{2+}-independent role in endocytosis based in the observation that *cmd1* mutants defective in binding Ca^{2+} are not defective in endocytosis whereas another temperature sensitive mutant is (Kübler *et al.*, 1994). Further analysis using the Ohya and Botstein collection of *cmd1* mutants identified several other endocytosis-defective mutants (*cmd1-226, cmd1-247*, and *cmd1-228*) (Geli *et al.,* 1998). Interestingly, intragenic complementation among the *cmd1-247* and *cmd1-228* mutants could be demonstrated for the endocytic defect, suggesting that at least two distinct Cmd1 targets are required for this process (Geli *et al*., 1998).

Myo5, an unconventional myosin type I heavy chain, was found to be one target for Cmd1 in endocytosis. Myo5 is required for internalization of the PM α-factor receptor (Ste2) at high temperature (Geli & Riezman, 1996) and its overexpression suppresses the endocytic defect of the *cmd1-247* but not the *cmd1-228* mutant (Geli *et al*., 1998). Myo5 contains two IQ sites that are both necessary and sufficient for its Ca^{2+}-independent interaction with Cmd1, and whose deletion partially overcomes the requirement for Cmd1 in endocytosis (Geli *et al*., 1998), suggesting a inhibitory role for Myo5 function in endocytosis. Consistent with the suppression data, the Cmd1-247 mutant was unable to bind Myo5 whereas the Cmd1-228 mutant did (Geli *et al*., 1998). Interestingly, the *cmd1-226* mutation also disrupted the Myo5-Cmd1 interaction. However, overexpression of Myo5 did not suppressed its endocytic defect, indicating the this mutation also alters the function of at least another relevant endocytic target. Consistently, the *cmd1-226*

mutantion did not complement neither the *cmd1-247* mutation, which specifically disrupted the Cmd1-Myo5 interaction, nor the *cmd1-228*, which presumably disrupted the interaction of Cmd1 with another endocytic protein (Geli *et al*., 1998).

More recently, the molecular bases for the inhibitory role of Cmd1 on Myo5 has been worked out. It has recently been shown that an inhibitory interaction between the Myo5 TH1 (Tail Homology 1) lipid binding domain and its C-terminal extension exists, which prevents the induction of Arp2/3-dependent actin polymerization by the Myo5 C-terminus and Myo5 recruitment to endocytic sites (Grötsch *et al.*, 2010). In addition, it was demonstrated that the autoinhibitory conformation was stabilized by binding of Cmd1 to the Myo5 neck and that autoinhibition was released by Cmd1 dissociation from Myo5 at the PM (Grötsch *et al.*, 2010). Type I myosins are also involved in endocytic uptake in higher eukaryotes (Krendel *et al.*, 2008) and Cmd binding to type I myosins in higher eukaryotes has also been reported (Lieto-trivedi & Coluccio, 2008). Even though increasing evidence points to a function of Cmd regulating endocytic uptake in mammals (Wu *et al.*, 2009), the role of Cmd regulating type I myosin function at endocytic sites *in vivo* has not been investigated in mammalian cells.

A second target for Cmd1 required for endocytosis is Arc35, an essential component of the Arp2/3 complex that stimulates branched actin polymerization (reviewed in (Rotty *et al*., 2013)). *arc35* mutants display defects in endocytosis as well as defects in actin cytoskeleton organization (Munn & Riezman, 1994; Winter *et al*., 1997), which can be suppressed by overexpression of Cmd1, but not by overexpression of mutant Cmd1-226 and Cmd1-228 (Schaerer-Brodbeck & Riezman, 2000a, 2000b). The genetic data is consistent with the view that the *cmd1-247* mutation specifically compromises Cmd1 binding to Myo5 and the *cmd1-228* mutation compromises Cmd1's interaction with Arc35, whereas the *cmd1-226* mutations affect the interaction with either target. Consistent with these findings, Arc35 was demonstrated to physically interact with Cmd1 *in vitro* and *in vivo*, but not with Cmd1-226 and Cmd1-228 (Schaerer-Brodbeck & Riezman, 2000a), although it is not clear whether these proteins´ interaction is direct or indirect. In addition, *arc35* mutants exhibited a defect in methaphase spindle formation resulting in cell cycle arrest (Schaerer-Brodbeck & Riezman, 2000b), that was suppressed by overexpression of Cmd1, Cmd1-226 and Cmd1-228 but not by

overexpression of Cmd1-239 (Schaerer-Brodbeck & Riezman, 2000b), which was shown to fall into the complementation group C that is unable to bind Nuf1 (Ohya & Botstein, 1994). Thus, an alternative Cmd1-dependent function that affects SPB function is disrupted in both mutants *arc35* and *cmd1-239*, or Arc35 might affect Nuf1 SPB function (Cyert, 2001).

1.2.3.2.2. Ca^{2+}-dependent calmodulin functions in *S. cerevisiae*

1.2.3.2.2.1. Role in stress response, Ca^{2+} homeostasis and cell cycle regulation

Calcineurin is a highly conserved Ca^{2+}-Cmd-dependent phosphoserine/ phosphothrenine-specific phosphatase that activates the NF-AT (Nuclear Factor of Activated T-cells) family of transcription factors, that upon calcineurin phosphorylation translocate to the nucleus for gene transcription (reviewed in (Rusnak & Mertz, 2000)). It is an heterodimer composed by a catalytic A subunit and a regulatory B subunit that contains an EF-hand (reviewed in (Rusnak & Mertz, 2000)). Under resting Ca^{2+} levels, the A and B subunits remain associated and inactive due to an autoinhibitory domain at the C-terminus of the A subunit. When Ca^{2+} concentration raise, Cmd binds to the A subunit releasing the autoinhibition (reviewed in (Klee *et al*., 1998)). In *S.cerevisiae*, complete disruption of calcineurin activity can be achieved by mutations in any of the subunit, by using calcineurin inhibitors or by expression of Ca^{2+}-binding defective *cmd1* mutants in a *cmd1* null mutant (reviewed in (Cyert, 2001)).

Yeast calcineurin has at least three different functions: 1) regulating a stress-activated transcriptional pathway, 2) regulating Ca^{2+} homeostasis, and 3) regulating the G2 to M transition of the cell cycle (reviewed in (Rusnak & Mertz, 2000)). These different functions reflect the activities of distinct calcineurin substrates.

1) Regulation of the stress response. Yeast calcineurin regulates a signal transduction pathway activated by intracellular Ca^{2+} that results in increased expression of various stress-induced genes. Under environmental stress conditions, such as exposure to high concentrations of ions, morphogenetic reprograming during matting, high temperature, or cell wall damage, calcineurin-mediated gene expression is activated (Cunningham & Fink, 1994; Fink, *et al.*, 1989; Mazur *et al.,* 1995; Mendizabal *et al.*, 1998; Mendozas *et al.,* 1994;

Stathopoulos & Cyert, 1997). Under these conditions, calcineurin is essential, whereas under standard laboratory growth conditions, the transduction pathway is inactive and calcineurin is dispensable for growth (Breuder et al., 1994; Cyertt & Thorner, 1992; Mendozas *et al.*, 1994; Nakamura *et al.,* 1993). Ca^{2+}/calcineurin-dependent transcription is mediated by a zinc-finger transcription factor, Crz1, that activates the expression of the structural genes for several P-type ATPases, cell wall biosynthetic enzymes, and many other genes (Matheos *et al.,* 1997; Stathopoulos & Cyert, 1997).

2) Regulation of Ca^{2+} homeostasis. Yeast Ca^{2+} is mainly stored in the vacuole, organelle that has an important role in regulating Ca^{2+} homeostasis (reviewed in (Cunningham, 2011)). Calcineurin is thought to regulate Ca^{2+} homeostasis by promoting the expression and activation of the vacuolar P-type ATPase that pumps Ca^{2+} into the vacuole against a concentration gradient, of the Ca^{2+}/H^{+} exchanger Vcx1 that allows rapid entry of Ca^{2+} into the vacuole upon V-type ATPase-dependent acidification of the vacuole, or of the PM H^{+}-ATPase ((Cunningham, 2011; Cyert, 2001) and references therein). However, the calcineurin-dependent regulation of Ca^{2+} homeostasis seems to be very complex, and needs to be further elucidated.

3) Cell cycle regulation. Calcineurin participates in the regulation of the G2 to M transition (Mizunuma *et al.,* 1998). It is thought that calcineurin interacts with Hsl1, a kinase that inhibits the kinase Swe1, which in turn phosphorylates and negatively regulates Cdc28 (the major cyclin-dependent kinase in *S. cerevisiae*) at the G2/M transition (Mizunuma *et al*., 2001).

In mammals, calcineurin regulates many processes including N-methyl-D-aspartate receptor (NMDA) signaling, Na^{+}/K^{+} ATPase function, cardiac and vasculature development, learning and memory, T-cell activation, and angiogenesis (reviewed in (Rusnak & Mertz, 2000)). In humans, highly specific inhibitors of calcineurin, as FK506 and cyclosporin A, are used as powerful immuno-suppressants (Liu, 1993) .

In yeast *S.cerevisiae*, Cmd1 also regulates the protein kinases Cmk1 and Cmk2 (Ohyas *et al.*, 1991), which resemble the mammalian multifunctional Cmd1 kinase type II (CamKII), whose activity is dependent on binding to Ca^{2+}/Cmd and has roles

in learning and memory (reviewed in (Means, 2000)). In yeast, they seem to have roles in a number of stress responses, as the ability of yeast to grow in the presence of weak organic acids, the acquisition of thermotolerance (Holyoak *et al.*, 2000; Iida *et al.,* 1995) or survival of pheromone induced growth arrest (Moser *et al.*, 1996).

1.2.3.2.2.2. Role in cytokinesis

Yeast Iqg1 is similar to the mammalian Iqgap proteins that regulate the cytoskeleton and are thought to act as effectors for several small GTPases (Epp & Chant, 1997; Weissbachs *et al*., 1994). In yeast, it localizes to the bud neck during anaphase and it is required for the formation and contraction of the actomyosin ring during cytokinesis (Epp & Chant, 1997). Iqg1 contains IQ motifs required for binding to Mlc1 (Shannon & Li, 2000), a myosin light chain that also interacts with Myo1 and Myo2 (Boyne *et al.,* 2000; Stevens & Davis, 1998), and the Iqg1-Mlc1 interaction mediates localization of Iqg1 to the cytokinetic ring, where it recruits actin (Shannon & Li, 2000). Although mammalian Iqgaps binding to Cmd is well established (Pathmanathan *et al.*, 2011) and the yeast Iqg1 binds Cmd1 *in vitro* in a Ca^{2+}-dependent manner independently of its IQ motifs (Shannon & Li, 1999), it is not clear if the interaction *in vivo* actually occurs. However, Cmd1 localization is perturbed in *iqg1* mutant cells, suggesting that these two proteins may associate *in vivo* (Osman & Cerione, 1998).

1.2.3.2.2.3. Role in membrane fusion

Some studies have evidenced that many intracellular fusion events, apart from requiring Rab and SNARE proteins for vesicle targeting, require lumenal Ca^{2+} release and Cmd function.

In vitro biochemical studies, suggest that Cmd1 plays a role in homotypic vacuole fusion in *S. cerevisiae* (Christopher Peters & Mayer, 1998). A complex composed of Ca^{2+}-Cmd1, and protein phosphatase type I on the vacuole membrane was found to be required during vacuole fusion *in vitro* for the final stage of bilayer mixing (Peters, 1999; Peters & Mayer, 1998). In addition, some *cmd1* mutants, in particular *cmd1-239*, display fragmented vacuoles *in vivo* at restrictive temperature (Ohya & Botstein, 1994a). A search for Cmd1-binding partners on the vacuolar membrane using chemical cross-linking identified the V0 sector of the

vacuolar-H^+ATPase (Peters *et al.,* 2001). It was found that reconstituted V0 proteolipids could respond to Ca^{2+} (released from the vacuole) and Cmd1 by forming a proteolipid ring in each membrane that interact with each other to form a dimer. Thus, Cmd1 is thought to act as a Ca^{2+} sensor to regulate the final stages of the vacuolar fusion process (Peters *et al.*, 2001; Peters & Mayer, 1998). Although this biochemical characterization strongly supported a role for yeast Cmd1 in vacuole fusion, the *in vivo* observations were not that clear ((Cyert, 2001) and references therein).

Regulated exocytosis in mammalian cells was also thought to involve Ca^{2+} and Cmd (Burgoyne, 1984; Burgoyne & Morgan, 1995). However, it has later become clear that Cmd is not an essential Ca^{2+} sensor for exocytosis in most cells types (reviewed in (Burgoyne & Clague, 2003; Burgoyne & Morgan, 1998)), although it is required in a few specialized cells such as neurons, where Cmd has a well-established role in synaptic transmission (Hilfiker *et al.,* 1999; Sakaba & Neher, 2001). For example, Ca^{2+}-Cmd-dependent activation of Cmd-dependent kinase II and consequent phosphorylation of synapsins is required for efficient release of synaptic vesicles ((Hilfiker *et al.*, 1999) and references therein). In addition, Ca^{2+}-Cmd has a role in vesicle fusion and neurotransmitter release, through the regulation of SNAREs assembly (Di Giovanni *et al.,* 2010; Liu *et al.,* 2014; Wang *et al.,* 2014).

Other *in vitro* studies reconstituting fusion among mammalian endosomes, have shown a role for Cmd in the regulation of homotypic endosome fusion, suggesting the Cmd-dependent kinase II, EEA1 and SNAREs as possible targets for Cmd (Colombo *et al.*, 1997; Mills *et al.*, 2001). Cmd is also thought to have a role in LE-lysosome fusion (Pryor *et al.*, 2000). Nevertheless, it remains to be resolved exactly how Cmd regulates the different membrane traffic events *in vivo*.

1.2.4. Physiological functions of calmodulin in multicellular organisms

As already described, Cmd is widely expressed in all higher eukaryotic cells, and several Cmd-stimulated proteins have been described, such as Serine/Threonine protein kinases, calcineurin, nitric oxide synthases, ion transporters and cytoskeletal proteins (Figure 18). The Cmd regulation of these targets mediates a variety of important cellular processes such as signaling, metabolism, cytoskeletal

regulation, ion channel regulation, cell survival, regulation of enzymatic activities, synaptic transmission and plasticity, fast axonal transport, regulation of gene expression, smooth muscle contraction, secretion, growth cone elongation, organelle tubulation, cell motility and chemotaxis (Bachs *et al.*, 1994; Deisseroth *et al*., 1998; Dick *et al*., 2008; Hinrichsen, 1993; Lladó *et al*., 2008; Lu & Means, 1993; McLaughlin & Murray, 2005; Walsh, 1994; Wayman *et al.*, 2009; Xia *et al.,* 1998). Thus, Cmd plays a uniquely important role in vital physiological processes in higher organisms, including inflammation, short-term memory, or the immune response. It also seems to be implicated in the entry of certain virus in the cells (Radding *et al.*, 2000). Therefore, it is not surprising that its misfunction is associated with the development of AIDS, Alzheimer disease, some cancers, neuropsychiatric disorders and other diseases (Berchtold & Villalobo, 2014; Coticchia *et al.* , 2013; O'Day & Myre, 2004; Radding *et al*., 2000; Robison, 2014)

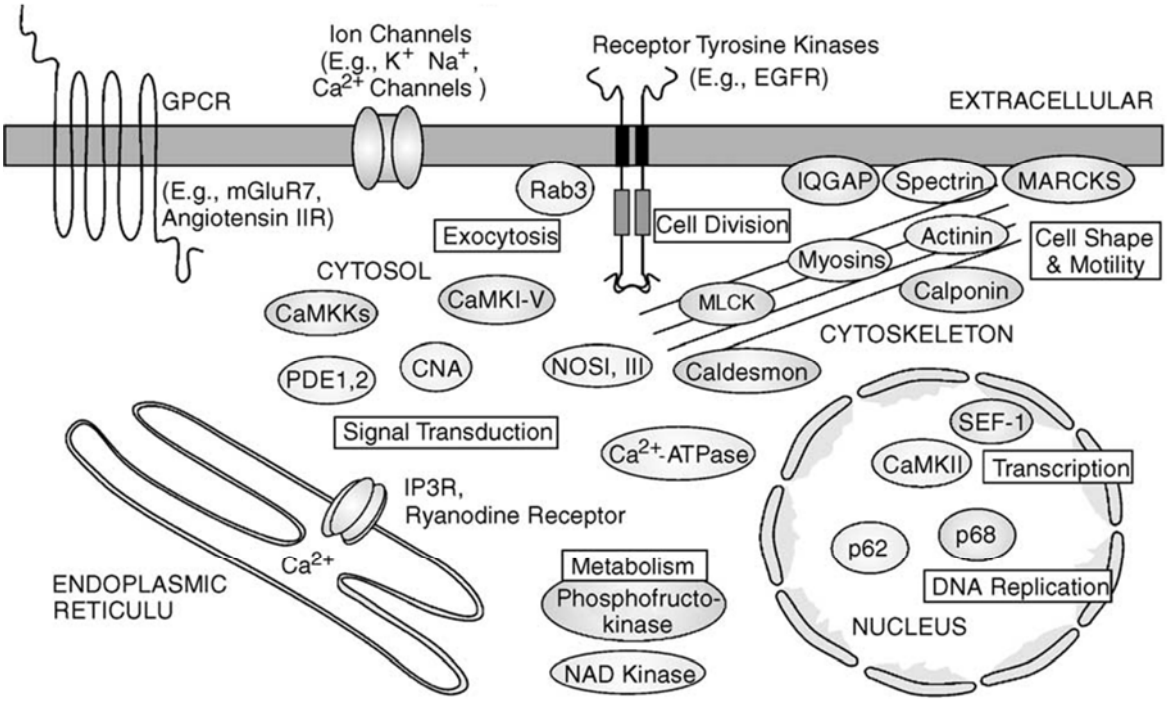

Figure 18. Some calmodulin binding proteins with their cellular localizations and functions in higher eukaryotes. Some Cmd binding proteins (CmdBPs) are targets for Ca^{2+}-Cmd mediated signal transduction, and have been shown to regulate G-protein coupled receptors (GPCRs), such as the metabotropic glutamine receptor 7 (mGluR7) and the angiotensin II receptor (Angiotensin IIR), as well as receptor tyrosine kinases such as the epidermal growth factor receptor (EGFR). On the ER, Cmd interacts with ryanodine and inositol 1,4,5 trisphosphate receptors (IP3R) for example. In the cytosol, Cmd binds the A subunit of calcineurin (CNA), a Ca^{2+}-Cmd-dependent phosphatase, Cmd-dependent kinases (CaMKI-V), CaMK kinases (CaMKKs), nitric oxide synthases I and III (NOSI, III) and phosphodiesterases 1 and 2 (PDE1,2), to name a few. At the cell membrane, Cmd regulate various ion channels as Na^{+}, K^{+} and Ca^{2+} channels, and other membrane associated proteins (often transiently) includimg Rab3 (a monomeric GTPase involved in exocytosis) and several proteins that interact with the cytoskeleton including IQGAP, spectrin and myristoylated arginine-rich C kinase substrate (MARCKS). Some cytoskeletal regulatory components such as α-actinin, caldesmon, calponin, various myosin isoforms, and myosin light chain kinase (MLCK) have been shown to bind Cmd, as well as various enzimes as Ca^{2+}-ATPase, phosphofructo-kinase and NAD kinase. In the nucleus, some CmdBPs regulate transcription (SEF-1, CaMKII), DNA replication (p68) and other nuclear events (p62). (Figure taken from (O´Day, 2003)).

2. OBJECTIVES

Previous studies from other laboratories showed that mammalian and yeast purified coated vesicles, triskelions and light and heavy chains bound calmodulin *in vitro* in a calcium dependent manner (Linden *et al*., 1981; Lisanti *et al*., 1982; Merisko *et al.*, 1988; Pley, 1995; Salisbury *et al.*, 1980a; Silveira *et al*., 1990). However, despite the extensive clathrin functional and biochemical studies, the exact role of clathrin interaction with calmodulin is still unknown. The objective of this Thesis is to address the study of this aspect of the biology of clathrin that has not been studied thus far, using yeast *Saccharomyces cerevisiae* as a model system. The objectives we present are:

- Determine if the clathrin-calmodulin interaction occurs *in vivo* and if it is calcium dependent.
- If so, identify the Chc1 and Clc1 regions involved in the interaction and generate clathrin mutants unable to interact with calmodulin.
- Identify Cmd1 point mutants that specifically affect the clathrin-calmodulin interaction.
- Characterize the common membrane traffic defects installed in the Cmd1 and clathrin mutants that disrupt their interaction, to precisely define its cellular function.
- If a specific clathrin-dependent membrane traffic event is altered by the disruption of the clathrin-calmodulin interaction, start dissecting the molecular mechanism behind.

3. RESULTS

3.1. Analysis of yeast clathrin heavy and light chain interaction with calmodulin

3.1.1. Chc1 and Clc1 bind Cmd1 in yeast in a calcium-dependent manner

It was already shown in previous studies from other laboratories that mammalian purified coated vesicles, triskelions and light chains bind to Cmd-sepharose columns and that Cmd specifically binds to purified coated vesicles *in vitro,* in a calcium-dependent manner (Linden *et al*., 1981; Lisanti *et al*., 1982; Pley, 1995; Salisbury *et al.*, 1980; Silveira *et al.*, 1990). In addition, it was also demonstrated that mammalian clathrin heavy chain binds Cmd when purified and immobilized on nitrocellulose membranes (Merisko *et al*.,1988) and that the mammalian and yeast clathrin light chain binds Cmd *in vitro* via its C-terminal region (Pley, 1995). However, it has not been assessed whether the clathrin heavy or light chains interact with Cmd *in vivo*.

To test for a physical interaction between Cmd1 and Chc1 or Clc1 in yeast, we performed immunoprecipitation assays (see section 6.4.4.2.) with a polyclonal serum against Cmd1 (Geli *et al.,* 1998) bound to protein A-Sepharose, from protein extracts of *chc1Δ* and *clc1Δ* yeast strains expressing HA-tagged clathrin heavy or light chains or the untagged versions form centromeric plasmids (*CHC1-HA, CLC1-HA, CHC1* and *CLC1)*. Immunoprecipitations using a pre-immune serum bound to protein A-Sepharose and immunoprecipitations from the untagged clathrin were used as controls. The immunoprecipitations were performed in the presence (Ca^{2+}) or absence (EDTA) of calcium to investigate if the putative Cmd1-clathrin interaction might be calcium-regulated. As shown in Figure 19, the results of the relative amount of Chc1 or Clc1 co-immunoprecipitated with Cmd1 revealed that Cmd1 binds to Chc1 (Figure 19A and 19B) and Clc1 (Figure 19C and 19D) in yeast, and that this interaction occurs mainly in the presence of calcium.

3.1.2. Analysis of the Chc1 and Clc1 domains that bind Cmd1

3.1.2.1. The C-terminal domain of Chc1 and Clc1 binds Cmd1 *in vitro* with the highest affinity

To investigate which domains of Chc1 and Clc1 directly bind Cmd1, we used three different GST-fused fragments of Chc1 (Figure 20A) comprising different

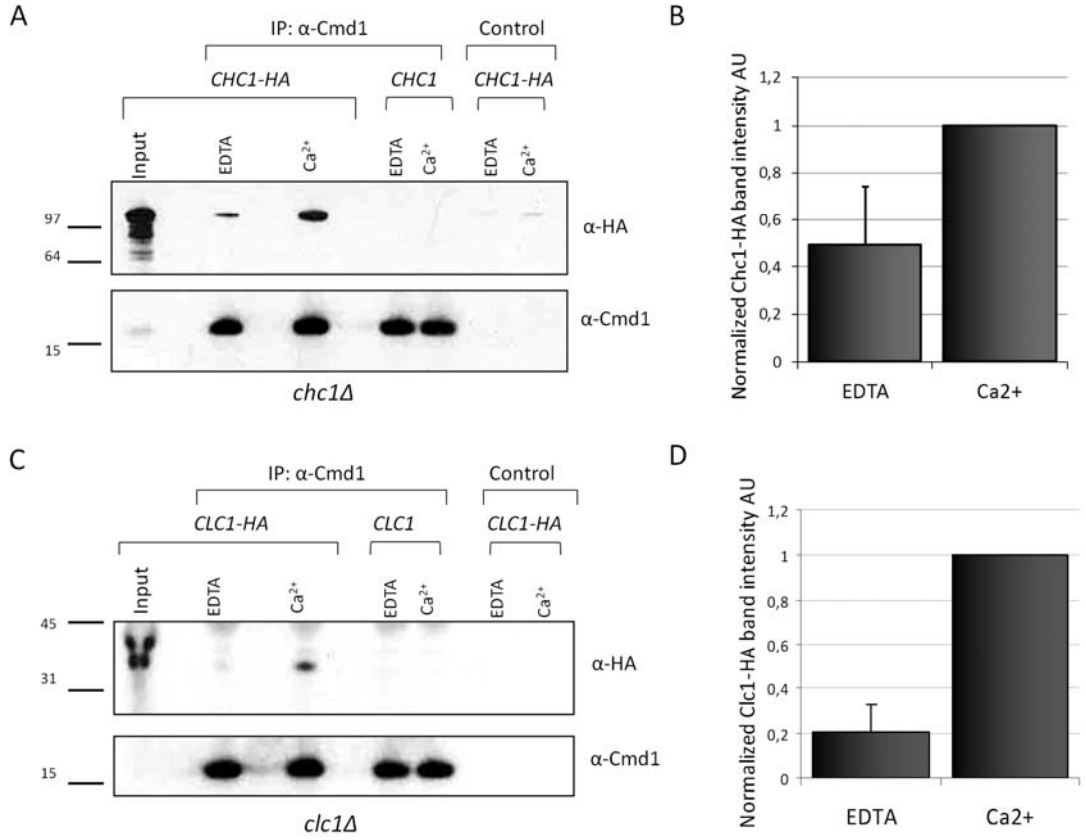

Figure 19. Cmd1 interacts with the clathrin heavy and light chains in yeast and this interaction is calcium-dependent. (A, C) α-Cmd1 and α-HA immunoblots of immunorecipitations with a polyclonal serum against Cmd1 pre-bound to Protein A-Sepharose from non-denaturing extracts of *chc1*Δ (SL114) (A) or *clc1*Δ (SL1620) (C) strains, expressing HA-tagged Chc1 (A) or Clc1 (C) or the untagged versions. Chc1-HA, Clc1-HA, Chc1 and Clc1 were expressed from centromeric plasmids under the control of their own promotor (*CHC1-HA, CLC1-HA, CHC1 and CLC1;* p50-*CHC1-HA*, p111-*CLC1-HA*, p50-*CHC1* and p111-*CLC1,* respectively). Immunoprecipitations with pre-immune serum pre-bound to Protein A-Sepharose were used as controls. The immune or pre-immune Sepharose beads were incubated with the yeast extracts in the presence of 5 mM $CaCl_2$ (Ca^{2+}) or 5 mM EDTA (EDTA) for 1 hour at 4ºC, and then they were pelleted, rinsed several times and boiled in the presence of SDS-PAGE sample buffer. Proteins were separated in a NuPAGE Bis-Tris 4-12 % gradient gel and transferred to a nitrocellulose filter. A peroxidase-conjugated anti-HA antibody (α-HA) and an antibody against Cmd1 (α-Cmd1) combined with an appropriate secondary antibody, were used to detect HA-tagged proteins and Cmd1, respectively. (B, D) Average band intensity of the co-immunoprecipitated Chc1-HA (B) or Clc1-HA (D) for the experiments described in (A, C). At least three independent experiments were performed per sample. Quantifications were performed with ImageJ. The average of the Chc1-HA or Clc1-HA band intensities was normalized to the band intensity of the immunoprecipitated Cmd1 for each sample, deducting also the band intensity for the control samples. Results were then normalized to the maximum value. The statistical significance was tested using the two-tailed Student's t-test ($p \geq 0.05$). AU: arbitrary units.

domains of Chc1: the terminal domain (Te) and the linker (L) (GST-Chc1-N); the distal domain (D) (GST-Chc1-D); and the proximal (P) and the trimerization domains (Tr) (GST-Chc1-C). Two Clc1 GST-fused constructs were used (Figure 20B), one containing the full length protein (GST-Clc1) (Newpher & Lemmon, 2006) and

another lacking the described Cmd1 binding site (Cbs) defined in (Newpher *et al*., 2006; Pley, 1995) (GST-Clc1-cbsΔ). The constructs were expressed in and purified from *E. coli* and we analyzed the interaction of these purified polypeptides with purified 6His-Cmd1 by pull down assays with glutathione-Sepharose beads in the presence of $CaCl_2$ or EDTA (see section 6.4.4.1.) (Figure 20C and 20D). The results showed that the C-terminal fragment (aa 1062-1653) of Chc1, which contained the proximal and trimerization domains, interacted with Cmd1 with the highest affinity in a calcium-dependent manner. The N-terminal Chc1 fragment (aa 1-500) also bound Cmd1, albeit with lower affinity. As previously described (Newpher *et al*., 2006; Pley, 1995), we found that Clc1 bound Cmd1 through a region in its C-terminal domain (aa 212-225), since deleting this region (cbs) significantly impaired the interaction. These results revealed that Chc1 and Clc1 both bind Cmd1 *in vitro* in a calcium-dependent manner through a region in their C-terminus and that this interaction is direct.

3.1.2.2. Identification of a Cmd1 binding site in the C-terminus of Chc1

3.1.2.2.1. Deletion of a putative Cmd1 binding site in Chc1 predicted *in silico* significantly affects its interaction with Cmd1 *in vitro*

Since the C-terminal part of Chc1 binds Cmd1 *in vitro* with the highest affinity (Figure 20), we decided to characterize in more detail the Cmd1 binding site in Chc1. For that, we performed an *in silico* analysis of the amino acid sequence of Chc1 using the tool "Binding site search" in the "Calmodulin Target Database" (Yap *et al*., 2000) that searches for possible Cmd-binding site motifs in the protein sequence of interest based on hydropathy, alpha-helical propensity, residue weight, residue charge and weight and hydrophobic residue content. The analysis indeed found a highly probable putative Cmd1 binding site in the C-terminal domain of Chc1, between amino acids 1491 and 1539, next to the trimerization domain (Figure 21A). The analysis of the protein sequence of Clc1 also predicted a highly probable Cmd1 binding site between amino acids 208 to 233, which actually comprises the previously defined Cmd1 binding site (aa 212-225, (Newpher *et al*., 2006; Pley, 1995)) (Figure 21C). As it is represented in the crystal structure of a clathrin heavy and light chain complex from *Bos Taurus* shown in Figure 21E (http://www.ncbi.nlm.nih.gov/Structure/mmdb/mmdbsrv.cgi)

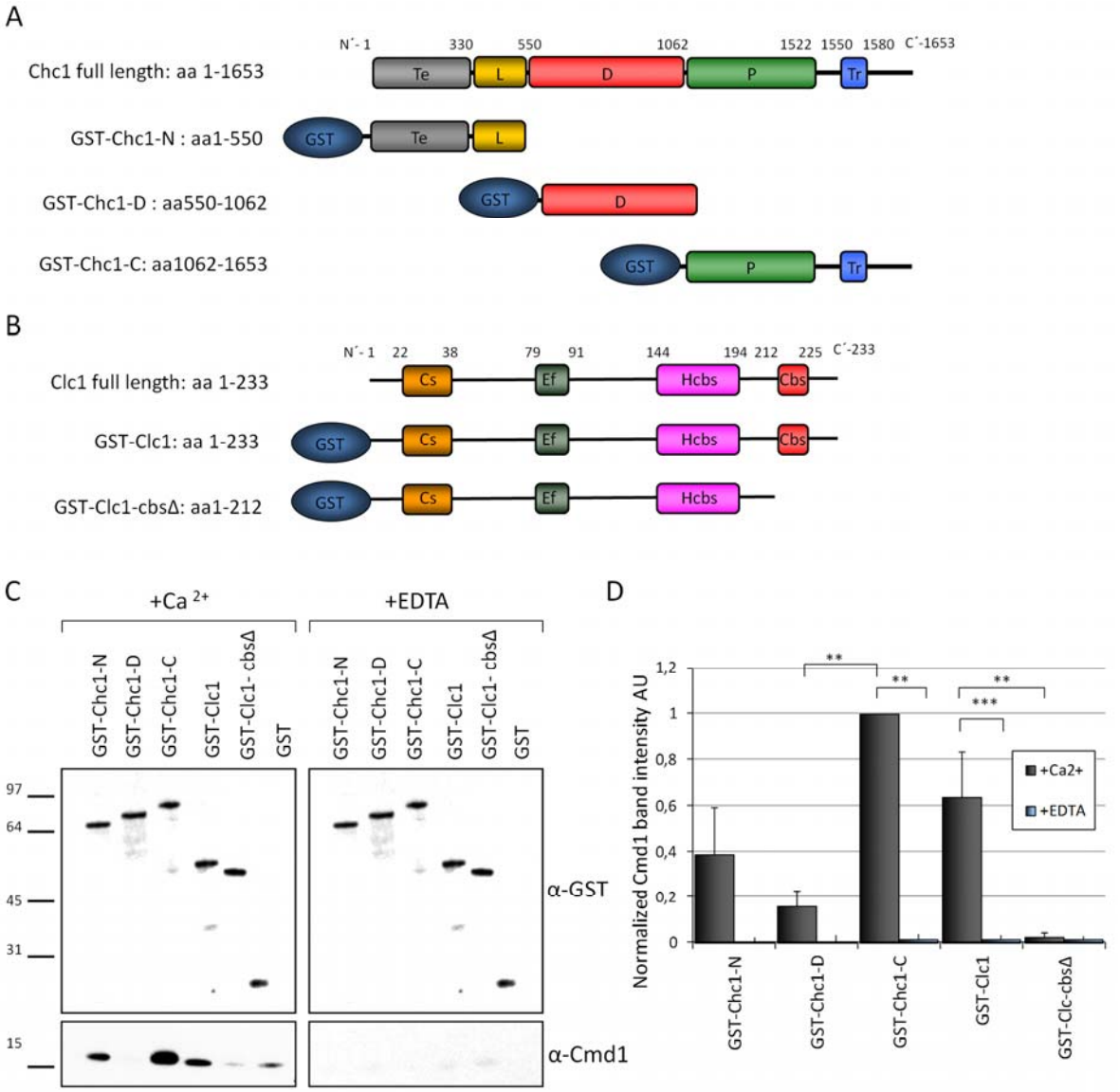

Figure 20. The C-terminal domain of Chc1 directly interacts with Cmd1 *in vitro* with the highest affinity, and this interaction is calcium-dependent. (A) Domain organization of the yeast clathrin heavy chain (Chc1) and the different GST-tagged constructs used in the pull down experiment showed in (C, D). Te: terminal domain. L: linker. D: distal domain. P: proximal domain. Tr: trimerization domain. (B) Domain organization of the yeast clathrin light chain (Clc1) and the different GST-tagged constructs used in the pull down experiment showed in (C, D). Cs: Sla2 binding conserved sequence. Ef: Ca^{2+} binding EF-hand. Hcbs: clathrin heavy chain binding site. Cbs: calmodulin binding site. (C) Immunoblots of glutatione-Sepharose pull downs of the different GST-fused clathrin constructs or GST alone, incubated 1 hour at 4ºC with purified 6xHis-Cmd1 (expressed from pQE11-*CMD1*) in the presence of $CaCl_2$ 5 mM (+Ca^{2+}) or EDTA 5 mM (+EDTA). Beads were pelleted, rinsed several times and boiled in the presence of SDS-PAGE sample buffer. GST-fusion proteins were separated in a NuPAGE Bis-Tris 4-12 % gradient gel and transferred to a nitrocellulose filter. Antibodies against GST (α-GST) and against Cmd1 (α-Cmd1), combined with an appropriate secondary antibody, were used to detect the GST fusion proteins (to demonstrate equivalent protein loading) and Cmd1, respectively. (D) Quantification of the pull down shown in (C). The graph shows the average band intensity of the 6xHis-Cmd1 pulled down by the different GST constructs, with respect to the band intensity of the corresponding GST fusion protein. The band intensity of the 6xHis-Cmd1 pulled down by the GST control was deducted from the rest of the samples, and results were normalized to the maximum value. Quantifications were performed with ImageJ. At least three independent experiments were performed per sample. The statistical significance was tested using

the two-tailed Student's t-test. ** represents a p-value ≤ 0.01; *** represents a p-value ≤ 0.001. AU: arbitrary units.

the putative Cmd binding site in heavy and light chains lied within the same region of the triskelion, next to the trimerization domain.

Interestingly, when analyzing the putative Cmd binding motifs in the sequence of clathrin heavy and light chains in different eukaryotic species (*Saccharomyces cerevisiae, Homo sapiens, Drosophila melanogaster* and *Caenorhabditis elegans*) using the same tool "Binding site search" of the "Calmodulin Target Database" (Figure 21B and 21D), we found that the putative Cmd1 binding site found *in silico* in the clathrin heavy chains analyzed was highly conserved, being located in the same C-terminal region of the heavy chain near the trimerization domain, being a conserved feature of all clathrins. On the contrary, the putative Cmd binding site sequence found *in silico* in the different light chain sequences was not so conserved, given the fact that the general clathrin light chain amino acid sequence is not highly conserved along evolution.

To analyze the ability of the putative Cmd1 binding site (cbs) in Chc1 to bind Cmd1 *in vitro*, we created a Chc1 C-terminal mutant lacking the putative Cmd1 binding site (cbsΔ; aa 1491-1539), fused to GST (GST-Chc1-C-cbsΔ) (Figure 22A) and performed pull down experiments in the presence of $CaCl_2$ (Ca^{2+}) or EDTA. The experiments revealed that the deletion of this putative Cmd1 binding site, significantly affected the calcium-dependent Chc1-Cmd1 interaction *in vitro*, as compared with the wild type C-terminal Chc1 fragment (Figure 22B and 22C). No significant effect was found in the presence of EDTA, as both the WT and mutant C-terminal domain of Chc1 did not bind Cmd1. Thus, the putative Cmd1 binding site identified *in silico* is responsible for the binding of Cmd1 to the C-terminal domain of Chc1.

3.1.2.2.2. The Chc1-cbsΔ and Clc1-cbsΔ mutants are unstable and bind Cmd1 with less affinity in yeast

To further characterize the effect of the deletion of the putative Cmd1 binding site (cbs) of Chc1 or Clc1 on the ability to bind Cmd1 in yeast , we generated

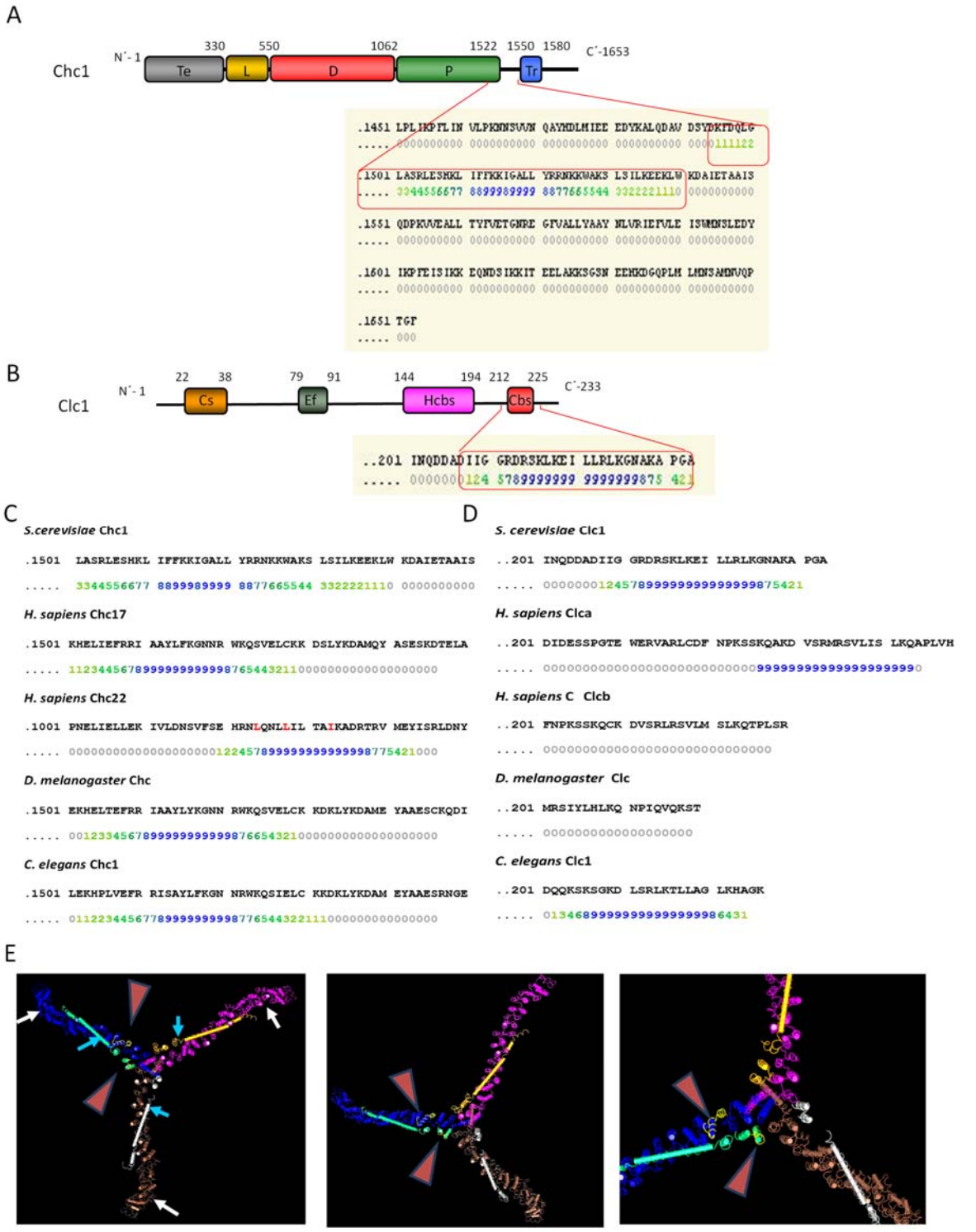

Figure 21. The *in silico* search for putative Cmd1 binding sites in Chc1 and Clc1 finds a high scored region at their C-terminus of both chains. (A, B) Domain organization of the yeast clathrin heavy chain (Chc1) (A) and light chain (Clc1) (B) showing the most probable Cmd1 binding site found using the Cmd binding motif prediction tool "Binding site search" (http://calcium.uhnres.utoronto.ca/ctdb/ctdb/sequence.html) in the "Calmodulin Target Database". Normalized scores (0 to 9) are shown below the sequence. Scoring is based on the evaluation criteria for determining the putative Cmd1 binding motifs (hydropathy, α-helical propensity, residue weight, residue charge, hydrophobic residue content, helical class, occurrence of particular residues). Scores were evaluated for a sliding twenty-residue window and normalized for the entire sequence. A consecutive string of high values

indicates the location of a putative binding site: amino acids 1491 to 1539 in Chc1 and amino acids 208 to 233 in Clc1. Te: terminal domain. L: linker. D: distal domain. P: proximal domain. Tr: trimerization domain. Cs: Sla2 binding conserved sequence. Ef: Ca^{2+} binding EF-hand. Hcbs: clathrin heavy chain binding site. Cbs: calmodulin binding site. (C,D) Amino acid sequence of the clathrin heavy chain (B) or light chain (D) putative Cmd binding site regions found in the indicated different species using the same tool "Binding site search" in the "Calmodulin Target Database". (E) Crystal structure of a clathrin heavy chain (white arrows) and a clathrin light chain (blue arrows) complex from *Bos Taurus.* The putative Cmd binding site in clathrin heavy and light chains is coloured in yellow and marked with a red pointer. Source: http://www.ncbi.nlm.nih.gov/Structure/mmdb/mmdbsrv.cgi.

HA-tagged Chc1 and Clc1 mutants lacking the Cmd1 binding site under the control of their own promoter (Figure 23A). Analysis of the expression of the WT and mutant clathrin heavy or light chain constructs expressed from centromeric plasmids (*CHC1-HA* CEN and *chc1- cbsΔ-HA* CEN or *CLC1-HA* CEN and *clc1-cbsΔ-HA* CEN) in *chc1Δ* or *clc1Δ* cells, respectively (Figure 23B and 23C), showed that the mutants were unstable comparing to the WT proteins, since the Chc1-cbsΔ-HA was expressed ten fold less that the WT and the Clc1-cbsΔ-HA mutant was undetectable by immunoblot. To obtain similar expression levels to the WT clathrin chains, we cloned the mutant ORFs in multicopy plasmids (*chc1-cbsΔ-HA* 2µ and *clc1-cbsΔ- HA* 2µ). When expressed from multicopy plasmids, the Clc1-cbsΔ mutant was expressed to a similar level than the WT Clc1-HA expressed from a centromeric plasmid, and the Chc1-cbsΔ mutant, was expressed approximately double, as compared to the WT Chc1, expressed from a centromeric plasmid.

Next, we performed co-immunoprecipitation experiments with a polyclonal serum against Cmd1 bound to protein A-Sepharose, from non-denaturing extracts of *chc1Δ* strains expressing either the HA-tagged WT Chc1 from a centromeric plasmid (*CHC1-HA* CEN) or the Chc1-cbsΔ mutant from centromeric (*chc1-cbsΔ*-HA CEN) (Figure 24A and 24B) or from multicopy (*chc1-cbsΔ-HA* 2µ) plasmids (Figure 24C and 24D).

Immunoprecipitations using a pre-immune serum bound to protein A-Sepharose and immunoprecipitations from the untagged Chc1 were used as controls. Analysis of the relative amount of Chc1 or Chc1-cbsΔ that co-immunoprecipitated with Cmd1 indicated that the Chc1-cbsΔ mutant (*chc1-cbsΔ* CEN) (Figure 24A and 24B) bound less Cmd1 in the presence of calcium, as compared with the WT Chc1. Co-

immunoprecipitations from yeast extracts expressing the Chc1-cbsΔ mutant from a multicopy plasmid (*chc1-cbsΔ* 2μ) (Figure 24C and 24D) after adjusting the Chc1-cbsΔ concentration to the Chc1 concentration from WT cells, and from three different serial dilutions, revealed that whereas Cmd1 could still co-precipitate

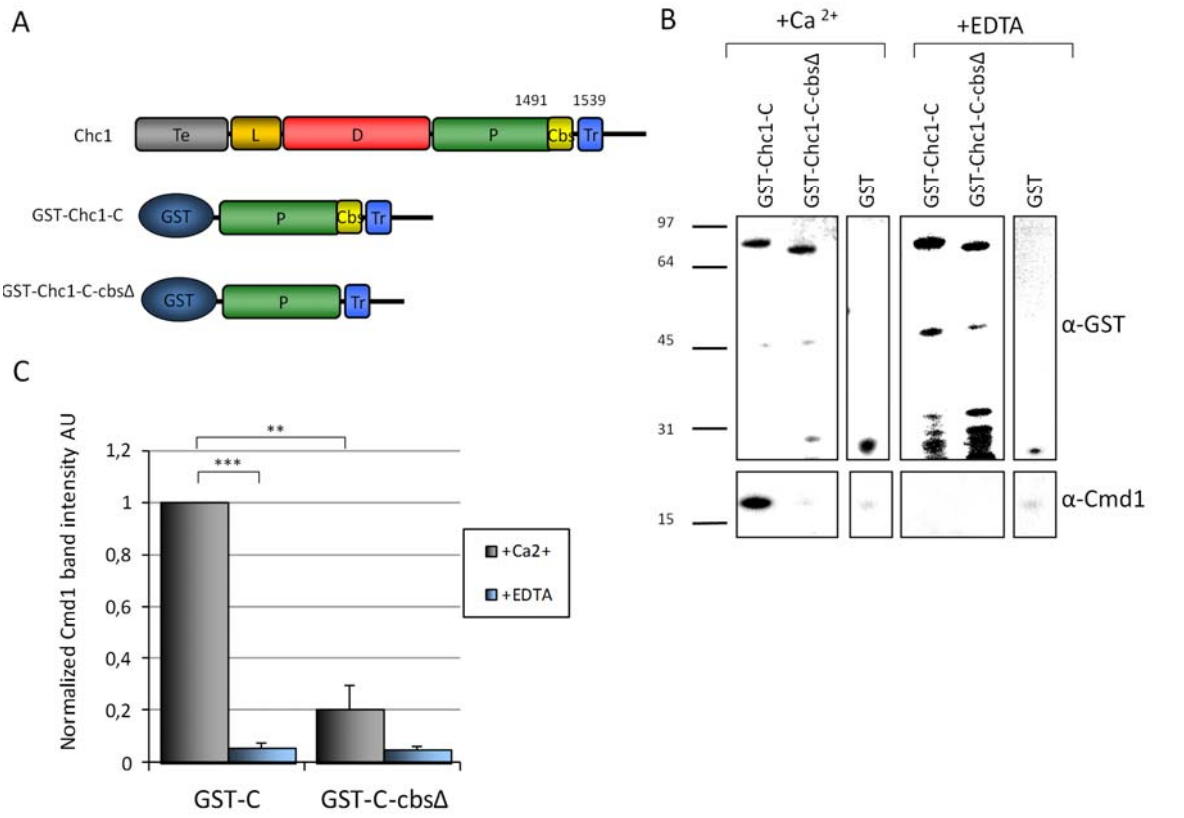

Figure 22. The Chc1 C-terminus that lacks the putative Cmd1 binding site does not bind Cmd1 *in vitro*. (A) Domain organization of the yeast clathrin heavy chain (Chc1) and the different GST-tagged constructs used in the pull down experiment showed in (B, C). Te: terminal domain. L: linker. D: distal domain. P: proximal domain. Cbs: putative Cmd1 binding site. Tr: trimerization domain. (B) Immunoblots of pull downs with the indicated GST-fused clathrin constructs or GST alone pre-bound to glutathione-Sepharose beads, incubated with purified 6xHis-Cmd1 (expressed from pQE11-*CMD1*) in the presence of $CaCl_2$ 5 mM (+Ca^{2+}) or EDTA 5 mM (+EDTA). Beads were pelleted, rinsed several times and boiled in the presence of SDS-PAGE sample buffer. GST-fusion proteins were separated in a NuPAGE Bis-Tris 4-12 % gradient gel and transferred to a nitrocellulose filter. Antibodies against GST (α-GST) and against Cmd1 (α-Cmd1), combined with an appropriate secondary antibody, were used to detect the GST fusion proteins (to demonstrate equivalent protein loading) and Cmd1, respectively. (C) Quantification of the pull downs shown in (B). The graph shows the average band intensity of the 6xHis-Cmd1 pulled down by the different GST constructs with respect to the band intensity of the corresponding GST fusion protein. The band intensity of the 6xHis-Cmd1 pulled down by the GST control was deducted from the rest of the samples, and results were normalized to the maximum value. Quantifications were performed with ImageJ. At least three independent experiments were performed per sample. The statistical significance was tested using the two-tailed Student's t-test. ** represents a p-value ≤ 0.01; *** represents a p-value ≤ 0.001. AU: arbitrary units.

WT Chc1 from highly diluted yeast extracts (1/10), it bound much less Chc1-cbsΔ. The result indicated that the affinity of Chc1 for Cmd1 was greatly diminished when its putative Cmd1 binding site was deleted. However, the Chc1-cbsΔ was still able to bind Cmd1 to a certain extent, probably via a less affinity binding site located at the N-terminus of Chc1 (Figure 20) or via an indirect interaction mediated by the Clc1.

These results suggested that a major Cmd1 binding site in Chc1 is located in the Chc1 C-terminal domain.

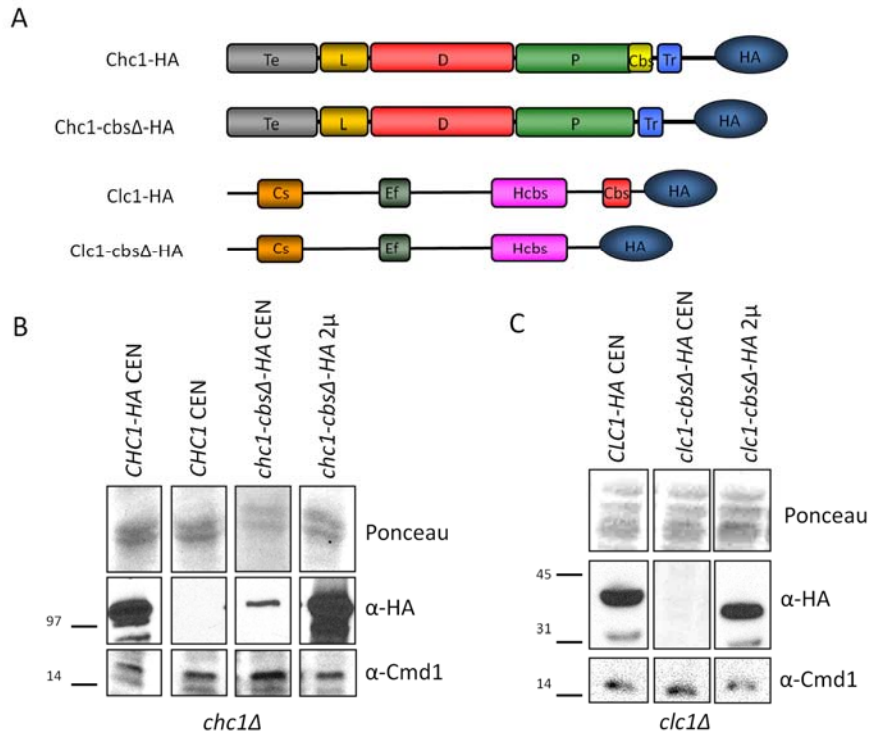

Figure 23. Analysis of the expression of the HA-tagged Chc1-cbsΔ and Clc1-cbsΔ mutants in *chc1Δ* and *clc1Δ* strains, respectively. (A) Domain organization of the HA-tagged Chc1 and Clc1 constructs analyzed in (B, C). Te: terminal domain. L: linker. D: distal domain. P: proximal domain. Cbs: putative Cmd1 binding site. Tr: trimerization domain. Cs: Sla2 binding conserved sequence. Ef: Ca^{2+} binding EF-hand. Hcbs: clathrin heavy chain binding site. (B,C) Immunoblots of total protein extracts from *chc1Δ* (SL114) (B) or *clc1Δ* (SL1190) (C) cells, expressing Chc1, Chc1-HA and Chc1-cbsΔ-HA (B) or Clc1-HA or Clc1-cbsΔ-HA (C), respectively. Chc1, Chc1-HA and Clc1-HA were expressed from centromeric plasmids (*CHC1 CEN*, *CHC1-HA* CEN, and *CLC1-HA* CEN; p50-*CHC1*, p50-*CHC1-HA* and p111-*CLC1-HA,*respectively) and Chc1-cbsΔ-HA and Clc1-cbsΔ-HA mutants were expressed from either centromeric or multicopy plasmids, all under the control of their own promotor (*chc1-cbsΔ-HA* CEN or 2μ and *clc1-cbsΔ-HA* CEN or 2μ*;* p50-*chc1-cbsΔ-HA* or p195-*chc1-cbsΔ-HA* and p111-*clc1-cbsΔ-HA* or p181-*clc1-cbsΔ-HA,* respectively). Ponceau red staining was used to demonstrate equivalent protein loading. A peroxidase-conjugated antibody against HA (α-HA) was used to detect the HA-tagged constructs and an antibody against Cmd1 (α-Cmd1), combined with an appropriate secondary antibody, was used to detect Cmd1. 25 μg of total protein was loaded per lane.

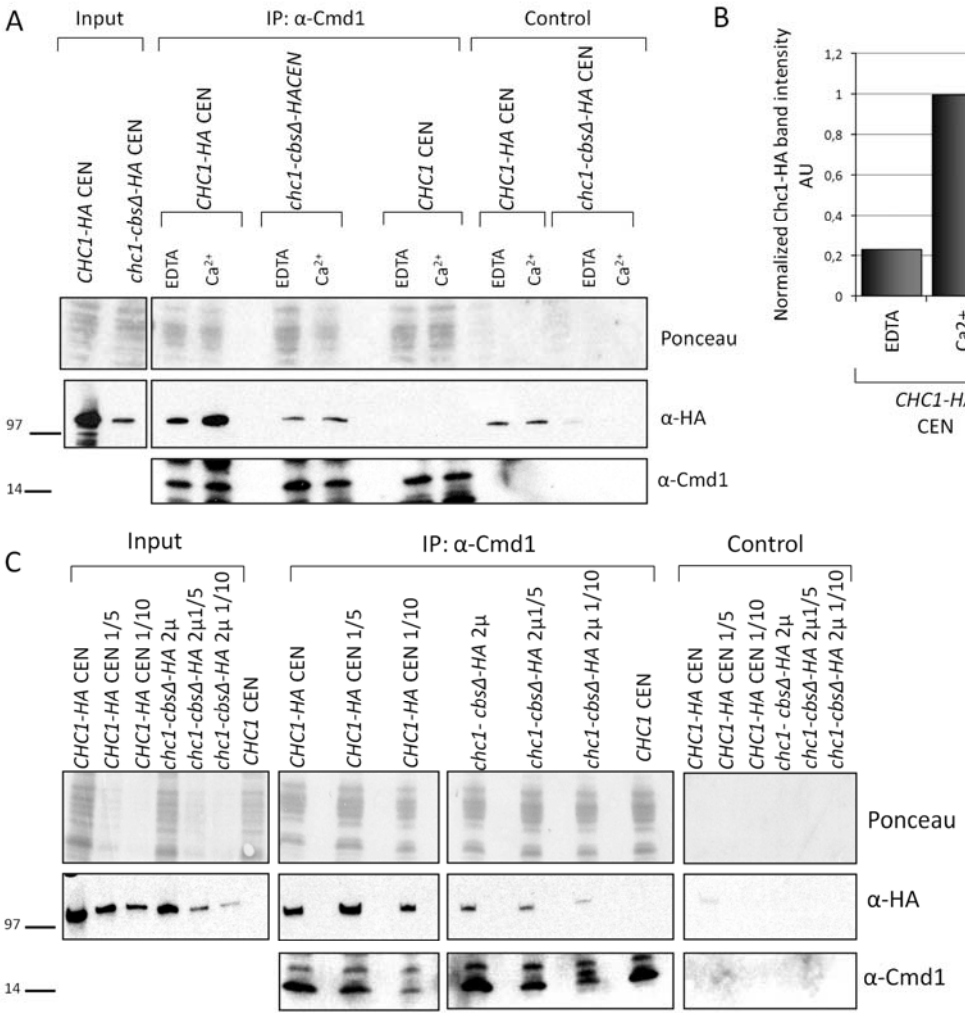

Figure 24. The Chc1-cbsΔ mutant binds Cmd1 in yeast with less affinity than the WT Chc1. (A, C) Immunoblots of immuniorecipitations with a polyclonal serum against Cmd1 pre-bound to Protein A- Sepharose from non-denaturing extracts of a *chc1*Δ (SL114) strain, expressing Chc1-HA, Chc1 and Chc1-cbsΔ-HA. Chc1-HA and Chc1 were expressed from centromeric plasmids, (*CHC1* CEN and *CHC1-HA* CEN; p50-*CHC1-HA* and p50-CHC1, respectively), and Chc1-cbsΔ-HA was expressed from either centromeric (A) or multicopy (C) plasmids (*chc1-cbsΔ-HA* CEN and 2μ; p50-*chc1-cbsΔ-HA* and p195-*chc1-cbsΔ-HA,* respectively), all under the control of their own promotor. Immunoprecipitations with pre-immune serum pre-bound to Protein A-Sepharose beads for each construct were used as controls. The immune or pre-immune Sepharose beads were incubated with the different yeast extracts at equivalent protein concentrations (A) or with serial dilutions of yeast extracts adjusted at equivalent protein concentrations (C) in the presence of 5 mM $CaCl_2$ (Ca^{2+}) or 5 mM EDTA (EDTA) (A) or incubated only in the presence of 5 mM $CaCl_2$ (C). The beads were pelleted, rinsed several times and boiled in the presence of SDS-PAGE sample buffer. Proteins were separated in a NuPAGE Bis-Tris 4-12 % gradient gel and transferred to a nitrocellulose filter. Ponceau red staining was used to demonstrate equivalent protein loading. A peroxidase-conjugated anti-HA antibody (α-HA) and an antibody against Cmd1 (α-Cmd1), combined with an appropriate secondary antibody, were used to detect HA-tagged proteins and Cmd1, respectively (B, D). Average band intensity of the immunoprecipitated Chc1-HA and Chc1-cbsΔ-HA for the immunoblots shown in (A, C). Quantifications were performed with ImageJ. The average of the HA-tagged constructs band

intensity was normalized to the band intensity of the immunoprecipitated Cmd1 for each sample, deducting also the band intensity for the control samples. Results were then normalized to the corresponding input band size and then to the maximum value (B) or to the WT Chc1 (D). AU: arbitrary units.

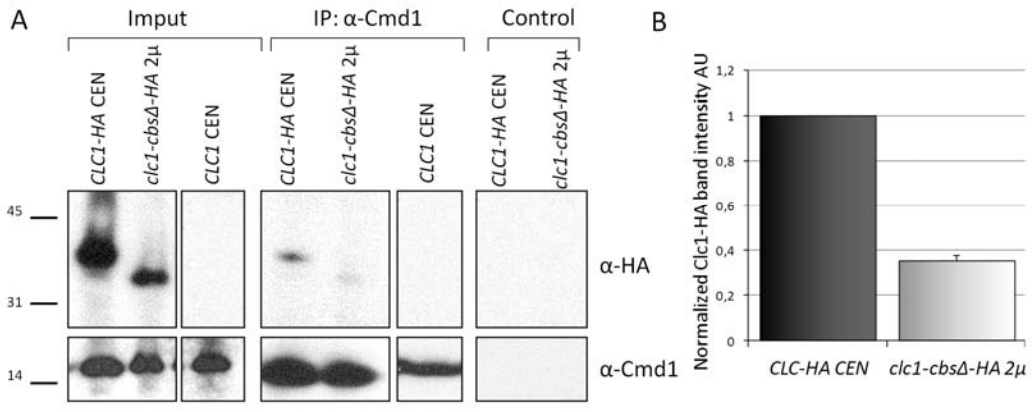

Figure 25. The Clc1-cbsΔ mutant binds Cmd1 in yeast with less affinity than the WT Clc1. (A) Immunoblot of immunoprecipitations with a polyclonal serum against Cmd1 pre-bound to Protein A-Sepharose, from non-denaturing extracts of a *clc1*Δ (SL1620) strain, expressing Clc1-HA, Clc1 and Clc1-cbsΔ-HA. Clc1-HA and Clc1 were expressed from centromeric plasmids (*CLC1-HA* CEN and *CLC1* CEN; p111-*CLC1-HA* and p111-*CLC1*, respectively), and Clc1-cbsΔ-HA was expressed from a multicopy plasmid (*chc1-cbsΔ-HA* 2μ; p181-*clc1-cbsΔ-HA*), all under the control of their own promotor. Immunoprecipitations of pre-immune serum pre-bound to Protein A-Sepharose beads were used as controls. The immune or pre-immune Sepharose beads were incubated with the different yeast extracts at equivalent protein concentration in the presence of 5 mM $CaCl_2$. The beads were pelleted, rinsed several times and boiled in the presence of SDS-PAGE sample buffer. Proteins were separated in a NuPAGE Bis-Tris 4-12 % gradient gel and transferred to a nitrocellulose filter. A peroxidase-conjugated anti-HA antibody (α-HA) and an antibody against Cmd1 (α-Cmd1), combined with an appropriate secondary antibody, were used to detect HA-tagged proteins and Cmd1, respectively. (B) Average band intensity of the immunoprecipitated Clc1-HA and Clc1-cbsΔ-HA for the experiment shown in (A). Two independent experiments were performed for each sample. Quantifications were performed with ImageJ. The average of the HA-tagged constructs band intensity was normalized to the band intensity of the immunoprecipitated Cmd1 for each sample, deducting also the band intensity for the control samples. Results were then normalized to the corresponding input band size and then to the maximum value. AU: arbitrary units.

We also performed co-immunoprecipitation experiments of a yeast *clc1Δ* strain expressing the HA-tagged WT Clc1 (*CLC1-HA* CEN) from a centromeric plasmid or the Clc1-cbsΔ mutant from a multicopy plasmid (*clc1-cbsΔ* 2μ) (Figure 25A and 25B). The results indicated that, although the Clc1-cbsΔ mutant was expressing at similar levels to the Clc1 WT, it bound significantly less Cmd1 in yeast. This result corroborated, together with the pull down experiments with purified components (Figure 20), that the Cmd1 binding site in Clc1 is located within its C-terminal domain (aa 212-225), as previously described.

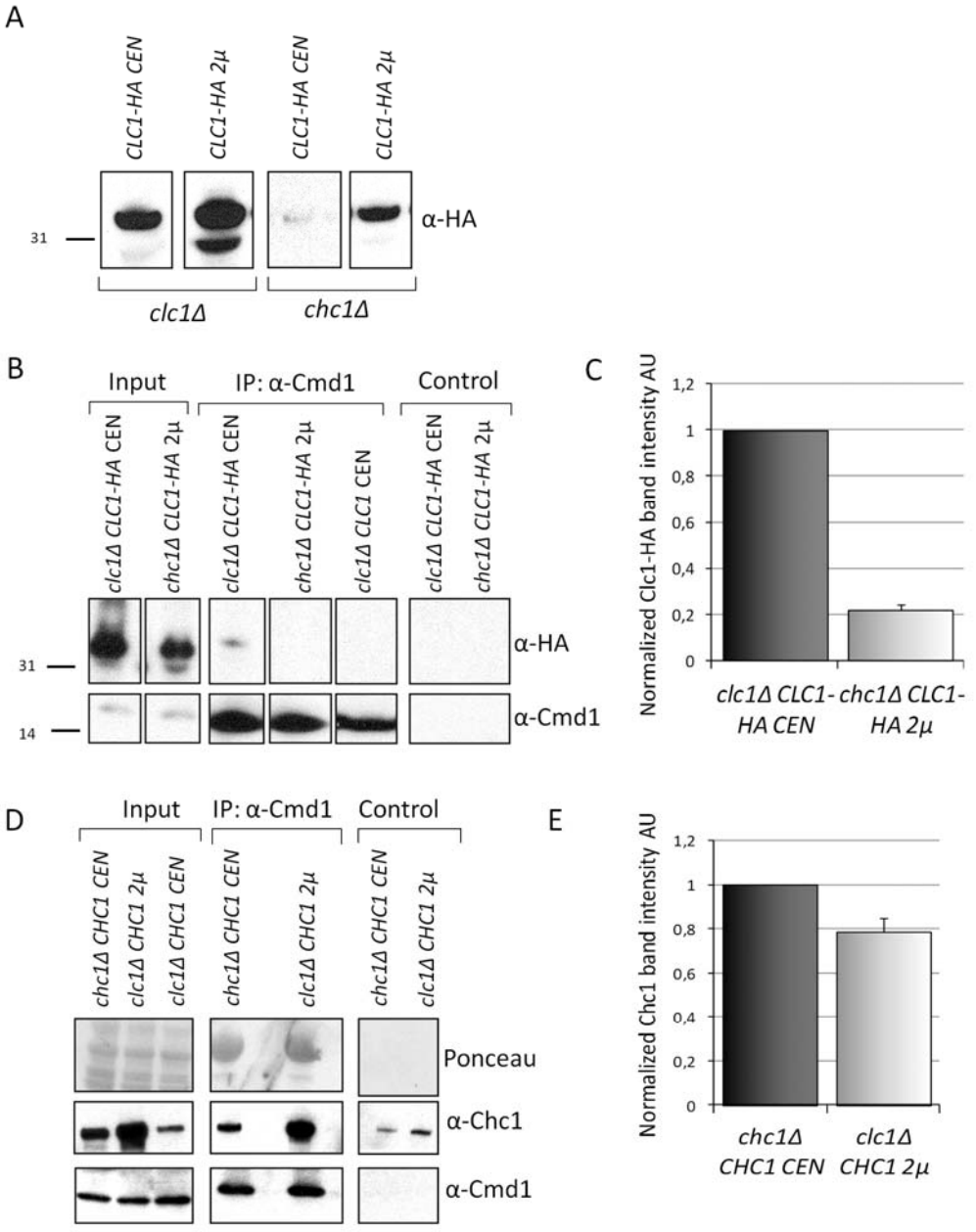

Figure 26. Clc1 binds significantly less Cmd1 in the absence of Chc1, but Chc1 can still bind Cmd1 in the absence of Clc1. (A) Immunoblot of total protein extracts from a *clc1Δ* strain (SL1620) and a *chc1Δ* strain (SL114), expressing Clc1-HA from centromeric or multicopy plasmids under the control of their own promotor *(CLC1-HA* CEN or 2μ; p111-*CLC1-HA* or p181-*CLC1-HA* respectively). An antibody against HA (α-HA) was used to detect the Clc1-HA. 25μg of total protein was loaded per lane. (B, D) Immunoblots of co-inmuniorecipitations with a polyclonal serum against Cmd1 pre-bound to Protein A-Sepharose from *clc1Δ* (SL1620) and *chc1Δ* (SL114) strains expressing Clc1 from a centromeric plasmid (*CLC1* CEN; p111-*CLC1*) or Clc1-HA from centromeric or multicopy plasmids, under the control of their own promotor (*CLC1-HA* CEN or 2 μ; p111-*CLC1-HA* or p181-*CLC1-HA,* respectively) (B) and co-immunoprecipitations from *chc1Δ* (SL114) or *clc1Δ* (SL1620) strains expressing Chc1 from a centromeric or a multicopy plasmid under the control of their own promotor (*CHC1* CEN and *CHC1* 2μ; p50-*CHC1* and Yep24-*CHC1*, respectively) (D). Immunoprecipitations with pre-immune serum pre-bound to Protein A-Sepharose beads from all the strains were used as controls. The immune or pre-immune Sepharose beads were incubated for 1 hour at 4ºC with the yeast extracts in the presence of 5 mM $CaCl_2$ and then they were pelleted, rinsed several times and boiled in the presence of SDS-PAGE sample buffer. Proteins were separated in a NuPAGE Bis-Tris 4-

12 % gradient gel and transferred to a nitrocellulose filter. Ponceau red staining was used to demonstrate equivalent protein loading. A peroxidase-conjugated anti-HA antibody (α-HA), and antibodies against Chc1 (α-Chc1) (D) and Cmd1 (α-Cmd1), combined with an appropriate secondary antibody, were used to detect HA-tagged Clc1, Chc1 and Cmd1, respectively. (C, E) Average band intensity of the immunoprecipitated Clc1-HA (C) or Chc1 (E) for the experiments described in B and D. Two independent experiments were performed per sample. Quantifications were performed with ImageJ. The average of Clc1-HA and Chc1 band intensities was normalized to the band intensities of the immunoprecipitated Cmd1 for each sample, deducting also the band intensities for the corresponding pre-immune control sample. Results were then normalized to the corresponding input band size and then to the maximum value. AU: arbitrary units.

3.1.2.3. Characterization of the contribution of Chc1 and Clc1 to the interaction with Cmd1

3.1.2.3.1. Chc1 is still able to bind Cmd1 in yeast in the absence of Clc1, but Clc1 is not able to bind Cmd1 in yeast in the absence of Chc1

We first analyzed the ability of Chc1 and Clc1 to bind Cmd1 when the other partner chain was not present, in order to investigate if both chains must be present to bind Cmd1 *in vivo* (Figure 26). For that purpose, we performed co-immunoprecipitations with a polyclonal serum against Cmd1 pre-bound to Protein A-Sepharose from *chc1Δ* or *clc1Δ* yeast protein extracts and measured the ability of Clc1 or Chc1 to co-immunoprecipitate with Cmd1, respectively.

As Clc1-HA is unstable when the Chc1 is not present and its expression is barely detectable by immunoblot (Figure 26A), we cloned the *CLC1* gen in a multicopy plasmid to reach expression levels of Clc1-HA in a *chc1Δ* strain similar to that in a *clc1Δ* strain expressing the WT Chc1 (Figure 26A). The results from the relative amount of Clc1-HA that co-immunoprecipitated with Cmd1 in a *chc1Δ* or a *clc1Δ* strain (Figure 26B and 26C) indicated that Clc1 was not able to bind Cmd1 in the *chc1Δ* strain, thus in the absence of Chc1.

Chc1 is also unstable in the absence of Clc1 (in a *clc1Δ* strain) and expresses at least 1/10 the levels of Chc1 in a WT strain (Chu *et al*., 1996), so the *CHC1* gen was also cloned in a multicopy plasmid to increase its expression level in a *clc1Δ* background (Figure 26D, input). As shown in Figures 26D and 26E, Chc1 was still able to bind Cmd1 in the absence of Clc1, when its expression level was increased in the *clc1Δ* background to the levels observed in the WT.

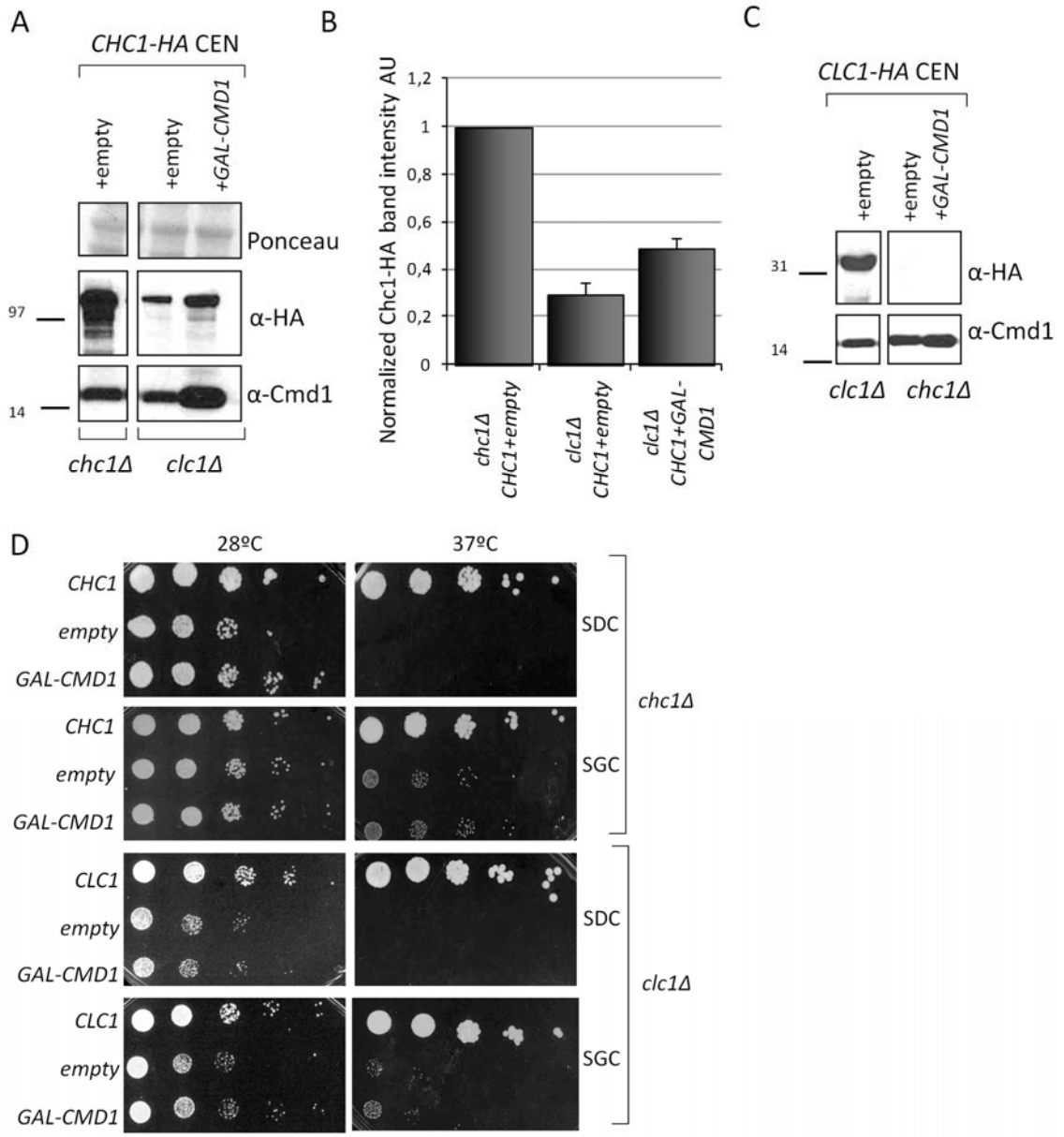

Figure 27. Overexpression of Cmd1 in a *clc1Δ* strain slightly increased Chc1 expression and slightly suppressed its growth defect at restrictive temperature. However, overexpression of Cmd1 in a *chc1Δ* strain neither increased Clc1 expression nor it suppressed its growth defect at restrictive temperature. (A) Immunoblots of total protein extracts from a *chc1Δ* strain (SL114) transformed with a multicopy empty plasmid (+empty; YEplac112) or a centromeric plasmid expressing Chc1-HA under the control of its own promotor (*CHC1-HA* CEN; p50-*CHC1-HA*) and a *clc1Δ* (SL1620) strain expressing Chc1-HA from a centromeric plasmid under the control of its own promotor (*CHC1-HA* CEN; p50-*CHC1-HA*), co-transformed with either a multicopy empty plasmid (+empty; pXY243) or the pXY243-*CMD1* multicopy plasmid expressing Cmd1 under the control of a galactose-inducible promotor (+GAL-*CMD1*). (C) Immunoblots of total protein extracts from a *clc1Δ* strain (SL1620) transformed with either a multicopy empty plasmid (+empty; YEplac112) or with a centromeric plasmid expressing Clc1-HA under the control of its own promotor (*CLC1-HA* CEN; p111-*CLC1-HA*), and a *chc1Δ* (SL114) strain transformed with a centromeric plasmid expressing Clc1-HA under the control of its own promotor (*CLC1-HA* CEN; p111-*CLC1-HA*), and co-transformed with either an empty plasmid (+empty; YEplac112) or a pXY243-*CMD1*-W multicopy plasmid expressing Cmd1 under the control of a galactose-inducible promotor (+GAL-*CMD1*). (A, C) Ponceau red staining was used to demonstrate equivalent protein loading. A peroxidase-conjugated anti-HA antibody (α-HA) was used to detect the

HA-tagged Chc1 and an antibody against Cmd1 (α-Cmd1), combined with an appropriate secondary antibody, was used to detect Cmd1. 25 µg of total protein was loaded per lane. (B) Average band intensity of the expressed Chc1-HA for the experiment described in (A). Quantifications were performed with ImageJ. Two independent experiments were done for each sample. The average Chc1 band intensity was normalized to the Ponceau stainning for each sample. Results were then normalized to the WT Cmd1. AU: arbitrary units. (D) Serial dilutions of *chc1Δ* cells (SL114) transformed with either an empty plasmid (empty; YEplac112), a centromeric plasmid encoding *CHC1,* under the control of its own promotor (*CHC1*; p50-*CHC1*), or a multicopy plasmid encoding *CMD1*, under the control of a galactose-inducible promotor (GAL-*CMD1*; pXY243-*CMD1-W)*, and a *clc1Δ* strain (SL1620) transformed with either a multicopy empty plasmid (empty; pXY243), a centromeric plasmid encoding *CLC1* under the control of its own promotor (*CLC1*; p111-*CLC1*), or a multicopy plasmid encoding *CMD1* under the control of a galactose-inducible promotor (GAL-*CMD1*; pXY243-*CMD1)*. Cells from mid-log phase culture were spotted into SDC (glucose) or SGC (galactose) plates and let grown for 72 hours at either 28ºC or 37ºC.

These results confirmed those obtained by the *in vitro* pull down assays (Figure 20), that indicated that the Cmd1 binding to Chc1 is more robust than the binding to the light chain

3.1.2.3.2. Overexpression of Cmd1 slightly increased Chc1 expression in a *clc1Δ* strain and slightly suppressed its growth defect at restrictive temperature

As Chc1 could still bind Cmd1 in the absence of Clc1, we wanted to assess if overexpression of Cmd1 could stabilize Chc1 expression in the *clc1Δ* strain. For that purpose, we transformed a *clc1Δ* strain with a centromeric plasmid encoding Chc1-HA (*CHC1* CEN) with either a multicopy empty plasmid (+empty) or with a multicopy plasmid encoding Cmd1 under the control of the galactose-inducible promotor (+*GAL-CMD1*), and we analyzed Chc1-HA expression after inducing Cmd1 overexpression in the presence of galactose (see Materials and Methods section 6.1.2.). The results from the immunoblot (Figure 27A and 27B) showed that the Chc1-HA expression was slightly stabilized in the *clc1Δ* strain upon overexpression of Cmd1. On the contrary, and consistent with the observation that Clc1 is not able to bind Cmd1 in the absence of Chc1, overexpression of Cmd1 could not stabilize Clc1 expression in a *chc1Δ* strain.

As overexpression of Chc1 partially rescues the temperature sensitive defect of *clc1Δ* cells (Chu *et al*., 1996) and we have observed that overexpression of Cmd1 increases Chc1 expression in *clc1Δ* cells, we wondered if overexpression of Cmd1 could also suppress the growth defect of a *clc1Δ* strain. Serial dilution cell growth assays in plates containing galactose, showed indeed that Cmd1 overexpression

could slightly rescue the growth defect of *clc1Δ* cells but not the growth defect of *chc1Δ* cells (Figure 27D). The suppression was dependent on the overexpression of Cmd1 since pGAL-*CMD1* failed to suppress the growth defect of the *clc1Δ* in the absence of galactose and the empty plasmid neither suppressed the growth defect of the *clc1Δ* strain in the galactose media.

Altogether the genetic and biochemical experiments indicated a functional and physical interaction between clathrin and Cmd1, which is predominantly hold by the clathrin heavy chain.

3.2. Identification of Cmd1 point mutants that specifically disrupt the interaction with Chc1 and Clc1

3.2.1. The mutations in the Cmd1-228 and Cmd1-242 mutants specifically disrupt the interaction with clathrin *in vitro*

Having identified Chc1 and Clc1 mutations that affected their calcium-dependent interactions with Cmd1 both *in vitro* and in yeast, we next tried to identify Cmd1 point mutations that specifically disrupted the direct Cmd1-Chc1 or Cmd1-Clc1 interaction. For this purpose, 6xHIS tagged versions of the WT and mutant Cmd1s were created and expressed in and purified from *E.coli*, to test their ability to interact with the purified GST-C-terminal fragments of Chc1 or the GST-Clc1. The Cmd1 mutants chosen belong to the collection generated by Ohya and Botstein (Yoshikazu Ohya & Botstein, 1994b), which were created by the combinatorial mutation of phenylalanines, expected to differentially interfere with binding to different targets. Temperature sensitive mutants, representatives of the original complementation groups defined were chosen (Cmd1-226, Cmd1-228, Cmd1-231 and Cmd1-239) (Yoshikazu Ohya & Botstein, 1994a, 1994b). From those, Cmd1-226 and Cmd1-228 were known to interfere with endocytic uptake by altering the interaction with different targets, whereas Cmd1-231 and Cmd1-239 were not defective for endocytosis (M I Geli et al., 1998). We also included the Cmd1-242 mutant, which in spite of not complementing the growth defect of any of the other mutants, exhibited WT uptake kinetics (M I Geli et al., 1998; Yoshikazu Ohya & Botstein, 1994b). Glutathione-Sepharose beads coated with GST or the indicated clathrin constructs were incubated in the presence of $CaCl_2$ and either the purified WT or mutant Cmd1s (Figure 28).

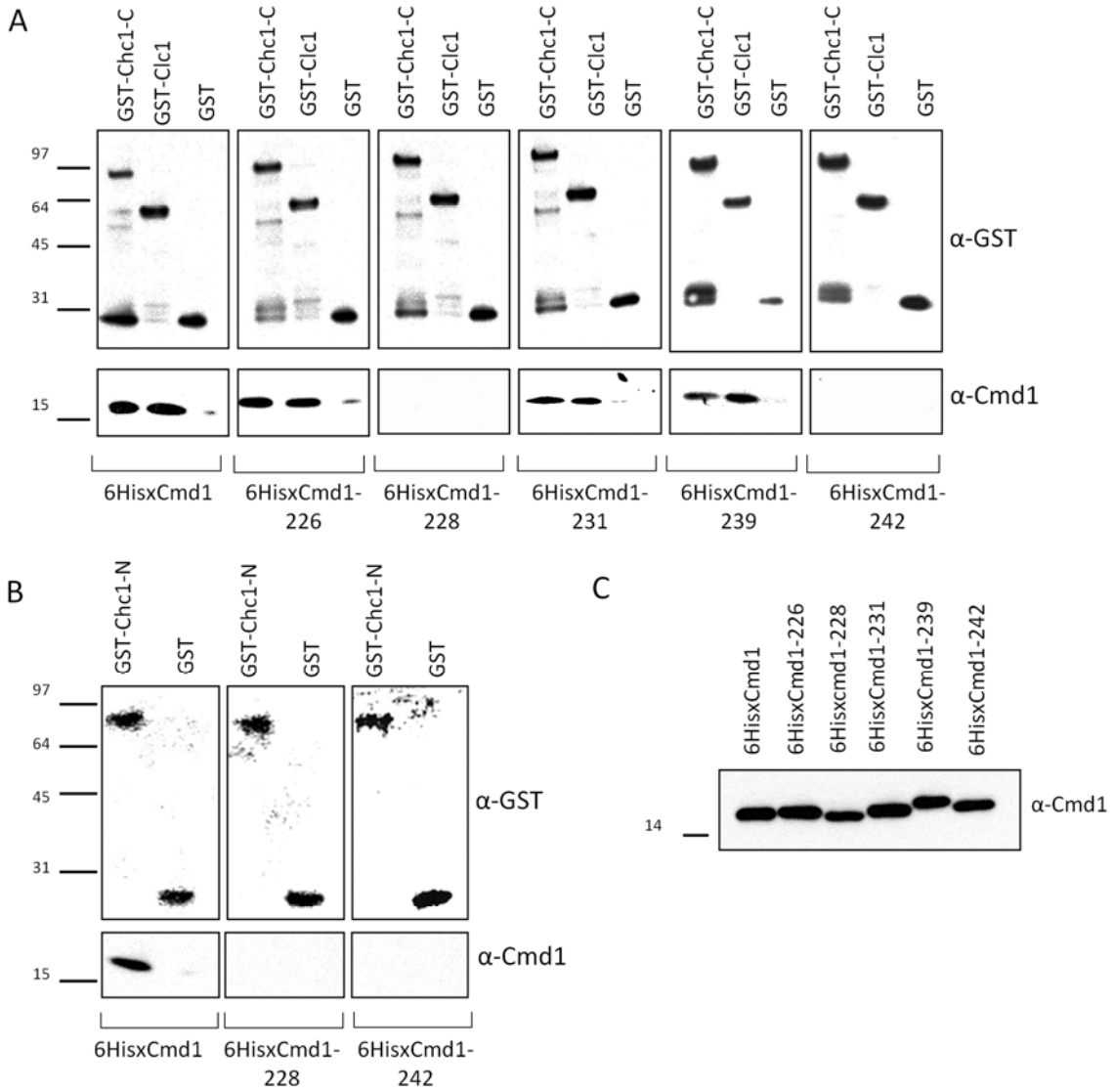

Figure 28. The mutations in the Cmd1-228 and Cmd1-242 mutants specifically disrupted the interaction with clathrin *in vitro*. (A,B) Immunoblots of pull downs of WT or mutant Cmd1 with GST or the indicated GST fusion proteins pre-bound to glutathione-Sepharose beads. Beads were incubated 1 hour at 4ºC with purified 6xHis-tagged WT (Cmd1) or the indicated mutant Cmd1s, expressed in E. coli from plasmids pQE11-*CMD1*, pQE11-*cmd1-226*, pQE11-*cmd1-228*, pQE11-*cmd1-231*, pQE11-*cmd1-239* and pQE11-*cmd1-242* in the presence of 5 mM $CaCl_2$. Beads were pelleted, rinsed several times and boiled in the presence of SDS-PAGE sample buffer. GST-fusion proteins were separated in a NuPAGE Bis-Tris 4-12 % gradient gel and transferred to a nitrocellulose filter. Antibodies against GST (α-GST) and against Cmd1 (α-Cmd1), combined with an appropriate secondary antibody, were used to detect the GST fusion proteins (to demonstrate equivalent protein loading) and Cmd1, respectively. (C) Immunoblot showing the input of the different purified 6xHis-Cmd1 constructs to demonstrate that equivalent concentration of the purified proteins were used in the pull downs shown in A and B. The same volume of the purified constructs was loaded, and an antibody against Cmd1 (α-Cmd1), combined with an appropriate secondary antibody, was used to detect the Cmd1 WT and mutant purified proteins. At least three independent experiments were performed for each sample.

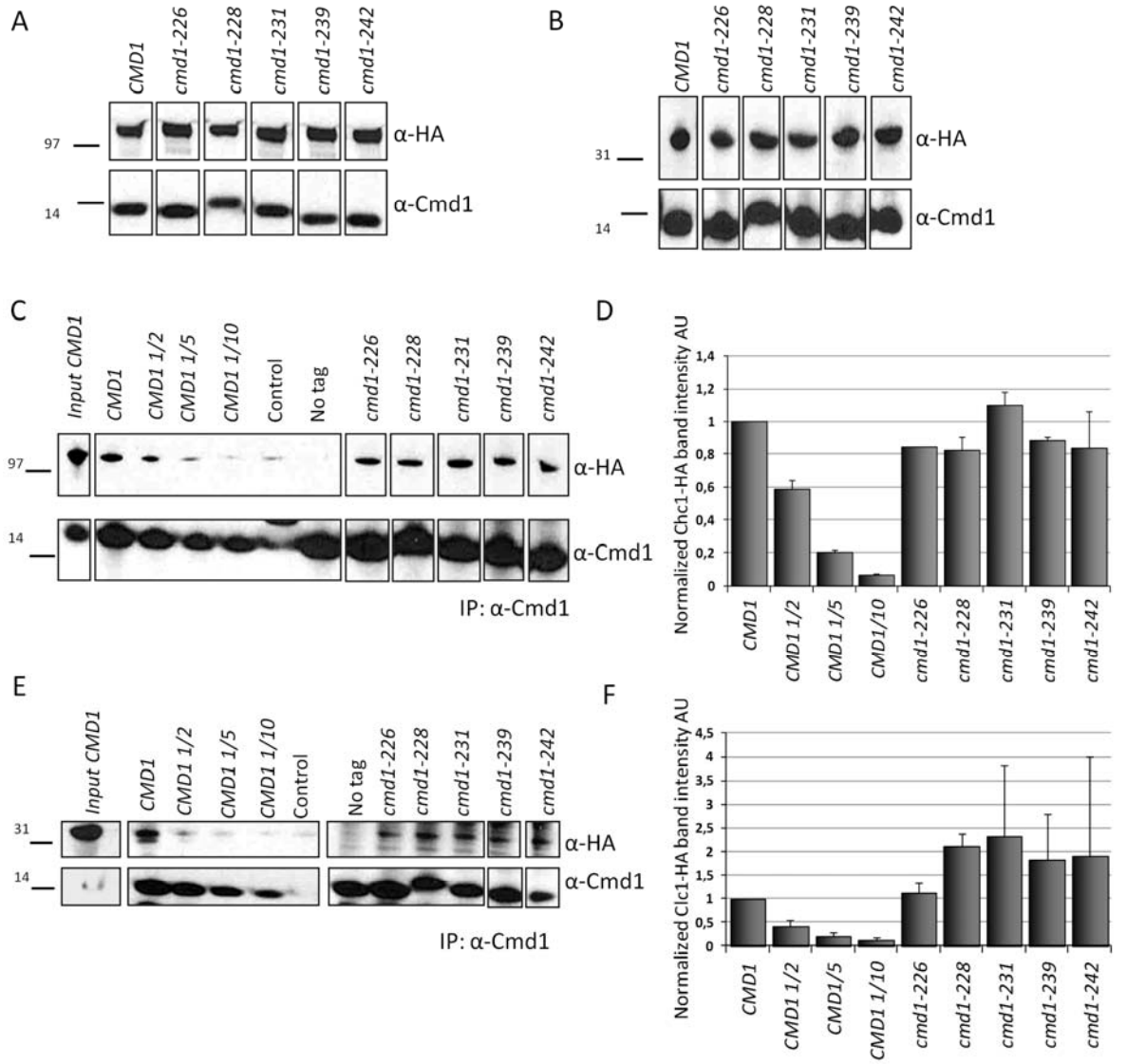

Figure 29. None of the Cmd1 point mutations affect the Cmd1 binding to Chc1 or Clc1 in yeast at permissive temperature (28ºC). (A, B) Immunoblots of total protein extracts from *cmd1Δ* strains bearing a HA-genome-tagged Chc1 (A) or Clc1 (B), grown at 28ºC and expressing either the WT Cmd1 or the Cmd1-226, Cmd1-228, Cmd1-231, Cmd1-239 or Cmd1-242 mutants from centromeric plasmids under the control of their own promotor (SCMIG1268, CSMIG1269, SCMIG1270, SCMIG1271, SCMIG1272 and SCMIG1273 or SCMIG1275, SCMIG1276, SCMIG1277, SCMIG1278, SCMIG1279 and SCMIG1280, respectively). A peroxidase-conjugated antibody against HA (α-HA) was used to detect the HA-tagged Chc1 or Clc1 and an antibody against Cmd1 (α-Cmd1), combined with an appropriate secondary antibody, was used to detect the different Cmd1 constructs. 25 µg of total protein was loaded per lane. (C,E) Immunoblots of co-immunoprecipitations with a polyclonal serum against Cmd1 pre-bound to Sepharose from non-denaturing extracts of a *cmd1*Δ strain grown at 28ºC bearing a HA-genome-tagged Chc1 (C) or Clc1 (E) and expressing either the WT Cmd1 or the Cmd1-226, Cmd1-228, Cmd1-231, Cmd1-239 or Cmd1-242 mutants, which were expressed from centromeric plasmids under the control of their own promotor (SCMIG1268, CSMIG1269, SCMIG1270, SCMIG1271, SCMIG1272 and SCMIG1273 or SCMIG1275, SCMIG1276, SCMIG1277, SCMIG1278, SCMIG1279 and SCMIG1280 respectively). Immunoprecipitations with pre-immune serum pre-bound to Sepharose beads (control) from the strain transformed with WT Cmd1 and immunoprecipitations from a non-tagged strain (no tag) were used as controls. The immune or pre-immune Sepharose beads were incubated with the yeast extracts in the presence of 5 mM $CaCl_2$ for 1 hour at 4ºC, and then they were pelleted, rinsed several times and boiled in the presence of SDS-

PAGE sample buffer. Proteins were separated in a NuPAGE Bis-Tris 4-12 % gradient gel and transferred to a nitrocellulose filter. Antibodies against HA (α-HA) and against Cmd1 (α-Cmd1), combined with an appropriate secondary antibody, were used to detect HA-tagged clathrin and Cmd1, respectively. (D, F) Average band intensity of the co-immunoprecipitated Chc1-HA (D) or Clc1-HA (F) for the experiments described in (C, E). At least three independent experiments were performed per sample. Quantifications were performed with ImageJ. The average of Chc1-HA or Clc1-HA band intensity was normalized to the band intensity of the immunoprecipitated Cmd1 for each sample, deducting also the band intensity for the pre-immune control sample. Results were then normalized to the WT Cmd1. At least three independent experiments were performed per sample. The statistical significance was tested using the two-tailed Student's t-test ($p \geq 0.05$). AU: arbitrary units.

The pull down experiments with purified components unveiled that mutants Cmd1-228 and Cmd1-242, did not bind to neither purified GST-C-terminal regions of Chc1 nor to GST-Clc1, whereas the other Cmd1 mutants did, similar to the WT Cmd1 (Figure 28A). Since Chc1 was found also to bind Cmd1 through its N-terminal domain via a lower affinity binding site (Figure 20C and 20D), we wonder if those Cmd1-228 and Cmd1-242 mutants also disrupted the interaction with the Chc1 N-terminus. Pull down experiments with purified components were performed to assess the ability of Cmd1 WT or mutants to bind the GST-N-terminal fragment of Chc1 (Figure 28B). The results indicated that neither Cmd1-228 nor Cmd1-242 were able to bind the N-terminal fragment of Chc1. The same volume of purified Cmd1 dilution used in the pull down experiments was loaded in a gel for immunoblot analysis to demonstrate that equivalent concentrations of WT or mutant Cmd1 were utilized (Figure 28C). Hence, the *cmd1-228* and *cmd1-242* point mutations severely disrupted the interaction of Cmd1 with Chc1 and Clc1 *in vitro*.

3.2.2. The *cmd1-242* mutant exhibits a disrupted clathrin-Cmd1 interaction in yeast at restrictive temperature

3.2.2.1. None of the *cmd1* point mutations analyzed significantly affected the interaction of Cmd1 with Chc1 and Clc1 in yeast at permissive temperature (28ºC)

In order to investigate the ability of the Cmd1 point mutants to bind Chc1 or Clc1, we performed co-inmuprecipitations in the presence of calcium expressing genome HA-tagged Chc1 or Clc1, and either the WT Cmd1 (*CMD1*) or the mutants

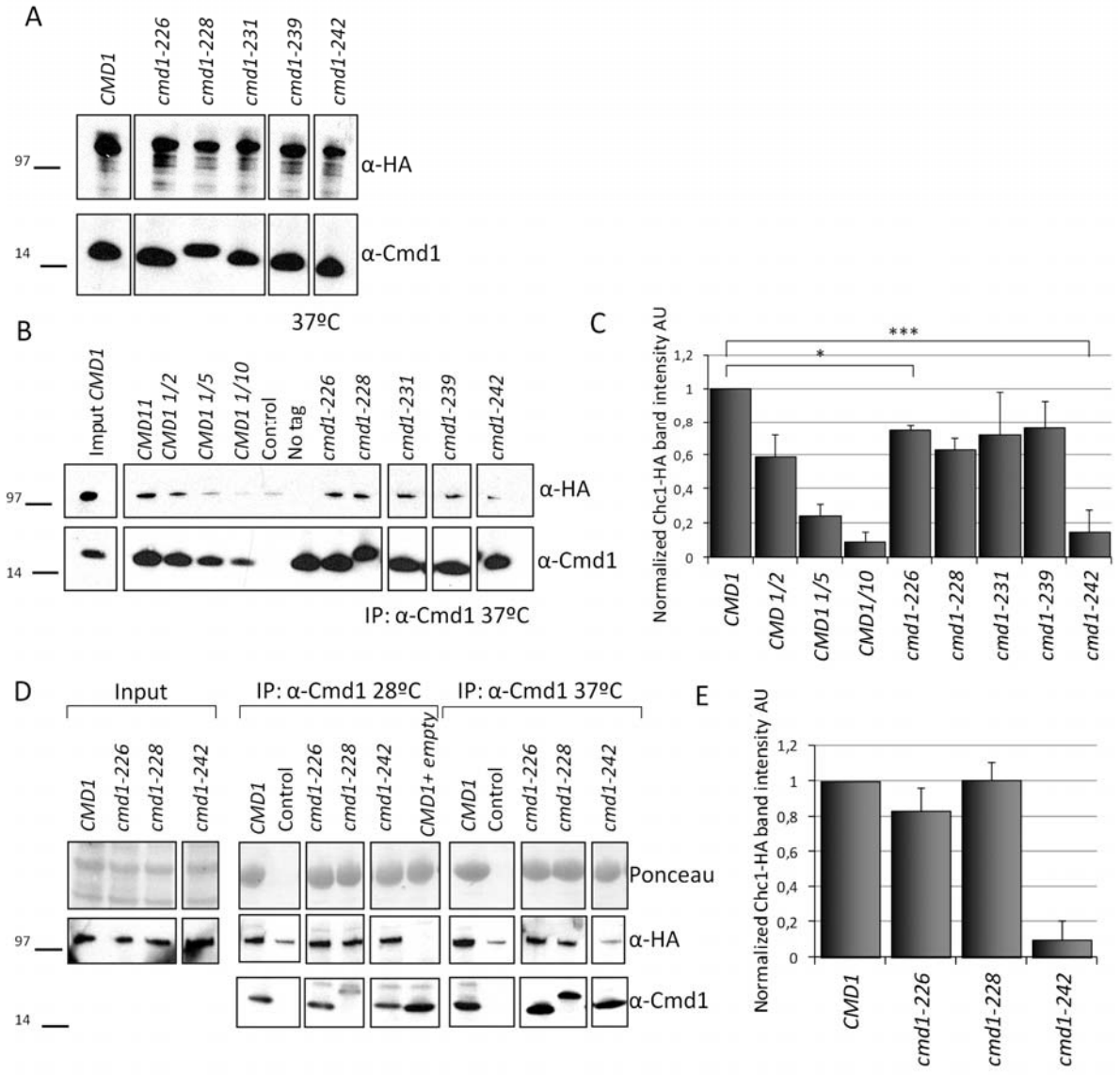

Figure 30. Cmd1-242 binds significantly less Chc1 *in vivo* at non-permissive temperature (37ºC). (A) Immunoblot of total protein extracts from a *cmd1Δ* strain grown at 28ºC and then 1 hour at 37ºC, bearing HA-genome-edited Chc1 and expressing either the WT Cmd1 or the Cmd1-226, Cmd1-228, Cmd1-231, Cmd1-239 or Cmd1-242 mutants, expressed from centromeric plasmids under the control of their own promotor (SCMIG1268, CSMIG1269, SCMIG1270, SCMIG1271, SCMIG1272, respectively). A peroxidase-conjugated antibody against HA (α-HA) was used to detect the HA-tagged Chc1 or Clc1 and an antibody against Cmd1 (α-Cmd1), combined with an appropriate secondary antibody, was used to detect the different Cmd1 constructs. 25 µg of total protein was loaded per lane. (B, D) Immunoblots of co-immunoprecipitations with an anti-Cmd1 serum pre-bound to Protein A-Sepharose, from non-denaturing extracts of a *cmd1*Δ strain grown at 28ºC and then 1 hour at 37ºC, expressing a HA-genome-edited Chc1 and either the WT Cmd1 or the Cmd1-226, Cmd1-228, Cmd1-231, Cmd1-239 or Cmd1-242 mutants, expressed from centromeric plasmids under the control of their own promotor (SCMIG1268, CSMIG1269, SCMIG1270, SCMIG1271, SCMIG1272 respectively) (B), or co-immunoprecipitations from *WT CMD1* (RH3983)*, cmd1-226* (RH3984)*, cmd1-228* (RH3985)*, cmd1-231 (*RH3986)*, cmd1-239 (*RH3988) and *cmd1-242* (RH3990) strains grown at 28ºC and then 1 hour at 28ºC or 37ºC, expressing Chc1-HA from a centromeric plasmid under the control of its own promotor (p50-*CHC1-HA*) (D). Immunoprecipitations with pre-immune serum pre-bound to Protein-A Sepharose beads as controls were performed from the *cmd1Δ CHC1-HA* strain transformed with WT *CMD1* (control) (SCMIG1268) (B) or from the *WT CMD1* strain (SCMIG947) transformed with p50-*CHC1-HA* (D). Immunoprecipitations with the anti-Cmd1 serum pre-bound to Protein A-Sepharose

from a non-tagged strain (no tag) (SCMIG1261) (B) or a WT *CMD1* strain transformed with an empty vector (*CMD1* empty) (D) were also used as controls. The immune or pre-immune Sepharose beads were incubated for 1 hour at 4ºC with the yeast extracts in the presence of 5 mM $CaCl_2$ (B, D) and then, they were pelleted, rinsed several times and boiled in the presence of SDS-PAGE sample buffer. Proteins were separated in a NuPAGE Bis-Tris 4-12 % gradient gel and transferred to a nitrocellulose filter. Ponceau red staining was used to demonstrate equivalent protein loading. Antibodies against HA (α-HA) and against Cmd1 (α-Cmd1), combined with an appropriate secondary antibody, were used to detect HA-tagged clathrin and Cmd1, respectively. (C, E) Average band intensity of the immunoprecipitated Chc1-HA for the experiments described in (B, D). Two (E) or three (C) independent experiments were performed per experiment. Quantifications were performed with ImageJ. The average of Chc1-HA band intensity was normalized to the band intensity of the immunoprecipitated Cmd1 for each sample, deducting also the band intensity for the pre-immune control sample. Results were then normalized to the WT Cmd1. The statistical significance was tested using the two-tailed Student's t-test. * represents a p-value ≤ 0.05; *** represents a p-value ≤ 0.001. AU: arbitrary units.

described above (*cmd1-228, cmd1-226, cmd1-231, cmd1-239* and *cmd1-242*) grown first at permissive temperature (28ºC) (Figure 29C, 29D, 29E and 29F).

We first analyzed the expression either of Chc1-HA (Figure 29A) or Clc1-HA (Figure 29B) from total protein extracts of the strains described to examine whether the *cmd1* point mutations affected the expression or stability of either of the clathrin chains. As shown in figure 29A and 29B, Chc1-HA and Clc1-HA were expressed in the *cmd1* mutants similar to the Cmd1 WT.

The analysis of the Chc1-HA and Clc1-HA co-precipitating with Cmd1 from protein extracts of the strains described above revealed that, in contrast to the *in vitro* pull down assays using purified components, Cmd1-228 and Cmd1-242 co-precipitated Chc1-HA and Clc1-HA amounts, similar to the WT Cmd1 when the strains had been grown at permissive temperature. The immunoprecipitations of *CMD1* WT and mutant strains expressing Clc1-HA showed great variability (Figure 29F), as the Cmd1-Clc1 interaction in yeast extracts is much weaker than that of Chc1 and the detection of the co-precipitated Clc1-HA by immunoblot was difficult. However, more than three co-immunoprecipitation experiments were done and no significant differences in the Cmd1-Clc1 interaction were found in the distinct Cmd1 mutants (Figure 29F).

3.2.2.2. The Cmd1-242 interaction with Chc1 and Clc1 is disrupted in yeast at restrictive temperature (37ºC)

In spite of the clear effect found *in vitro* for some of the *CMD1* mutations in its ability to interfere with the clathrin-Cmd1 interaction, no significant defect was found for any of the Cmd1 mutants in their ability to bind Chc1 or Clc1 in yeast when the cells were grown at 28ºC. However it is often the case in yeast that thermosensitive mutant strains do not exhibit phenotypes demonstrated for the purified components *in vitro*, unless the cells are pre-incubated at restrictive temperature (in the case of the *cmd1* mutants, 37ºC), possibly because a complex molecular environment maintain better its native WT-like conformation (Ben-Aroya *et al*. , 2010; Forsburg, 2001). Therefore, we re-examined the clathrin-Cmd1 interaction of the *cmd1* mutant strains after pre-incubation of the yeast cells at 37ºC (Figures 30 and 31).

We first analyzed the expression of Chc1-HA (Figure 30A) or Clc1-HA (Figure 31A) from total protein extracts of yeast strains expressing genome HA-tagged Chc1 or Clc1 and either the WT or mutant Cmd1, expressed from centromeric plasmids (*CMD1, cmd1-228, cmd1-226, cmd1-231, cmd1-239* and *cmd1-242*) in a *cmd1Δ* background, grown first at 28ºC to mid-log phase, and then for 1 hour at 37ºC. Longer incubations at 37ºC, resulted in high levels of cell death. The immunoblots showed that neither Chc1-HA nor Clc1-HA expression was affected in any of the mutants grown at 37ºC, comparing to the WT *CMD1* strain.

Next, we performed co-immuprecipitations using Protein-A-Sepharose pre-bound to an anti-Cmd1 antibody, in the presence of calcium, from non-denaturing extracts of yeast expressing the HA-tagged clathrin chains and either the WT or mutant *CMD1* alleles. The results clearly revealed that Cmd1-242 bound significantly less Chc1-HA in yeast at restrictive temperature (37ºC) (Figure 30B and 30C), as compared to the wild type Cmd1 or the other mutant Cmd1s analyzed, including Cmd1-228, which did not bind Chc1 in the pull down assays with purified components. The same result was confirmed by performing immunoprecipitation experiments with genome-integrated WT *CMD1* or the mutant *cmd1-226*, *cmd1-228* and *cmd1-242* alleles and Chc1-HA or Chc1 (as a control) expressed from a centromeric plasmids (Figure 30D and 30E). The results clearly demonstrated that the interaction of Cmd1-242 with Chc1 in the presence

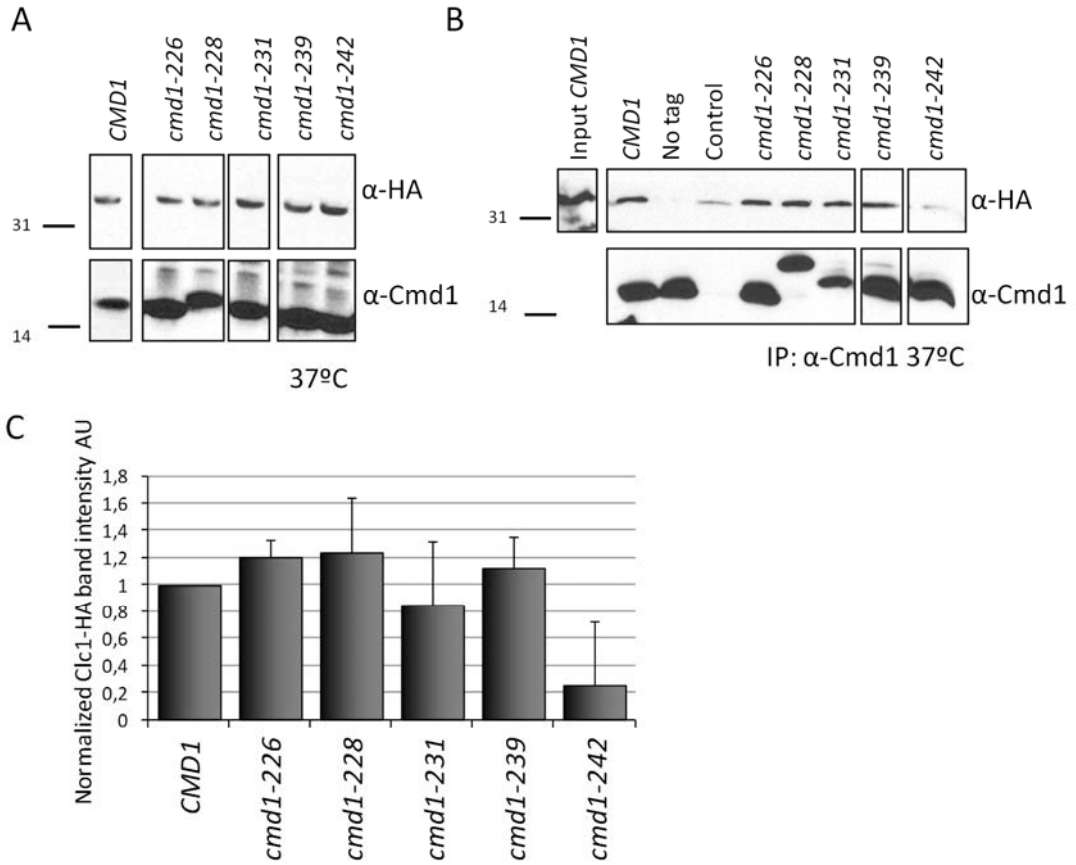

Figure 31. Cmd1-242 binds significantly less Clc1 in yeast at 37ºC. (A) Immunoblot of total protein extracts from a *cmd1Δ* strain grown at 28ºC and then 1 hour at 37ºC bearing a HA-genome-tagged Clc1 and expressing either the WT Cmd1 or the Cmd1-226, Cmd1-228, Cmd1-231, Cmd1-239 or Cmd1-242 mutants, expressed from centromeric plasmids under the control of their own promotor (SCMIG1275, SCMIG1276, SCMIG1277, SCMIG1278, SCMIG1279 and SCMIG1280, respectively). A peroxidase-conjugated anti-HA antibody (α-HA) was used to detect the HA-tagged Chc1 or Clc1 and an antibody against Cmd1 (α-Cmd1), combined with an appropriate secondary antibody, was used to detect the different Cmd1 constructs. 25µg of total protein was loaded per lane. (B) Immunoblots of co-immunoprecipitations with a polyclonal serum against Cmd1 pre-bound to Protein A-Sepharose from non denaturing extracts of a *cmd1Δ* strain grown at 28ºC and then 1 hour at 37ºC, bearing an HA-genome-edited Clc1 and expressing either the WT Cmd1 or the Cmd1-226, Cmd1-228, Cmd1-231, Cmd1-239 or Cmd1-242 mutants, expressed from centromeric plasmids under the control of their own promotor (SCMIG1275, SCMIG1276, SCMIG1277, SCMIG1278, SCMIG1279 and SCMIG1280, respectively). Immunoprecipitations of pre-immune serum pre-bound to Protein A-Sepharose beads from the *cmd1Δ CLC1-HA* strain transformed with the WT Cmd1 (control) and immunoprecipitation from a non-tagged strain (no tag) were used as controls. The immune or pre-immune Sepharose beads were incubated for 1 hour at 4ºC with the yeast extracts in the presence of 5 mM $CaCl_2$ and then, they were pelleted, rinsed several times and boiled in the presence of SDS-PAGE sample buffer. Proteins were separated in a NuPAGE Bis-Tris 4-12 % gradient gel and transferred to a nitrocellulose filter. Antibodies against HA (α-HA) and against Cmd1 (α-Cmd1), combined with an appropriate secondary antibody, were used to detect HA-tagged clathrin and Cmd1, respectively. (C) Average band intensity of the immunoprecipitated Clc1-HA for the experiments described in (B). Two independent experiments were performed per sample. Quantifications were performed with ImageJ. The average of the Clc1-HA band intensities was normalized to the band intensities of the immunoprecipitated Cmd1 for each sample, deducting also the band intensity for the pre-immune control sample. Results were then normalized to the WT Cmd1. AU: arbitrary units.

of calcium was not affected when cells were grown at 28ºC, as compared with the WT Cmd1, but Cmd1-242 bound significantly less Chc1 in yeast extracts at restrictive temperature (37ºC).

Immunoprecipitations performed from non-denaturing extracts of yeast expressing HA-tagged Clc1 and WT or mutant Cmd1s (Figure 31B and 31C) also indicated that Cmd1-242 also bound less Clc1 in yeast at restrictive temperature (37ºC), even though the levels of Cmd1 and clathrin were similar to the WT.

Interestingly though, no significant disruption of the Chc1-Cmd1 or Clc1-Cmd1 interaction neither at permissive nor at restrictive temperature could be demonstrated for the Cmd1-228 mutant, which, similar to Cmd1-242, exhibited very low affinity for clathrin *in vitro*, indicating that this mutation was less penetrating *in vivo* than the *cmd1-242* mutation, or that clathrin could still bind to this mutant indirectly via an intermediate binding partner. No significant disruption of the Chc1-Cmd1 or Clc1-Cmd1 interaction could be demonstrated for any other of the Cmd1 mutants that showed unaltered affinities for clathrin in pull down experiments, as compared to the wild type Cmd1.

As interfering with the clathrin-Cmd1 interaction in the Cmd1 point mutants did not affect the Chc1 or Clc1 expression levels, neither at 28ºC or 37ºC (Figures 29A, 29B, 30A and 31A), we could infer that despite the Chc1 and Clc1 mutants lacking the Cmd1 binding site are less expressed, the clathrin-Cmd1 interaction was not essential to maintain the clathrin expression levels.

3.3. Analysis of the growth phenotype at restrictive temperature of the different Cmd1 and clathrin mutants

3.3.1. The Chc1-cbsΔ and Clc1-cbsΔ mutants partially rescue the temperature sensitive growth defect of the clathrin null mutations

In order to analyze the phenotype of the clathrin Cmd1 binding site mutants for their ability to grow at restrictive temperature, we performed serial dilution cell growth assays (see Materials and Methods section 6.2.4) (Figure 32). *chc1Δ* or *clc1Δ* strains which grow slowly at 37ºC, as compared to the WT (K. M. Huang et al., 1997; Silveira et al., 1990), were transformed with a multicopy empty plasmid (empty) or with either centromeric plasmid encoding *CHC1* or *CLC1* (*CHC1* CEN or

CLC1 CEN, respectively) or a multicopy plasmid encoding *chc1-cbsΔ* or *clc1-cbsΔ (chc1-cbsΔ* or *clc1-cbsΔ* 2µ, respectively). The growth assays showed that the overexpression of the *chc1-cbsΔ* and *clc1-cbsΔ* partially rescued the growth defect of the *chc1Δ* and *clc1Δ* mutants, indicating that although the clathrin mutants are not able to completely complement the growth defects of clathrin null mutants, the essential functions of clathrin at 37ºC do not require an intact Cmd1 interaction with the C-terminus of Chc1 or Clc1.

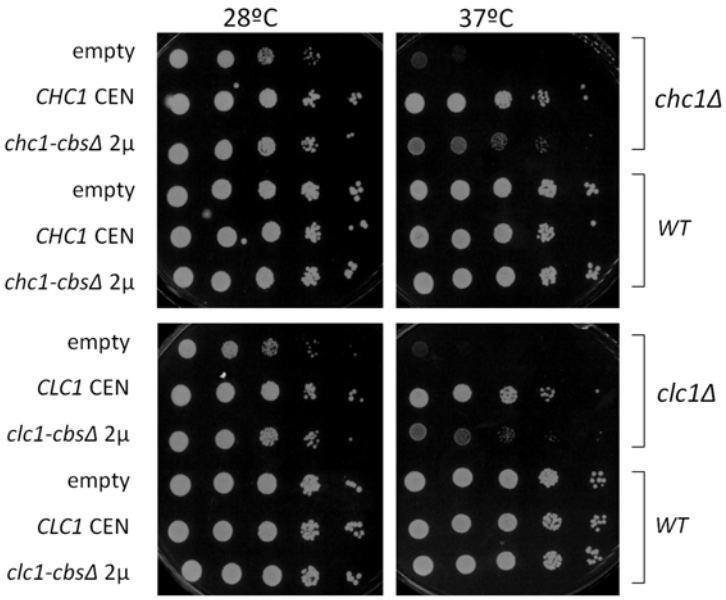

Figure 32. The Chc1-cbsΔ and Clc1-cbsΔ mutants partially rescue the temperature sensitive growth defect of the clathrin null mutations. The partial growth defect of clathrin mutants is not dominant when the endogenous WT clathrin is present. Serial dilutions of *chc1Δ* (SL114) and *WT* (SCMI381) cells transformed with either a multicopy empty plasmid (*empty*), a centromeric plasmid encoding *CHC1* (*CHC1* CEN), a multicopy plasmid encoding *chc1-cbsΔ* (*chc1-cbsΔ* 2µ) all of them expressed under the control of their own promotor (YEplac195, p50-*CHC1,* and p195-*chc1-cbsΔ,* respectively), and *clc1Δ* (SL1620) and *WT* (SCMI381) strains transformed with either a multicopy empty plasmid (*empty*), a centromeric plasmid encoding *CLC1* (*CLC1* CEN), a multicopy plasmid encoding *clc1-cbsΔ* (*clc1-cbsΔ* 2µ), all expressed under the control of their own promotor (YEplac181, p111-*CLC1*, and p181-*clc1-cbsΔ*). Cells from mid-log phase culture were spotted into the appropriate SDC plates and let grown for 72 hours at either 28ºC or 37ºC.

3.3.2. The partial growth defect of the clathrin mutants is not dominant when the WT clathrin is present

As a temperature sensitive growth phenotype for the Cmd1 binding site deletion clathrin mutants was revealed when expressed in *chc1Δ* and *clc1Δ* strains, we wanted to investigate if this defect was dominant when the endogenous Chc1 or Clc1 was present. For that purpose, we performed serial dilution cell growth assays of *WT* and *chc1Δ* and *clc1Δ* (controls) strains, transformed with either a multicopy empty plasmid (empty), a centromeric plasmid encoding either the Chc1 or Clc1 (*CHC1* CEN or *CLC1* CEN, respectively), or a multicopy plasmid encoding either the Chc1-cbsΔ or the Clc1-cbsΔ mutants (*chc1-cbsΔ* 2µ and *clc1-cbsΔ* 2µ, respectively) (Figure 32). The results revealed that overexpressing the Chc1-cbsΔ or Clc1-cbsΔ mutants in a WT strain that also expressed the endogenous WT Chc1 and Clc1, had no effect in their ability to grow at 37ºC, suggesting that the temperature sensitive phenotype of clathrin mutants is not dominant.

3.3.3. The *cmd1-228* and *cmd1-242* mutants are defective in growing at restrictive temperature but this defect is not necessarily dependent on the clathrin-Cmd1 interaction

To investigate if the defective clathrin-Cmd1 interaction is the main cause of temperature sensitive growth defect observed in the *cmd1-228* and *cmd1-242* mutants (Yoshikazu Ohya & Botstein, 1994b), we analyzed their ability to grow at 37ºC upon overexpression Chc1 or Clc1, also using serial dilution cell growth assays (Figure 33). The reasoning behind the suppression experiments in yeast is that over-expression of one of the components of a protein complex, in the presence of a partial lack-function point mutation in the partner component might favor the formation of the complex in the "WT" conformation, thereby restoring its cellular function.

cmd1 mutant strains were transformed with either a multicopy empty plasmid, or multicopy plasmids encoding either WT Chc1 or Clc1 or the clathrin mutants lacking the Cmd1 binding site (*CHC1* 2µ, *CLC1* 2µ, *chc1-cbsΔ* 2µ or *chc1-cbsΔ* 2µ, respectively) and they were spotted in SDC plates and incubated at 28ºC or 37ºC.

The results showed that the *cmd1-228* and *cmd1-242* mutants, which had the clathrin-Cmd1 interaction altered at least *in vitro*, exhibited a strong defect in

growing at 37ºC, which was not rescued by overexpressing neither Chc1 nor Clc1 nor the clathrin Cmd1 binding site mutants. This result indicates that clathrin is not at least the only relevant protein whose altered function caused the inability of the Cmd1 mutants to grow at 37ºC, consistent with the previous result that an intact clathrin-Cmd1 interaction is not essential in yeast to sustain growth.

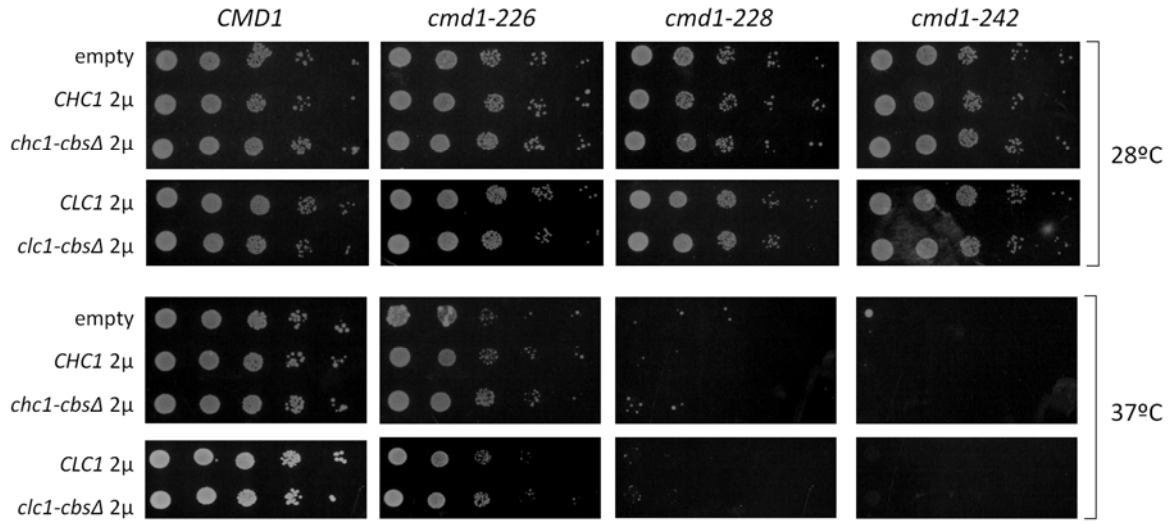

Figure 33. The overexpression of Chc1, Clc1 or the Chc1-cbsΔ or Clc1-cbsΔ mutants does not rescue the thermosensitive growth defect of the *cmd1-228* and *cmd1-242* mutants. Serial dilutions of *WT CMD1* (RH3983), *cmd1-226* (RH3984), *cmd1-228* (RH3985) and *cmd1-242* (RH3990) strains transformed with multicopy plasmids either empty (empty), or encoding *CHC1* (*CHC1* 2µ), *CLC1* (*CLC1* 2µ), *chc1-cbsΔ* (*chc1-cbsΔ* 2µ) or *clc1-cbsΔ* (*clc1-cbsΔ* 2µ), all expressed under the control of their own promotor (YEplac195, YEp24-*CHC1*,p181-*CLC1*, p195-*chc1-cbsΔ* or p181-*clc1-cbsΔ*, respectively). Cells from mid-log phase culture were spotted on the appropriate SDC plates and let them grow for 72 hours at either 28ºC or 37ºC.

3.4. Analysis of the membrane traffic phenotype of the mutants that specifically affect the clathrin-Cmd1 interaction

3.4.1. Disruption of the clathrin-Cmd1 interaction does not necessarily alter endocytic uptake

3.4.1.1. The *cmd1-226* and *cmd1-228,* but not the *cmd1-242* mutants, are defective in endocytic uptake at restrictive temperature

Once mutants that specifically disrupted the clathrin-Cmd1 interaction were identified, we wanted to study more in detail their phenotype, investigating their effect in membrane traffic events that require clathrin such as endocytic uptake and forward and retrograde traffic from the Golgi to the endosomes. We first analyzed the endocytic activity of the Cmd1 mutants by the Lucifer yellow uptake (LY) assay (see Materials and Methods section 6.5.2), measuring the ability of the WT and clathrin binding defective *cmd1-242* and *cmd1-228* mutant strains to internalize the fluorescent membrane-impermeable dye, which accumulates in the vacuole only when taken up by fluid phase endocytosis (Figure 34). We also included in all the analysis the *cmd1-226* strain as a Cmd1 mutant that do not alter the clathrin-Cmd1 interaction as a control. The *cmd1-226* mutation has previously been shown to affect the Cmd1 interaction with the type I myosin and cause a temperature sensitive endocytic defect (M I Geli et al., 1998).

The results showed that the *cmd1-226* and *cmd-228*, but importantly not the *cmd1-242* mutant, had a strong endocytic defect at restrictive temperature compared with that displayed at 28ºC and with the *CMD1* WT strain (Figure 34A and 34B). The result was consistent with the phenotype already described for the Cmd1 mutants using an α-factor uptake assay (M I Geli et al., 1998), which measures receptor-mediated endocytosis. Since the *cmd1-242* mutation strongly interfered with the clathrin-Cmd1 interaction, both in yeast extracts and *in vitro*, whereas the *cmd1-226* mutation was unaltered in that respect, the result clearly indicated that the clathrin-Cmd1 interaction was not necessarily relevant for endocytic vesiculation from the PM. As it is demonstrated in Figures 34A and 34C, overexpression of Chc1 (*CHC1* 2µ) did not rescue the uptake defect at 37ºC of the *cmd1-226* and *cmd1-228* mutants, further indicating that the relevant endocytic protein whose function was disrupted in these mutants was not clathrin.

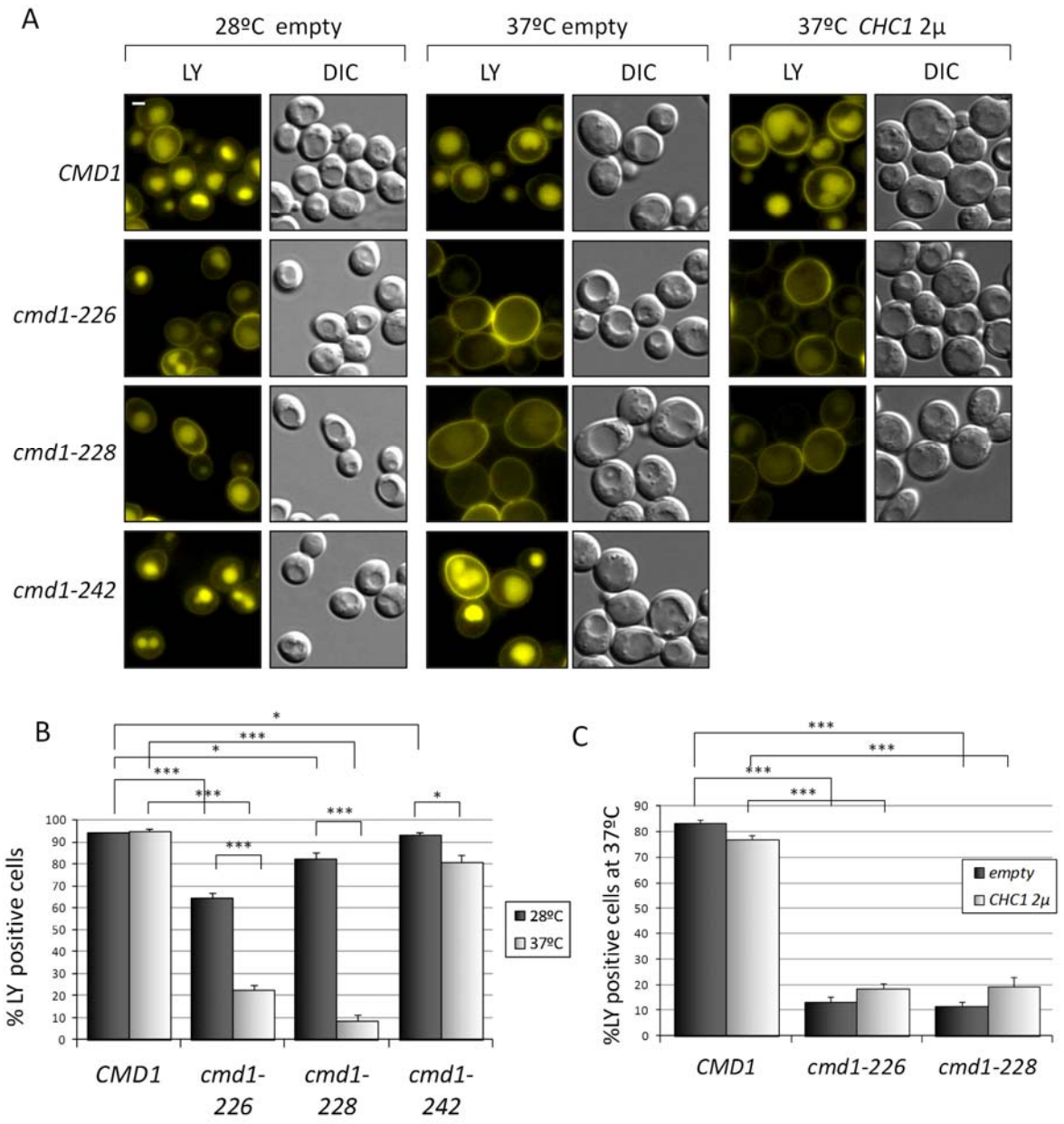

Figure 34. The *cmd1-226* and *cm1-228* mutant strains are defective in the Lucifer yellow endocytic uptake assay at restrictive temperature, and this defect is not rescued by overexpressing Chc1. (A) Fluorescence micrographs of a Lucifer yellow endocytic uptake of *CMD1* (RH3983)*, cmd1-226* (RH3984), *cmd1-228* (RH3985) and *cmd1-242 (*RH3990) strains transformed with a multicopy plasmid either empty or encoding *CHC1* under the control of its own promotor (empty or *CHC1* 2µ; YEplac195 or YEp24-*CHC1,* respectively). Cells were incubated with Lucifer yellow for 1 hour at 28ºC or at 37ºC. LY: Lucifer yellow fluorescence images. DIC: differential interference contrast images. Scale bar = 2 µm. (B) Average percentage of cells transformed with the empty plasmid that internalized Lucifer yellow at 28ºC or 37ºC, and delivered it to the vacuole (% LY positive cells) for the experiment described in (A). (C) Average percentage of cells transformed with the empty plasmid (*empty*) and the multicopy *CHC1* plasmid (*CHC1* 2µ) that internalized Lucifer yellow at 37ºC and delivered it to the vacuole (% LY positive cells at 37ºC) for the experiment described in (A). At least three independent experiments were done for each sample. The statistical significance was tested using the two-tailed Student's t-test, * represents a p-value ≤ 0.05, *** represents a p-value ≤ 0.001.

3.4.1.2. The *chc1-cbsΔ* and *clc1-cbsΔ* mutants have a partial defect in endocytosis

Next, we investigated the endocytic phenotype of the *chc1-cbsΔ* and *clc1-cbsΔ* clathrin mutants, performing Lucifer yellow uptake assays at 28ºC and 37ºC with a *chc1Δ* or *a clc1Δ* strain transformed with a multicopy empty plasmid (empty) or with either centromeric plasmids encoding *CHC1* or *CLC1*, or *chc1-cbsΔ* or *chc1-cbsΔ (chc1-cbsΔ* or *clc1-cbsΔ* CEN, respectively) or multicopy plasmids encoding *chc1-cbsΔ* or *clc1-cbsΔ (chc1-cbsΔ* or *clc1-cbsΔ* 2µ, respectively) (Figures 35 and 36). Surprisingly in light of the results obtained with the *cmd1-242* mutant, the expression, and even the overexpression of the Chc1-cbsΔ (Figures 35) or Clc1-cbsΔ (Figures 36) mutants did not rescue the Lucifer yellow endocytic uptake defect of the *chc1Δ* or *clc1Δ* strains neither at 28ºC nor 37ºC, which exhibit a partial defect in endocytosis (Chu *et al.*, 1996; Payne *et al.*, 1988). In addition, the *chc1-cbsΔ* and *clc1-cbsΔ* mutants did not have a dominant effect on endocytosis when the endogenous WT clathrin was present (Figure 37).

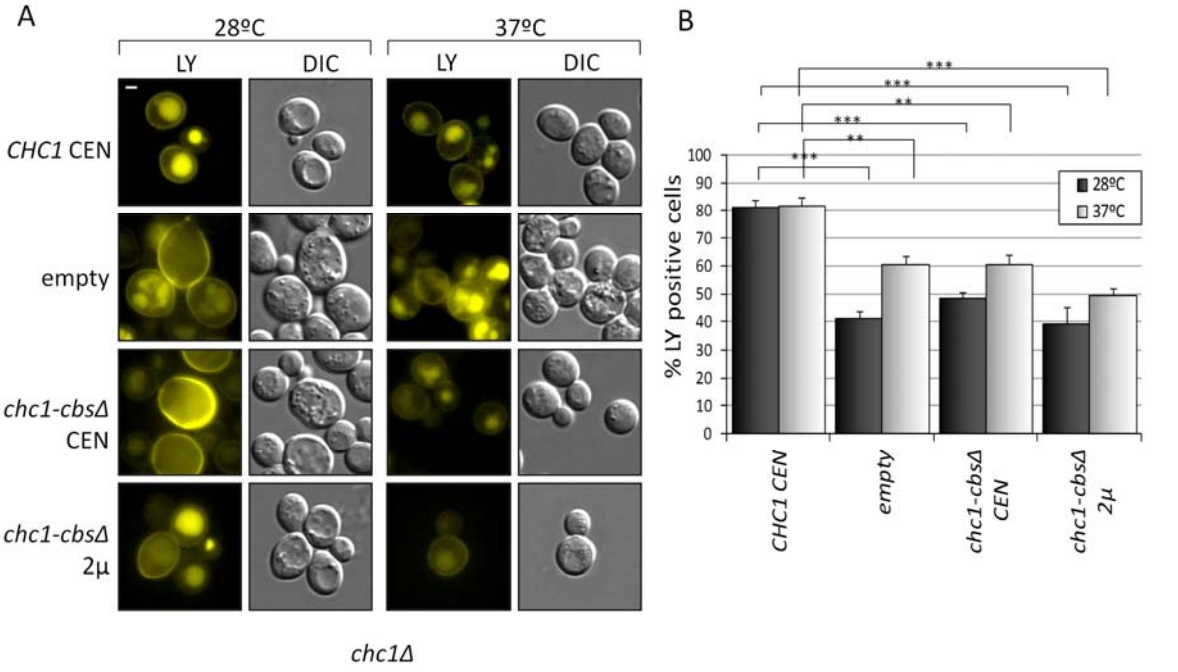

Figure 35. The *chc1-cbsΔ* mutant has a partial defect for Lucifer yellow fluid-phase endocytosis, comparable to the *chc1Δ* strain. (A) Fluorescence micrographs of a Lucifer yellow endocytic uptake of a *chc1Δ* strain (SL114) transformed with either a multicopy empty plasmid (empty), a centromeric plasmid encoding *CHC1* (*CHC1* CEN), or a centromeric or multicopy plasmid encoding *chc1-cbsΔ* (*chc1-cbsΔ* CEN, *chc1-cbsΔ* 2µ, respectively), all of them expressed under the control of their own promotor (YEplac195, p50-*CHC1,* p50-*chc1-cbsΔ* or p195-*chc1-cbsΔ,* respectively). Cells were incubated with Lucifer yellow for 1 hour at 28ºC or 37ºC. LY: Lucifer yellow fluorescence images. DIC:

differential interference contrast images. Scale bar: 2 µm. (B) Average percentage of cells that internalized Lucifer yellow and delivered it to the vacuole (% LY positive cells) for the experiment described in (A). At least three independent experiments were done for each sample. Statistical significance was tested using the two-tailed Student's t-test, * represents a p-value ≤ 0.05; ** represents a p-value ≤ 0.01,*** represents a p-value ≤ 0.001.

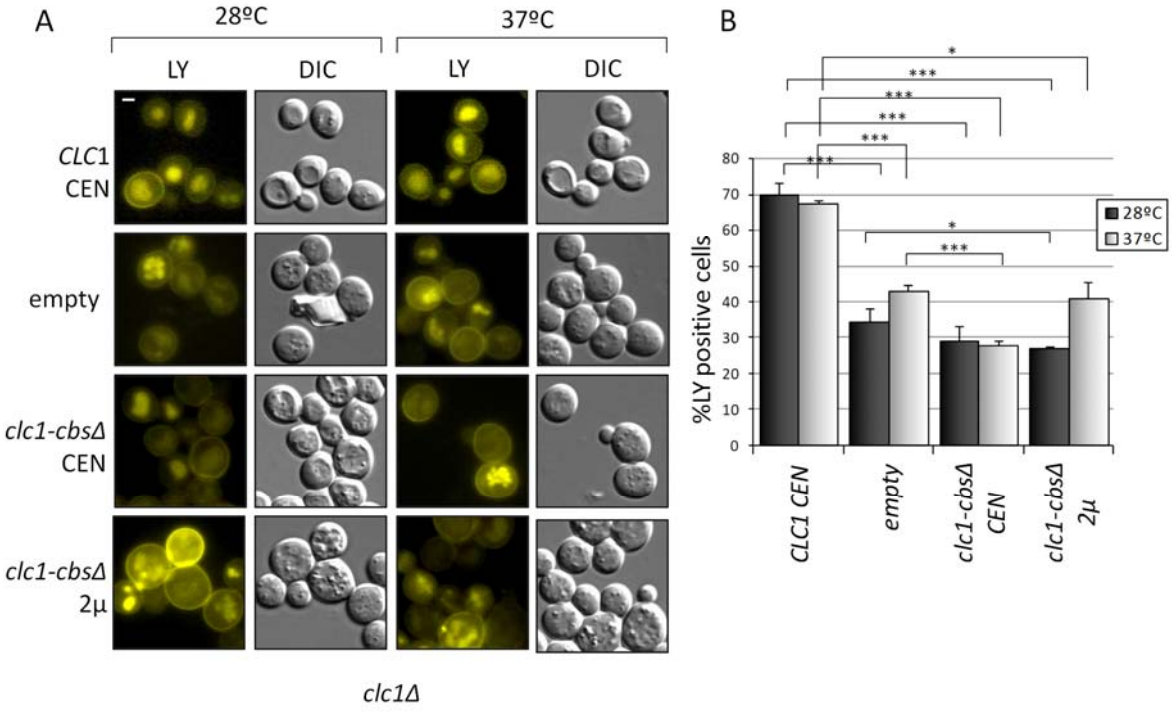

Figure 36. The *clc1-cbsΔ* mutant has a partial defect for Lucifer yellow fluid-phase endocytosis, comparable to the *clc1Δ* strain. (A) Fluorescence micrographs of a Lucifer yellow endocytic uptake assay of a *clc1Δ* strain (SL1620) transformed with either an empty plasmid (empty), a centromeric plasmid encoding *CLC1* (*CLC1* CEN), or a centromeric or multicopy plasmid encoding *clc1-cbsΔ* (*clc1-cbsΔ* CEN or *clc1-cbsΔ* 2µ), all expressed under the control of their own promotor (YEplac181, p111-*CLC1,* p111-*clc1-cbsΔ* or p181-*clc1-cbsΔ,* respectively). Cells were incubated with Lucifer yellow for 1 hour at 28ºC or 37ºC. LY: Lucifer yellow fluorescence images. DIC: differential interference contrast images. Scale bar: 2 µm. (B) Average percentage of cells that have internalized Lucifer yellow and delivered it to the vacuole (% LY positive cells) for the experiment described in (A). At least three independent experiments were done for each sample. The statistical significance was performed using the two-tailed Student's t-test, * represents a p-value ≤ 0.05; ** represents a p-value ≤ 0.01, *** represents a p-value ≤ 0.001.

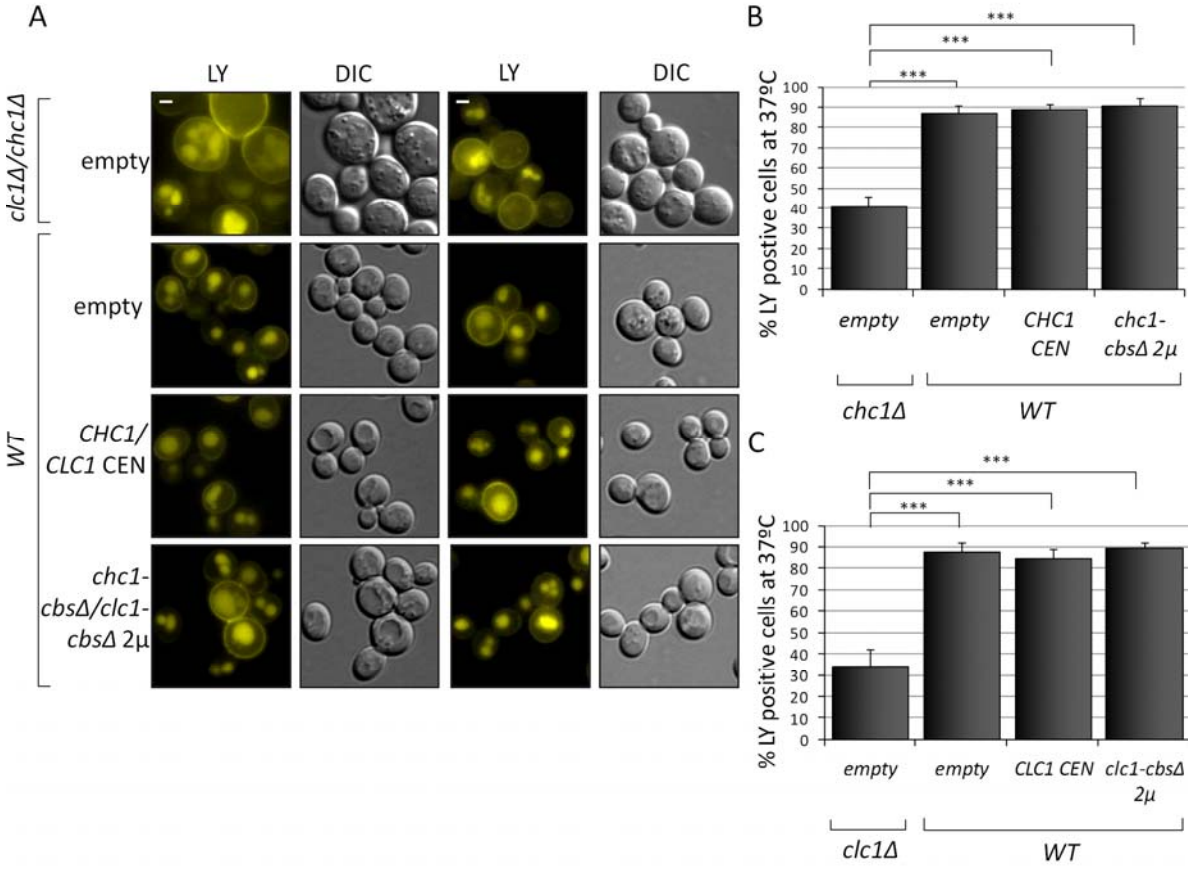

Figure 37. The *chc1-cbsΔ* and *clc1-cbsΔ* mutants do not have a dominant effect on endocytosis when the endogenous WT clathrin is present. (A) Fluorescence micrographs of a Lucifer yellow endocytic uptake of *chc1Δ* (SL114) and *clc1Δ* (SL1620) strains transformed with a multicopy empty plasmid (empty; YEplac195), and a WT strain (BY4742) transformed with a centromeric plasmid encoding either *CHC1* or *CLC1* (*CHC1* CEN or *CLC1* CEN), and a multicopy plasmid encoding either *chc1-cbsΔ* or *clc1-cbsΔ* (*chc1-cbsΔ* 2μ or *clc1-cbsΔ* 2μ), all expressed under the control of their own promotor (p50-*CHC1,* p111-*CLC1,* p195-*chc1-cbsΔ* or p181-*clc1-cbsΔ,* respectively). Cells were incubated with Lucifer Yellow for 1 hour at 37ºC. LY: Lucifer yellow fluorescence images. DIC: differential interference contrast images. Scale bar: 2 μm. (B, C) Average percentage of cells that have internalized Lucifer yellow and delivered it to the vacuole at 37ºC (% LY positive cells at 37ºC) for the experiment described in (A). At least three independent experiments were done for each sample. The statistical significance was tested using the two-tailed Student's t-test, *** represents a p-value ≤ 0.001.

3.4.2. Study of the contribution of the clathrin-Cmd1 interaction on clathrin stability and on the interaction between Chc1 and Clc1

We observed that deletion of the Cmd1 binding site in clathrin resulted in lower expression of Chc1 and Clc1 and endocytic defects (Figures 23B, 23C, 35 and 36). However, interfering with the clathrin-Cmd1 interaction in the *cmd1-242* mutant did not affect the Chc1 or Clc1 expression or endocytosis neither at 28 º C nor at

37ºC (Figures 29A, 30A, 31A and 34). Therefore, we could infer that deletion of the Cmd1 binding site in Chc1 and Clc1 altered interactions of clathrin with molecules other than Cmd1.

Since the Cmd1 binding site lies within the region implicated in the Chc1-Clc1 interaction, and altering the Chc1-Clc1 interaction also results in low expression of the clathrin chains and altered triskelion assembly and endocytosis defects (Chu *et al.*, 1996; Payne, *et al*., 1987), we wondered if depletion of the Cmd1 binding site might affect the Chc1-Clc1 binding and in turn, the clathrin triskelion assembly and the clathrin stability.

If this was the case, the uptake defect in the Cmd1 binding site mutant might probably be caused by the defective Chc1-Clc1 interaction or triskelion formation rather than by a defective clathrin-Cmd1 interaction. For that, we investigated the effect of the Cmd1 binding site deletion in the Chc1-Clc1 interaction and their ability to form triskelions, and we compared the effects with those installed in the *cmd1-242* mutant at 37ºC, to differentiate between the phenotypes directly caused by the interference of the clathrin-Cmd1 interaction and those installed by other reasons.

3.4.2.1. Deletion of the Cmd1 binding site on Chc1 affects its interaction with Clc1 and the interaction of Clc1 with Cmd1 in yeast

First, we analyzed the protein expression of WT or mutant Chc1 and Clc1 in a *chc1Δ* strain, expressing or not either Chc1 from a centromeric plasmid (*CHC1 CEN*), or Chc1-cbsΔ or Clc1-HA from centromeric or a multicopy plasmids (*chc1-cbsΔ* CEN or 2µ and *CLC-HA1* CEN or 2µ, respectively) (Figure 38A). Immunoblots from total protein extracts from the cells mentioned showed that Clc1, as well as Chc1 in *chc1Δ* strain, were expressed at very low levels upon deletion of the Cmd1 binding site in Chc1.

Next we wanted to assess if the Chc1-cbsΔ mutant interaction with Clc1 was disrupted, so that the lost of Chc1 and Clc1 and the phenotypes displayed in the *chc1-cbsΔ* could be explained as a consequence of interfering with the Chc1-Clc1 interaction rather than with the Chc1-Cmd1 interaction. Therefore, we performed co-immunoprecipitations using anti-HA agarose from *chc1Δ* cells expressing Clc1-

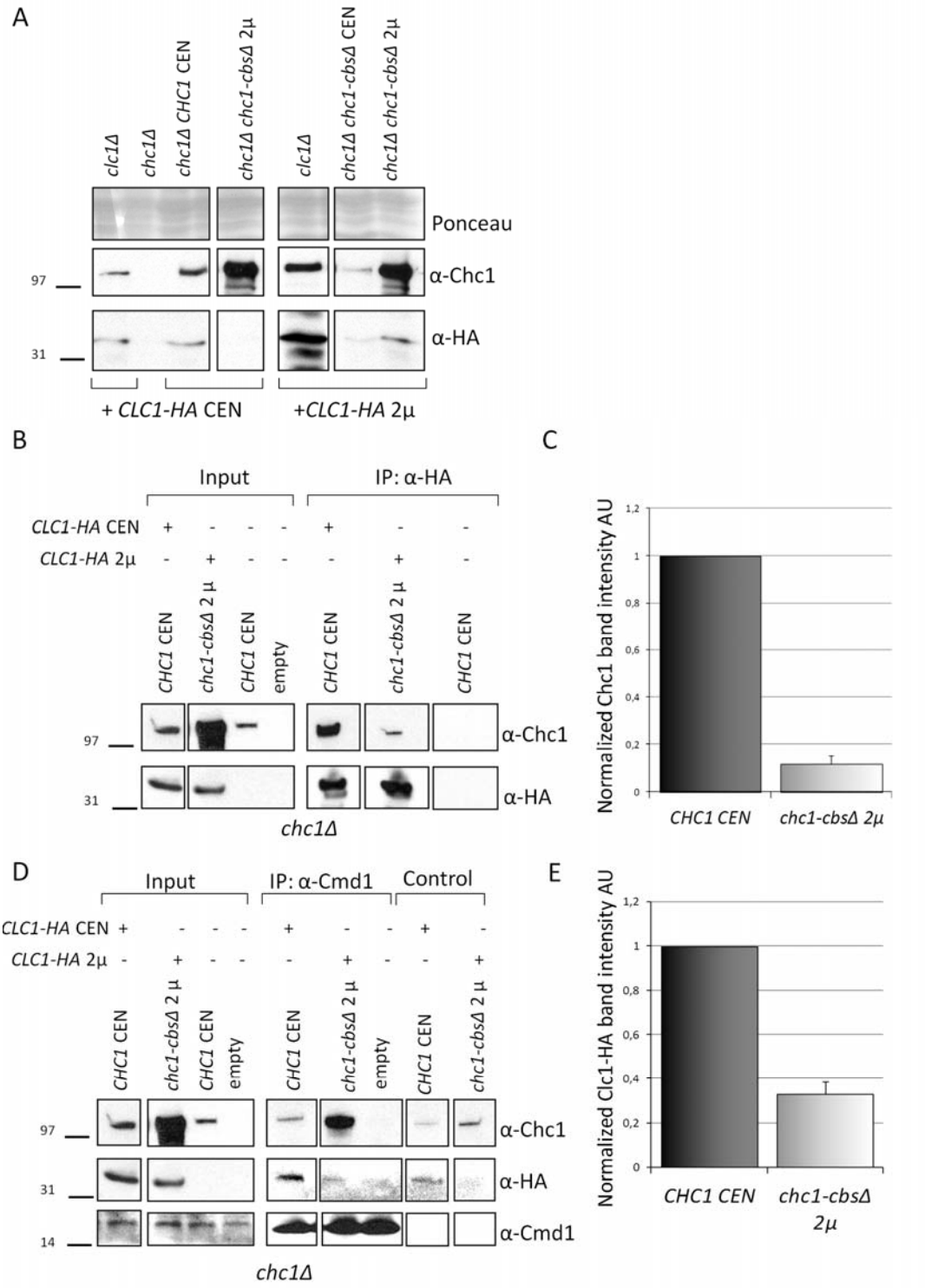

Figure 38. The Cmd1 binding site deletion in Chc1 negatively affects its interaction with Clc1 and the Clc1 interaction with Cmd1 in yeast. (A) Immunoblot of total protein extracts from a *clc1Δ* strain (SL1620) expressing Clc1-HA from centromeric or multicopy plasmids under the control of their own promotor (*CLC1-HA* CEN and 2μ; p111-*CLC1-HA* and p181-*CLC1-HA,* respectively) and a *chc1Δ* strain (SL114) expressing Clc1-HA from centromeric or multicopy plasmids (*CLC1-HA* CEN or 2μ) and Chc1 expressed from a centromeric plasmid (*CHC1* CEN) or Chc1-cbsΔ expressed from centromeric or multicopy plasmids (*chc1-cbsΔ* CEN or 2μ), all under the control of their own promotor (p111-*CLC1-HA*, p181-*CLC1-HA,* p50-*CHC1,* p50-*chc-cbsΔ* and p195-*chc1-cbsΔ,* respectively). Ponceau red staining was used to demonstrate equivalent protein loading. An antibody against Chc1 (α-Chc1) combined

with an appropriate secondary antibody and a peroxidase-conjugated antibody against HA (α-HA) was used to detect the Chc1 or Chc1-cbsΔ and the Clc1-HA, respectively. 25 µg of total protein was loaded per lane. (B) Immunoblot of co-immunoprecipitations with anti-HA agarose from a *chc1Δ* (SL114) strain expressing or not Clc1-HA from centromeric or multicopy plasmids (*CLC1-HA* CEN or 2µ) and Chc1 expressed from a centromeric plasmid (*CHC1* CEN) or Chc1-cbsΔ expressed from a multicopy plasmid (*chc1-cbsΔ* 2µ), all under the control of their own promotor (p111-*CLC1-HA*, p181-*CLC1-HA*, p50-*CHC1* and p195-*chc1-cbsΔ,* respectively). (D) Immunoblot of co-immunoprecipitations with a polyclonal serum against Cmd1 pre-bound to Protein A-Sepharose from a *chc1Δ* (SL114) strain expressing or not Clc1-HA from centromeric or multicopy plasmids (*CLC1-HA* CEN or 2µ) and Chc1 expressed from a centromeric plasmid (*CHC1* CEN) or Chc1-cbsΔ expressed from a multicopy plasmid (*chc1-cbsΔ* 2µ), all under the control of their own promotor (p111-*CLC1-HA*, p181-*CLC1-HA*, p50-*CHC1* and p195-*chc1-cbsΔ,* respectively). Immunoprecipitations of pre-immune serum pre-bound to Sepharose beads were used as controls. (B, D) The anti-HA, the immune or the pre-immune beads were incubated for 1 hour at 4ºC with the yeast extracts in the presence of 5 mM $CaCl_2$ and then they were pelleted, rinsed several times and boiled in the presence of SDS-PAGE sample buffer. Proteins were separated in a NuPAGE Bis-Tris 4-12 % gradient gel and transferred to a nitrocellulose filter. A peroxidase-conjugated anti-HA antibody (α-HA), and antibodies against Chc1 (α-Chc1) and Cmd1 (α-Cmd1), combined with an appropriate secondary antibody, were used to detect Clc1-HA, Chc1 or Chc1-cbsΔ, and Cmd1, respectively. (C) Average band intensity of the immunoprecipitated Chc1 or Chc1-cbsΔ for the experiment described in (B). Two independent experiments were performed per sample. The average Chc1 band intensity was normalized to the band intensity of the immunoprecipitated Clc1-HA for each sample. (D) Average band intensity of the immunoprecipitated Clc1-HA for the experiment described in (D). Two independent experiments were performed per sample. The average of the Clc1-HA band intensities was normalized to the band intensities of the immunoprecipitated Cmd1 for each sample, deducting also the band intensity for the corresponding pre-immune control sample. (C, E) Quantifications were performed with ImageJ. Results were then normalized to the corresponding input band size and then to the maximum value. AU: arbitrary units.

HA (*CLC1-HA* CEN) with Chc1 WT (*CHC1* CEN) or overexpressing Clc1-HA (*CLC-HA1* 2µ) together with Chc1-cbsΔ (*chc1-cbsΔ* 2µ). Cells transformed only with *CHC1* CEN were used as a control for unspecific binding (Figures 38A and 38B). The results revealed that Chc1-cbsΔ was in fact not able to bind *Clc1* in yeast (Figures 38B and 38C).

Consistent with our previous observation that binding of Clc1 to Chc1 was required for efficient binding of Clc1 to Cmd1, we observed that the Clc1-Cmd1 interaction was affected in a *chc1-cbsΔ* mutant (Figures 38D and 38E). Thus, the Clc1 binding to Cmd1 was analyzed by co-immunoprecipitations with a polyclonal serum against Cmd1 pre-bound to protein A-Sepharose from *chc1Δ* cells expressing Clc1-HA (*CLC1-HA* CEN) with Chc1 WT (*CHC1* CEN) or overexpressing Clc1-HA (*CLC1-HA* 2µ), together with overexpressed Chc1-cbsΔ (*chc1-cbsΔ* 2µ). Cells transformed only with an empty plasmid were used as a control for unspecific antibody detention and a pre-immune serum pre-bound to protein A-Sepharose was used as control for unspecific binding (control) (Figures 38D and 38E). Clc1-HA co-immunoprecipitation with Cmd1 was negatively affected in *the chc1-cbsΔ* mutant.

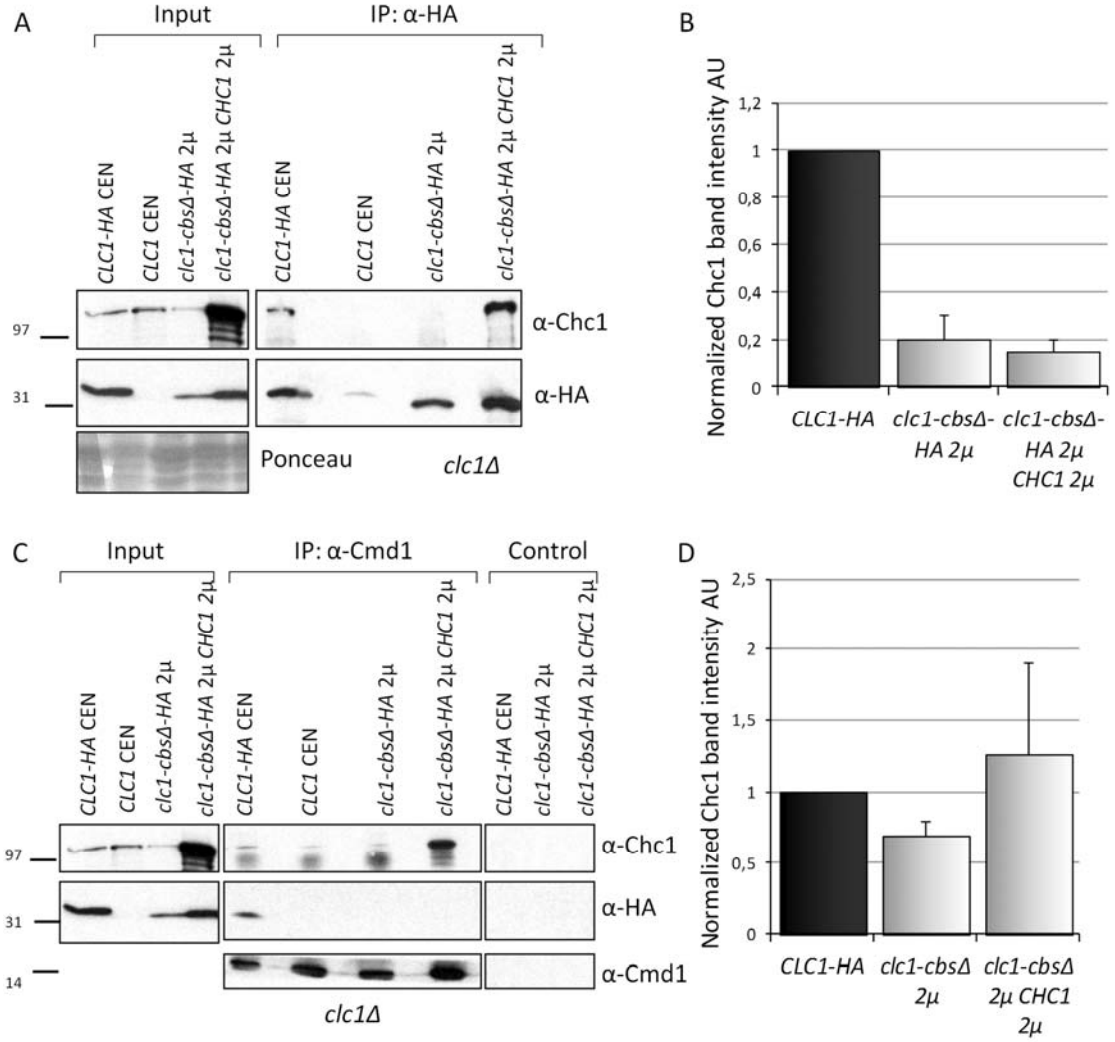

Figure 39. The Clc1-cbsΔ mutant interaction with Chc1 is affected, but it does not affect the Chc1 interaction with Cmd1. (A) Immunoblot of an anti-HA agarose co-immunoprecipitations from a *clc1Δ* strain (SL1620) expressing non tagged or HA-tagged Clc1 from centromeric plasmids (*CLC1* or *CLC1-HA*) and Clc1-cbsΔ expressed from a multicopy plasmid (*clc1-cbsΔ* 2μ), all under the control of its own promotor (p111-*CLC1*, p111-*CLC1-HA* and p181-*clc1-cbsΔ*, respectively), co-transformed or not with Chc1 expressed from a multicopy plasmid under the control of its own promotor (*CHC1* 2μ; YEp24-*CHC1*). (C) Immunoblot of co-immunoprecipitations with a polyclonal serum against Cmd1 pre-bound to Protein A-Sepharose from a *clc1Δ* strain (SL1620) expressing non tagged or HA-tagged Clc1 from centromeric plasmids (*CLC1* or *CLC1-HA*) and Clc1-cbsΔ expressed from a multicopy plasmid (*clc1-cbsΔ* 2μ), all under the control of its own promotor (p111-*CLC1*, p111-*CLC1-HA* and p181-*clc1-cbsΔ*, respectively), co-transformed or not with Chc1 expressed from a multicopy plasmid, under the control of its own promotor (*CHC1* 2μ; YEp24-*CHC1*). Immunoprecipitations with pre-immune serum pre-bound to Protein A-Sepharose beads were used as controls. (A, C) The anti-HA, the immune or pre-immune beads were incubated for 1 hour at 4ºC with the yeast extracts in the presence of 5 mM $CaCl_2$ and then they were pelleted, rinsed several times and boiled in the presence of SDS-PAGE sample buffer. Proteins were separated in a NuPAGE Bis-Tris 4-12 % gradient gel and transferred to a nitrocellulose filter. Ponceau red staining was used to demonstrate equivalent protein loading. A peroxidase-conjugated anti-HA antibody (α-HA), and antibodies against Chc1 (α-Chc1) and Cmd1 (α-Cmd1), combined with an appropriate secondary antibodies, were used to detect Clc1-HA, Chc1 or Clc1-cbsΔ-HA, and Cmd1, respectively. (B) Average band intensity of the immunoprecipitated Chc1 for the experiment described in (A). Two independent experiments were performed per sample. The average Chc1 band intensity was normalized to the band intensity of the immunoprecipitated Clc1-HA or Clc1-cbsΔ-HA for each sample. (D) Average band intensity of the immunoprecipitated Chc1 for

the experiment described in (C). Two independent experiments were performed per sample. The average Chc1 band intensity was normalized to the band intensity of the immunoprecipitated Cmd1 for each sample, deducting also the band intensity for the corresponding pre-immune control sample. (B, D) Quantifications were performed with ImageJ. Results were then normalized to the corresponding input band size and then to Clc1-HA. AU: arbitrary units.

3.4.2.2. Deletion of the Cmd1 binding site on Clc1 affects its interaction with Chc1 but it does not affect the interaction of Chc1 with Cmd1 in yeast

Next, we analyzed Clc1 and Chc1 expression when Clc1 lacked the Cmd1 binding site, and the capacity of Clc1-cbsΔ mutant to bind Chc1 in yeast. For that, we performed co-immunoprecipitations using anti-HA agarose from *clc1Δ* cells expressing either Clc1-HA (*CLC1-HA* CEN), Clc1 (*CLC1* CEN), or Clc1-cbsΔ expressed from a multicopy plasmid (*clc1-cbsΔ* 2µ) and co-expressed or not with overexpressed Chc1 (*CHC1* 2µ). Cells transformed with p*CLC1* CEN were used as a control for unspecific binding (Figures 39A). Analysis of the protein expression from the total protein extracts showed in the input (Figure 39A) revealed that Chc1 as well as Clc1 showed low expression levels in a *clc1Δ* strain complemented with *clc1-cbsΔ*. *CHC1* and *clc1-cbsΔ* were expressed from multicopy plasmids to be able to detect them easily by immunoblot.

As represented in Figures 39A and 39B, the results revealed that the Clc1-cbsΔ interaction with Chc1 in yeast was affected.

Next, we wanted to analyze the influence of *clc1-cbsΔ* mutation on the ability of Chc1 to bind Cmd1. Thus co-immunoprecipitations with a polyclonal serum against Cmd1 bound to protein A-Sepharose were performed from non-denaturing protein extracts of the strains indicated above. A pre-immune serum pre-bound to protein A-Sepharore was used as control for unspecific binding (control) (Figures 39C and 39D). The results unveiled that the deletion of the Cmd1 binding site in Clc1 did not affect the ability of Chc1 to interact with Cmd1 in yeast, consistent with the previous result indicating that Chc1 can bind Cmd1 in the absence of Clc1 (Figures 26D and 26E).

3.4.2.3. The *cmd1* point mutations that alter the clathrin-Cmd1 interaction do not affect the Chc1 interaction with Clc1

Having confirmed that Chc1 and Clc1 mutants are not able to bind to their partner chain in the absence of the Cmd1 binding site and this probably cause the instability of the Cmd1 binding site deletion mutants, we wanted to test if the Cmd1 point mutants that are not able to bind clathrin in yeast or *in vitro* also altered the interaction between clathrin chains. Therefore, we did co-immunoprecipitations with anti-HA agarose from *CMD1 WT, cmd1-226, cmd1-228* and *cmd1-242* mutant strains grown at 28ºC and then 1 hour at 37ºC expressing Clc1-HA to analyze the relative amount of endogenous Chc1 co-precipitating with Clc1-HA (Figure 40). The results indicated that none of the point mutations that impaired the clathrin-Cmd1 interaction (*cmd1-228* and *cmd1-242*) affected the Chc1-Clc1 interaction, as compared with the WT Cmd1 or a Cmd1 mutant that did not altered the clathrin-Cmd1 interaction.

Thus, we concluded that altering of clathrin-Cmd1 interaction did not necessarily affect Chc1 binding to Clc1.

3.4.2.4. Chc1-cbsΔ fails to form triskelions, but Chc1 can still form triskelions in the *cmd1-228* and *cmd1-242* mutants

Chc1 is not able to form triskelions in the absence of Clc1 (Chu *et al.,* 1996; Payne *et al.*, 1987). Therefore, we postulated that the Chc1-cbsΔ mutant, which was unable to bind Clc1, might also be unable to form triskelions. To test this hypothesis, we investigated the capacity of Chc1-cbsΔ to form triskelions, as compared to Chc1, expressed in either a WT *CMD1* background or in the *cmd1* point mutants in which the Chc1-Clc1 interaction was not altered but the clathrin-Cmd1 interaction was. We analyzed the native protein conformation using Native PAGE (see Materials and Methods section 6.4.5.), from cytosolic non-denaturing protein extracts from *chc1*Δ expressing either Chc1-HA or Chc1-cbsΔ-HA (*chc1Δ CHC1-HA*, or *chc1Δ Chc1-cbsΔ-HA*), *clc1*Δ expressing Chc1-HA (*clc1Δ CHC1-HA)*, and *CMD1 WT, cmd1-226, cmd1-228* and *cmd1-242* strains expressing Chc1-HA grown for 1 hour at 37ºC previous to harvesting (Figure 41).

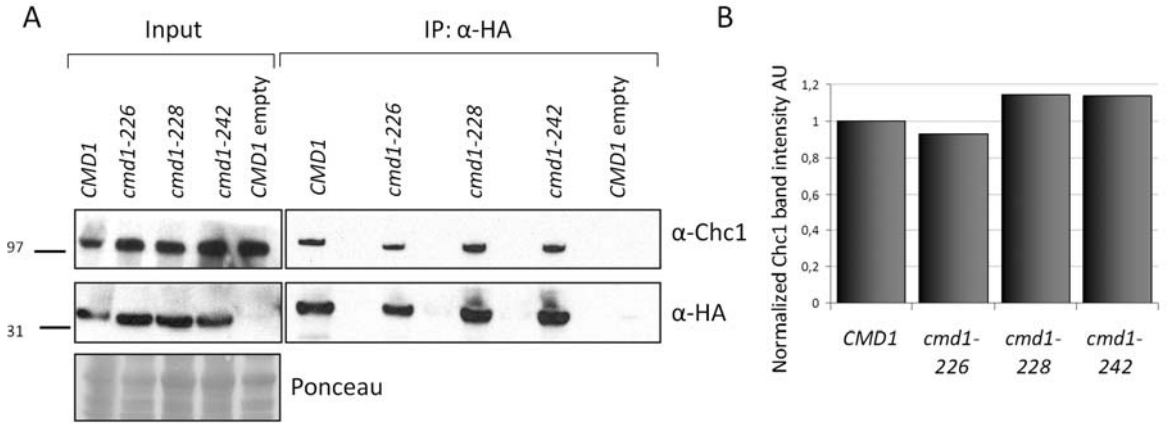

Figure 40. The Chc1-Clc1 interaction does not seem to be affected in the Cmd1 point mutants grown at 37ºC. Immunoblot of co-immunoprecipitations with an anti-HA agarose from *WT CMD1 (*RH3983*), cmd1-226 (*RH3984*), cmd1-228 (*RH3985*), cmd1-231 (*RH3986*), cmd1-239(*RH3988) and *cmd1-242 (*RH3990) cells, grown at 28ºC and then 1 hour at 37ºC, expressing Clc1-HA from a centromeric plasmid, under the control of its own promotor (p111-*CLC1-HA*). The anti-HA agarose beads were incubated for 1 hour at 4ºC with the yeast extracts in the presence of 5 mM $CaCl_2$ and then they were pelleted, rinsed several times and boiled in the presence of SDS-PAGE sample buffer. Proteins were separated in a NuPAGE Bis-Tris 4-12 % gradient gel and transferred to a nitrocellulose filter. Ponceau red staining was used to demonstrate equivalent protein loading. A peroxidase-conjugated anti-HA antibody (α-HA) and an antibodies against Chc1 (α-Chc1) combined with an appropriate secondary antibody, were used to detect Clc1-HA and the endogenous Chc1, respectively. (B) Average band intensity of the co-immunoprecipitated Chc1 for the experiment described in A. Two independent experiments were done for each sample. Quantifications were performed with ImageJ. The average Chc1 band intensity was normalized to the band intensity of the immunoprecipitated Clc1-HA for each sample. Results were then normalized to the corresponding input band size and then to the WT Cmd1. AU: arbitrary units.

Protein extracts were treated under non-denaturing conditions, to preserve the triskelion conformation. A control sample of *chc1Δ* expressing WT Chc1-HA was denatured in conventional SDS-PAGE sample buffer and loaded separated from the rest to have the reference where the monomer of the protein of interest run.

The results presented in Figure 41 confirmed that the Chc1-cbsΔ mutant, which is not able to bind Clc1, is not able to form triskelions neither, similar to Chc1 expressed in a *clc1Δ* strain. In contrast, Chc1 was capable of forming triskelion in all the *cmd1* mutants analyzed one hour after incubation at restrictive temperature, consistent with the fact that the Chc1-Clc1 interaction is not altered. Consequently, we can assume that altering the clathrin-Cmd1 interaction does not directly affect the ability of Chc1 to form triskelions.

In summary, these results indicated that the Chc1-cbsΔ and Clc1-cbsΔ mutants were less expressed, showed an altered Chc1-Clc1 interaction and failed to form triskelions. Therefore, the uptake and growth defects installed in these mutants are not necessarily caused by the impaired clathrin-Cmd1 interaction, but might be an indirect consequence of the impaired Chc1-Clc1 interaction and /or the failure to form clathrin triskelions and most likely also to form clathrin cages. Importantly, the stability of Chc1, its capacity to form triskelions and its ability to interact with Clc1 appeared unaltered in the *cmd1-228* and *cmd1-242* mutants at restrictive temperature, indicating that the clathrin-Cmd1 interaction does not play an essential role in the assembly of these clathrin suprastructures.

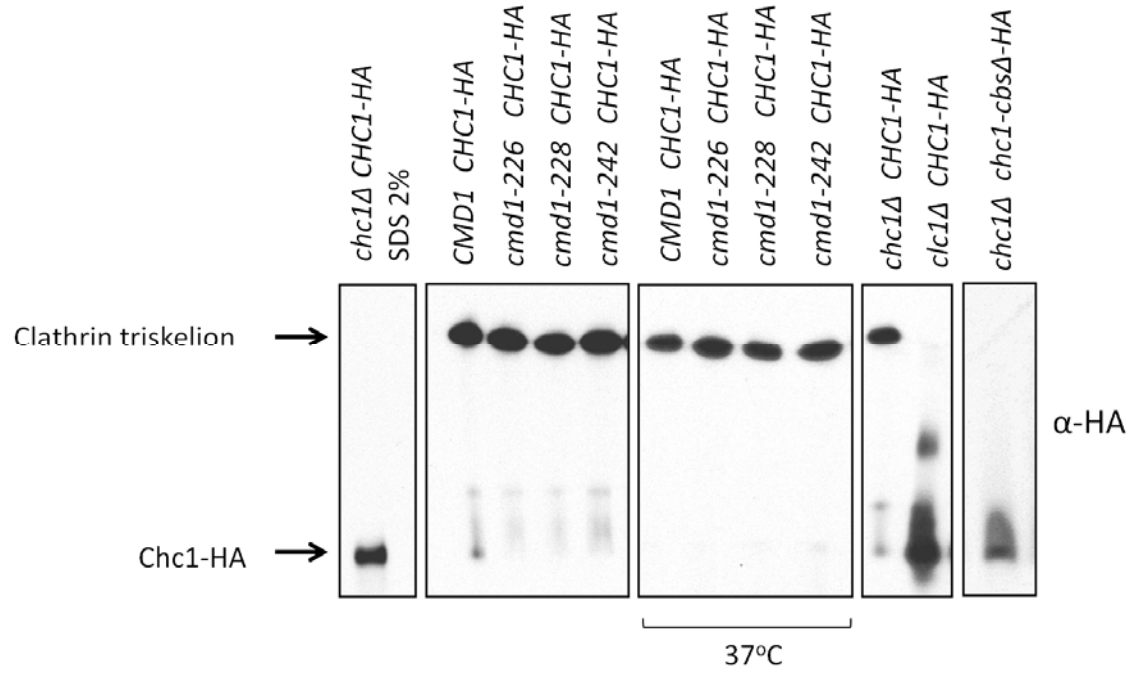

Figure 41. The Chc1-cbsΔ mutant is defective in the formation of triskelions, but Chc1 is able to form triskelions in the *cmd1-228* and *cmd1-242* mutants. Immunoblots of cytosolic non-denaturing protein extracts from *chc1*Δ (SL114), *clc1*Δ (SL1620)*, CMD1* (RH3983), *cmd1-226* (RH3984)*, cmd1-228* (RH3985) *and cmd1-242* (RH3990) strains, expressing either Chc1-HA (*CHC1-HA*) or Chc1-cbsΔ-HA (*chc1-cbsΔ-HA*) from centromeric plasmids, under the control of their own promotor (p50-*CHC1-HA* and p50-*chc1-cbs*Δ, respectively). When indicated, cells were incubated for 1 hour at 37°C (37ºC), previous to harvesting. Proteins were separated in NativePAGE 3-12 % Bis-Tris gels and transferred to PVDF membranes. A peroxidase-conjugated anti-HA antibody (α-HA) was used to detect the clathrin triskelion or the Chc1 monomers.

3.4.3. Disruption of the clathrin-Cmd1 interaction alters the clathrin TGN-endosomal function

3.4.3.1. The *cmd1-228* and *cmd1-242* mutants are defective in the endosomal to TGN retrograde transport of the α-factor processing enzyme Kex2

3.4.3.1.1. The *cmd1-228* and *cmd1-242* mutants exhibit an halo formation defect on *Mat***a** *sst1 sst2* lawns at 30ºC that is most likely a consequence of interfering with clathrin function

Once verified that the clathrin-Cmd1 interaction does not have an essential role in endocytic uptake from the PM, we wondered if it may function in the traffic between the TGN and endosomes, where clathrin is also involved. To analyze possible TGN-endosomal trafficking defects installed upon disruption of the clathrin-Cmd1 interaction, we initially performed halo assays on lawns of *Mat***a** *sst1 sst2* cells (see Materials and Methods section 6.5.1.). This assay measures the defect in bioactive α-factor production by *Mat***α** cells, caused by the mislocalization of Kex2, a protease that normally localizes at the TGN and processes the α-factor yeast pheromone expressed in and secreted from *Mat***α** cells (Fuller *et al*., 1989a; Fuller *et al*., 1989b; Redding *et al*., 1996). Once processed, the α-factor is secreted to the media and causes the matting response in *Mat***a** cells, which express the α-factor receptor Ste2. As part of the matting response, *Mat***a** *SST1 SST2* cells suffer a cell cycle arrest. The *SST1* gene, encodes a protease secreted into the cellular periplasmic space that cleaves and inactivates the α-factor allowing cells to recover from the α-factor-induced cell cycle arrest, whereas the *SST2* gene encodes for a GTPase that regulates desensitization to α-factor pheromone and is also required to prevent receptor-independent signalling of the mating pathway (Dohlman *et al.,* 1996). The assay is based on the observation that *MAT***a** cells bearing double *sst1* and *sst2* mutations cannot recover from the cell cycle arrest induced by the α-factor pheromone (Chan & Otte, 1982). So, when *Mat***α** cells are spotted on a loan of hyper-sensitive *Mat***a** *sst1* and *sst2* mutant cells, the cell cycle arrest can be visualized as an halo surrounding the cells secreting the active α-factor. Kex2 is maintained at the TGN by continuous recycling of the enzyme from the TGN to the endosomes and back to the TGN, both trafficking pathways being dependent on clathrin (Black & Pelham, 2000; Lemmon & Traub, 2000; Redding *et al.*, 1996; Valdivia *et al*., 2002;

Vida *et al.*, 1993). When a defect is installed upon any of these pathways, Kex2 mislocalizes from the TGN and cannot process the α-factor, which is secreted as a pre-processed inactive form that is unable to arrest the *Mat***a** cells growth and thus, the halo will not be observed.

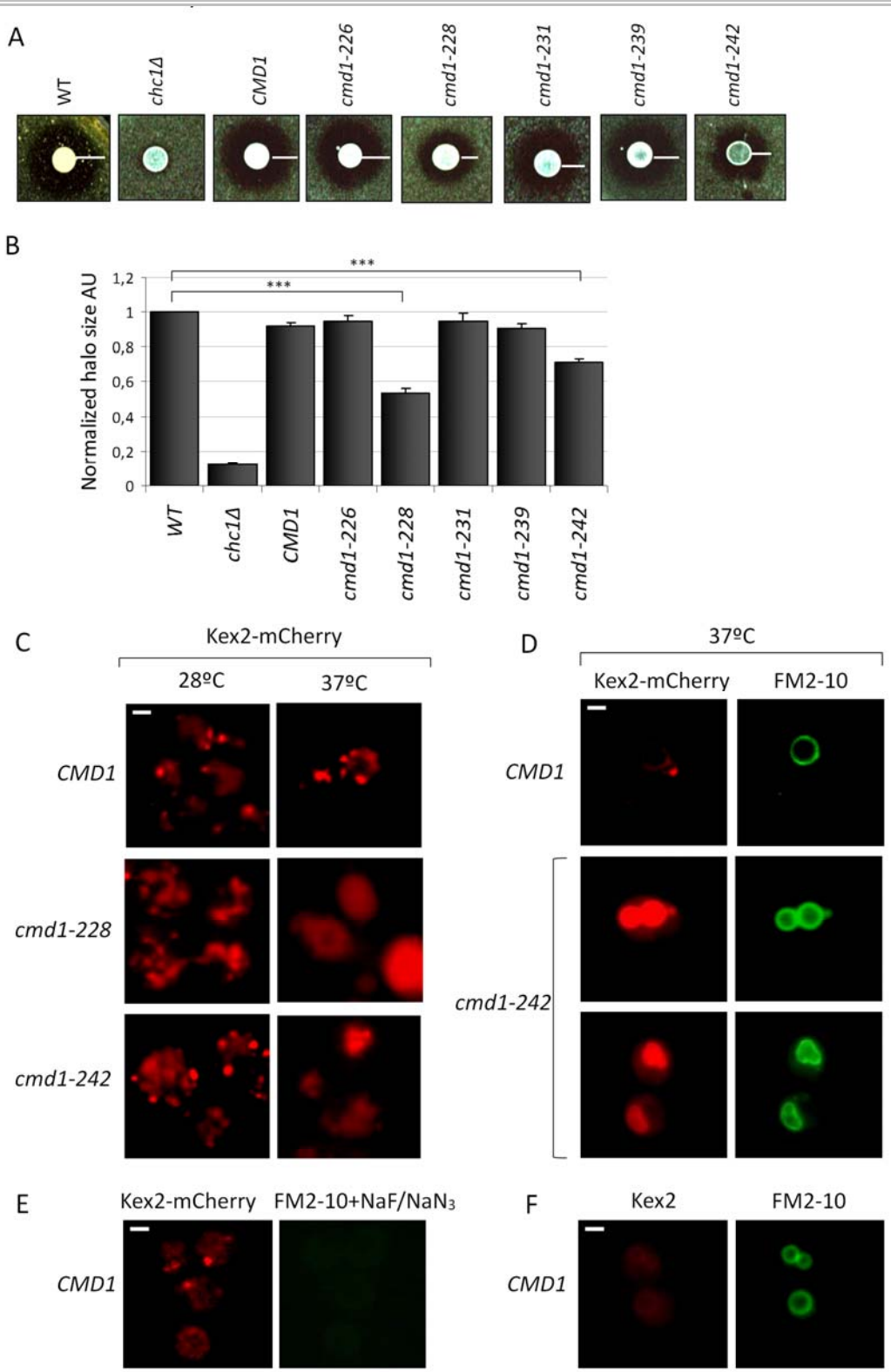

Figure 42. The *cmd1-228* and *cmd1-242* mutants misssort the α-factor processing enzyme Kex2 from the TGN to the vacuole. (A) Halo assay for a *cmd1Δ* strain expressing either the WT Cmd1 or the Cmd1-226, Cmd1-228, Cmd1-231, Cmd1-239 or Cmd1-242 mutants from centromeric plasmids under the control of their own promotor (SCMIG1261, SCMIG1262, SCMIG1263, SCMIG1264, SCMIG1265 and SCMIG1266, respectively). Cells from a mid-log phase culture were patched over a *MAT***a** *sst1 sst2* yeast lawn and let grown for 48 hours at 30ºC. A zone of growth inhibition (halo) demonstrates secretion of mature α-factor. (B) Average halo size for the experiment described in A. Quantifications were performed with ImageJ. At least three independent experiments were done for each sample. The average halo size for each sample was normalized to the halo size of the WT strain. Statistical significance was tested using the two-tailed Student's t-test.*** represents a p-value ≤ 0.001. AU: arbitrary units.(C,D) Fluorescence micrographs of *cmd1Δ KEX2-mCherry* cells expressing either the WT Cmd1, the Cmd1-228 or Cmd1-242 mutants from centromeric plasmids under the control of their own promotor (SCMIG1294, SCMIG1295 and SCMIG1296, respectively), and grown at the indicated temperature and treated (D) or not (C) with the styril dye FM2-10 for 45 minutes at 37ºC. (E) Control for the internalized FM2-10. *cmd1Δ KEX2-mCherry* cells expressing the WT Cmd1 (SCMIG1294) were treated with FM2-10 and 10 mM NaF/NaN_3 to avoid internalization. (F) Control for the FM2-10 cross-exciting. *cmd1Δ* cells expressing the WT Cmd1 (SCMIG1261) were treated with FM2-10 for 45 minutes at 28ºC. (D,E,F) Fluorescence images for mCherry (left) and FM2-10 (right) were taken. Scale bar: 2 µm.

Interestingly, as shown in Figures 42A and 42B our results from the halo assays from *CMD1 WT* and *cmd1* mutants from each complementation group demonstrated that the *cmd1-228* and *cmd1-242* mutants that alter the direct clathrin-Cmd1 interaction, but not the *cmd1-226*, *cmd1-231* and *cmd1-239* mutants that do not alter the interaction, showed a strong halo formation defect at 30ºC (*chc1Δ* strain, known to have a strong defect in the halo assay (Newpher *et al.*, 2006), was used as negative control). Interestingly, this defect was significantly rescued by overexpressing either Chc1 (*CHC1* 2µ) or Clc1 (*CLC1* 2µ), but not the Chc1-cbsΔ (*chc1-cbsΔ* 2µ) and Clc1-cbsΔ (*clc1-cbsΔ* 2µ) mutants (Figure 43A and 43B). This result suggested that the halo formation defect in the Cmd1 mutants is a direct consequence of interfering with clathrin function. It must be mentioned that overexpression of Chc1-cbsΔ rescued to some extent the halo defect on *cmd1-242,* maybe because Cmd1 could still bind the N-terminus of the Chc1-cbsΔ mutant and compensate for the lack of binding of to the C-terminus, as previously demonstrated by *in vitro* (Figure 20) and in yeast extracts (Figure 24) experiments. Small differences in the halo size between strains and replicas might be consequence of differences in the pH of the solid media in the plate that can affect the halo formation. An immunoblot from total protein extracts from the strains used in the halo assays (Figure 43C) was made to control for the overexpression of WT or mutant Chc1 and Clc1.

3.4.3.1.2. Kex2 is mislocalized to endosomal structures and vacuoles in *cmd1-228* and *cmd1-242* mutants

In order to narrow down the trafficking defect installed upon disruption of the clathrin-Cmd1 interaction, we analyzed the *in vivo* localization of genome-edited Kex2-mCherry in the *cmd1-228* and the *cmd1-242* mutants at 28ºC and at 37ºC (Figure 42C) (See Materials and Methods section 6.6.1.). Kex2-mCherry in *CMD1* WT cells either at 28ºC or 37ºC, localized mostly in discrete patches that co-localize with TGN and endosomal markers (Newpher *et al*., 2005). On the contrary, we observed that at 28ºC, in the *cmd1* mutants Kex2 appeared in abnormal endosomal-like enlarged structures and discrete patches were reduced. At 37ºC, the aberrant phenotype was even more obvious, as Kex2 patches mostly disappeared and a Kex2 appeared localized in a big structure that resembled the vacuole. This phenotype was more notable in the *cmd1-228* mutant.

Kex2 mislocalization from the TGN can be caused by a defect in the TGN endosomal forward or retrograde transport to or from the endosomes. In the first case, Kex2 is secreted to the cell surface, and can reach the vacuole by endocytosis (Black & Pelham, 2000; Nothwehr et al., 1995; Seeger & Payne, 1992) whereas in the second case Kex2 will rather accumulate rapidly in endosomal-vacuolar compartments (Redding *et al.*, 1996; Wilcox *et al.*, 1992). For the purpose of verifying that the structures where Kex2 accumulated in the mutants were of endocytic origin, we analyzed the localization of Kex2-mCherry in the *cmd1-242* mutant at restrictive temperature in the presence of the fluorescent styryl dye FM2-10 (green version of the FM4-64) (Figure 42D) which labels the endosomal and lysosomal system in cells that do not have endocytic defects (Vida & Emr, 1995)(See Material and Methods 6.5.3.). This analysis revealed that at restrictive temperature, Kex2 was mislocalizing to vacuoles, and no significant labeling could be detected at the PM, not even in the *cmd1-228* mutant, whose capacity to endocytose is completely blocked at restrictive temperature so Kex2 cannot reach the vacuole via the PM. Thus, these results suggest that disruption of the clathrin-Cmd1 interaction mainly causes a defect in the retrograde transport from the endosomes to the TGN.

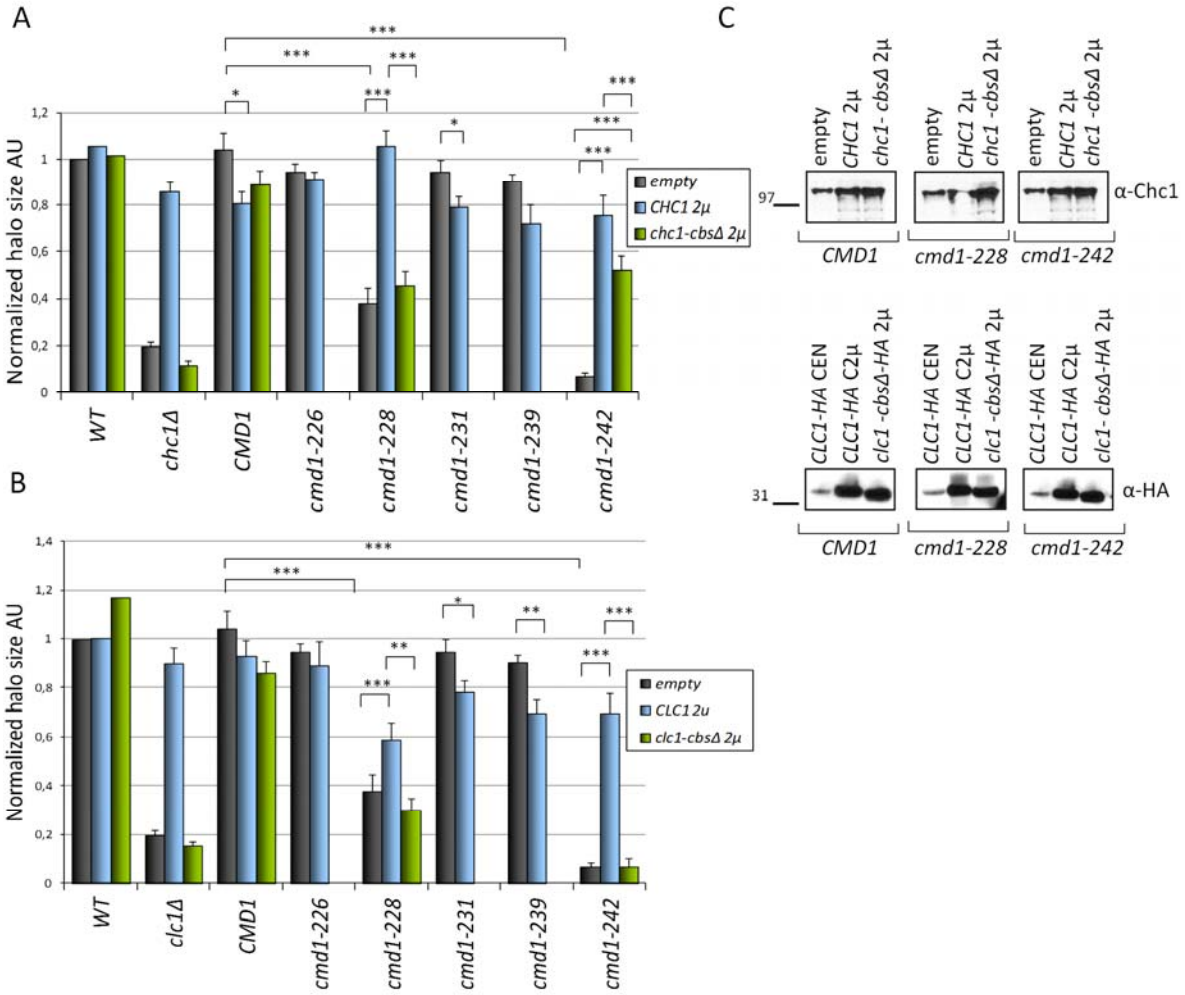

Figure 43. The *cm1-228* and *cmd1-242* defect in bioactive α-factor production is significantly rescued by overexpressing the Chc1 or Clc1 but it is rescued to a lesser extent by overexpressing Chc1-cbsΔ or Clc1-cbsΔ. (A, B) Average halo size for assays performed for a *cmd1Δ* strain expressing either the WT Cmd1 or the Cmd1-226, Cmd1-228, Cmd1-231, Cmd1-239 or Cmd1-242 mutants from centromeric plasmids under the control of their own promotor (SCMIG1261, SCMIG1262, SCMIG1263, SCMIG1264, SCMIG1265 and SCMIG1266, respectively), transformed with a multicopy empty plasmid (*empty*; YEplac195) , or a multicopy plasmid encoding either *CHC1* or *chc1-cbsΔ* (*CHC1* 2µ or *chc1-cbsΔ* 2µ ; YEp24-*CHC1* or p195-*chc1-cbsΔ*, respectively) (A) or *CLC1* or *clc1-cbsΔ* (*CLC1* 2µ or *clc1-cbsΔ* 2µ; p181-*CLC1* or p181- *clc1-cbsΔ*, respectively) (B), expressed under the control of their own promotor. Cells from a mid-log phase culture were spotted over a *MAT***a** *sst1 sst2* lawn and let grown for 48 hours at 30ºC. The size of the zone of growth inhibition (halo) was quantified with ImageJ. At least three independent experiments were done for each sample. The average halo size for each sample was normalized to the halo size of the WT strain transformed with the empty plasmid. Statistical significance was tested using the two-tailed Student's t-test, * represents a p-value ≤ 0.05; ** represents a p-value ≤ 0.01,*** represents a p-value ≤ 0.001. AU: arbitrary units. (C) Immunoblot of total protein extracts performed as a control for the overexpression of Chc1, Chc1-cbsΔ, Clc1-HA and Clc1-cbsΔ-HA for strains described in A and B. An antibody against Chc1 (α-Chc1), combined with an appropriate secondary antibody, was used to detect Chc1, and a peroxidase-conjugated anti-HA antibody (α-HA) was used to detect the HA-tagged Clc1. 25 µg of total protein was loaded per lane.

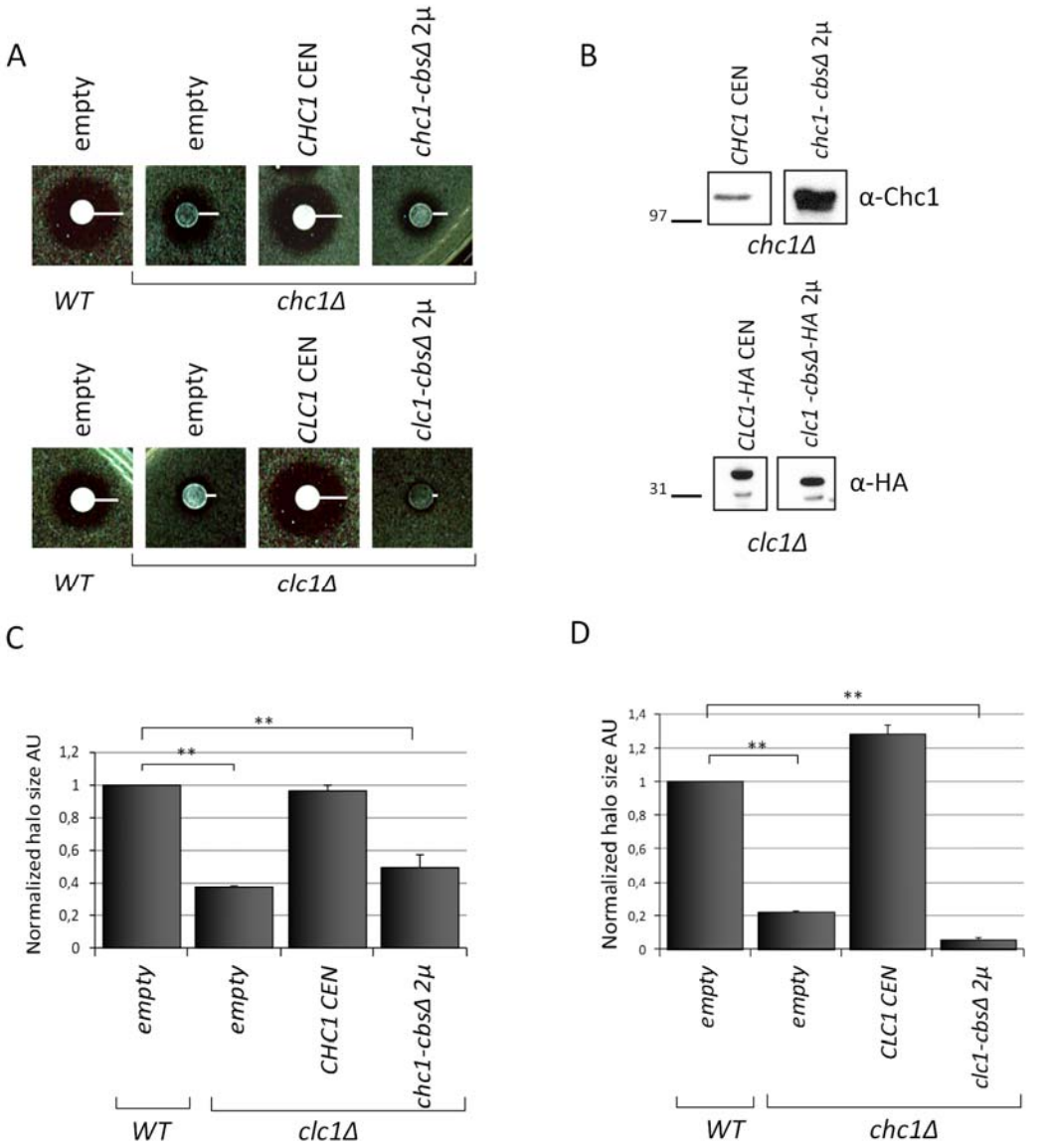

Figure 44. The *chc1-cbsΔ* and *clc1-cbsΔ* mutants have a defect in bioactive α-factor production. (A) *Mat***a** *sst1 sst2* cells halo assay for a *chc1Δ* strain (SL114) transformed with a multicopy empty plasmid (*empty*; YEplac195), a centromeric plasmid encoding Chc1 (*CHC1* CEN; p50-*CHC1*), and a multicopy plasmid encoding Chc1-cbsΔ (*chc1-cbsΔ* 2µ; p195-*chc1-cbsΔ*), and a *clc1Δ* strain (SL1620) transformed with a multicopy empty plasmid (*empty*; YEplac181), a centromeric plasmid encoding Clc1 (*CLC1* CEN; p111-*CLC1*), and a multicopy plasmid encoding Clc1-cbsΔ (*clc1-cbsΔ* 2µ; p181-*chc1-cbsΔ*). All the proteins were expressed under the control of their own promotor. A WT (BY4742) and a *chc1Δ* (SL114) or *clc1Δ* (SL1620) strains transformed with multicopy empty plasmids (YEplac195 or YEplac181) were used as controls. Cells from a mid-log phase culture were spotted over a *MAT***a** *sst1 sst2* lawn and let grown for 48 hours at 30ºC. A zone of growth inhibition (halo) demonstrates secretion of mature α-factor. (B) Immunoblot of total protein extracts to analyze the expression of Chc1 expressed from a centromeric plasmid (*CHC1* CEN or 2µ; p50-*CHC1*) and of Chc1-cbsΔ expressed from a multicopy plasmid (*chc1-cbsΔ* 2µ; p195-*chc1-cbsΔ)* in a *chc1Δ* strain (SL114) and the expression of Clc1-HA expressed from a centromeric plasmid (*CLC1-HA* CEN or 2µ; p111-*CLC1-HA*) and Clc1-cbsΔ-HA expressed from a multicopy plasmid (*clc1-cbsΔ-HA* 2 µ; p181-*clc1-cbsΔ-HA)* in a *clc1Δ* strain (SL1620). An antibody against Chc1 (α-Chc1), combined with an appropriate secondary antibody, was used to detect Chc1, and a peroxidase-conjugated anti-HA antibody (α-HA) was used to detect the HA-tagged Clc1. 25 µg of total protein was loaded per lane. (C, D) Average halo size for the experiment described in (A). Quantifications were performed with ImageJ. At least three independent experiments were done for each sample. The average halo size for each sample was

normalized to the halo size of the WT strain. Results were then normalized to the WT. Statistical significance was tested using the two-tailed Student's t-test. * represents a p-value ≤ 0.05; ** represents a p-value ≤ 0.01, *** represents a p-value ≤ 0.001. AU: arbitrary units.

3.4.3.2. The clathrin cbsΔ mutants also have a defect in TGN retention of the α-factor processing enzyme Kex2

We also analyzed the ability of the *chc1-cbsΔ* and *clc1-cbsΔ* mutants to process the α-factor. A *chc1Δ* expressing the WT Chc1 (*CHC1* CEN) or overexpressing the Chc1-cbsΔ mutant (*chc1-cbsΔ* 2μ) and a *clc1Δ* strain expressing the WT Clc1-HA (*CLC1-HA* CEN) or overexpressing the Clc1-cbsΔ-HA mutant (*clc1-cbsΔ-HA* 2μ) were subjected to halo assays (Figure 44). The results indicated that the Chc1-cbsΔ (Figures 44A and 44C) and Clc1-cbsΔ (Figures 44A and 44D) mutants exhibited clear defects in halo formation, similar to clathrin delta strains. Immunoblots from total protein extracts from the indicated strains were performed in order to verify the expression and overexpression of the WT or mutant clathrin chains (Figure 44B).

Thus, unlike the LY uptake assay, the halo assay performed with the clathrin mutants demonstrated a strong correlation between the TGN-endosomal trafficking defects and the capacity of clathrin and Cmd1 to directly interact *in vitro*. However, it must be taken into account that this halo formation defect might also be a consequence of the clathrin cbsΔ mutants´ inability to form triskelions and/or their incapacity to interact with their partner clathrin chain (Chu *et al*., 1996; Newpher *et al*., 2006).

3.4.3.3. The defect in Kex2 TGN retention of clathrin mutants is not dominant when the endogenous clathrin WT is present

As an halo formation defect for the Cmd1 binding site clathrin mutants was revealed when expressed in *chc1Δ* and *clc1Δ* strains, we wanted to investigate if this defect was dominant when the endogenous Chc1 or Clc1 was present (Figure 45). For that we performed halo assays for *chc1Δ* and *clc1Δ* strains transformed with a multicopy empty plasmid (controls) and for a WT strain transformed with either a multicopy empty plasmid or a plasmid encoding either the Chc1 (*CHC1* CEN) or Chc1-cbsΔ (*chc1-cbsΔ* 2μ) (Figures 45A and 45B) or transformed with

either a plasmid encoding Clc1 (*CLC1* CEN) or Clc1-cbsΔ (*clc1-cbsΔ* 2µ) (Figures 45A and 45C). The results revealed that overexpressing the Chc1-cbsΔ or Clc1-cbsΔ mutants in a WT strain that also expressed the endogenous WT Chc1 and Clc1, had no effect in their ability to arrest the growth of a hyper-sensitive *Mat***a** *sst1 sst2* cells lawn, suggesting that the halo formation defect of clathrin mutants is not dominant.

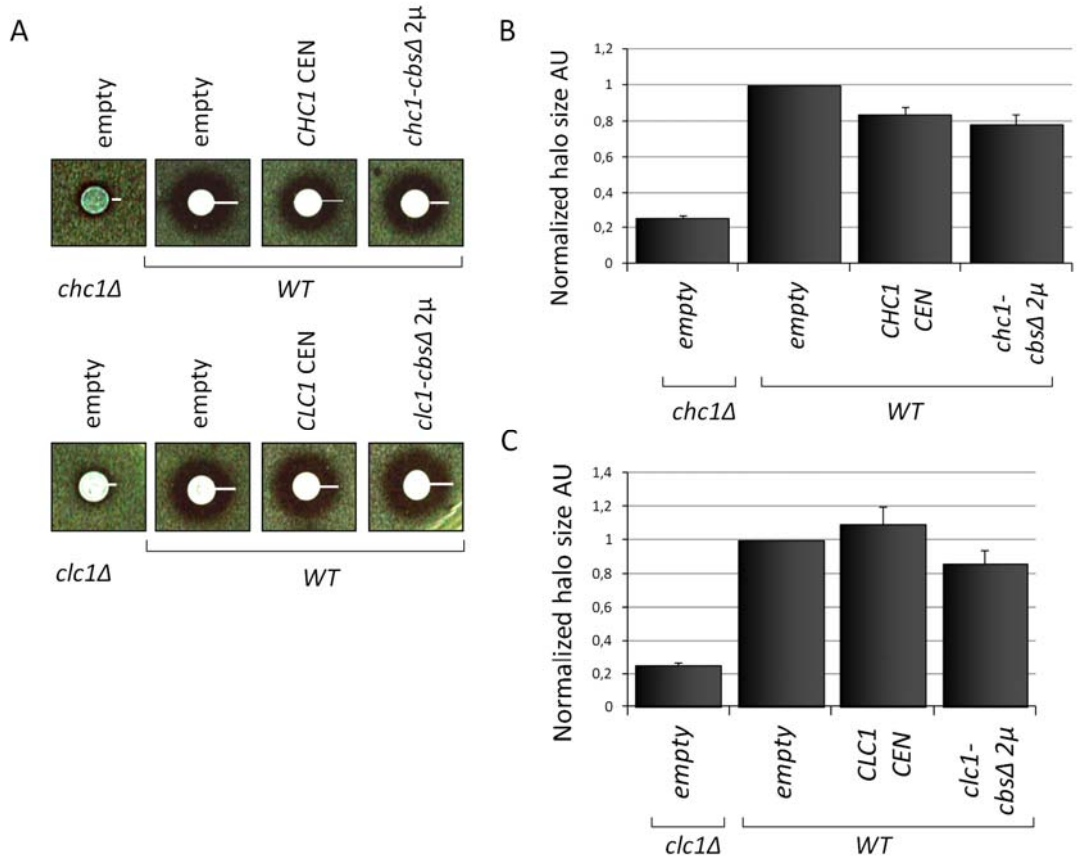

Figure 45. The *chc1-cbsΔ* and *clc1-cbsΔ* mutants do not have a dominant phenotype in the halo assay when the endogenous WT clathrin is present. (A) *Mat***a** *sst1 sst2* cells halo assay for a *chc1Δ* (SL114) or a *clc1Δ* (SL1620) strains transformed with a multicopy empty plasmid (YEplac195 or YEplac181, respectively), and a WT strain (BY4742) transformed with a multicopy empty plasmid (YEplac195 or YEplac181), a centromeric plasmid encoding Chc1 (*CHC1* CEN) or Clc1 (*CLC1* CEN) (p50-*CHC1* or p111-*CLC1*, respectively), and a multicopy plasmid encoding Chc1-cbsΔ (*chc1-cbsΔ* 2µ) or Clc1-cbsΔ (*clc1-cbsΔ* 2µ) (p195-*chc1-cbsΔ* or p181-*clc1-cbsΔ*, respectively). Cells from a mid-log phase culture were spotted over a *MAT***a** *sst1 sst2* lawn and let grown for 48 hours at 30ºC. A zone of growth inhibition (halo) demonstrates secretion of mature α-factor. (B, C) Average halo size for the experiment described in (A). Quantifications were performed with ImageJ. At least three independent experiments were done for each sample. The average halo size for each sample was normalized to the halo size of the WT strain transformed with the empty plasmid. AU: arbitrary units.

The results from the phenotypes analyzed for the *cmd1* or clathrin mutants so far are resumed in Table 9.

Phenotype / Strain	Expression		Interaction	Interaction	Interaction	Trimeri-	LY 37ºC			Growth 37ºC			Halo		
	Chc1	Clc1	Chc1-Clc1	Cmd1-Chc1	Cmd1-Clc1	zation	ø	*CHC1* 2µ	*CLC1* 2µ	ø	*CHC1* 2µ	*CLC1* 2µ	ø	*CHC1* 2µ	*CLC1* 2µ
WT	++++	++++	++++	++++	++++	++++	++++	++++	++++	++++	++++	++++	++++	++++	++++
chc1Δ		+			+	-	++	++++		+	++++		+	++++	
clc1Δ	++			+++		-	++		++++	+		++++	+		++++
chc1-cbsΔ	++	+	+	++	+	-	++	++++		+	++++		+	++++	
clc1-cbsΔ	++	+	+	++++	+	-	++		++++	+		++++	+		++++
CMD1	++++	++++	++++	++++	++++	++++	++++	++++	++++	++++	++++	++++	++++	++++	++++
cmd1-226	++++	++++	++++	++++	++++	++++	+	+	+	+++	+++	+++	++++		
cmd1-228	++++	++++	++++	+++ (37ºC)	++++	++++	+	+	+	+	+	+	++	++++	+++
cmd1-242	++++	++++	++++	++ (37ºC)	++(37ºC)	++++	++++			+	+	+	++	++++	+++

Table 9. Summary of the different phenotypes that exhibit the indicated strains in yeast. Expression of Chc1 or Clc1 analyzed by immunoblot, interaction between Chc1 and Clc1, between Cmd1 and Chc1 or between Cmd1 and Clc1 analyzed by co-immunoprecipitations, ability to from triskelions analyzed by Native PAGE gels, endocytic activity analyzed by Lucifer yellow uptake assays, ability to grow at 37ºC, and ability to produce bioactive α-factor analyzed by halo assays, in strains overexpressing either Chc1 (*CHC1* 2µ) or Clc1 (*CLC1* 2µ) or not (ø). Most relevant results are highlighted.

3.5. Analysis of the co-localization of clathrin with endosomal and TGN markers and Cmd1 in WT and mutant strains with an altered clathrin-Cmd1 interaction

Since a defect on TGN-endosome trafficking was revealed upon disruption of the clathrin-Cmd1 interaction, we postulated that this interaction might be required for the proper recruitment of clathrin in the TGN endosomal systems (Chu et al., 1996; Newpher et al., 2006; Mary Seeger & Payne, 1992). To investigate this matter, we used live-cell fluorescence microscopy (see Materials and Methods section 6.6.1.) of cells expressing GFP-tagged versions of WT (Newpher *et al*., 2005) or mutated Chc1 and Clc1 together with genome edited mCherry- tagged versions of the cortical endocytic markers **Sla1** (an endocytic clathrin adaptor)(Aghamohammadzadeh & Ayscough, 2010; Ayscough *et al*., 1999) and **Abp1** (an endocytic actin binding protein)(Ayscough *et al*., 1999), the **Gga2**

clathrin adaptor, which function in protein sorting from the TGN to the endosomes (Black & Pelham, 2000; De *et al*., 2012), **Apl2**, the β1 subunit of the AP-1 clathrin adaptor complex, which functions downstream of Gga2 in the TGN endosomal anterograde transport, but also, in the endosome-TGN retrograde traffic (Valdivia *et al*., 2002), and **Snf7,** a subunit of the ESCRT-III (Endosomal Sorting Complex Required for Transport III) complex, that labels the late, prevacuolar endocytic compartment and which is involved in the sorting of ubiquitinated transmembrane proteins into the ILV of the MVB (Babst *et al*. , 2002). All those traffic markers have been already shown to clearly co-localize with clathrin in WT strains by live-cell fluorescence microscopy (Newpher *et al*., 2005; Raymond *et al.*, 1992).

3.5.1. Clathrin accumulates on enlarged structures together with TGN and endosomal markers in the *cmd1-228* and *cmd1-242* mutants

3.5.1.1. GFP-Clc1 partially co-localizes with cortical endocytic markers Sla1 and Abp1 in Cmd1 WT and mutant strains

We used GFP-Clc1 as a reporter for clathrin co-localization, since Clc1 and Chc1 completely co-localize (Newpher *et a*l., 2005). In WT cells, co- localization of Abp1 and Sla1 with clathrin is rather poor because the strong signal given by the highly dynamic internal clathrin structures mask the cortical signal, making imaging difficult (Kaksonen *et al.,* 2005; Newpher *et al.*, 2005). Consistent with previous observations, our fluorescence microscopy analysis in WT *CMD1* strains expressing GFP-Clc1 and either Sla1-mCherry (Figures 46) or Abp1-mCherry (Figure 47) revealed poor co-localization (in approximately 10% of cells). However co-localization was evident at the cell poles and cytokinetic sites, where endocytic cortical patches accumulate. Double channel fluorescence microscopy analysis of GFP-Clc1 with either Sla1-mCherry or Abp1-mCherry in *cmd1-228* and *cmd1-242* mutants showed no significant differences with the WT *CMD1* strain, neither at 28ºC nor at 37ºC. This result was consisted with our previous observations indicating that the clathrin-Cmd1 interaction does not necessarily alter endocytic uptake.

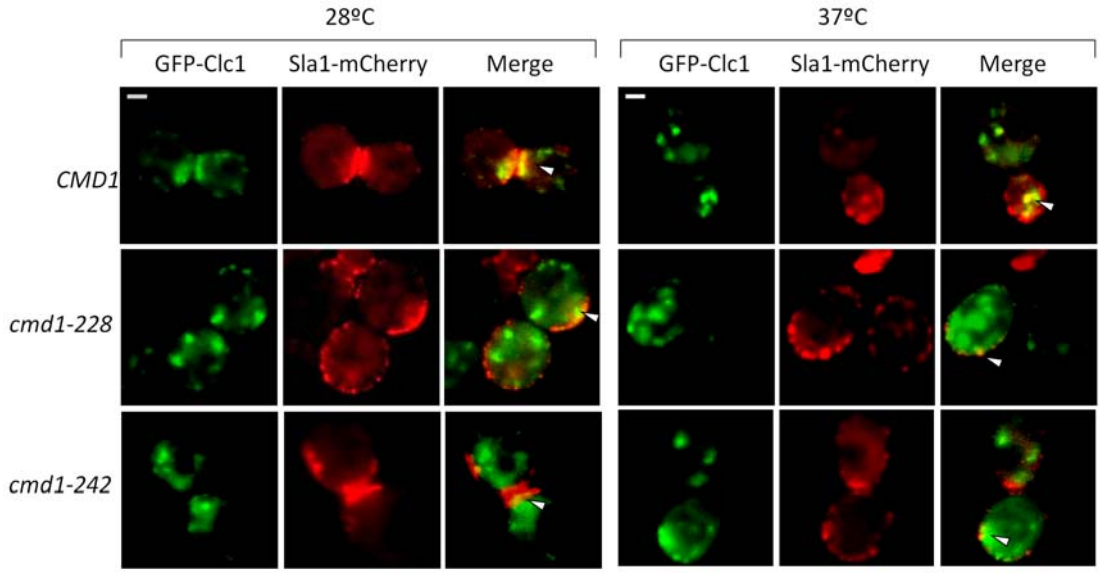

Figure 46. The endocytic marker Sla1 co-localizes with Clc1 in WT *CMD1* and *cmd1-228* and *cmd1-242* mutants to a similar extent. (A) Representative fluorescence micrographs from a *cmd1Δ SLA1-mCherry* strain grown at 28ºC or at 37ºC expressing either Cmd1 or the Cmd1-228 or Cmd1-242 mutants (SCMIG1077, SCMIG1283 and SCMIG1284, respectively) and GFP-Clc1 (pGFP-*CLC1-U*), all expressed from centromeric plasmids under the control of their own promotor. Fluorescence images for GFP (left) and mCherry (middle) were taken and merged (right). Patches of Clc1 associated with Sla1 are seen as yellow in the merge. At least 300 cells were imaged. Scale bar: 2 µm. A figure with brighter micrographs showing the cytosolic signal to evidence the cell contour is provided in Appendix I.

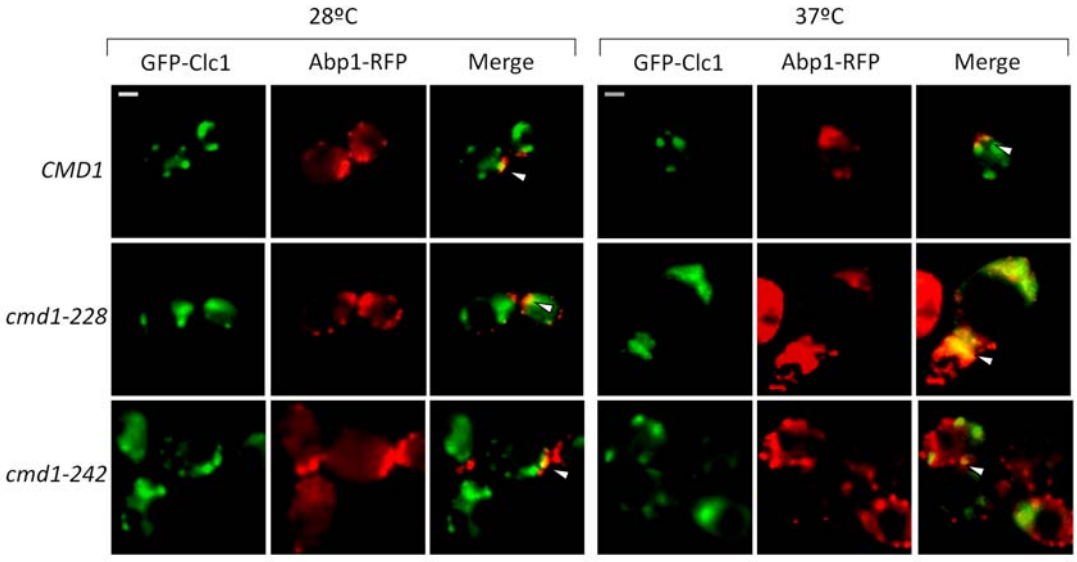

Figure 47. The endocytic marker Abp1 co-localizes with Clc1 in WT *CMD1* and *cmd1-228* and *cmd1-242* mutants to a similar extent. Representative fluorescence micrographs from a *cmd1Δ ABP1-RFP* strain grown at 28ºC or at 37ºC expressing either Cmd1 or the Cmd1-228 or Cmd1-242 mutants (SCMIG1063, SCMIG1281 and SCMIG1282, respectively) and GFP-Clc1 (pGFP-*CLC1-U*), all expressed from centromeric plasmids under the control of their own promotor. Fluorescence images for GFP (left) and mCherry (middle) were taken and merged (right). Patches of Clc1 associated with Abp1 are seen as yellow in the merge. At least 300 cells were imaged. Scale bar: 2 µm. A figure with brighter micrographs showing the cytosolic signal to evidence the cell contour is provided in Appendix I.

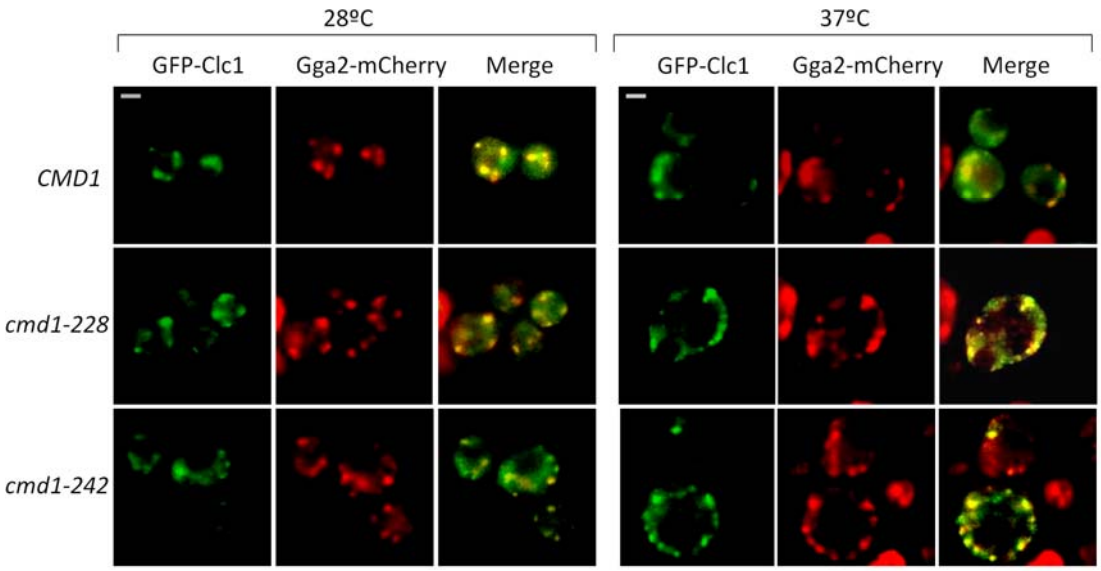

Figure 48. The endocytic marker Gga2 co-localizes with Clc1 in WT *CMD1* and *cmd1-228* and *cmd1-242* mutants to a similar extent. Representative fluorescence micrographs from a *cmd1Δ GGA2-mCherry* strain grown at 28ºC or at 37ºC, expressing either Cmd1 or the Cmd1-228 or Cmd1-242 mutants (SCMIG1286, SCMIG1287 and SCMIG1288, respectively) and the GFP-Clc1 (pGFP-*CLC1-U*) expressed all from a centromeric plasmid under the control of their own promotor. Fluorescence images for GFP (left) and mCherry (middle) were taken and merged (right). Patches of Clc1 associated with Gga1 are seen as yellow in the merge. At least 300 cells were imaged. Scale bar: 2 µm. A figure with brighter micrographs showing the cytosolic signal to evidence the cell contour is provided in Appendix I.

3.5.1.2. GFP-Clc1 extensively co-localizes with mCherry-tagged Apl2 and Snf7 on enlarged structures in *cmd1-228* and *cmd1-242* mutants

In order to characterize the effect of altering the clathrin-Cmd1 interaction on the recruitment of clathrin to the endosomal compartments, we analyzed the co-localization extend of GFP-Clc1 with mCherry-tagged TGN and endosomal markers Gga2 and Apl2, and with the late endosomal or prevacuolar marker Snf7 in the *cmd1-228* and *cmd1-242* mutants at permissive and restrictive temperature, and we compared it with cells expressing the WT Cmd1.

In WT cells, clathrin extensively co-localizes with Gga2 and Apl2 in discrete punctuated structures corresponding to the TGN and endosomal compartments (Daboussi *et al.*, 2012). Accordingly, we observed that approximately 80% of the WT *CMD1* cells had at least one co-localization patch (Figures 48 and 49). GFP-Clc1 only partially co-localizes with the late endosomal marker Snf7 (Newpher *et al.*,

2005). For this marker we found 40% of WT *CMD1* cells exhibiting at least one patch of Snf7 co-localizing with GFP-Clc1 (Figure 50A).

Double channel fluorescence microscopy analysis of GFP-Clc1 with Gga2-mCherry in *cmd1-228* and *cmd1-242* mutants showed no significant differences with the WT *CMD1* strain, neither at 28ºC nor at 37ºC (Figure 48). Surprisingly, we found that in the *cmd1-228* and *cmd1-242* mutants the GFP-Clc1 staining appeared more dispersed and greatly co-localized with Apl2 (Figure 49), associated with bigger structures. This effect was significantly more evident when cells were incubated at 37ºC. Co-localization with Snf7 (Figure 50A) appeared most significantly enhanced.

These observations suggested that clathrin accumulated on rather enlarged compartments that captured early and late endosomal markers.

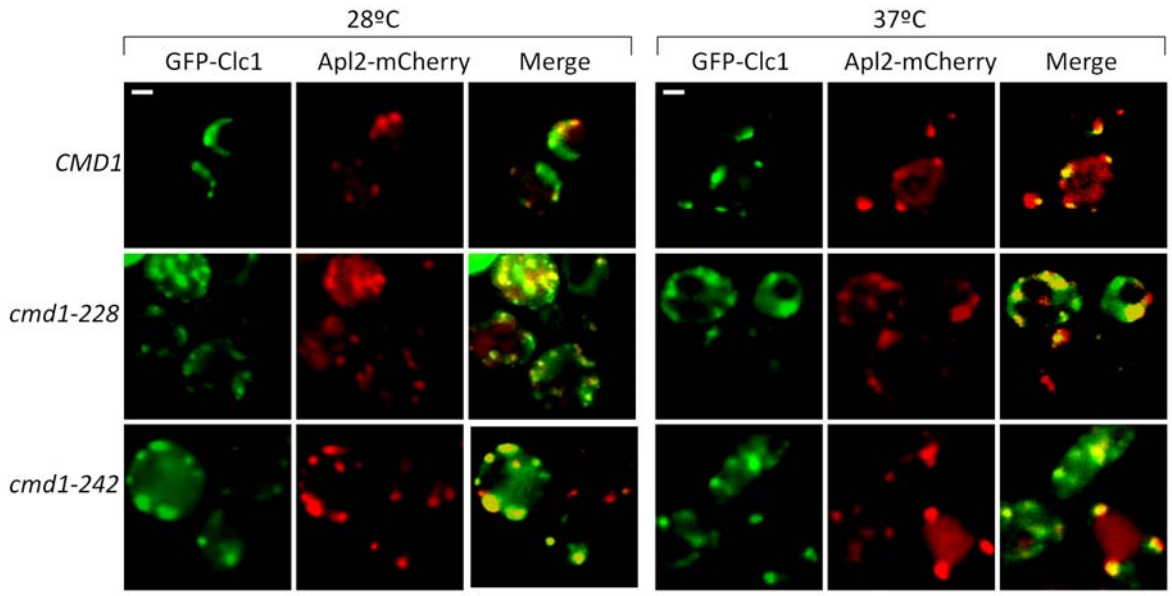

Figure 49. The TGN marker Apl2 co-localizes to a higher extent and on bigger punctae structures with Clc1 in the *cmd1-228* and *cmd1-242* mutants than in WT *CMD1* cells. Representative fluorescence micrographs from a *cmd1Δ APL2-mCherry* strain grown at 28ºC or 37ºC, expressing either Cmd1, the Cmd1-228 or Cmd1-242 mutants (SCMIG1290, SCMIG1291 and SCMIG1292, respectively) and the GFP-Clc1 (pGFP-*CLC1-U*), expressed all from centromeric plasmids under the control of their own promotor. Fluorescence images for GFP (left) and mCherry (middle) were taken and merged (right). Patches of Clc1 associated with Apl2 are seen as yellow in the merge. At least 300 cells were imaged. Scale bar: 2 µm. A figure with brighter micrographs showing the cytosolic signal to evidence the cell contour is provided in Appendix I.

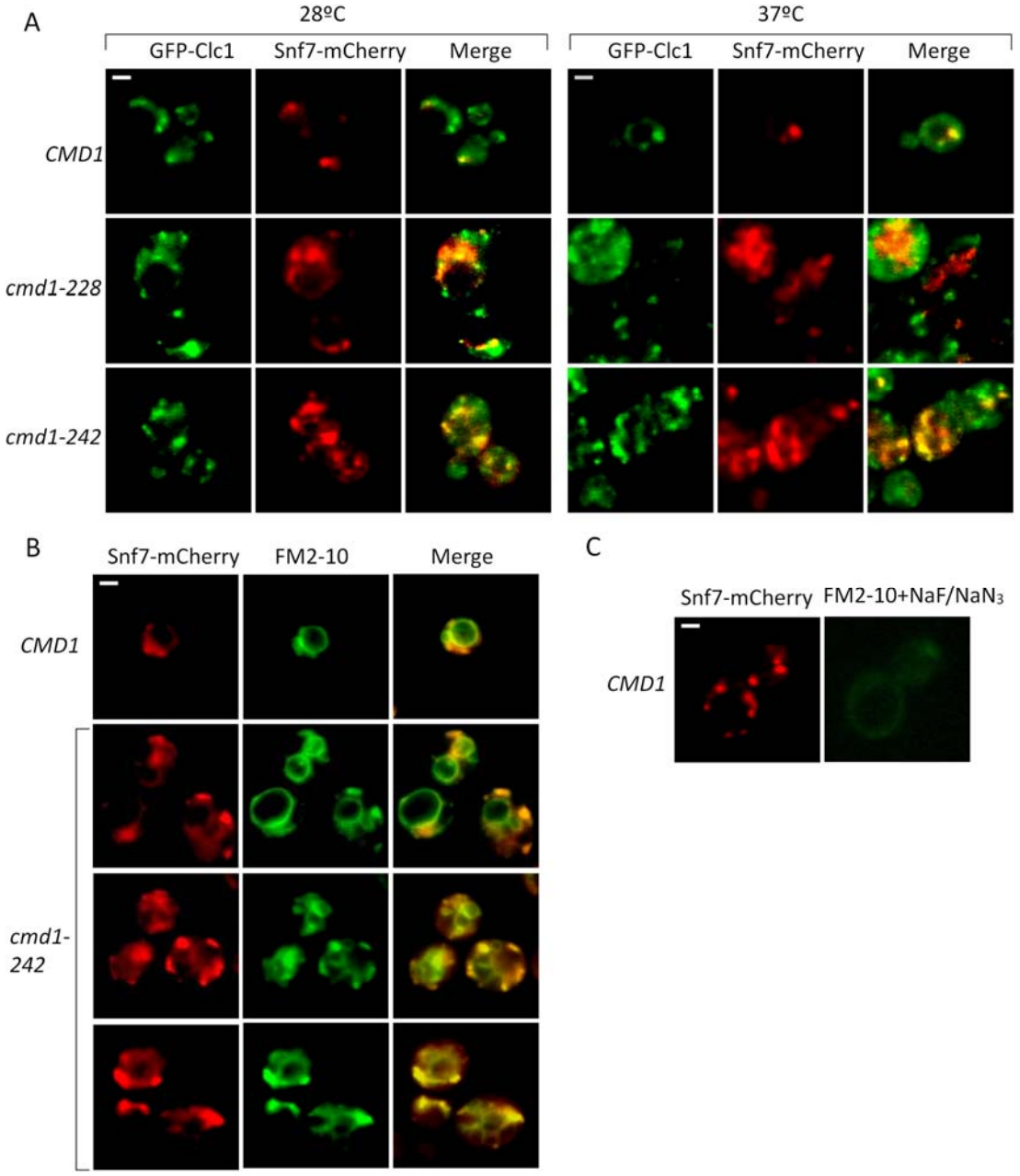

Figure 50. The prevacular compartment marker Snf7 co-localizes with GFP-Clc1 on enlarged structures in the *cmd1-228* and *cmd1-242* mutants. (A) Representative fluorescence images of a *cmd1Δ SNF7-mCherry* strain grown at 28ºC or 37ºC expressing either Cmd1 or the Cmd1-228 or Cmd1-242 mutants (SCMIG1298, SCMIG1299 and SCMIG1300, respectively) and GFP-Clc1 (pGFP-*CLC1-U*), expressed all from centromeric plasmids under the control of their own promotor. Fluorescence images for GFP (left) and mCherry (middle) were taken and merged (right). Patches of Clc1 associated with Snf7 are seen as yellow in the merge. (B) Fluorescence micrographs of *cmd1Δ SNF7-mCherry* cells expressing either the WT Cmd1 or the Cmd1-242 mutant from centromeric plasmids under the control of their own promotor (SCMIG1298 and SCMIG1300, respectively) and incubated with the styril dye FM2-10 for 45 minutes at 37ºC. Fluorescence images for mCherry (left) and FM2-10 (middle) were taken and merged (right). Patches of Snf7 associated with FM2-10 -dyed membranous structures are seen as yellow in the merge. (C) Control for the internalized FM2-10. *cmd1Δ SNF7-mCherry* cells expressing the WT Cmd1 (SCMIG1298) were treated with FM2-10 and 10 mM NaF/NaN_3 to avoid internalization. At least 300 cells were imaged. Scale bar: 2 µm. A figure with brighter micrographs showing the cytosolic signal to evidence the cell contour is provided in Appendix I.

3.5.1.3. Snf7 is localized on enlarged endosomal structures in *cmd1-228* and *cmd1-242* mutants

In order to verify the endosomal nature of the aberrant expanded structure where clathrin co-localized with Snf7 and Apl2, we performed a staining with FM2-10 of the *cmd1Δ* cells expressing Snf7-mCherry and the Cmd1-228 and Cmd1-242 mutant Cmd1 grown at 37ºC (Figure 50B). The analysis revealed that Snf7 indeed localized on enlarged endosomal structures in the *cmd1* mutants.

A control for the endocytic-dependent endosomal staining with FM2-10 was done in WT *CMD1* cells by inhibiting endocytosis with NaF and NaN_3 along with the incubation with the dye (Figure 50C). As expected, no perceptible FM2-10 was observed upon inhibition of endocytosis.

3.5.1.4. Clathrin also accumulates on enlarged endosomal compartments in *cmd1-228* and cmd1-*242* mutants

To further confirm the endosomal nature of the compartment where clathrin and Snf7 co-localized, we also stained *CMD1* and *cmd1-242* cells expressing GFP-Clc1 grown at 37ºC with the endocytic marker FM4-64 (Figure 51A). GFP-Clc1 labeling was coincident with endosomal membranes, corroborating the endosomal nature of the structures (Figure 50B).

3.5.1.5. Kex2 does not co-localize with clathrin but it mislocalizes to endosomal structures and vacuoles in the *cmd1-228* and *cmd1-242* mutants at restrictive temperature

In WT cells, clathrin co-localizes with Kex2 in discrete punctuated structures corresponding to the TGN compartments (60% of GFP-Clc1 patches overlapping with Kex2) (Newpher *et al*., 2005). In *cmd1-228* and *cmd1-242* mutants, as they might exhibit TGN-endosome trafficking defects and Kex2 is mislocalized from the TGN, clathrin co-localization with the protease might probably be prevented. Dual channel fluorescence microscopy of GFP-Clc1 and Kex2-mCherry in the WT and mutant Cmd1 strains both at 28ºC and at 37ºC (Figure 52), confirmed that co-localization was almost completely absent at 37ºC in the *cmd1* mutants, a phenotype more strongly exhibited by the *cmd1-228* mutant, being Kex2 localized (as previously shown in Figures 42C and 42D) in the vacuoles reflecting

most likely a defect in retrograde transport from LE to the TGN (Redding *et al.*, 1996; Wilcox *et al.*, 1992). Moreover, although at 28ºC some co-localization patches were still observable, Kex2 was partially accumulating to endosomal structures, indicating again a defect in retrograde traffic.

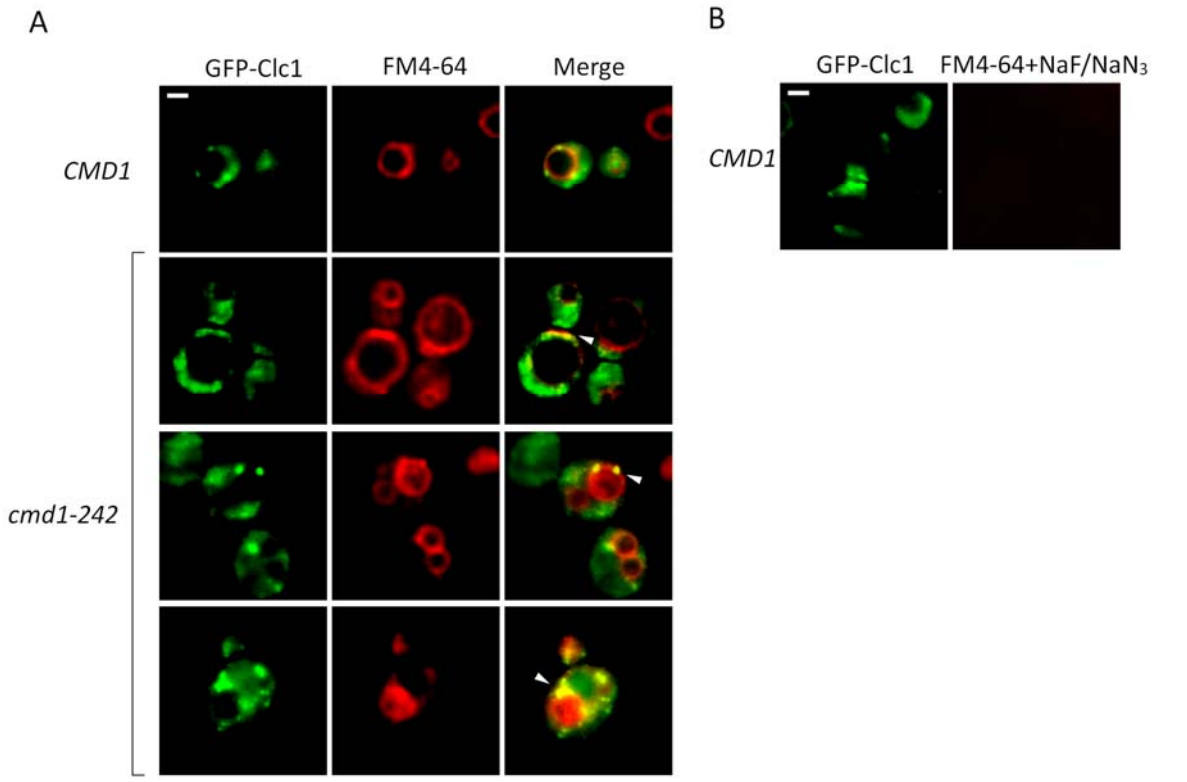

Figure 51. The Clc1-decorated enlarged compartment in the *cmd1-242* mutant at 37ºC is at least partially of endocytic origen. (A) Representative fluorescence micrographs of a *cmd1Δ* strain grown at 37ºC expressing GFP- Clc1 (pGFP-*CLC1-U*) and either Cmd1 or the Cmd1-242 mutant (SCMIG1261 and SCMIG1266, respectively) all from centromeric plasmids under the control of their own promotor, treated with the styril dye FM4-64 for 45 minutes at 37ºC. Fluorescence images for GFP (left) and FM4-64 (middle) were taken and merged (right). Patches of Clc1 associated with FM4-64-dyed membranous structures are seen as yellow in the merge. (B) Control for the internalized FM4-64. *cmd1Δ* cells expressing the WT Cmd1 (SCMIG1261) and the GFP-Clc1 expressed from a centromeric plasmid under the control of its ownpromotor (pGFP-*CLC1-U*) were treated with FM4-64 and 10 mM NaF/NaN_3 to avoid internalization. At least 300 cells were imaged .Scale bar: 2 µm. A figure with brighter micrographs showing the cytosolic signal to evidence the cell contour is provided in Appendix I.

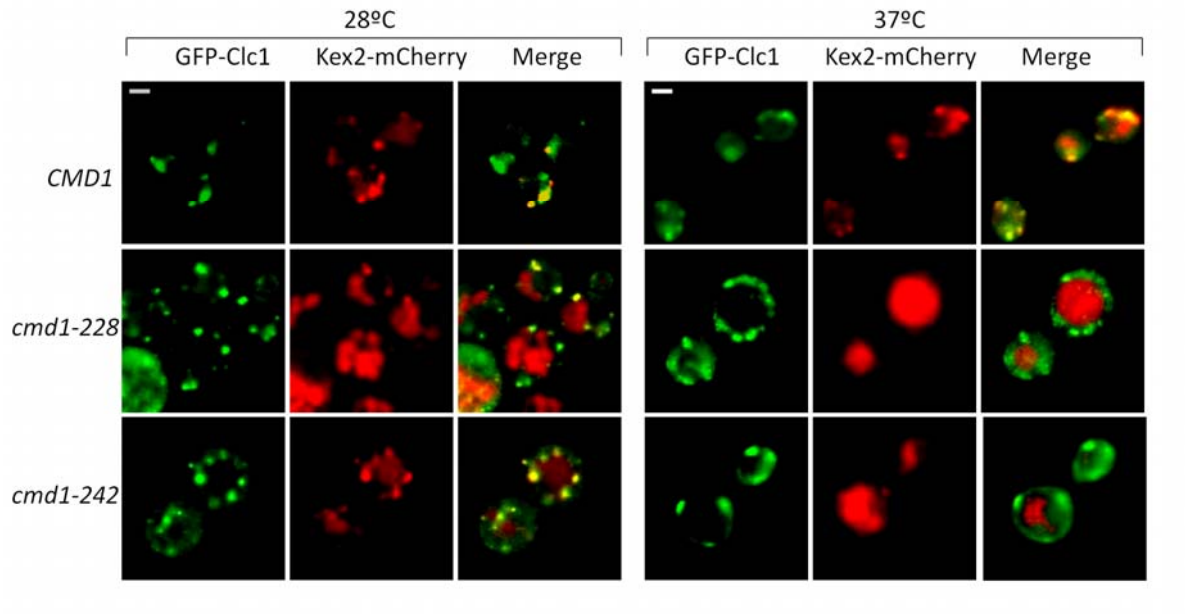

Figure 52. The TGN α-factor processing enzyme Kex2 mislocalizes from the TGN and accumulates in vacuolar structures in *cmd1-228* and *cmd1-242* mutants. Representative fluorescence micrographs from a *cmd1Δ KEX2-mCherry* strain grown at 28ºC or 37ºC expressing either Cmd1, or the Cmd1-228 or Cmd1-242 mutants (SCMIG1294, SCMIG1295 and SCMIG1296, respectively) and the GFP-Clc1 (pGFP-*CLC1-U*) all expressed from centromeric plasmids under the control of their own promotor. Fluorescence images for GFP (left) and mCherry (middle) were taken and merged (right). Patches of Clc1 associated with Kex2 are seen as yellow in the merge. At least 300 cells were imaged. Scale bar: 2 µm. A figure with brighter micrographs showing the cytosolic signal to evidence the cell contour is provided in Appendix I.

3.5.2. The clathrin cbsΔ mutants occasionally accumulate on enlarged prevacuolar compartments co-localizing with some TGN and endosomal markers

3.5.2.1. The clathrin cbsΔ mutants are mainly delocalized but occasionally accumulate on large endosomal prevacuolar compartments

We also wanted to investigate the localization of the clathrin mutants that had their Cmd1 binding site deleted to investigate possible correlated phenotypes regarding the endosomal accumulation observed in the *cmd1* mutants. As GFP-fused clathrin mutants expressed from centromeric plasmids were poorly expressed, we expressed them from multicopy plasmids (*chc1-cbsΔ* 2µ and *clc1-cbsΔ* 2µ) in either a WT, a *chc1Δ* or a *clc1Δ* strain using Chc1-GFP or GFP-Clc1 expressed from centromeric plasmids *(CHC1* or *CLC1*) as positive controls. We

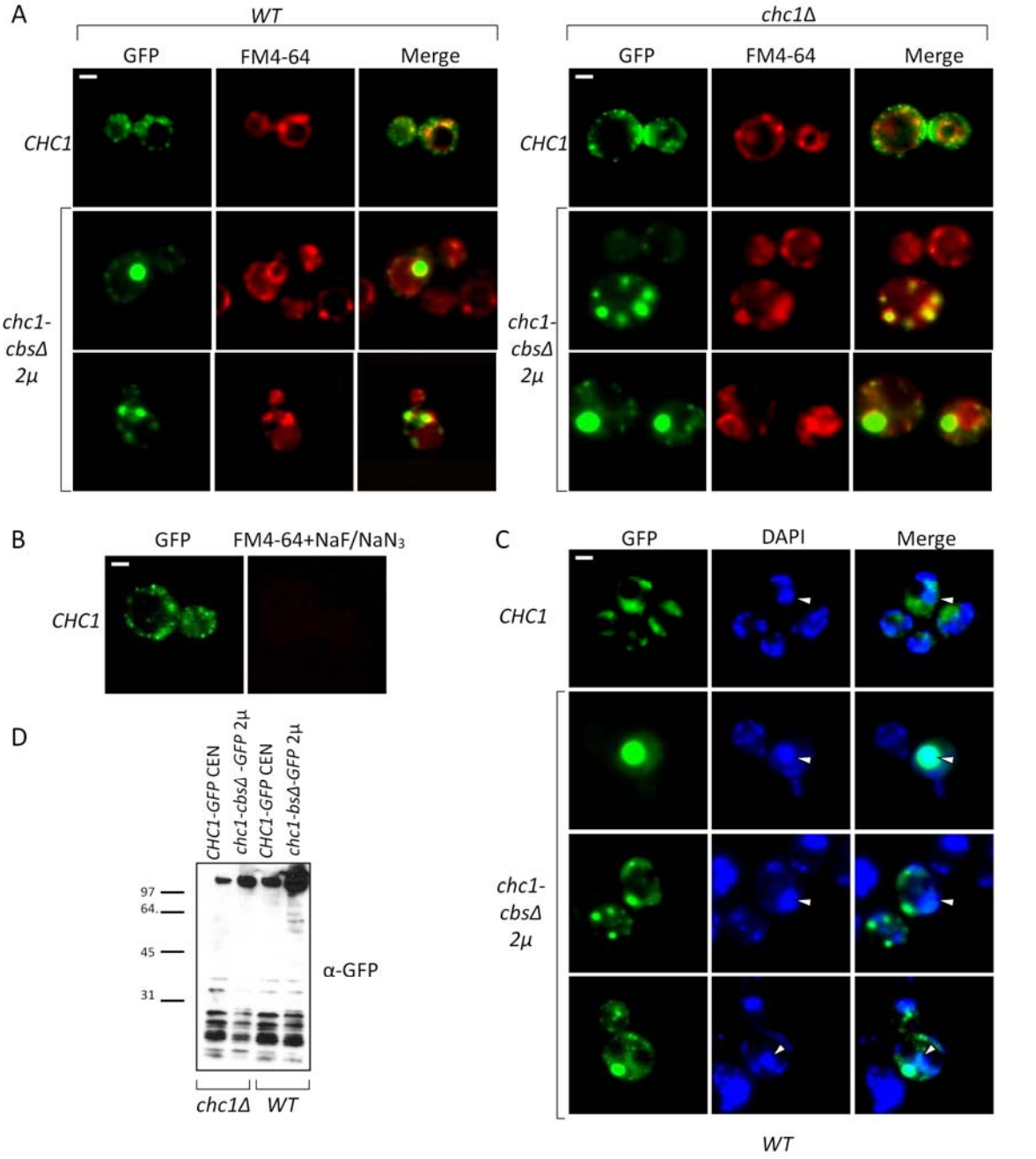

Figure 53. The Chc1-cbsΔ mutant expressed from a multicopy plasmid is delocalized and occasionally accumulates on endosomal structures. (A) Representative fluorescence micrographs of *WT* (BY4742) (left panels) or *chc1Δ* (SL114) (right panels) strains grown at 28ºC expressing either the Chc1-GFP (*CHC1*) or the Chc1-cbsΔ-GFP mutant (*chc1-cbsΔ* 2μ) from centromeric and multicopy plasmids, respectively, under the control of their own promotors (p50-*CHC1-GFP* and p195-*chc1-cbsΔ-GFP*, respectively). Cells were incubated with the styril dye FM4-64 for 45 minutes at 28ºC. Fluorescence images for GFP (left) and FM4-64 (middle) were taken and merged (right). Patches of Chc1 or Chc1-cbsΔ associated with FM4-64-dyed membranous structures are seen as yellow in the merge. (B) Control for the internalized FM4-64. *WT* cells (BY4742) expressing Chc1-GFP (*CHC1-GFP*; p50-*CHC1-GFP*) were incubated with FM4-64, and 10 mM NaF/NaN_3 to avoid internalization. (C) Representative fluorescence micrographs of a *WT* strain (BY4742) expressing either the Chc1-GFP (*CHC1*) or the Chc1-cbsΔ-GFP mutant (*chc1-cbsΔ* 2μ) from centromeric and multicopy plasmid, respectively, under the control of their own promotors (p50-*CHC1-GFP* and p195-*chc1-cbsΔ-GFP*, respectively) (right images) and incubated with DAPI for nucleus visualization (middle images). Patches of Chc1 or Chc1-cbsΔ accumulated at the DAPI-dyed nucleus are seen as light blue in the

merge. The nucleus is indicated by a small white arrow. Scale bar: 2 µm. A figure with brighter micrographs showing the cytosolic signal to evidence the cell contour is provided in Appendix I. (D) Immunoblot of total protein extracts to analyze the expression and degradation of Chc1-GFP (*CHC1*-GFP CEN) or Chc1-cbsΔ-GFP (*chc1-cbsΔ*-GFP 2µ) expressed from a centromeric and a multicopy plasmid, respectively under the control of their own promotors (p50-*CHC1-GFP* and p195-*chc1-cbsΔ-GFP*, respectively) in *WT* (BY47421) or *chc1Δ* (SL114) cells. An antibody against GFP (α-GFP), combined with an appropriate secondary antibody, was used to detect GFP-tagged proteins.

observed that both Chc1-cbsΔ-GFP (Figure 53A) and GFP-Clc1-cbsΔ (Figure 54A) expressed in both a WT or a clathrin delta strain, were mainly delocalized and diffuse, in accordance with the localization pattern already described for GFP-Clc1 in a *chc1Δ* strain (Newpher *et al*., 2005). In addition, some cells (20%) showed Chc1-cbsΔ-GFP and GFP-Clc1-cbsΔ accumulations near the vacuole in the WT and clathrin delta strains. As judged by its co-localization with FM4-64 (Figures 53A and 54A) and DAPI (see Materials and Methods section 6.6.2.) stainings (Figures 53C and 54C), the clathrin cbsΔ mutants accumulated mostly on endosomal structures and occasionally in the nucleus. A probable explanation for the GFP labelling of the nucleus is that the clathrin mutants might be degraded, generating GFP fragments that would translocate to the nucleus (Seibel *et al*., 2007). To confirm degradation of these clathrin mutant proteins *in vivo*, we did immunoblots from total protein yeast extracts of a WT and a *chc1Δ* strains expressing either Chc1-GFP or Chc1-cbsΔ-GFP (*CHC1-GFP* CEN and *chc1-cbsΔ-GFP* 2µ, respectively) (Figure 53D) or WT and *clc1Δ* strains expressing either GFP-Clc1 or GFP-Clc1-cbsΔ (GFP-*CLC1* CEN and *GFP-clc1-cbsΔ* 2µ, respectively) (Figure 54D) with an antibody against GFP. The results showed that clathrin mutants were indeed degraded *in vivo* generating smaller GFP-tagged fragments. However, WT Chc1-GFP and GFP-Clc1, which did not show any accumulation in the nucleus, were also degraded to a similar extend.

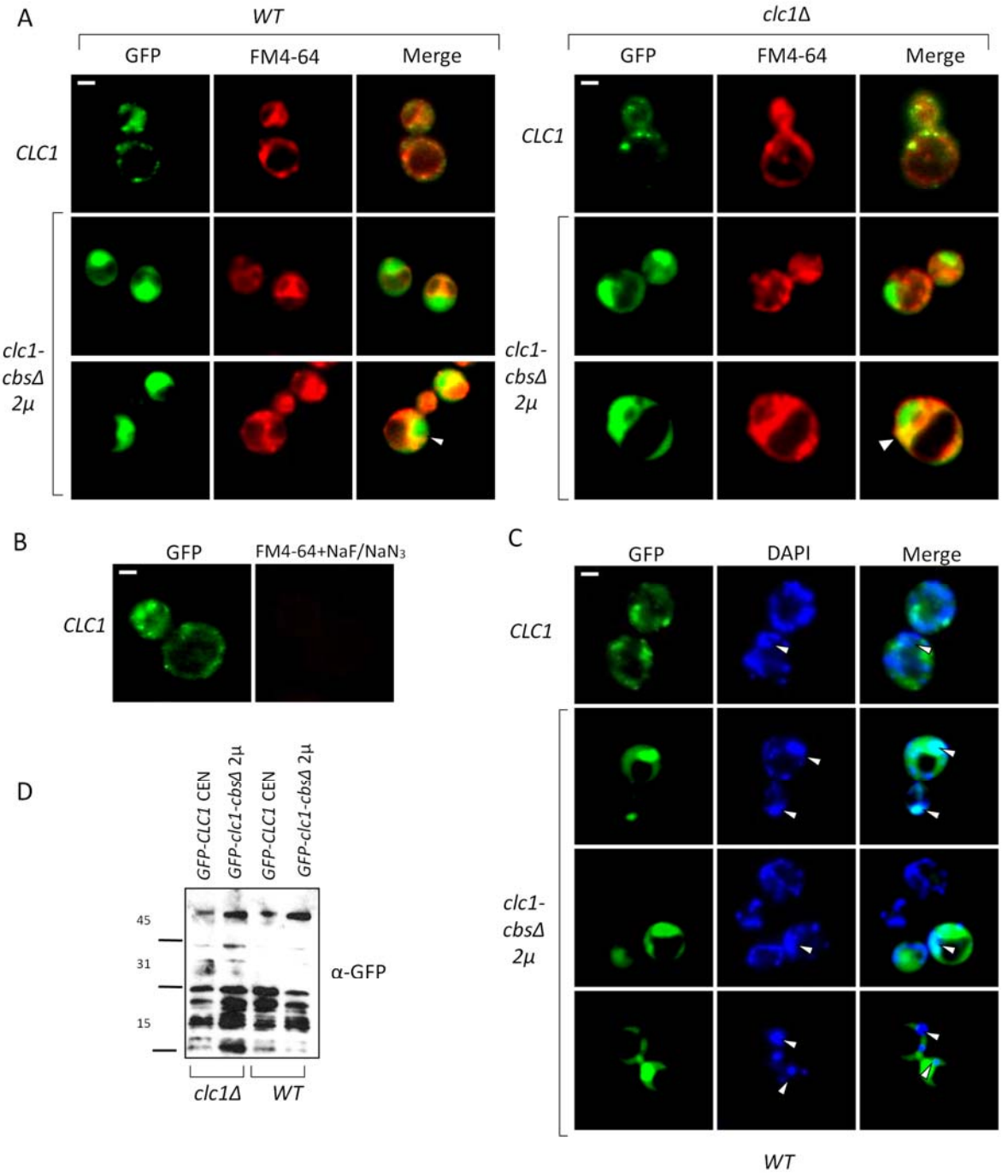

Figure 54. The Clc1-cbsΔ mutant expressed from a multicopy plasmid is delocalized and occasionally accumulates on endosomal structures. (A) Representative fluorescence micrographs of *WT* (BY4742) (left panels) or *clc1Δ* (SL1620) (right panels) strains grown at 28ºC expressing either the GFP-Clc1 (*CLC1*) or the GFP-Clc1-cbsΔ mutant (*clc1-cbsΔ* 2μ) from centromeric and multicopy plasmids, respectively, under the control of their own promotors (pGFP-*CLC1-U* and pGFP-*clc1-cbsΔ,* respectively). Cells were treated with the styril dye FM4-64 for 45 minutes at 28ºC. Fluorescence images for GFP (left) and FM4-64 (middle) were taken and merged (right). Patches of Clc1 or Clc1-cbsΔ associated with FM4-64-dyed membranous structures are seen as yellow in the merge. (B) Control for the internalized FM4-64. *WT* cells (BY4742) expressing GFP-Clc1 (*CLC1;* pGFP-*CLC1-U*) were treated with FM4-64, and 10 mM NaF/NaN_3 to avoid internalization. (C) Representative fluorescence micrographs of a *WT* strain (BY4742) expressing either the GFP-Clc1 (*CLC1*) or the GFP-Clc1-cbsΔ mutant (*clc1-cbsΔ* 2μ) from a centromeric and a multicopy plasmid, respectively, under the control of their own promotor (pGFP-*CLC1-U* and pGFP-*clc1-cbsΔ,* respectively) (right images) and

incubated with DAPI for nucleus visualization (middle images). Patches of Chc1 or Chc1-cbsΔ accumulated at the DAPI-dyed nucleus are seen as light blue in the merge. The nucleus is indicated by a small white arrow. Scale bar: 2 µm. A figure with brighter micrographs showing the cytosolic signal to evidence the cell contour is provided in Appendix I. (D) Immunoblot of total protein extracts to analyze the expression and degradation of GFP-Clc1 (GFP-*CLC1* CEN) or GFP-Clc1-cbsΔ (GFP-*clc1-cbsΔ* 2µ) expressed from a centromeric and a multicopy plasmid, respectively, under the control of their own promotors (pGFP-*CLC1-U* and pGFP-*clc1-cbsΔ,* respectively) in *WT* (BY4742) or *clc1Δ* (SL1620) cells. An antibody against GFP (α-GFP) combined with an appropriate secondary antibody, was used to detect GFP-tagged proteins.

3.5.2.2. The clathrin cbsΔ mutant-accumulations occasionally co-localize with cortical endocytic and TGN-endosomal markers

To investigate whether the mutant clathrin accumulations also co-localized with TGN, endosomal and cortical endocytic markers, we performed fluorescence microscopy studies of cells expressing GFP-tagged Chc1 and Clc1 from centromeric plasmids (*CHC* and *CLC1*) and Chc1-cbsΔ and Clc1-cbsΔ mutants from multicopy plasmids (*chc1-cbsΔ* 2µ and *clc1-cbsΔ* 2µ, respectively) in a WT strain expressing genome-edited mCherry tagged versions of either Sla1, Abp1, Gga1, Apl2, Kex2 or Snf7. Tagging the genes of interest with mCherry in *chc1Δ* or *chc1Δ* strains was not possible probably due to the tendency of clathrin mutants to become polyploid (Lemmon *et al*., 1990), making their genetic manipulation very difficult.

Interestingly, the Chc1-cbsΔ-GFP labelled structures also accumulated Snf7, Gga1, Apl2 and Sla1 (Figure 55). A control for GFP cross-excitation was done to discard possible GFP signal capturated by the mCherry microscopy filters (Figure 55G). On the contrary, the GFP-Clc1-cbsΔ labeled enlarged structures did not co-localize with Sla1, Gga2, Apl2 or Snf7 (Figure 56). In agreement with the results that verified a non dominant phenotype of the clathrin mutants expressed in a WT strain, Kex2 still appeared in discrete patches that yet did not co-localize with the clathrin mutants (Figures 55E and 56E).

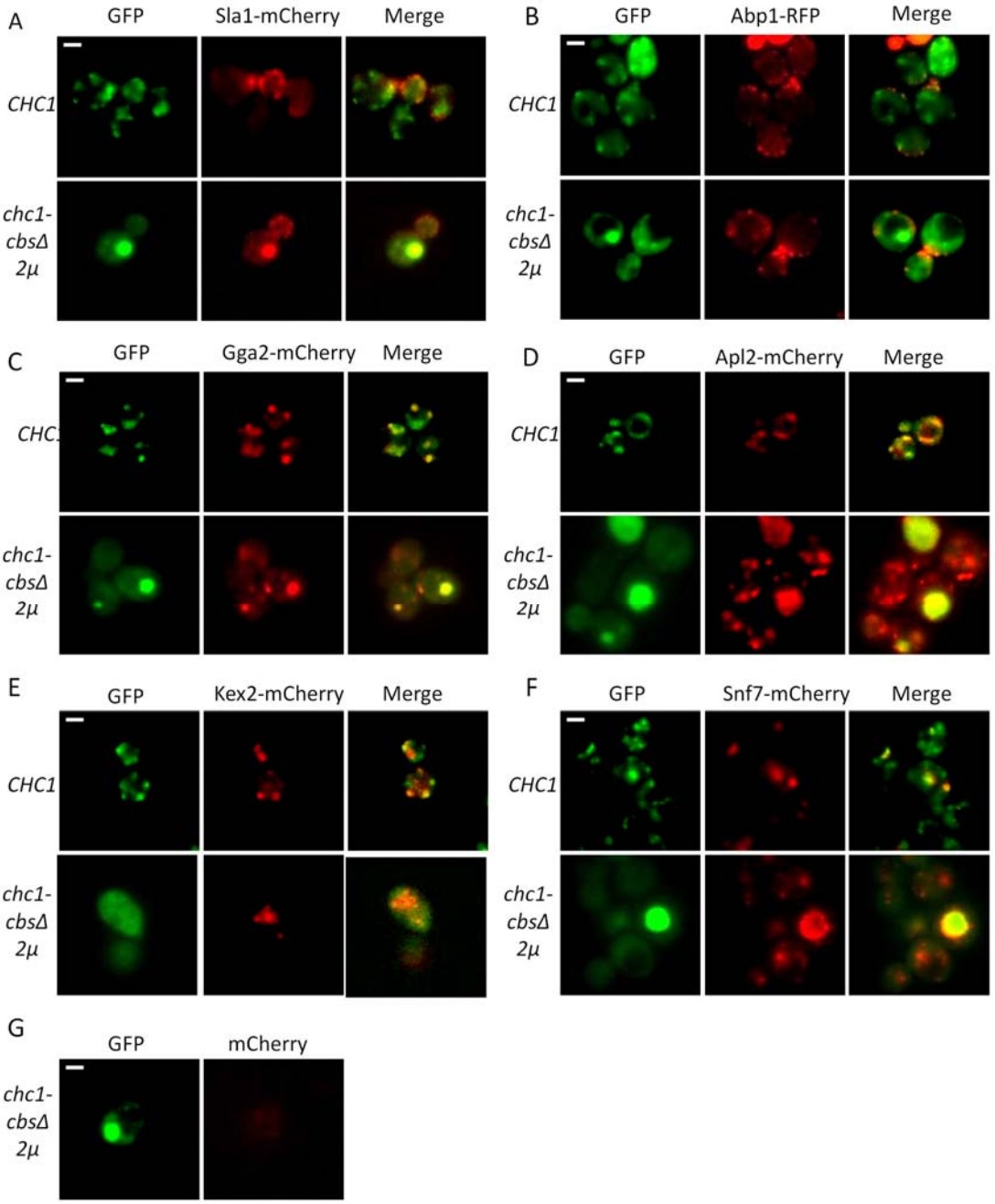

Figure 55. The Chc1-cbsΔ mutant expressed from a multicopy plasmid accumulates on endosomal structures where it co-localizes with Sla1, Gga1, Apl2 and Snf7. Representative fluorescence micrographs from cells expressing either Sla1-mCherry (SCMIG1141)(A), Abp1-RFP *(*SL5156*)* (B)*,* Gga1-mCherry (SCMIG1301) (C), Apl2-mCherry *(SCMIG1302)*(D)*,* Kex2-*mCherry* (SCMIG1303) (E) or Snf7-mCherry (SCMIG1304) (F) strains grown at 28ºC and expressing either the Chc1-GFP (*CHC1*) or the Chc1-cbsΔ-GFP mutant (*chc1-cbsΔ* 2μ) from centromeric and multicopy plasmid, respectively, under the control of their own promotors (p50-*CHC1-GFP* and p195-*chc1-cbsΔ-GFP*, respectively). Fluorescence images for GFP (left) and mCherry (middle) were taken and merged (right). Patches of Chc1 or Chc1-cbsΔ associated with each of the mCherry-tagged markers are seen as yellow in the merge. (G) Fluorescence images from a *WT* strain (BY4742) expressing only Chc1-cbsΔ-GFP (*chc1-cbsΔ* 2μ) from a multicopy plasmid under the control of its own promotor (p195-*chc1-cbsΔ-GFP)* (left) image with the filters for mCherry (right) as control for cross-excitation. Scale bar: 2 μm. A figure with brighter micrographs showing the cytosolic signal to evidence the cell contour is provided in Appendix I.

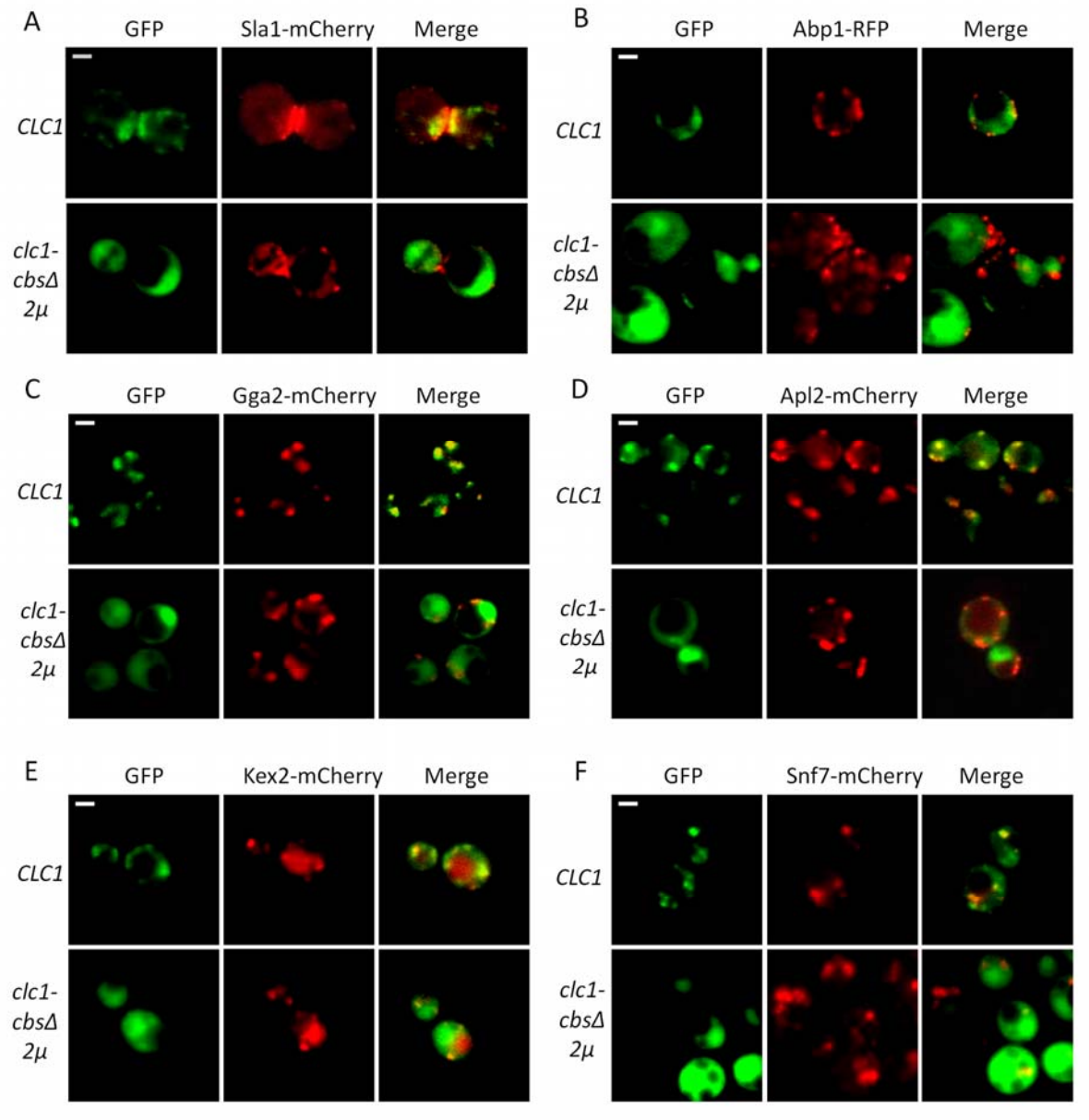

Figure 56. The Clc1-cbsΔ mutant expressed from a multicopy plasmid does not co-localize with the endocytic or TGN-endosomal markers. Representative fluorescence micrographs from cells expressing Sla1-mCherry (SCMIG1141)(A), Abp1-TFP (SL5156) (B), Gga1-mCherry (SCMIG1301) (C), Apl2-mCherry (SCMIG1302)(D), Kex2-mCherry (SCMIG1303) (E) and Snf7-mCherry (SCMIG1304) (F) strains grown at 28ºC and expressing either GFP-Clc1 (*CLC1*) or the GFP-Clc1-cbsΔ mutant (*clc1-cbsΔ* 2μ) from a centromeric and a multicopy plasmid, respectively, under the control of their own promotors (GFP-*CLC1-U* and GFP-*clc1-cbsΔ*, respectively). Fluorescence images for GFP (left) and mCherry (middle) were taken and merged (right). Patches of Clc1 or Clc1-cbsΔ associated with each of the mCherry-tagged markers are seen as yellow in the merge. Scale bar: 2 μm. A figure with brighter micrographs showing the cytosolic signal to evidence the cell contour is provided in Appendix I.

3.5.3. Clathrin partially co-localizes with Cmd1 probably on endosomal structures in WT cells

To further explore the possibility that the clathrin-Cmd1 interaction played a role in endosomal trafficking, we investigated if Cmd1 and clathrin co-localized in endosomal structures, at least transiently. For that purpose, we analyzed co-localization of WT cells expressing Cmd1-mCherry from the chromosomal gene and either Chc1-GFP or GFP-Clc1 from centromeric plasmids (*CHC1* and *CLC1,* respectuvely) or Chc1-cbsΔ-GFP or GFP-Clc1-cbsΔ from multicopy plasmids (*chc1-cbsΔ* 2µ and *clc1-cbsΔ* 2µ, respectively). WT Cmd1 localizes to sites of cell growth (bud tips and bud necks) overlapping with the location of actin patches, and to internal patches that mainly correspond to the spindle pole body (Brockerhoff & Davis, 1992; Moser *et al.*, 1997; Sun *et al.*, 1992). Co-localization of WT Chc1-GFP (Figure 57A) and GFP-Clc1 (Figure 57B) with Cmd1-mCherry was observed in about 5% of cells and this co-localization was seen mainly at cytokinesis sites and bud tips, and within some of the internal patches (2% of the cells).

In order to test whether some of the internal patches of Cmd1 had endosomal nature, we analyzed by fluorescence microscopy cells expressing Cmd1-mCherry and incubated with the endocytic marker FM2-10 (Figure 57C). The results indicated that some of the internal Cmd1 patches co-localized with endosomal structures (around 3% of the cells). Thus, this result strongly supports a role of a transient clathrin-cmd1 interaction in endosomal trafficking.

Analysis of the co-localization of Cmd1 with mutants Chc1-cbsΔ-GFP or GFP-Clc1-cbsΔ (Figures 57A and 57B) showed that clathrin co-localization with Cmd1 in these internal structures was disrupted by deletion of the Chc1 and Clc1 Cmd1-binding sites.

The results obtained from the co-localization analysis of clathrin WT and mutants with endocytic or endosomal markers and Cmd1, are resumed in Table 10.

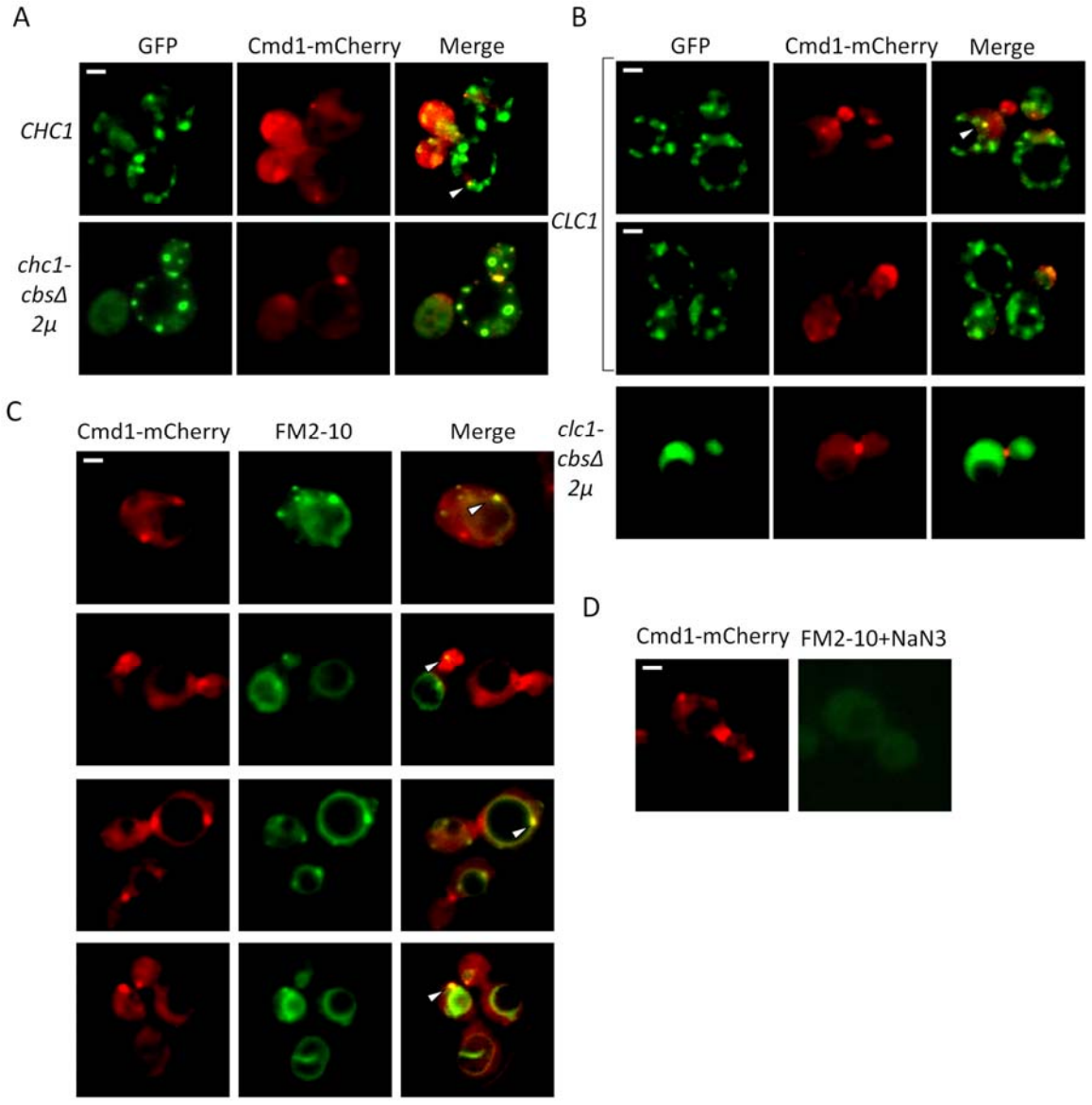

Figure 57. Cmd1 partially co-localizes with Chc1 and Clc1 in a WT strain at the cell poles, at cytokinesis ring, and on a few internal patches of endocytic origin. (A, B) Representative fluorescence micrographs of a *WT CMD1-mCherry* strain (SCMI1080) grown at 28ºC expressing either Chc1-GFP (*CHC1*) (A) or GFP-Clc1 (*CLC1*) (B) from centromeric plasmids (p50-*CHC1-GFP* or pGFP-*CLC1-U,* respectively), or the Chc1-cbsΔ-GFP (*chc1-cbsΔ* 2μ) (A) or GFP-Clc1-cbsΔ (*clc1-cbs*Δ 2μ) (B) mutants from multicopy plasmids (p195-*chc1-cbsΔ* or pGFP-*clc1-cbsΔ*, respectively), all under the control of their own promotors. Fluorescence images for GFP (left) and mCherry (middle) signals were taken and merged (right). Patches of Chc1 or Clc1 associated with Cmd1 are seen as yellow in the merge (white arrows indicate internal patches). (C) Representative fluorescence micrographs of *WT CMD1-mCherry* cells (SCMIG1080) incubated with the styril dye FM2-10 for 45 minutes at 28ºC. Images for mCherry (left) and FM2-10 (middle) were taken and merged (right). Patches of Cmd1 associated with FM2-10-dyed membranous structures are seen as yellow in the merge (indicated by white arrows). (D) Control for the internalized FM2-10. *WT CMD1-mCherry* cells (SCMIG1080) were treated with FM2-10 and 10 mM NaF/NaN_3 to avoid internalization. Scale bar: 2 μm. A figure with brighter micrographs showing the cytosolic signal to evidence the cell contour is provided in Appendix I.

Strain / mCherry marker	*CMD1* *GFP-CLC1* (Discrete punctuated patches)	*cmd1-228* *GFP-CLC1* (Dispersed and enlarged patches)	*cmd1-242* *GFP-CLC1* (Dispersed and enlarged patches)	*WT* *CHC1-GFP* (Discrete punctuated patches)	*WT* *chc1 cbsΔ-GFP 2μ* (Cytosolic and accumulated in endosomal structures.)	*WT* *GFP-CLC1* (Normal cells Discrete punctuated patches)	*WT* *GFP-clc1 cbsΔ 2μ* (Cytosolic and accumulated in endosomal structures.)
Sla1	Poor coloc.(10% cells) at poles & cytokinesis sites	Poor coloc. (10% cells) Coloc. at poles & cytokinesis sites	Poor coloc. (10% cells) Coloc. at poles & cytokinesis sites	Poor coloc. (10% cells) Coloc. at poles & cytokinesis sites	No coloc. in patches . Coloc. in GFP endosomal massive accumulation	Poor coloc. (10% cells) Coloc. at poles & cytokinesis sites	No coloc.
Abp1	Poor coloc. (10% cells) at poles & cytokinesis sites	Poor coloc. (10% cells) at poles & cytokinesis sites	Poor coloc. (10% cells) at poles & cytokinesis sites	Poor coloc. (10% cells) at poles & cytokinesis sites	No coloc.	Poor coloc. at poles & cytokinesis sites	No coloc.
Gga1	Good coloc. (≈80% cells)	Good coloc. (≈80%);	Good coloc.(≈80%);	Good coloc. (≈80%)	No coloc. in patches . Coloc. with GFP endosomal massive accumulation	Good coloc. (≈80%)	No coloc.
Apl2	Good coloc. (≈80% cells)	Good coloc.(≈90%); more dispersed and bigger patches (more at 37ºC)	Good coloc. (≈90%); more dispersed and bigger patches (more at 37ºC)	Good coloc. (≈60% cells	No coloc. in patches. Coloc. with GFP endosomal massive accumulation	Good coloc. (≈60% cells	No coloc.
Kex2	Good coloc (≈0% cells)	Coloc. ≈30% (28ºC) and ≈5% cells (37ºC) Less patches, much Kex2 localized at endosomal structures and vacuoles.	Coloc. ≈50% (28ºC) and ≈10% cells (37ºC) Less patches, localized at endosomal structures and vacuoles	Good coloc (≈60% cells)	No coloc.	Good coloc (≈60% cells)	No coloc.
Snf7	Coloc. ≈40%cells	Coloc. in enlarged endosomal perivacuolar structures (	Coloc. in enlarged endosomal perivacuolar structures	Coloc. ≈40%cells	No coloc. in patches. Enlarged Snf7 around GFP endosomal massive accumulation	Coloc. ≈40%cells	No coloc. in patches. Enlarged Snf7 around GFP endosomal massive accumulation
Cmd1	Coloc.(5% cells) at poles , cytokinesis sites & internal endosomal patches (2%)			Coloc.(5% cells) at poles, cytokinesis sites & internal endosomal patches (2%)	Coloc.(3% cells) at poles , cytokinesis sites	Coloc.(5% cells) at poles, cytokinesis sites & internal endosomal patches (2%)	Coloc.(3% cells) at poles , cytokinesis sites

Table 10. Table summarizing the live-cell fluorescence microscopy data for GFP-clathrin and the different mCherry-tagged TGN, cortical endocytic and endosomal markers in the indicated strains.

4. DISCUSSION

Even though most of the conserved interactions between clathrin and the proteins involved in membrane traffic have been extensively studied and their functionally relevance is understood, at least to a certain extent, the functional significance of the clathrin-calmodulin interaction has remained elusive, possibly because the multiple functions of calmodulin hinders identification of mutations that specifically alter the clathrin-calmodulin interaction. It was already shown in previous studies that both the clathrin heavy and light chains bind calmodulin *in vitro* (Lisanti *et al.*, 1982; Merisko *et al.*, 1988; Pley, 1995; Silveira *et al*., 1990) However, it was not clarified whether clathrin and calmodulin interact *in vivo* and what is the functional significance of this interaction.

In this study, we reveal that the clathrin heavy and light chains bind Cmd1 not only *in vitro* but also in yeast, most likely in a calcium-dependent manner. Further, we describe a not-previously-characterized Cmd1 binding site at the C-terminus of the clathrin heavy chain, and identify Cmd1 point mutations that specifically disrupt its interaction with clathrin. Finally, we provide evidence supporting a specific role of the clathrin-calmodulin interaction in the retrograde transport from endosomes to the TGN.

4.1. A novel conserved Cmd1 binding site at the C-terminus of the clathrin heavy chain: a putative role in the disassembly of the clathrin cages

4.1.1. A conserved Cmd1 binding site at the C-terminus of the clathrin heavy and light chains

Many *in vitro* studies have evidenced the calcium-dependent interaction of Cmd with purified clathrin (Lisanti *et al.*, 1982; Merisko *et al.*, 1988; Pley, 1995; Silveira *et al*., 1990) and isolated CCV (Linden *et al.,* 1981; Lisanti *et al.*, 1982; Pley, 1995) Further, a C-terminal Cmd binding site has been described both for the mammalian and yeast clathrin light chains (Lisanti *et al.*, 1982; Pley, 1995; Silveira *et al.*, 1990). However, it has not been assessed whether clathrin interacts with Cmd *in vivo*.

In this study, we have revealed that both Chc1 and Clc1 bind Cmd1 in yeast extracts in a calcium-dependent manner (Figure 19). We have also experimentally confirmed with purified components that Chc1 and Clc1 both directly bind Cmd1 in

the presence of calcium (Figure 20). In addition, we have corroborated by co-immunoprecipitation experiments from non-denaturing yeast protein extracts and by pull down experiments with purified components that the Cmd1 binding site of Clc1 is located within its C-terminus, as previously defined (Pley, 1995; Silveira *et al.,* 1990) (Figures 20 and 25). Most unexpectedly thought, we found that the predominant Cmd1 binding site in clathrin is located at the C-terminus of Chc1 (Figure 20, 21, 22 and 24). Experiments in yeast and *in vitro* defined the existence of a previously uncharacterized Cmd1 binding site located near the trimerization domain of Chc1. This Cmd1 binding site was initially identified *in silico* using the calmodulin binding motif prediction tool "Binding site search" (http://calcium.uhnres.utoronto.ca/ctdb/ctdb/sequence.html) in the "Calmodulin Target Database" (Figure 21). Subsequent immunoprecipitation and pull downs experiments with the WT Chc1 and Clc1, or the mutants lacking the putative Cmd1 binding sites indicated that the C-terminal Chc1 binding site was the predominant Cmd1 binding region of clathrin in yeast (Figures 20, 22, 24 and 26). However, other lower-affinity Cmd1 binding sites seem to be present within the N-terminus of Chc1 and in Clc1 (Figure 20, 24 and 26).

Interestingly, *in silico* analysis predicted that the newly characterized Chc1 Cmd1 binding site is conserved throughout evolution (Figure 21), suggesting an important conserved role for this interaction. Besides, when assembled in the triskelion, the Cmd1 binding site at the C-terminus of the heavy and light chains lie within the same region, next to the trimerization domain (Figure 21E). By altering the triskelion pucker, Cmd binding at this position could influence the triskelion stability or the assembly/disassembly cycle of the clathrin lattices (Pishvaee *et al*., 1997).

To further characterize the Cmd1 binding site and the extent of its conservation, we compared the sequence of the predicted binding site of the clathrin heavy and light chains of different eukaryotic species (*Saccharomyces cerevisiae, Homo sapiens, Drosophila melanogaster* and *Caenorhabditis elegans*), in search for hydrophobic residues with a conserved spacing that fit with any of those defined for Cmd binding targets. Different recognition modes have been identified in Ca^{2+}-dependent target peptides. The most common are 1–10 and 1–14, where each residue interacts with one hydrophobic cavity of the C- terminal or N-terminal domain of Cmd. However, modes 1–12, 1–16 , 1–17 and subclasses 1–8–14 and 1-

5-10 (where two hydrophobic residues from the peptide lie in the same pocket of Cmd) have also been identified in crystal structures ((Kursula, 2014; O'Day, 2003; Yap *et al*., 2000) and references therein).

First, we analyzed the clathrin heavy chain amino acid sequences of *S.cerevisiae* Chc1, *H. sapiens* Chc17 (closest human clathrin heavy chain homologue to the yeast Chc1) and Chc22, *D.melanogaster* Chc and *C. elegans* Chc1 (Figure 58A) using the calmodulin binding motif prediction tool "Binding site search" (http://calcium.uhnres. utoronto.ca/ctdb/ctdb/sequence.html) in the "Calmodulin Target Database". The position of a highly probable Cmd binding site in the different clathrin heavy chain sequences was highly conserved, being located in the C-terminal region, near the trimerization domain. A defined consensus sequence for Cmd-binding sites does not exist. However, Cmd-binding sites usually contain several characteristic features such as a high helix propensity, a net positive charge of the binding region and two hydrophobic anchor residues spaced by a certain number of residues (Tidow & Nissen, 2013). Based on the distance between the anchor residues, Cmd-binding sites can be classified into several motifs (Figure 58) (Tidow & Nissen, 2013; Yap *et al.*, 2000). Thus, we searched for different consensus Cmd-binding motifs previously described (Figure 58A). We identified a 1-8-14 (L1520-W1573-I1533) and a 1-7-10 (L1510, I1516, L1519) putative Cmd binding sites as well as additional 1-10, 1-16 and 1-18 motifs, conserved among the different species (Figure 58B).

We analyzed the α-helix composition of the yeast Chc1 Cmd1 binding site region that contained all putative conserved motifs by an *in silico* analysis using the "HeliQuest" program (http://heliquest.ipmc.cnrs.fr/) (Figure 58C) and found that L1520-W1573-I1533 motif forms a hydrophobic surface on the predicted α-helix predisposed to interact with other small molecules (Young *et al*., 1994), including Cmd1. In addition, analysis of the location of the clathrin heavy chain Cmd binding site and its conserved motifs in a crystal structure of a clathrin heavy chain and a clathrin light chain complex showed that this site partially overlaps with the proximal domain where light chains bind (Figure 59), and the conserved motifs are located within an hydrophobic surface that most probably is interacting with the light chain (Figure 59C). Thus, Cmd1 binding to this site could alter the Chc1-Clc1 interactions near the trimerization domain, which might also affect the triskelion conformation. In fact, clathrin triskelion bound to calmodulin in the presence of

calcium has been showed to have extended legs as compared to the free triskelions, in rotary shadow experiments (Merisko et al., 1988).

The human isofom Chc22, despite a 1-5-10 putative Cmd binding site is also present (L1024-L1028-I1033; Leucine-Leucine-Isoleucine), its sequence and location within the protein is not conserved, as it is located between the distal domain and the knee, instead of being located near the trimerization domain. Chc22 is specifically more expressed in muscle cells, where it targets the GLUT4 transporter to the insulin-responsive GLUT4 storage compartment (GSC) that regulates GLUT4 expression during postprandial glucose metabolism (Frances M Brodsky, 2012; Towler et al., 2004). In other cell types, Chc22 is much lower expressed but it competes with Chc17 to bind LEs, probably through interactions with AP-1 and the

A

Described calmodulin binding motifs

HXXHXXXXXHXXH	1-4-10-13
HXXXHXXH	1-5-8
HXXXHXXXXH	1-5-10
HXXXHXXXXHXXXH	1-5-10-14
HXXXXXHXXH	1-7-10
HXXXXXXHXXXXXH	1-8-14
HXXXXXXXXH	1-10
HXXXXXXXXHXXXH	1-10-14
HXXXXXXXXHXXXXXH	1-10-16
HXXXXXXXXXXXXXH	1-14
HXXXXXXXXXXXXXXXH	1-16
HXXXXXXXXXXXXXXXXXH	1-18

B

Putative calmodulin binding motifs in the clathrin heavy chains

KFDQLGLASRLESHKLIFFKKIGALLYRRNKKWAKSLSILKEEKL	S. cerevisiae
NFDNISLAQRLEKHELIEFRRIAAYLFKGNNRWKQSVELCKKDSL	H. sapiens CHC17
NFDNIALAQKLEKHELTEFRRIAAYLYKGNNRWKQSVELCKKDKL	D. melanogaster
NFDNITLAQQLEKHPLVEFRRISAYLFKGNNRWKQSIELCKKDKL	C. elegans
HXXXXHHXHXXHXXHHHXXXXXHXXXHXH	Consv. Hydrophobic Resid
HXXXXXXXXXXXXXXXH	1-16
HXXXXXHXXH	1-7-10
HXXXXXXXXXXXXXXXXXH	1-18
HXXXXXXXXH	1-10
HXXXXXXXXXXXXXXXH	1-16
HXXXXXXXXXXXXXXXXXH	1-18
HXXXXXXHXXXXXH	1-8-14

Putative calmodulin binding motifs in the clathrin light chains

INQDDADIIGGRDRSKLKEILLRLKGNAKAPGAS	S. Cerevisiae
CDFNPKSSKQAKDVSRMRSVLISLKQAPLVH	H. sapiens CLTA
CDFNPKSSKQCKDVSRLRSVLMSLKQTPLSR	H. sapiens CLTB
CDFNPKVNKAGKDVSRMRSIYLHLKQNPIQVQKST	D melanogaster
TVNKLVDQQKSKSGKDLSRLKTLLAGLKHAGK	C. elegans
XXXXXXXHXXHHHXHXXXXX	Consv. Hydrophobic Residues
HXXXHXXH	1-5-8

C

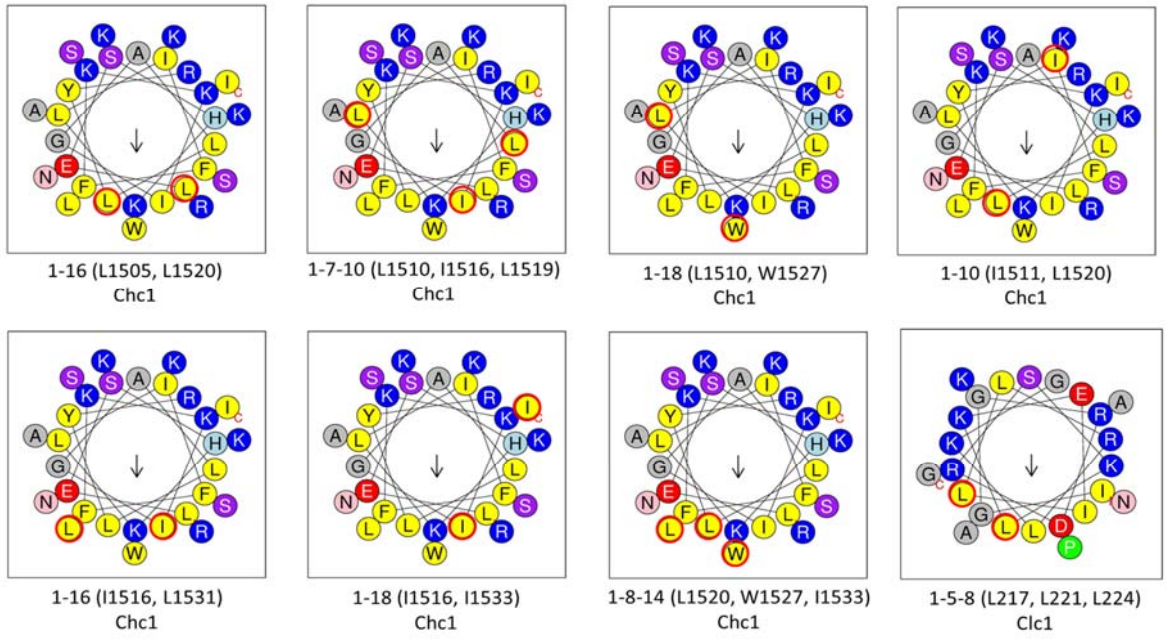

Figure 58. Analysis of the clathrin putative calmodulin binding site and calmodulin binding motifs homology between different species. (A) Representation of the Cmd-binding motifs described in (Tidow & Nissen, 2013), where X represents any amino acid and H represent anchor hydrophobic amino acids. The anchor hydrophobic residues usually lie within an amino acid sequence with net positive charge and with high propensity to form an α-helix. (B) Sequence alignment of the putative Cmd-binding sites of the indicated clathrin heavy and light chains of different organisms, indicating conserved hydrophobic residues. Putative conserved Cmd-binding sites defined for the spacing between the hydrophobic anchor residues (See A) are indicated. (C) α-helix representation of the Chc1 or Clc1 Cmd1 binding site amino acid sequence highlighted, based on the program "HeliQuest" (http://heliquest.ipmc.cnrs.fr/) that calculates from the amino acid sequence of an helix its physicochemical properties and the polar amino acid composition. The polar positive amino acids are coloured in blue (arginine (R) and lysine(K)), the polar neutral amino acids in purple and pink (tyrosine (Y), serine (S) and asparagines (N)), the polar negative amino acids in red (glutamic acid (E) and aspartatic acid (D)), and the hydrophobic non polar amino acids in yellow ((isoleucine (I), leucine (L), phenylalanine (F) and tryptophan (W)). The putative Cmd1 anchor hydrophobic residues are encircled in red.

retromer subunit SNX5 and contributes to retrograde sorting of MPR and Shiga toxin (Esk *et al.,* 2010; Towler *et al.*, 2004). These observations indicate a preferential specificity for Chc22 function in this site, so Chc22 could operate adjacent to retromer sorting patches, as observed for Chc17 (Frances M Brodsky, 2012; Esk et al., 2010). Chc22 has not been found in PMs nor in the mitotic spindle, and it associates with AP-1 or AP-3 but not AP-2, and not even with the clathrin light chains, although it is able to form triskelions (Brodsky, 2012; Esk et al., 2010; Liu *et al.*, 2001). The lack of clathrin light chain association with Chc22

suggests that Chc22 assembly or disassembly is regulated differently from Chc17, and indicates that the probably conserved Cmd binding site in the other clathrin heavy chains might be require to regulate the interaction between the clathrin heavy and light chains.

Subsequently, we analyzed the clathrin light chain amino acid sequence of *S.cerevisiae* Clc1, *H. sapiens* Clca and Clcb, *D.melanogaster* Clc and *C. elegans* Clc1 (Figure 58B). The putative Cmd binding site sequence found *in silico* in the different light chain sequences was not so conserved, reflecting the fact that the clathrin light chain amino acid sequence is not so highly conserved along evolution, as compared to the heavy chain. We searched for consensus Cmd binding motifs in the different clathrin light chain sequences, and we found a 1-5-8 motif (L217-L221-L224) (Yap *et al*., 2000) that was also present in the human CLTb and in Clc1 from *C.elegans* (Figure 58B). Analyzing the α-helix composition of the yeast Clc1 Cmd1-binding site region that contained the conserved motif using the "HeliQuest" program (Figure 58C), we found that the L-L-L motif was also located within the α-helix constituting a non-polar hydrophobic surface. In addition, analysis of the location of the clathrin light chain Cmd-binding site in the crystal structure of triskelion Hub showed that this site is located in the C-terminus of light chains which interacts with the trimerization domain in heavy chains (Figure 59), again consistent with a putative role of Cmd1 binding to this site in altering the Chc1-Clc1 interactions (Pishvaee *et al*., 1997).

In mammals, the neuron-specific light chains have been shown to interact more efficiently with Cmd *in vitro*, and purified triskelions and coated vesicles from brain, but not from adrenal gland bind calmodulin *in vitro,* which may suggest a specific role of Cmd-clathrin interaction in neurons, such as the recycling of synaptic vesicle membrane proteins or the transport of unpolymerized triskelions transport axons to the nerve terminal (Pley, 1995; Royle, 2006). Although a tissue-specific heavy chain binding to Cmd has not been assessed, the neuron-specific insertions in mammalian clathrin light chains may account for this differential binding efficiency, affecting the conformation or accessibility of Cmd binding sites in triskelions or coats (Pley, 1995). In the same way, these neuron-specific insertions could facilitate clathrin binding to Hsc70 that would maintain clathrin in an uncoated form to be transported though axonal transport and thus supplying

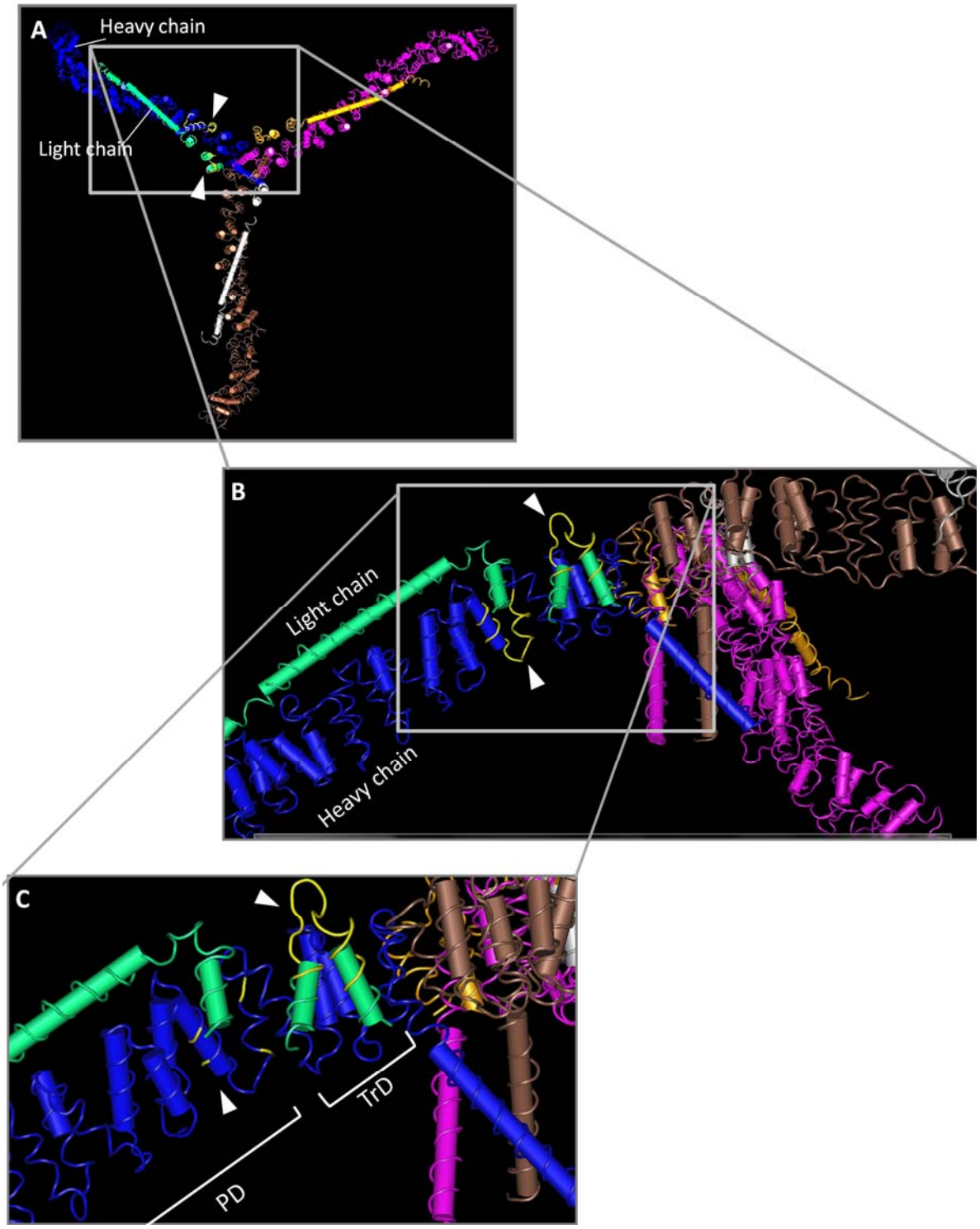

Figure 59. Crystal structure of clathrin heavy and a clathrin light chains complex from *Bos Taurus.* The putative Cmd binding site in clathrin heavy and light chains (A; B; C) are coloured in yellow and marked with a white arrow. Source: http://www.ncbi.nlm.nih.gov/Structure/ mmdb/mmdbsrv.cgi. PD: clathrin heavy chain proximal domain. TrD: clathrin heavy chain trimerization domain

polymerizable clathrin to the nerve terminal (Pley, 1995). This idea would be consistent with a role of Cmd in clathrin uncoating.

4.1.2. An unlikely role of the clathrin-Cmd1 interaction regulating the assembly or the stability of the clathrin triskelion

The position of the Cmd binding site in the clathrin heavy and light chains, and the observations that the clathrin heavy and light chain mutants lacking the Cmd1 binding sites are less expressed (Figure 26), fail to interact with their partner chain (Figures 38 and 39) and to form triskelions (Figure 41), made us hypothesize that

the clathrin-Cmd interaction could play an important role in the assembly of the triskelions or in the assembly/disassembly of clathrin cages or plaques. Four pieces of information indicate that a sustained clathrin-Cmd interaction is certainly not required for the assembly or the stability of the triskelions. First, one hour after shift to restrictive temperature, the Chc1-Clc1 interaction and the amount of triskelions present in conditional *cmd1* mutants that show impaired clathrin-Cmd1 interaction, do not seem to be altered, as compared to the WT strain (Figures 40 and 41). Under the same conditions, trafficking defects associated to clathrin miss function in the *cmd1* mutants are clearly installed (Figures 34 and 42), indicating that those are not the result of the instability of Chc1 or Clc1 or the disassembly of triskelions. Second, the observation that the co-localization of clathrin and Cmd1 is scarce (Figure 39) indicates that the interaction is transient and/or it occurs in a very particular cellular location. On the contrary, most clathrin heavy and light chains in WT cells are assembled in triskelions (Figure 41). Third, the Cmd1 binding to clathrin seems to be calcium-dependent, indicating that the interaction is regulated by an internal or external signal. In contrast, there is no evidence indicating that the triskelions assemble or disassemble in response to cellular signaling (Frances M Brodsky, 2012). Fourth, *in silico* analysis of the structure of the mutants generated suggests that the deletions imposed, besides altering the interaction with Cmd1, might also alter the Chc1-Clc1 interaction and therefore, the assembly in triskelions. The region deleted in Chc1 (aa 1491-1539) is adjacent to the Chc1 trimerization domain (aa 1550-1580). Clc1 binds to Chc1 through the Chc1 proximal domain between residues 1213 and 1522 (Liu *et al.,* 1995; Näthke *et al.,* 1992; Pishvaee *et al*., 1997), but also depends on some leucine and

phenylalanine residues on the trimerization domain, as shown by Clc1 co-precipitation and gel

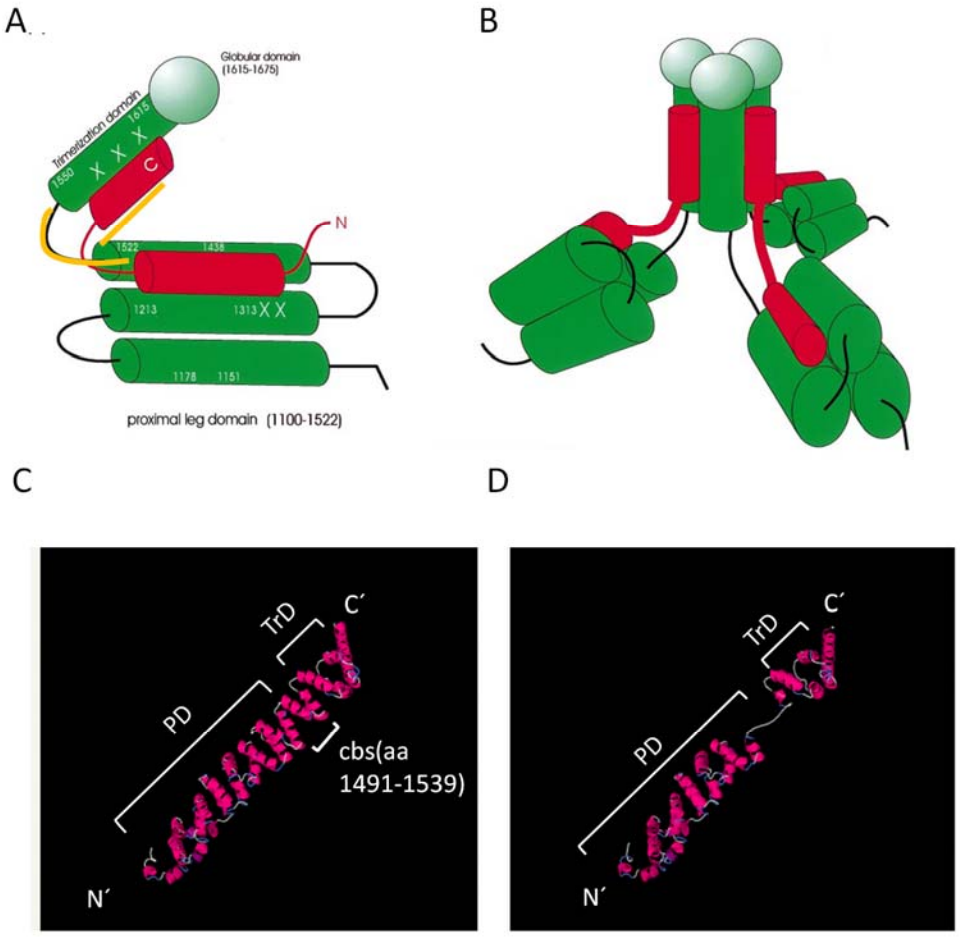

Figure 60. Structural analysis of the deletion of the clathrin putative Cmd1 binding site. (A) Model for the interaction of Clc1 (in red) with the trimerization domain and the vertex-proximal leg segment of Chc1 (in green) in yeast. Cylinders represent the putative helices involved in Chc1-Clc1 binding. Illustration taken from Pishvaee *et al.,* 1997. The globular Chc1 domain at the trimer vertex, is represented as a sphere. The orange line indicates the position of the putative Cmd1 binding site in both chains. (B) Three dimensional model of the triskelion vertex region involved in Clc1 binding. The Clc1 is positioned as a molecular hinge connecting the Chc1 proximal leg to the trimerization domain. By extending into the trimerization domain, Clc1 is strategically positioned to influence the flexibility around the trimerization domain-proximal leg joint. Changes in the angles at the trimer vertex could affect the pucker of the triskelion and consequently the curvature and/or stability of clathrin lattices. Taken from (Pishvaee *et al.*, 1997).C) D) 3D secondary structure prediction of a Chc1 segment containing the proximal (PD; aa 1062-1522) and trimerization domains (TrD; aa1550-1580) of either a WT Chc1 (C) or a Chc1 carrying a deletion of the Cmd1 binding site (aa 1491-1539). The 3D structure was predicted using the program "Phyre 2" (**P**rotein **H**omology/analog**Y** **R**ecognition **E**ngine V 2.0)(http://www.sbg.bio.ic.ac.uk/phyre2/html/page.cgi?id=index).

filtration analysis with Chc1 point mutations on these residues (Pishvaee *et al.,*1997)(Figure 60A). On the other hand, even though the trimerization domain is necessary for Chc1 to form trimmers it is not sufficient in yeast, as Chc1 cannot trimerize without the Clc1 (Chu *et al*., 1996; Huang *et al*., 1997) (Figure 23). Therefore, deletion of the Cmd1 binding site in Chc1 might change the Chc1 C-terminal structure preventing proper Clc1 binding and / or formation of triskelions. Indeed, a prediction of the secondary structure of a Chc1 segment containing the proximal (aa 1062-1522) and trimerization (aa1550-1580) domains of either a WT Chc1 or a Chc1-cbsΔ (Figures 60C and 60D), and the crystal structure of a clathrin heavy and light chain complex (Figure 59), show on one hand, that the Cmd1 binding site in Chc1 (aa1491-1539) partially overlaps with the region required for binding to Clc1 in the proximal domain (aa 1213-1522) (Figures 60A, 60B and 59). On the other hand, the deletion of this binding site affects the α-solenoid secondary structure of the C-teminal part of the proximal domain, that in WT conditions constitutes a superhelical rod of modular CHCR repeats each one comprising 10 α-helixes (Ybe *et al.*, 1999). Upon deletion of the entire sequence of the Cmd1 binding site, the α-helical structure of the last CHCR repeat (CHCR7) is impaired (Figures 60C and 60D), which might affect the Chc1 C-terminal conformation and in turn the Clc1 binding. In the case of the Clc1-cbsΔ mutant, the Cmd1 binding site is situated at the most C-terminal region (aa 212-225). This truncation is also predicted to affect binding to Chc1 (Figures 59 and 60).

Thus, deleting the Cmd1 binding site of either clathrin chain, possibly alters the Chc1-Clc1 interaction and therefore, the assembly in triskelions. At the moment though, we cannot completely discard that Cmd1 works in the assembly of triskelions in a chaperon-like fashion. If clathrin triskelions are really stable, we might fail to detect differences in the stability of the triskelions, upon incubation for 1 hour at restrictive temperature of the *cmd1* mutants. Longer incubations at restrictive temperature result in high levels of cell death making the results inconclusive. Further analysis of this matter will now require the analysis of point mutations that disrupt the clathrin-Cmd1 interaction without altering the Chc1-Clc1 interaction (if at all possible) and the analysis of the assembly of clathrin triskelions in the calmodulin mutants using pulse and chase experiments.

We are currently generating point mutations in Chc1 and Clc1 predicted to specifically disrupt their interaction with Cmd1, trying to minimally perturb their

structure, their capacity to interact with their partner chain and to form triskelions, if possible, to carefully investigate the cellular function of the clathrin-Cmd1 interaction. The hydrophobic anchor residues of the different predicted conserved Cmd1 binding motifs in Chc1 (Figure 58B) and the L217-L221-L224 motifs in Clc1 will be mutated to alanines to minimize alterations in the secondary structure of the protein. Once the point mutants will be generated, we will analyze their ability to bind Cmd1 by *in vitro* pull down experiments and immunoprecipitations in yeast, and their stability, trimerization, and Chc1-Clc1 interaction capability. Nevertheless, it must be considered that the conformation of the clathrin heavy and light chains is influenced by interaction with their partner chain, which may affect the accuracy of predictions based on the conformation of the isolated heavy or light chain.

4.1.3. A possible role of the clathrin-Cmd1 interaction in the disassembly of clathrin cages

Our results and the structural information available indicate that a role of Cmd1 binding in the disassembly of clathrin lattices is likely. The Clc1 extending from the Chc1 proximal domain into the trimerization domain, suggest a model in which changes in Clc1-Chc1 interactions near the trimerization domain might influence the angle between the trimerization domain and the proximal segments, which in turn would influence the concavity of the triskelion (Pishvaee *et al.*, 1997; Ybe *et al.*, 2007). Regulatory parameters such as Cmd1 binding to clathrin could modulate the tripod angles by altering Clc1 or Chc1 conformation or Clc1 positioning on Chc1, thus affecting the concavity of the triskelion and consequently the curvature and/or stability of clathrin lattices (Pishvaee *et al.*, 1997; Ybe *et al.*, 2007). Hence, Cmd1 binding to the Chc1 and Clc1 C-terminus would modulate the Clc1 binding to the trimerization domain and in turn influence the pucker of the trimer in a Ca^{2+}/Cmd1-dependent way, allowing the hinge to acquire the flexibility needed to accommodate curvature changes, required during coated vesicle biogenesis or uncoating reactions (Pishvaee *et al.*, 1997; Ybe *et al.*, 2007). In contrast, in the absence of Cmd1, the stable binding of Clc1 to the trimerization domain could restrict the flexibility of the triskelion and either prevent clathrin coat disassembly, or assembly.

A model in which the clathrin-Cmd1 interaction regulates clathrin coat disassembly seems more likely, since disruption of the interaction caused clathrin accumulation on endosomal structures (Figure 51). The coat disassembly could be induced directly by Cmd1 binding next to the trimerization domain, or by altering the Chc1-Clc1 interaction and/or allowing the recruitment of a chaperone that would promote clathrin uncoating. Indeed, it has been previously suggested that the regulation of the Chc-Clc interaction could control disassembly by promoting a clathrin conformational change that would facilitate mammalian auxilin-dependent Hsc70 recruitment and activity (Pishvaee *et al*., 1997; Ybe *et al.*, 1998; Young *et al.*, 2013). As discussed, a few hints point to the hypothesis that the activity of Cmd in disassembly of clathrin cages implies the regulation of the Chc-Clc interaction, including the facts that: : 1) the human Chc22, which do not bind light chains, does not have the conserved Cmd binding site (Figure 58), 2) the Cmd1 binding site in the Chc1 overlaps with the Clc1 binding site and, 3) the conserved motifs found within this site are located in an helix surface that interacts with Clc1 (Figures 59 and 60).

Yeast also has an auxilin (Swa2) and Hsc70 (Ssa1/2/3/4) orthologs, which have ATPase activity, and are able to bind clathrin and partially uncoat yeast clathrin cages *in vitro* (Krantz *et al.*, 2013). Although Swa2 has not been found at endocytic sites (Toret *et al.,* 2008), it has been shown to also bind clathrin and stimulate Ssa1 ATPase activity (Gall *et al.*, 2000). Besides, *swa2* mutants grow slowly, have TGN-endosome trafficking defects, and accumulate assembled clathrin coats, as compared to WT cells (Gall *et al.*, 2000). It will be interesting in the future to genetically evaluate the functional interaction between Cmd1, the yeast auxilin and Hsc70 homologues by investigating for example if overexpression of Swa2 or Ssa1 can suppress the temperature sensitive trafficking defects of the Cmd1 mutants specifically impaired in their capacity to interact with clathrin.

In addition, experiments to directly investigate the role of Cmd1 in regulating clathrin disassembly *in vitro* could be performed using perpendicular light scattering. In these assays, disassembly of purified clathrin cages incubated in the presence or absence of Cmd1, calcium, auxilins, or chaperone ATPases could be monitored spectrometrically at 320 nm thanks to a differential light-scattering of the triskelions in solution versus the clathrin assembled in cages (Blank & Brodsky, 1986; Liu *et al.*, 1995; Ybe *et al.*, 2003; Young *et al.*, 2013).

4.1.4. Identification of Cmd1 amino acids involved in the interaction with clathrin

Further, we have identified two point mutations in Cmd1 that specifically disrupted the direct interaction with Chc1 and Clc1 *in vitro*: *cmd1-228* and *cmd1-242* (Figure 28). In yeast, only Cmd1-242 had an observable significant decrease in Chc1 and Clc1 binding under pre-incubation at restrictive temperature (Figures 30 and 31). The *cmd1-228* mutantions, although clearly disrupted the interaction with Chc1 and Clc1 *in vitro,* did not altered the interaction in yeast, even at restrictive temperature. Both mutants have different single mutations in different locations of the Cmd1 sequence which might affect Cmd1 binding to clathrin in a distinct way. The *cmd1-228* mutation could be less penetrating *in vivo*. Other molecules interacting with clathrin or Cmd1 *in vivo* might be capable of stabilizing a WT conformation for the Cmd1-228 but not for the Cmd1-242 mutant. Interestingly, mutations in the Cmd1-228 affect only the N-terminal lobe whereas the Cmd1-242 mutant bears mutations in both, the N- and the C-terminal lobes (see below). It is possible that *in vivo* the C-terminal lobe is capable of maintaining the clathrin-Cmd1 interaction. Alternatively, the Cmd1-228 mutant could still bind clathrin in yeast through an intermediate binding partner whose interaction with Cmd1-242 is also disrupted.

The collection of *cmd1* point mutants generated by Ohya and Botstein (Ohya & Botstein, 1994) contain combinations of mutations in any of the 8 phenylalanine residues, which are the most conserved within the Cmd1 amino acid sequence between yeast and vertebrates. These residues are highly hydrophobic and are involved in hydrophobic interactions with target peptides (Ikura *et al.*, 1992), so that their combinatorial mutation to alanines was predicted to differentially affect the interaction of Cmd1 with distinct targets (Ohya & Botstein, 1994). In the case of the Cmd1-228 mutant, the residues mutated are F12, F16 and F19 (Table 8), which lie within the first Cmd1 α-helix belonging to the most N-terminal EF-hand (Figure 61). Mutant Cmd1-242, has F65, located within the Ca^{2+} binding loop in the second EF-hand, and F140, located in the fourth EF-hand, within the most C-terminal helix (Table 8, Figure 61), mutated. Thus, hydrophobic phenylalanine residues in the two EF- hands of the N-terminal lobe (3 in the EF-hand 1 and one

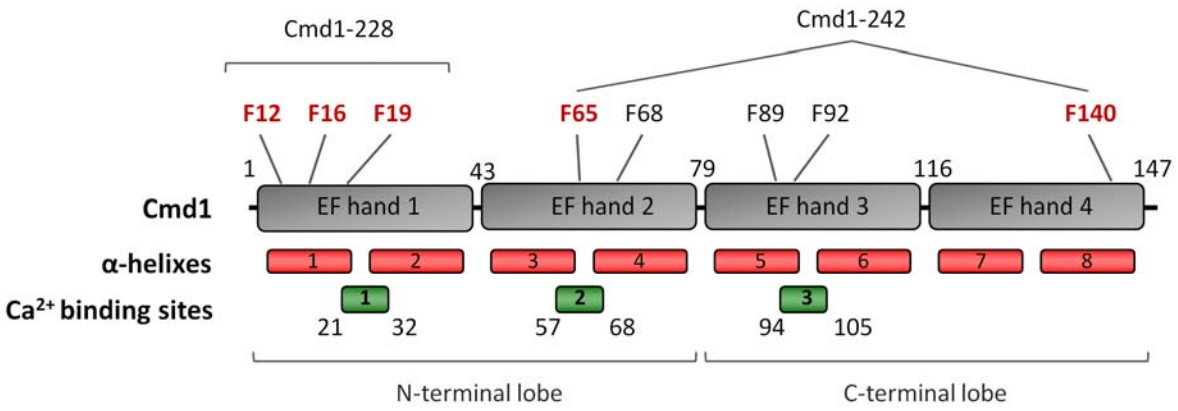

Figure 61. Yeast Cmd1 domain organization and position of the mutated phenylalanine residues in the Cmd1 mutants. Schematic representation of the domain organization and amino acid boundaries of the yeast Cmd1, indicating the positions of the four EF hands, the α-helixes and the calcium binding sites composing each EF-hand, and the different phenylalanine residues mutated to alanine in the generation of the *cmd1* point mutants collection (Ohya & Botstein, 1994). The residues mutated in the Cmd1-228 and Cmd1-242 mutants are shown in red.

in the EF-hand 2) and one residue in the EF-hand 4 in the C-terminal lobe might contribute to the Cmd1 interaction with clathrin. The Cmd1-239 mutant, which bear the F65A mutation alone (Yoshikazu Ohya & Botstein, 1994b) does not disrupt the Cmd1 clathrin interaction (Figure 30). It would be interesting to analyze if the F140 mutation by its own disrupt the clathrin-Cmd1 interaction or whether it needs to be combined with the F65A mutation. In any case, we can conclude that even though it is uncertain that the F65 contributes to the clathrin-Cmd1 interaction, the F140 certainly does. Whether it plays a redundant function with F65 remains to be explored. Smilingly, the F12 mutation in combination with F89 mutation in Cmd1-231 did not disturb the clathrin-Cmd1 interaction indicating that the F16 or the F19 necessarily contribute of the clathrin-Cmd1 interaction. In essence then, we can conclude that contacts with the α-helix belonging to the most N-terminal EF-hand are necessary but not sufficient to maintain the clathrin-Cmd1 interaction. In addition, we can assure that the F140 of EF hand 4 in the C-terminal loop of Cmd1 also contributes.

Hence, upon Ca^{2+} binding, Cmd1 would acquire an “open” conformation, and the phenylalanine residues would project from the hydrophobic interaction surfaces in the N-terminal and C-terminal lobes, being available to bind clathrin specifically

(Ohya & Botstein, 1994; Zhang *et al.*, 1995). It would now be interesting to do an *in silico* modeling of the secondary structure of the Ca^{2+}-bound Cmd1-clathrin complex analyzing the possible hydrophobic contacts of the Cmd1 phenylalanine residues that contribute to clathrin binding with the proposed conserved Cmd1 binding motifs found in Chc1 and Clc1 (Figure 58B) (see section 4.1.1.).

4.2. Cellular function of the clathrin-Cmd1 interaction

4.2.1. An unlikely role of the clathrin-Cmd1 interaction in endocytic uptake

Previous work from our laboratory that characterized the Ohya and Botstein collection of Cmd1 mutants with respect to their endocytic uptake defects, identified two Cmd1 complementation groups, indicating that Cmd1 regulates at least two different targets in the context of endocytic budding (Geli *et al.*, 1998). Three endocytic defective mutants were identified: *cmd1-247*, *cmd1-226* and *cmd1-228.* The *cmd1-247* and the *cmd1-228* mutations complemented each other for their endocytic defect, indicating that they interfere with the function of different targets. In contrast, the *cmd1-226* mutant did not complement neither the *cmd1-228* nor the *cmd1-247* mutants, suggesting that it exhibited altered binding to both putative endocytic targets. One of the Cmd1 targets was identified as the unconventional type I myosins Myo5, whose interaction with Cmd1 was disrupted in the *cmd1-247* and *cmd1-226* mutants but not in the *cmd1-228* mutant (Geli *et al.*, 1998).

In the present work, we found the *cmd1-228* mutation, which disrupted the clathrin-Cmd1 interaction, and the deletion of the clathrin Cmd1 binding sites, all caused strong endocytic uptake defects (Figures 34, 35 and 36), suggesting that the clathrin-Cmd1 interaction might be the second Cmd1 target required for endocytic internalization. However, strong evidence argued against this hypothesis. Most importantly, the mutations in Cmd1-242, which more dramatically interfered with the clathrin interaction *in vivo*, as compared to those in Cmd1-228, did not have a significant effect in endocytic uptake (Figure 34). Further, genetic evidence demonstrated that the mutations in Cmd1-226 that were expected to disrupt the interaction both with Myo5 and the second relevant Cmd1 endocytic target, showed instead WT affinity for clathrin, both *in vitro* and *in vivo* (Figures 28, 30 and 31). Finally, overexpression of clathrin did not rescue the

endocytic uptake defect of the *cmd1-228* mutant, indicating that clathrin was at least not the only relevant endocytic Cmd1 target, whose function was disrupted in this mutant. Experimental evidence indicate that Arc35 subunit of the Arp2/3 complex might be the second relevant endocytic target of Cmd1 (Geli *et al.,* 1998; Schaerer-Brodbeck & Riezman, 2000). Why then the Cmd1 binding site defective clathrin mutants also have a strong endocytic uptake defect? Our results demonstrate that deletion of the entire Cmd1 binding site in Chc1 and Clc1 also disturbed the Chc1-Clc1, and their capacity to form triskelions (Figures 38, 39 and 41), which in turn might have caused the uptake defect. An altered Chc1-Clc1 interaction or an impaired capacity to form clathrin triskelions was not observed in the *cmd1-242* (Figures 40 and 41) mutant at restrictive temperature, indicating that those effects are not a direct effect of disrupting the clathrin-Cmd1 interaction but rather they are an unwanted consequence of disrupting the clathrin structure.

Our data thus suggest that the clathrin-Cmd1 interaction does not play an essential role in endocytic budding from the PM. However, we cannot discard that it plays a regulatory role in the control of a subset of endocytic events. Compensatory endocytosis in neurons during depolarization at the nerve terminal has been shown to be regulated by calcium, suggesting that the calcium sensor mediating this form of endocytosis is Cmd. This Ca^{2+}/Cmd initiated endocytosis generates new vesicles, which replenishes the vesicle pool and is critical for maintaining exocytosis (Wu *et al.*, 2009). Indeed, we do observe co-localization of Cmd1 and clathrin in regions of polarized secretion (growing bud tips and cell abscission sites) (Figure 57), which would be consistent with a possible role of Cmd1/clathrin interaction regulating a subset of compensatory endocytosis events. Further experiments analyzing the endocytosis of polarized secreted cargo would be required to address this subject.

4.2.2. A role of the clathrin-Cmd1 interaction in TGN-endosomal trafficking

Our data is thought much more consistent with a role of the clathrin-Cmd1 interaction in retrograde traffic from the endosomes to the TGN.

Both, *cmd1-228* and *cmd1-242* mutants, which exhibited altered clathrin binding, have a defect in TGN-endosome trafficking, as demonstrated by *Mat***a** *sst1 sst2*

halo assays. In contrast, the *cmd1-226* mutant, which exhibited WT Cmd1 affinity for clathrin, did not show a TGN endosomal trafficking defect (Figure 42). The TGN trafficking defect of the *cmd1-228* and *cmd1-242* mutants was rescued by overexpressing the Chc1 and to a lesser extent, Clc1. However, it was not suppressed when we overexpressed the clathrin cbsΔ mutants (Figure 43). This result strongly indicates that the TGN endosomal trafficking defect in the *cmd1* mutants was mainly caused by clathrin miss-functioning. We also observed that the *cmd1* mutants that impaired the clathrin-Cmd1 interaction missorted Kex2 to the vacuole and accumulated clathrin in what seems a late endosomal compartment decorated with ESCTRIII subunit Snf7, relatively rapidly upon shift to restrictive temperature (Figures 42, 50 and 52). These results point to a role of Cmd1 in the disassembly endosomal clathrin and/or fission of clathrin coats from the endosomes, associated with a defect in retrograde transport from endosomes to the TGN. However, at this point, we cannot discard that the clathrin-Cmd1 interaction is also required for the forward traffic from the TGN to the endosomes because Kex2 can also be degraded in the vacuole when the Gga proteins involved in forward TGN endosomal traffic, are mutated or their interaction with Kex2 is disrupted (De *et al.,* 2012; Mullins & Bonifacino, 2001). In the *gga* mutants, Kex2 is diverted to the PM and it is thought to be transported to the vacuole through the endocytic pathway. We do not think that this is the case in the *cmd1* mutants, at least not in the *cmd1-228* mutant because this strain has a very strong uptake defect at restrictive temperature, which would block Kex2 internalization. Despite this, Kex2 is still missorted to the vacuole in the *cmd1-228* mutant (Figures 42 and 52). Further, a specific miss-function of the forward traffic would result in the enlargement of the TGN but possibly not the endosomal compartments, contrary to what we see in the *cmd1* mutants.

Nevertheless, further experiments need to be performed in order to completely discard a possible role of the clathrin-Cmd1 interaction in anterograde transport. The localization of Kex2 should be compared in temperature sensitive *gga1 gga2* and *vps1* mutants, which block anterograde traffic, and in the *cmd1* mutants that disrupt the clathrin-Cmd1 interaction, upon shift to the restrictive temperature and in the absence or in the presence of Latrunculin A to prevent endocytic uptake.

Designing point mutations in the clathrin heavy and light chains that specifically disrupt the clathrin-Cmd1 interaction without impairing their ability to assemble in triskelions, if at all possible, will also now be required to unequivocally demonstrate a specific role of the clathrin-Cmd1 interaction in retrograde traffic from the endosome to the TGN.

Interestingly, disruption of the clathrin-Cmd1 interaction did not prevent recruitment of clathrin to endosomal compartments in the *cmd1-228* and *cmd1-242* mutants but rather increased the co-localization of clathrin with the TGN and endosomal adaptor Apl2 and most strikingly also with the ESCRT-III subunit Snf7, in enlarged endosomal membranes (Figures 49 and 50), suggesting a role of Cmd1 in the disassembly of endosomal clathrin or fission of clathrin coats from the endosomes, associated with a defect in retrograde transport from endosomes to the TGN. We would favor a role of Cmd1 in the disassembly of endosomal clathrin because the position of the Cmd1 binding sites in the clathrin triskelion fits with such a molecular function (see previous section 4.1).

Even though the analysis of the clathrin cbsΔ mutants is not so informative because of the reasons outlined above, we observed that the GFP-tagged mutants were mainly cytosolic and in some cases they also accumulated clathrin in a big structure near the vacuole, which was confirmed to be at least in some cases of endocytic nature by FM4-64 staining (Figures 53 and 54). The fact that in the Chc1-cbsΔ mutant, Snf7 and Apl2 are also co-localizing with this big clathrin perivacuolar accumulation (Figure 55), fits with the co-localization results obtained in the *cmd1* mutants. However, in this case, we cannot be sure if this phenotype is caused by the loose of the clathrin-Cmd1 interaction, or by the altered Chc1-Clc1 interaction observed in these clathrin mutants. Clathrin mutants that cannot bind to their partner chain might form aggregates when overexpressed that are consumed by autophagosomes. The Chc1-cbsΔ-GFP still bears the terminal domain that interacts with most of the clathrin adaptors. That could explain why the putative Chc1-cbsΔ-GFP aggregates co-localizes with Apl2, Gga2 and Sla1 (Figure 55). The GFP-Clc1-cbsΔ mutant does not accumulate adaptors (Figure 56), as it does not have an interacting N-terminal domain. However, the GFP-Clc1 expressed in a *chc1Δ* strain (thus not able to bind Chc1) has not been found to form aggregates nor to accumulate in enlarged endosomal structures (Newpher *et al.*, 2005).

The trafficking phenotype in the *cmd1-242* and *cmd1-228* mutants is reminiscent of that of the Class E *vps* mutants, which affect members of the ESCRT complexes that mediate the budding of ILVs at LE (reviewed in (Hurley, 2010)). Mutation of the class E Vps proteins causes changes in endosome morphology, which are manifested in *Saccharomyces cerevisiae* by the formation of aberrant perivacuolar endosomes, the class E compartment (Raymond *et al.*, 1992), and are defective both in sorting to the vacuole and in the retrieval to the TGN. However, they are not defective in PM internalisation (Lemmon & Traub, 2000; Russell *et al.*, 2012). The presence of an enlarged perivacuolar endosomal compartment where Snf7 and clathrin accumulate (Figures 50 and 51), together with a defective endosome to TGN transport and an intact endocytic function (Figures 34 and 42), would fit with a role of Cmd1 disassembling the flat clathrin coat present on endosomes (Sachse *et al.*, 2002), and consequently in the proper function of ESCRT complexes in ILVs sorting and /or fusion of late endosomes with vacuole. However, the fact that we have observed Kex2 accumulating in the lumen of those vacuoles in the *cmd1-228* and *cmd1-242* mutants (Figures 42 and 52) does not agree with this hypothesis, because it probably means that the mutants with the altered clathrin-Cmd1 interaction are still sorting Kex2 to ILVs. Thus, a role of clathrin-Cmd1 interaction specifically in retrograde transport from endosome to TGN is actually more likely.

4.2.3. A role of the clathrin-Cmd1 interaction in the disassembly or fission of endosomal clathrin coats: a possible function in AP-1/clathrin- or retromer-dependent endosome to TGN retrograde trafficking

Various transport pathways and carriers may function in the retrograde transport for cargo from endosomes to the TGN. The evidence support a model in which multiple pathways for return to the Golgi take place, in some cases through the cooperation of more than one sorting device (reviewed in (Bonifacino & Rojas, 2006; Pfeffer, 2011; Seaman, 2012). The retromer, clathrin, and AP-1 have been implicated in this retrieval pathway being likely all to be components of conserved molecular machinery for retrograde transport, although their physical and functional relationships are unclear. On one side, AP-1 and clathrin have been suggested to sort some specific cargo into CCV from the EE and LE in mammals and presumably from EE in yeast, to the TGN (Crump *et al.*, 2001; Lauvrak *et al.*, 2004; Mallard *et al.*, 1998; Meyer *et al.,* 2000; Saint-Pol *et al.*, 2004; Stoorvogel *et al*.,

1996; Valdivia *et al*., 2002). On the other side, clathrin, and possibly AP-1, have also been found to function in the retrograde transport to the TGN, cooperating with retromer (Chin *et al*., 2001; Popoff *et al.,* 2007, 2009).

It has been proposed that flat clathrin lattices present on endosomes (and presumably AP-1) (Sachse *et al.*, 2002), not only interact with the ESCRT complexes (Raiborg *et al.*, 2006) but also with retromer, being not only involved in the degradative sorting, but also acting with retromer as a platform to enrich a subset of cargos destined for retrograde traffic to the TGN (Popoff *et al.,* 2009). It has been proposed that clathrin is removed before as retromer-dependent tubulation occurs, since retromer decorated carriers are not decorated with clathrin by fluorescence microscopy (McGough & Cullen, 2013; Popoff *et al.*, 2007, 2009). Even though clathrin and retromer seem to co-localized in certain endosomal subdomains at the ultrastrucutral level (Popoff *et al.*, 2007) clathrin seem to be excluded from retromer coated tubules (McGough & Cullen, 2013). It has been proposed that retromer is recruited to the edge of flat clathrin coats where cargo is confined, and then it removes the clathrin coat to subsequently generate the tubules and target the enriched cargo into the tubular carrier (McGough & Cullen, 2013; Popoff *et al*., 2009). Thus, clathrin would be required for cargo enrichment, but not for tubule formation (McGough & Cullen, 2013). Indeed, knocking down clathrin causes a defect in cargo retrogade transport, but not in retromer sorting nexin-dependent tubular carrier formation (McGough & Cullen, 2013). Consistent with our observation that Kex2 is transported to the lumen of the vacuole in the Cmd1 clathrin-binding defective mutants and with the hypothesis that Cmd1-induced clathrin disassembly interferes with retromer-mediated retrograde transport to the TGN, interfering with retromer causes cargo sorting into the degradative pathway to the lysosome/vacuole (Seaman *et al.*, 1997).

Interestingly, it has been proposed that retromer promotes clathrin uncoating by an interaction with RME-8 (Popoff *et al.,* 2009; Shi *et al.*, 2009). RME-8 is an endosomal specific auxilin-like protein that has been described in mammalian cells, *D. melanogaster, C.elegans* and plants, which contains a DNA J-domain that stimulates the chaperone Hsc70 (Chang *et al.*, 2004; Girard *et al.,* 2005; Silady *et al.,* 2008; Zhang *et al.,* 2001) (Figure 62). RME-8 strongly co-localizes with retromer components and it interacts with the retromer component SNX1 but it does not

bind clathrin (McGough & Cullen, 2013; Popoff *et al.*, 2009; Shi *et al.*, 2009). Loss of RME-8, Hsc70 or the retromer component SNX1 led to an increase in the amount of clathrin on endosomes, a slower turnover of endosomal clathrin, and cargo missorting into the degradative pathway (Popoff *et al.*, 2009; Shi *et al.*, 2009). However, loss of RME-8 did not increase the co-localisation between retromer and clathrin, and tubules generated were still clathrin negative (McGough & Cullen, 2013). These data support a role of RME-8 in recruiting Hsc70 onto sites of retrograde tubule formation, thereby regulating clathrin dynamics that is critical for functional retrograde transport. RME-8-mediated clathrin uncoating would not be necessary for retromer-dependent tubule formation, but it would be necessary for efficient cargo targeting to the TGN (McGough & Cullen, 2013). In addition, it has also been recently suggested that other key role of RME-8 in endosomal trafficking is to coordinate WASH and sorting nexins activities for efficient retromer-mediated endosomal protein sorting (Freeman *et al.*, 2014). Upon deletion of RME-8, SNX1 maintains an abnormally tight association with the membrane, causing an exacerbated tubulation activity of its BAR domain (Freeman *et al.*, 2014).

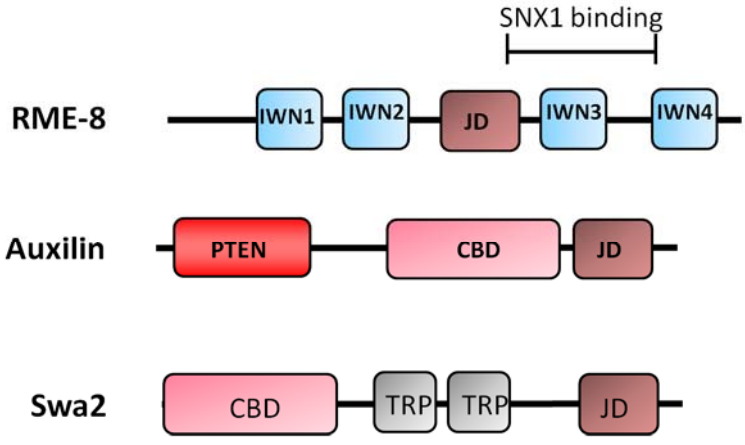

Figure 62. **Schematic representation of the domain organization of human RME-8, and auxilin and yeast Swa2**. JD: DNA J-domain that binds Hsc70 ; IWN: four IWN repeats of unknown function ; PTEN: phosphatase-and-tensin-homologue domain; CBD: clathrin-binding domain; TRP: tetratricopeptide repeats.

RME-8 does not appear to bind clathrin (Girard *et al.*, 2005), contrary to the other DNA J-domain protein auxilin, that binds clathrin and destabilizes the lattice, recruiting then Hsc70 and allowing it to bind the released clathrin C-terminus (Ernst Ungewickell et al., 1995). Thereby, RME-8 recruited to endosomes through an interaction with retromer, recruits Hsc70 to clathrin but other factor would be needed to destabilize the clathrin coat and promote Hsc70 binding. We would like to propose that Cmd1 might fulfil this function on the endosomes.

Auxilin and Hsc70 yeast orthologues, Swa2 and Ssa1, respectively, are also able to bind clathrin and partially uncoat yeast clathrin cages *in vitro* (Krantz *et al*., 2013). *In vivo*, cytoplasmic Swa2 binds clathrin and stimulate Hsc70 and Ssa1 ATPase activity (Gall *et al.*, 2000). However, Swa2 has not been observed at cortical endocytic sites and its deletion does not seem to affect the dynamics of endocytic clathrin adaptors such as Sla2 (Toret *et al.,* 2008). *swa2* mutants display TGN-endosome trafficking defects, and accumulate membrane assembled clathrin coats comparing to WT cells (Gall *et al.*, 2000; Pishvaee *et al.*, 2000), which suggest a role of Swa2 and Ssa1 in disassembling clathrin *in vivo* in TGN-endosomal pathways. There is no sequence similarity between RME-8 and auxilin or between RME-8 and Swa2, outside the J-domain (Figure 62). Other J-domain proteins have been described in yeast, but they have different specific locations, as nucleoplasm, mitochondria or ER membranes, and diverse specific functions as translation and folding, peroxisome biogenesis or protein translocation (Walsh *et al*., 2004), different from clathrin uncoating. For example, one yeast RME-8-like protein, Sec63, is an ER transmembrane protein required in protein secretion (Walsh *et al*. , 2004). Besides, *swa2* activity defects are not recovered by overexpression of other J proteins (Gillies *et al.*, 2013), suggesting that Swa2 is specialized in yeast for the Ssa1 function in clathrin uncoating. Interestingly, expression of a Swa2 fragment containing only the J and the TRP domains (necessary to bind and activate Hsc70) but not the clathrin binding domain can partially restore the α-factor processing defects of *swa2Δ* cells (Xiao *et al.*, 2006), suggesting that at least some function of Swa2 in clathrin-dependent TGN-endosomal traffic can take place without binding clathrin. In this context, we could hypothesize that Cmd1, Swa2 and Hsc70 might cooperate to disassemble clathrin assembled on the TGN or endosomes either upon fission of bona fide CCVs or on endosomal flat clathrin layers. In the case of

Cmd1, this last option seems more likely since enlarge endosomal structures coated with clathrin rather than individual CCVs seem to accumulate in the Cmd1 clathrin-binding defective mutants. Due to the different flat and non-curved clathrin coat conformation, clathrin might not be accessible to Hsc70 so then disassembly would require Cmd1 as a co-chaperone to assist destabilize the Chc1-Clc1 interaction and promote recruitment of the yeast Hsc70 orthologue Ssa1 (Pishvaee *et al.*, 1997; Ybe *et al.*, 2007).

Further experiments to test this hypothesis will be performed in the future. For instance, we would like to analyze if overexpression of Ssa1 or Swa2 in clathrin-Cmd1 interaction defective mutants recovers the defective TGN-endosomal trafficking phenotypes, or if overexpression of Cmd1 would partially restore *swa2* or *ssa1* partial loss of function mutations. In addition, it would be interesting to study clathrin, Snf7 and AP-1 endosomal localization in *ssa1*, *swa2* mutants. Alternatively, a possible role in endosome clathrin uncoating of other yeast cytoplasmic J-domain proteins such as Jjj2/3 proteins (P. Walsh et al., 2004), could also be investigated.

Interestingly the existence of clathrin plaques on endosomes has not been demonstrated in yeast, probably due to the ribosome packed cytosol, which also prevents the observation of CCPs at the PM and the TGN, despite CCVs have been isolated from yeast and visualized by EM (Mueller & Branton, 1984). Our *cmd1* mutants now provide a tool to enlarge clathrin lattices on endosomes that could facilitate their ultrastructural analysis and subsequently help identifying them on endosomes of WT cells.

Thus, our data is in agreement with a model that needs to be further validated, in which the clathrin-Cmd1 interaction on endosomal membranes would facilitate clathrin uncoating possibly by displacing the Clc1 C-terminus from the trimerization domain, allowing the hinge of the trimer to acquire the flexibility needed to accommodate curvature changes required for uncoating reactions and/or by directly promoting J-domain proteins and Hsc70/Ssa1 to the endosomal clathrin plaques. Clathrin uncoating would then allow retromer to target the cargo enriched by clathrin subdomains into the retromer-generated endosomal tubular carriers for sorting into the retrograde pathway to the TGN. In complete agreement with this hypothesis, we find that when the clathrin-Cmd1 interaction

is affected, clathrin accumulates in an enlarged endosomal compartment (Figure 51), and the retromer-cargo Kex2 mislocalizes to vacuoles (Figure 52).

Overexpression of Chc1 and to a lesser extent Clc1, but not overexpression of Chc1-cbsΔ nor Clc1-cbsΔ, suppressed the halo formation defect of *cmd1-228* and *cmd1-242* mutants, which initially suggested that the halo formation defect is most likely a consequence of interfering with the clathrin-Cmd1 interaction (Figure 45). In yeast, suppression of a cellular defect (endosomal-TGN trafficking) in a strain bearing point mutations in a particular protein (*cmd1-242* and *cmd1-228*), by overexpression of a gene encoding an interacting partner (Chc1 or Clc1), but not by the overexpression of the mutant that cannot interact (Chc1-cbsΔ nor Clc1-cbsΔ) is taken as a proof that the interaction is required for that particular cellular process. It is assumed that increasing the cellular concentration of one of the components of the complex in the mutant background will favour the assembly of the complex in the WT conformation and restore its function. However, in the context of our hypothesis that Cmd1 might be required for endosomal clathrin uncoating, overexpression of WT clathrin in *cmd1* mutants, would instead be suppressing the halo defect by maybe increasing the clathrin triskelion pool, free to function in another clathrin-dependent retrograde pathway that might compensate the endosome to TGN trafficking defect.

Interestingly and correlating with our results, it has been found that in mammalian cells, Cmd is crucial to the regulation of endosomal trafficking (Lladó *et al.*, 2004, 2008; Tebar *et al.*, 2002). Chemical inhibition of Cmd blocks traffic from EE, associated with a dramatic alteration of its morphology and size. A cross-talk between Cmd and protein kinase C (PKC) has been shown to be involved in the regulation of the endosomal actin cytoskeleton promoted by cortactin and the Arp2/3 complex (Lladó *et al.*, 2004, 2008; Tebar *et al.*, 2002). Altering Cmd function, up-regulates the Arp2/3-dependent accumulation of actin around endosomes, leading to the inhibition of traffic out from the endosomes and an alteration of its morphology (Lladó *et al.*, 2004, 2008; Tebar et al., 2002). However, the enlarged endosomal phenotype upon Cmd inhibition could also be in part a consequence of a lack of clathrin disassembly that might be necessary for functional retromer-dependent retrieval of cargo. In addition, RME-8, which promotes clathrin uncoating in endosomes, has also been shown to coordinate the actin-dependent fission activity of WASH (which also promotes the Arp2/3 activity

on endosomes (Derivery *et al*., 2009)) and the retromer tubulation activity on sorting endosomes (Freeman *et al.*, 2014). These results evidence a common role of Cmd and RME-8, both in the regulation of endosomal actin dynamics and clathrin turnover, necessary for protein sorting and/or intermediate carrier formation, from endosomes.

Intriguingly, emerging clues suggest that some sort of crosstalk between retromer and the ESCRT machinery might occur. Some evidence support an interaction between retromer components SNX1 and Vps35 and the ESCRT-0 component Hrs/Vps27 (Chin *et al.,* 2001; Popoff *et al.,* 2009). Thus, retromer might interact with RME-8 and Hrs/Vps27, which both might have an impact in clathrin dynamics on endosomes to regulate sorting of cargo from clathrin subdomains into transport intermediates (Figure 63). In the absence of RME-8 or RME-8 activity, clathrin and cargo would probably remain associated with Hrs, being cargo then targeted to the lysosome/vacuole through the subsequent recruitment and activity of ESCRT complexes (McGough & Cullen, 2011). This would explain the Snf7 (ESCRT-III) accumulation and co-localization with clathrin in enlarged endosomal compartments upon disruption of the clathrin-Cmd1 interaction in the *cmd1-228* and *cmd1-242* mutants (Figure 50), although its function in cargo delivery to the vacuole would not seem to be significantly altered (Figure 42 and 52). A current model suggest that the opposing activities of Hrs promoting clathrin assembly on the endosomes and RME-8 and Hsc70 triggering disassembly could maintain an equilibrium between endosomal subdomains, such that degradative and recycling functions can coexist in the same endosome (McGough & Cullen, 2011, 2013; Popoff *et al.*, 2009). Thereby, sorting decisions on endosomes would be operated in an integrated manner, and the ability to switch between the ESCRT pathway and retromer would provide a mechanism for controlling the destination of cargos which alternate between degradation and recycling in response to certain stimuli, such as calcium.

An important issue in the context of the proposed hypothesis is that the clathrin-Cmd1 interaction seems to be calcium dependent (Figures 19 and 20), suggesting that clathrin disassembly from endosomes would be triggered by calcium. Consistent with the Ca^{2+} requirement for the clathrin-Cmd1 interaction found in this study, Ca^{2+} has been reported to have a regulatory function in the retrograde transport from the endosome to the TGN (Burgoyne & Clague, 2003; Hay, 2007;

Luzio *et al.*, 2007). The Ca^{2+} signal necessary for this clathrin-Cmd1 interaction, might be caused by a local release of Ca^{2+} from the endosome lumen through the activity of Ca^{2+} channels activated by stimulus such as the synthesis of specific phosphoinositides, luminal pH variations or the tension of the outer endosomal membrane, all consequences of endosome maturation (Abe & Puertollano, 2011; Bonilla & Cunningham, 2002; Huotari & Helenius, 2011). Two Ca^{2+} channels in yeast, Mid1, which is mainly found in the PM and Yvc1, which is mainly found in vacuoles (reviewed in (Abe & Puertollano, 2011; Bonilla & Cunningham, 2002) would be in a position to release Ca^{2+} from the endosomes. Even though it has not been investigated, Mid1 and/or Ycv1 might be present in endosomes via the endocytic recycling pathway (Mid1) or through the biosynthetic pathway to the vacuole (Ycv1). Interestingly *mid1* mutations show negative genetic interactions with mutations in *SWA2*, the auxilin homologue that involved in disassembly of clathrin cages, in *FAB1*, which encodes the PtdIns(3)P-5-kinase essential in endosomal maturation, and *BRO1* and *VPS27*, proteins involved in the recruitment of clathrin to endosomes (P. S. Aguilar et al., 2011; Hoppins et al., 2011). Interestingly Mid1 is a stretch-induced Ca^{2+} channel, raising the interesting possibility that accumulation of ILV as the endosome matures causes an increase in tension of the endosomal outer membrane, causing the release of Ca^{2+} and the Ca^{2+}-Cmd1 dependent disassembly of clathrin. It would be interesting to analyse in *yvc1* and *mid1* mutated cells, whether clathrin accumulates in endosomal membranes similar to the clathrin-Cmd1 interaction defective mutants.

AP-1 and clathrin have also been suggested to assemble at the endosome to sort specific cargo into bona fide CCV that traffic to the TGN (Bonifacino & Rojas, 2006). Recruitment of cargo into CCV at these sites could depend on the affinity of sorting signals for AP-1 or participation of different auxiliary proteins, as epsinR and OCRL1 (Oculocerebrorenal syndrome of Lowe 1, a Golgi-localized PtdIns(4,5)P_2 5-phosphatase), suggested to target clathrin to endosomal membranes in mammals (Choudhury *et al*., 2005). Our results revealed that upon disruption of clathrin-Cmd1 interaction, AP-1 and clathrin are accumulated in enlarged endosomal-like structures and endosome to TGN transport is defective (Figures 42, 49 and 51). Thus, with our present observations, we cannot discard an alternative role clathrin-Cmd1 interaction in fission of AP-1/clathrin-coated vesicles from endosomes rather than in the disassembly of planar endosomal clathrin coats. If

fission does not take place, clathrin/AP-1 coats might not able to uncoat and therefore, they will accumulate on endosomes. EM analysis needs to be done to further analyze the structure of the clathrin accumulated on endosomes upon disruption of the clathrin-Cmd1 interaction.

This study has brought to light new important molecular mechanisms that may cooperate in the regulation of membrane traffic from endosomes. The proposed model for the role of the Ca^{2+}-dependent clathrin-Cmd1 interaction in the regulation of clathrin dynamics at endosomes according to the presented results and the previously described data is summarized in Figure 63. However, the activity of a RME-8-like component or any other endosomal DNA J-domain protein as well as Ssa1 (Hsc70) and the presence of a flat clathrin coat on yeast endosomes need to be further investigated. Besides, an alternative role of clathrin-Cmd1 interaction in fission of clathrin/AP-1 coated vesicles from endosomes should be also explored by using electron microscopy.

Future experiments are now being designed to define more accurately the specifical Cmd1 binding motifs present in clathrin, as well as to validate and characterize the proposed endosomal trafficking function of the clathrin-Cmd1 interaction.

In addition, it would be worth in the future to explore a possible role of this interaction in the abscission step of cytokynesis, as Cmd1 and clathrin were shown to also co-localize at the cytokinetic ring (Figure 57). Indeed, Cmd, clathrin and ESCRT proteins, have already been implicated in cytokinesis (Carlton & Martin-Serrano, 2009; Cyert, 2001; Niswonger & O´Halloran, 1997; Ohya & Botstein, 1994; Smith & Chircop, 2012).

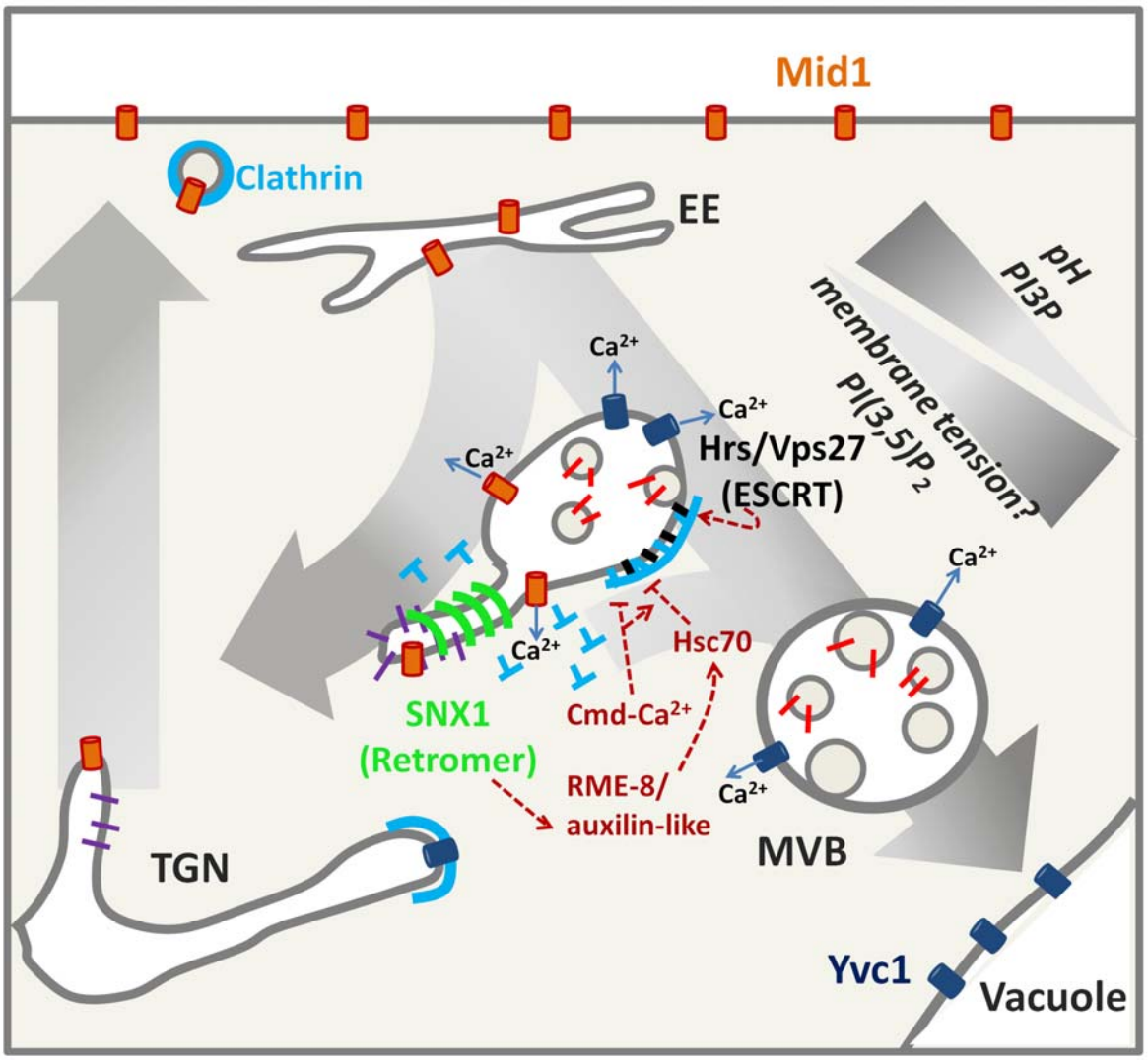

Figure 63. Speculative model for the calcium-induced Cmd1-dependent disassembly of endosomal clathrin. Clathrin is present at endosomal membranes as a flat coat that is recruited through an interaction with Hrs/Vps27, or clathrin adaptors such as AP-1. There, it is implicated in the formation of endosomal subdomains that enrich cargo for sorting to the degradative compartment in cooperation with Hrs/Vps27 and/or for sorting to the retromer-decorated endosomal tubules (adajacent to clathrin coats) for retrograde transport to the TGN and maybe also in the formation of bona fide AP-1 and clathrin coated vesicles destined to the TGN. Stimulus as synthesis of specific phosphoinositides, luminal pH variations, or the tension of the outer endosomal membrane, all consequences of endosome maturation, might activate Mid1 or the Yvc1 calcium channels, which might be present in endosomes via the endocytic recycling pathway (Mid1) or through the biosynthetic pathway to the vacuole (Ycv1). The local release of Ca^{2+} would recruit Cmd1 to the light and heavy chain, which might influence the pucker of the triskelium and allow the interaction with Hsc70/Ssa1, which will already be recruited and activated at the endosomes subdomains enriched in retromer by DNA J-domain proteins as RME-8, which interacts with both SNX1 and with Hsc70. Hsc70/Ssa1 would then split ATP and put strain leading to clathrin disassembly. Clathrin uncoating permits enriched cargo to be targeted to retromer-generated tubular endosomal membranes. If clathrin is not disassembled, cargo and clathrin would remain linked to ESCRT machinery (Hrs/Vps27) and subsequently targeted to lysosomes/vacuoles for degradation.

CONCLUSIONS

Based on the results described in this study, we confirm that yeast clathrin binds calmodulin *in vitro* in a calcium-dependent manner and we conclude that:

- Chc1 and Clc1 directly bind Cmd1 *in vitro* and in yeast in a calcium-dependent manner.
- The Cmd1 binding site in Chc1 is located at the C-terminus adjacent to the trimerization domain, between amino acids 1491-1539.
- *In silico* analysis predicts that the Cmd1 binding site in the clathrin heavy chain is conserved throughout evolution. However, in humans the conserved putative Cmd1 binding site is only present in the Chc17 but not in the Chc22 clathrin heavy chain.
- The Cmd1 binding site in Clc1 is located at the C-terminus, between amino acids 212-225. *In silico* analysis also predict the Cmd1 will bind to the Clc1 at the vertex of the clathrin triskelion.
- The Cmd1 binding site in Chc1 constitutes the predominant Cmd1 binding region for clathrin in yeast.
- The deletion of the complete putative Cmd1 binding site sequence of Chc1 and Clc1 negatively affects their expression, the Chc1-Clc1 interaction and their ability to form triskelions.
- The *cmd1-228* and *cmd1-242* mutations specifically disrupt the direct interaction with both Chc1 and Clc1 *in vitro*. Most likely though, interactions of Cmd1 with other proteins might be also affected *in vivo*.
- The *cmd1-242* mutation, but not the *cmd1-228* mutation, specifically disrupts the interaction with Chc1 and Clc1 in yeast, upon incubation at restrictive temperature (37ºC). The Cmd1-228-clathrin interaction in a cellular context might either be stabilized by a particular molecular microenviroment, or the Cmd1-228-clathrin interaction observed in the immunoprecipitation experiments is hold by indirect interactions with other proteins that co-precipitate with Cmd1 and clathrin.

- The clathrin-Cmd1 interaction might not be essential in yeast to sustain growth.

- Incubation of the *cmd1-242* mutant at restrictive temperature does not alter the expression level of Chc1 or Clc1, their ability to interact or their assembly in triskelions, suggesting that the clathrin-Cmd1 interaction is not essential to maintain Chc1-Clc1 interaction or the triskelions.

- Incubation of the *cmd1-242* mutant at restrictive temperature does not significantly affect the endocytic internalisation, suggesting that the clathrin-Cmd1 interaction is not directly involved in membrane budding form the plasma membrane.

- All the mutations affecting the clathrin-Cmd1 interaction *in vitro* display defects in the TGN retention of the Kex2 protease, indicating a strong disruption of the TGN /endosomal retrograde or forward traffic.

- The *cmd1-228* and *cmd1-242* mutants accumulate Kex2 on the vacuole, rapidly upon incubation at restrictive temperature, indicating a primary defect in the retrograde transport of Kex2 from the endosomes to the TGN.

- Cmd1 can be detected in internal compartments of endocytic origin. Clathrin and Cmd1 can be found co-localizing in internal structures. The data is consistent with a transient interaction of clathrin and Cmd1 on endosomes.

- The *cmd1-228* and *cmd1-242* mutants accumulate clathrin in a late endosomal compartment, suggesting that the clathrin-Cmd1 interaction is involved in clathrin uncoating from endosomes. Our results and the published data are consistent with a calcium-dependent calmodulin function in the disassembly of clathrin from endosomes, possibly required for retromer function in retrograde traffic from endosomes to TGN.

6. MATERIALS AND METHODS

6.1. Cell culture

6.1.1. Cell culture of *Escherichia coli*

E. coli cell culture was performed according to standard protocols (Sambrook & Russel, 2001). The DH5α strain was used for molecular cloning. DH5α cells were grown at 37ºC in LB media (0.5% yeast extract, 1% bactotryptone, 0.5% NaCl) supplemented with 50 mg/L ampicillin, when selection was required. The BL21 strain was used for the expression of GST-fusion proteins (see section 6.4.3.1). BL21 cells were grown at 37ºC in LB supplemented with 50 mg/L to an OD_{600} of 0.4, shifted to 24°C, and induced at an OD_{600} of 0.7-0.8 with 0.1 mM isopropyl-β-D-thiogalactopyranoside (IPTG) for 2 h.

E.coli was stored at -80ºC in 15% glycerol added to fresh culture.

6.1.2. Cell culture of *Saccharomyces cerevisiae*

S. cerevisiae cell culture was performed as described (Sambrook & Russel, 2001) . Yeast cells were grown at 28ºC unless otherwise mentioned. Strains were grown in complete yeast peptone dextrose media (YPD) or, if selection was required, in appropriate synthetic dextrose minimal media (SDC) (Sherman, 2002). Complete YPD media contained 1% yeast extract (Difco), 2% peptone (Difco) and 2% glucose (Duchefa or Difco). Synthetic minimal media consisted of 2% glucose (Duchefa), 0.67% yeast nitrogen base (Difco) and 0.075% of CSM (Complete Synthetic Mix, Qbiogene), which contains all required amino acids, purine- and pyrimidine-bases except those required for auxotrophic marker selection. The concentration of amino acids, purine- and pyrimidine-bases used in CSM were: 10 mg/l adenine, 50 mg/l L-arginine, 80 mg/l L-aspartate, 20 mg/l L-histidine-HCl, 50 mg/l L-leucine, 50 mg/l L-lysine, 20 mg/l L-methionine, 50 mg/l L-phenylalanine, 100 mg/l L-threonine, 50 mg/l tryptophan, 50 mg/l L-tyrosine, 20 mg/l uracil and 140 mg/l valine. Solid media additionally contained 2% agar (Pronadisa or Difco). In FOA-containing plates, 5'-fluoro-orotic acid (Fluorochem) was added to synthetic minimal solid medium at a concentration of 1 mg/ml. For the induction of proteins under a *GAL1*-promoter, yeast cells were grown until early logarithmic phase ($D.O_{600}$~0.3) in synthetic raffinose minimal media (SRC). Then, galactose (Fluka) was added to a final concentration of 2% and cells were grown for 3 more hours. For induction made in solid media, synthetic galactose minimal plates (SGC) were

used, which consisted in 1% galactose (Fluka), 2% raffinose (Fluka), 0.67% yeast nitrogen base (Difco) and 0.075% of CSM.

S.cerevisiae was stored at -80ºC in 20% glycerol added to fresh culture.

6.2. Genetic techniques

6.2.1. Transformation of *Escherichia coli*

Transformation of *E.coli* strains was performed according to standard protocols (Sambrook & Russel, 2001). Chemical transformation was used to transform intact plasmids in BL21 cells and DH5α cells. Electroporation was used to transform DNA ligations in DH5α cells.

6.2.2. Transformation of *Saccharomyces cerevisiae*

Transformation of yeast was accomplished by the lithium acetate method (Ito *et al.*, 1983). Briefly, yeast cells were grown on the appropriate media and recovered at exponential phase. Approximately 1-2 x 10^8 pelleted cells were washed on LiAc-TE buffer (100 mM lithium acetate, 10 mMTris-HCl pH 7.5, 1 mM EDTA), mixed with the required DNA (0.5 μg of plasmid DNA or 2 to 5 μg of linear DNA for genomic integration), 25 μg of herring sperm DNA (Clonthech), which act as carrier, and 75 μg of PEG-4000. Cells were incubated at room temperature for 30 min, and heat shocked at 42ºC for 15 min. The PEG was eliminated by centrifugation; cells were diluted with TE (10 mMTris pH 7.5, 1 mM EDTA) and plated on the adequate SDC media for selection.

6.2.3. Generation of yeast strains

6.2.3.1. Generation of yeast strains by homologous recombination

For epitope tagging, a PCR-product (see section 6.3.1) encoding the epitope of interest with a yeast marker flanked by DNA sequences homologous to the upstream and downstream sequences adjacent the stop codon of the gene of interest was generated. The PCR fragment was transformed into yeast cells as detailed in section 6.2.2. The DNA fragments containing the epitope plus the marker do not have origin of replication, so cells that grow in the selected marker have incorporated the DNA in its genome. Epitope tagging was confirmed by PCR

analysis and immunoblot or scoring under the fluorescent microscope depending on the tag adjoined to the gene of interest.

6.2.3.2. Scoring of genetic markers

Scoring of genetic markers was accomplished as indicated below.

6.2.3.2.1. Scoring for auxotrophies

Analysis of the nutritional requirements and temperature sensitivity of yeast cells was done by replica plating. Briefly, a master plate containing the strains of interest was stamped onto a velvet. A copy of this impression was transferred to plates made with the relevant selective media.

6.2.3.2.2. Scoring of *S. cerevisiae* synthetic lethality after contra-selection of cells bearing plasmids expressing *URA3* in a *ura3* mutant background

For contra-selection of cells expressing *URA3* plasmids, 5'-fluoro-orotic acid (FOA) (Fluorochem) was added to synthetic minimal solid medium at a concentration of 1 mg/ml. Cells were transferred by replica plating to FOA-containing plates. Cells encoding the WT *URA3* convert 5'-fluoro-orotic acid to 5'-fluoro-uracil, which is toxic for the yeast cell.

6.2.3.3. Construction of strains generated for this study

Yeast strains used in this study are listed in Table I. Not previously published strains were generated as follows.

Table I. Yeast strains

Strain	Genotype	Reference
BY4742	*MAT***α** *his3 leu2 lys2 ura3*	Euroscarf
SL114	*Mat***α** *leu2 ura3 trp1 chc1Δ::LEU2 scd1*	S. Lemmon
SL1620	*MAT***α** *leu2 ura3 trp1 GAL2 his3 scd1-v clc1Δ::HIS3*	(K. M. Huang et al., 1997)
SL5156	*MAT***α** *leu2 ura3 trp1 his3 ABP1-RPF::KMX*	S. Lemmon
SCMIG1141	*Mat***a** *his3 leu2 trp1 ura3 bar1 SLA1-mCherry::HIS3MX*	I. Fernández
RH123	*MAT***a** *ssa1 ssa2*	H. Riezman

SCMIG1022	*MATα cmd1Δ::KMX ura3 leu2 his3 trp1 ade2 lys2 met15 pURA3-CMD1*	M.I.Geli
SCMIG1261	*MATα cmd1Δ::KMX ura3 leu2 his3 trp1 ade2 lys2 met15 pTRP1-CMD1*	This study
SCMIG1262	*MATα cmd1Δ::KMX ura3 leu2 his3 trp1 ade2 lys2 met15 pTRP1-cmd1-226*	This study
SCMIG1263	*MATα cmd1Δ::KMX ura3 leu2 his3 trp1 ade2 lys2 met15 pTRP1-cmd1-228*	This study
SCMIG1264	*MATα cmd1Δ::KMX ura3 leu2 his3 trp1 ade2 lys2 met15 pTRP1-cmd1-231*	This study
SCMIG1265	*MATα cmd1Δ::KMX ura3 leu2 his3 trp1 ade2 lys2 met15 pTRP1-cmd1-239*	This study
SCMIG1266	*MATα cmd1Δ::KMX ura3 leu2 his3 trp1 ade2 lys2 met15 pTRP1-cmd1-242*	This study
SCMIG1267	*MATα cmd1Δ::KMX ura3 leu2 his3 trp1 ade2 lys2 met15 CHC1-3HA::HIS3MX6 pURA3-CMD1*	This study
SCMIG1268	*MATα cmd1Δ::KMX ura3 leu2 his3 trp1 ade2 lys2 met15 CHC1-3HA::HIS3MX 6 pTRP1-CMD1*	This study
SCMIG1269	*MATα cmd1Δ::KMX ura3 leu2 his3 trp1 ade2 lys2 met15 CHC1-3HA::HIS3MX6 pTRP1-cmd1-226*	This study
SCMIG1270	*MATα cmd1Δ::KMX ura3 leu2 his3 trp1 ade2 lys2 met15 CHC1-3HA::HIS3MX 6 pTRP1-cmd1-228*	This study
SCMIG1271	*MATα cmd1Δ::KMX ura3 leu2 his3 trp1 ade2 lys2 met15 CHC1-3HA::HIS3MX6 pTRP1-cmd1-231*	This study
SCMIG1272	*MATα cmd1Δ::KMX ura3 leu2 his3 trp1 ade2 lys2 met15 CHC1-3HA::HIS3MX6 pTRP1-cmd1-239*	This study
SCMIG1273	*MATα cmd 1Δ::KMX ura3 leu2 his3 trp1 ade2 lys2 met15 CHC1-3HA::HIS3MX6 pTRP1-cmd1-242*	This study
SCMIG1274	*MATα cmd1Δ::KMX ura3 leu2 his3 trp1 ade2 lys2 met15 CLC1-3HA::HIS3MX6 pURA3-CMD1*	This study
SCMIG1275	*MATα cmd1Δ::KMX ura3 leu2 his3 trp1 ade2 lys2 met15 CLC1-3HA::HIS3MX6 pTRP1-CMD1*	This study
SCMIG1276	*MATα cmd1Δ::KMX ura3 leu2 his3 trp1 ade2 lys2 met15 CLC1-3HA::HIS3MX6 pTRP1-cmd1-226*	This study
SCMIG1277	*MATα cmd1Δ::KMX ura3 leu2 his3 trp1 ade2 lys2 met15 CLC1-3HA::HIS3MX6 pTRP1-cmd1-228*	This study
SCMIG1278	*MATα cmd1Δ::KMX ura3 leu2 his3 trp1 ade2 lys2 met15 CLC1-3HA::HIS3MX6 pTRP1-cmd1-231*	This study
SCMIG1279	*MATα cmd1Δ::KMX ura3 leu2 his3 trp1 ade2 lys2 met15 CLC1-3HA::HIS3MX6 pTRP1-cmd1-239*	This study
SCMIG1280	*MATα cmd1Δ::KMX ura3 leu2 his3 trp1 ade2 lys2 met15 CLC1-3HA::HIS3MX6 pTRP1-cmd1-242*	This study

RH3983	*MAT***a** *ade2 ade3::CMD1::TRP1 his3 leu2 lys2 trp1 ura3 cmd Δ::HIS3MX6 bar1Δ::LYS2*	(M I Geli et al., 1998)
RH3984	*MAT***a** *ade2 ade3::cmd1-226::TRP1 his3 leu2 lys2 trp1 ura3 cmd1Δ::HIS3MX6 bar1Δ::LYS2*	(M I Geli et al., 1998)
RH3985	*MAT***a** *ade2 ade3::cmd1-228::TRP1 his3 leu2 lys2 trp1 ura3 cmd1Δ::HIS3MX6 bar1Δ::LYS2*	(M I Geli et al., 1998)
RH3986	*MAT***a** *ade2 ade3::cmd1-231::TRP1 his3 leu2 lys2 trp1 ura3 cmd Δ::HIS3MX6 bar1Δ::LYS2*	(M I Geli et al., 1998)
RH3988	*MAT***a** *ade2 ade3::cmd1-239::TRP1 his3 leu2 lys2 trp1 ura3 cmd1Δ::HIS3MX6 bar1Δ::LYS2*	(M I Geli et al., 1998)
RH3990	*MAT***a** *ade2 ade3::cmd1-242::TRP1 his3 leu2 lys2 trp1 ura3 cmd1Δ::HIS3MX6 bar1Δ::LYS2*	(M I Geli et al., 1998)
SCMIG1061	*MAT***a** *his3 leu2 trp1 ura3 met15 cmd Δ::KMX myo5Δ::KMX ABP1-RFP::KMX pURA3-CMD1*	(Grötsch *et al.*, 2010)
SCMIG1063	*MAT***a** *his3 leu2 trp1 ura3 met15 cmd1Δ::KMX myo5Δ::KMX ABP1-RFP::KMX pTRP1-CMD1*	(Grötsch *et al.*, 2010)
SCMIG1281	*MAT***a** *his3 leu2 trp1 ura3 met15 cmd1Δ::KMX myo5Δ::KMX ABP1-RFP::KMX pTRP1-cmd1-228*	This study
SCMIG1282	*MAT***a** *his3 leu2 trp1 ura3 met15 cmd1Δ::KMX myo5Δ::KMX ABP1-RFP::KMX pTRP1-cmd1-242*	This study
SCMIG1076	*MAT***a** *his3 leu2 trp1 ura3 met15 cmd Δ::KMX myo5D::KMX SLA1-mCherry::HIS3MX6 pURA3-CMD1*	(Grötsch *et al.*, 2010)
SCMIG1077	*MAT***a** *his3 leu2 trp1 ura3 met15 cmd1Δ::KMX myo5Δ::KMX SLA1-mCherry::HIS3MX6 pTRP1-CMD1*	(Grötsch *et al.*, 2010)
SCMIG1283	*MAT***a** *his3 leu2 trp1 ura3 met15 cmd1Δ::KMX myo5Δ::KMX SLA1-mCherry::HIS3MX6 pTRP1-cmd1-228*	This study
SCMIG1284	*MAT***a** *his3 leu2 trp1 ura3 met15 cmd1Δ::KMX myo5Δ::KMX SLA1-mCherry::HIS3MX6 pTRP1-cmd1-242*	This study
SCMIG1080	*MAT***a** *his3 leu2 ura3 met15 myo5Δ::KMX CMD1-mCherry::HIS3MX6*	(Grötsch *et al.*, 2010)
SCMIG1285	*MAT***α** *cmd1Δ::KMX ura3 leu2 his3 trp1 ade2 lys2 met15 GGA2-mCherry::HIS3MX6 pURA3-CMD1*	This study
SCMIG1286	*MAT***α** *cmd1Δ::KMX ura3 leu2 his3 trp1 ade2 lys2 met15 GGA2-mCherry::HIS3MX6 pTRP1-CMD1*	This study
SCMIG1287	*MAT***α** *cmd1Δ::KMX ura3 leu2 his3 trp1 ade2 lys2 met15 GGA2-mCherry::HIS3MX6 pTRP1-cmd1-228*	This study
SCMIG1288	*MAT***α** *cmd1Δ::KMX ura3 leu2 his3 trp1 ade2 lys2 met15 GGA2-mCherry::HIS3MX6 pTRP1-cmd1-242*	This study
SCMIG1289	*MAT***α** *cmd1Δ::KMX ura3 leu2 his3 trp1 ade2 lys2 met15 APL2-mCherry::HIS3MX6 pURA3-CMD1*	This study
SCMIG1290	*MAT***α** *cmd1Δ::KMX ura3 leu2 his3 trp1 ade2 lys2 met15 APL2-mCherry::HIS3MX6 pTRP1-CMD1*	This study

SCMIG1291	*MATα cmd1Δ::KMX ura3 leu2 his3 trp1 ade2 lys2 met15 APL2-mCherry::HIS3MX6 pTRP1-cmd1-228*	This study
SCMIG1292	*MATα cmd1Δ::KMX ura3 leu2 his3 trp1 ade2 lys2 met15 APL2-mCherry::HIS3MX6 pTRP1-cmd1-242*	This study
SCMIG1293	*MATα cmd1Δ::KMX ura3 leu2 his3 trp1 ade2 lys2 met15 KEX2-mCherry::HIS3MX6 pURA3-CMD1*	This study
SCMIG1294	*MATα cmd1Δ::KMX ura3 leu2 his3 trp1 ade2 lys2 met15 KEX2-mCherry::HIS3MX6 pTRP1-CMD1*	This study
SCMIG1295	*MATα cmd1Δ::KMX ura3 leu2 his3 trp1 ade2 lys2 met15 KEX2-mCherry::HIS3MX6 pTRP1-cmd1-228*	This study
SCMIG1296	*MATα cmd1Δ::KMX ura3 leu2 his3 trp1 ade2 lys2 met15 KEX2-mCherry::HIS3MX6 pTRP1-cmd1-242*	This study
SCMIG1297	*MATα cmd1Δ::KMX ura3 leu2 his3 trp1 ade2 lys2 met15 SNF7-mCherry::HIS3MX6 pURA3-CMD1*	This study
SCMIG1298	*MATα cmd1Δ::KMX ura3 leu2 his3 trp1 ade2 lys2 met15 SNF7-mCherry::HIS3MX6 pTRP1-CMD1*	This study
SCMIG1299	*MATα cmd1Δ::KMX ura3 leu2 his3 trp1 ade2 lys2 met15 SNF7-mCherry::HIS3MX6 pTRP1-cmd1-228*	This study
SCMIG1300	*MATα cmd1Δ::KMX ura3 leu2 his3 trp1 ade2 lys2 met15 SNF7-mCherry::HIS3MX6 pTRP1-cmd1-242*	This study
SCMIG1301	*MATα his3 leu2 lys2 ura3 GGA2-mCherry ::HIS3MX*	This study
SCMIG1302	*MATα his3 leu2 lys2 ura3 APL2-mCherry ::HIS3MX*	This study
SCMIG1303	*MATα his3 leu2 lys2 ura3 KEX2-mCherry ::HIS3MX*	This study
SCMIG1304	*MATα his3 leu2 lys2 ura3 SNF7-mCherry ::HIS3MX*	This study

SCMIG1261, SCMIG1262, SCMIG1263, SCMIG1264, SCMIG1265 and SCMIG1266

SCMIG1190, SCMIG1191, SCMIG1192, SCMIG1193, SCMIG1194 and SCMIG1195 were created by transforming SCMIG1022 with pRB1688, pRB1646, pRB1648, pRB1651, pRB1659 or pRB1662 respectively. Then contra-selection of cells bearing *pURA3-CMD1*, was performed on FOA plates (see section 6.2.3.2.2) and confirmed by replica-plating on SDC-URA (see section 6.2.3.2.1).

SCMIG1267, SCMIG1268, SCMIG1269, SCMIG1270, SCMIG1271, SCMIG1272 and SCMIG1273

SCMIG1267 was generated by tagging the *CHC1* gene with a DNA fragment encoding 3HA with the auxotrophically selectable *HIS3MX6* gene by homologous

recombination. To do this, a PCR product encoding the *3HA::HIS3MX6* cassette flanked by 40 nucleotides upstream and 40 nucleotides downstream the STOP codon was generated using the plasmid pFA6a-3HA-His3MX6 as template and primers Chc1.d.F2 and Chc1.u.R1. The amplified fragment was transformed into the SCMIG1022 and transformants were selected on SDC-His. Successful recombination was verified by immunoblot using an antibody against the HA epitope.

SCMIG1268, SCMIG1269, SCMIG1270, SCMIG1271, SCMIG1272 and SCMIG1273 were generated by transforming SCMIG1196 with pRB1688, pRB1646, pRB1648, pRB1651, pRB1659 or pRB1662 respectively. Then contra-selection of cells bearing *pURA3-CMD1*, was performed on FOA and confirmed by replica-plating on SDC-URA.

SCMIG1274, SCMIG1275, SCMIG1276, SCMIG1277, SCMIG1278, SCMIG1279 and SCMIG1280

SCMIG1274 was generated by tagging the *CLC1* gene with a DNA fragment encoding 3HA with the auxotrophically selectable *HIS3MX6* gene by homologous recombination. To do this, a PCR product encoding the *3HA::HIS3MX6* cassette flanked by 40 nucleotides upstream and 40 nucleotides downstream the *CLC1* STOP codon was generated using the plasmid pFA6a-3HA-His3MX6 as template and primers Clc1.d.F2 and Clc1.u.R1. The amplified fragment was transformed into the SCMIG1022 and transformants were selected on SDC-His. Successful recombination was verified by immunoblot using an antibody against the HA epitope.

SCMIG1275, SCMIG1276, SCMIG1277, SCMIG1278, SCMIG1279 and SCMIG1280 were created by transforming SCMIG1196 with pRB1688, pRB1646, pRB1648, pRB1651, pRB1659 or pRB1662 respectively. Then contra-selection of cells bearing *pURA3-CMD1*, was performed on FOA and confirmed by replica-plating on SDC-URA.

SCMIG1281 and SCMIG1282

SCMIG1281 and SCMIG1282 were generated by transforming SCMIG1061 with PRB1646 and PRB1662 respectively. Then contra-selection of cells bearing *pURA3-CMD1*, was performed on FOA and confirmed by replica-plating on SDC-URA.

SCMIG1283 and SCMIG1284

SCMIG1283 and SCMIG1284 were generated by transforming SCMIG1076 with pRB1646 and pRB1662 respectively. Then contra-selection of cells bearing *pURA3-CMD1*, was performed on FOA and confirmed by replica-plating on SDC-URA.

SCMIG1285, SCMIG1286, SCMIG1287, SCMIG1288 and SCMIG1301

SCMIG1285 and SCMIG1301 were created by tagging the *GGA2* gene with a DNA fragment encoding mCherry with the auxotrophically selectable *HIS3MX6* gene by homologous recombination. To do this, a PCR product encoding the *mCherry::HIS3MX6* cassette flanked by 40 nucleotides upstream and 40 nucleotides downstream the *GGA2* STOP codon was generated using the plasmid pBS34 as template and primers Gga2.d.F2 and Gga2.u.R1. The amplified fragment was transformed into the SCMIG1022 and SCMIG381, respectively and transformants were selected on SDC-His. Successful recombination was verified by PCR analysis of genomic DNA (see section 6.3.2.2) using the primers Gga2.1527.d and Gga2.1991.u.

SCMIG1286, SCMIG1287 and SCMIG1288 were generated by transforming SCMIG1214 with pRB1688, pRB1648 or pRB1662 respectively. Then contra-selection of cells bearing *pURA3-CMD1*, was performed on FOA and confirmed by replica-plating on SDC-URA.

SCMIG1289, SCMIG1290, SCMIG1291, SCMIG1292 and SCMIG1302

SCMIG1289 and SCMIG1302 were created by tagging the *APL2* gene with a DNA fragment encoding mCherry with the auxotrophically selectable *HIS3MX6* gene by homologous recombination. To do this, a PCR product encoding the *mCherry::HIS3MX6* cassette flanked by 40 nucleotides upstream and 40 nucleotides downstream the STOP codon was generated using the plasmid pBS34 as template and primers Apl2.d.F2 and Apl2.u.R1. The amplified fragment was

transformed into the SCMIG1022 and SCMIG381 strains, respectively and transformants were selected on SDC-His. Successful recombination was verified by PCR analysis of genomic DNA using the primers Apl2.1889.d and Apl2.2439.u.

SCMIG1290, SCMIG1291 and SCMIG1292 were generated by transforming SCMIG1218 with pRB1688, pRB1648 or pRB1662 respectively. Then contra-selection of cells bearing *pURA3-CMD1*, was performed on FOA and confirmed by replica-plating on SDC-URA.

SCMIG1293, SCMIG1294, SCMIG1295, SCMIG1296 and SCMIG1303

SCMIG1293 and SCMIG1303 were created by tagging the *KEX2* gene with a DNA fragment encoding mCherry with the auxotrophically selectable *HIS3MX6* gene by homologous recombination. To do this, a PCR product encoding the *mCherry::HIS3MX6* cassette flanked by 40 nucleotides upstream and 40 nucleotides downstream the *KEX2* STOP codon was generated using the plasmid pBS34 as template and primers Kex2.d.F2 and Kex2.u.R1. The amplified fragment was transformed into the SCMIG1022 and SCMIG381 respectively and transformants were selected on SDC-His. Successful recombination was verified by PCR analysis of genomic DNA using the primers Kex2.2161.d and Kex2.2663.u.

SCMIG1294, SCMIG1295 and SCMIG1296 were generated by transforming SCMIG1222 with pRB1688, pRB1648 or pRB1662 respectively. Then contra-selection of cells bearing *pURA3-CMD1*, was performed on FOA and confirmed by replica-plating on SDC-URA.

SCMIG1297, SCMIG1298, SCMIG1299, SCMIG1300 and SCMIG1304

SCMIG1297 and SCMIG1304 were generated by tagging the *SNF7* gene with a DNA fragment encoding mCherry with the auxotrophically selectable *HIS3MX6* gene by homologous recombination. To do this, a PCR product encoding the *mCherry::HIS3MX6* cassette flanked by 40 nucleotides upstream and 40 nucleotides downstream the *SNF7* STOP codon was generated using the plasmid pBS34 as template and primers Snf7.d.F2 and Snf7.u.R1. The amplified fragment was transformed into the SCMIG1022 and SCMIG381 strains respectively and transformants were selected on SDC-His. Successful recombination was verified by PCR analysis of genomic DNA using the primers Snf7.458.d and Snf7.995.u.

SCMIG1298, SCMIG1299 and SCMIG1300 were generated by transforming SCMIG1226 with pRB1688, pRB1648 or pRB1662 respectively. Then contra-selection of cells bearing *pURA3-CMD1*, was performed on FOA) and confirmed by replica-plating on SDC-URA.

6.2.4. Serial dilution cell growth assays

Cells from mid-log phase cultures were diluted to 10^7 cells/ml in the adequate fresh media and 4 x 1 to 10 serial dilutions were prepared on sterile 1.5 ml Eppendorf tubes. 5 µl of each dilution were spotted on plates with the adequate solid media. After the liquid was evaporated, plates were incubated for three days at the indicated temperature.

6.3. DNA and RNA techniques and plasmid construction

6.3.1. Standard molecular biology techniques: amplification and purification of plasmids in *E. coli*, enzymatic restriction of DNA, DNA ligation, polimerase chain reaction, agarose gels, purification of DNA fragments, and DNA sequencing

Standard DNA manipulations such as polymerase chain reactions (PCRs), gel electrophoresis, enzymatic digestion, DNA ligation, and plasmid purification were performed as described (Sambrook & Russel, 2001). Standard PCRs were performed with a DNA polymerase with proof reading activity (Vent polymerase, New England Biolabs) and a TRIO-thermoblock (Biometra GmbH). Oligonucletides were synthesized by Thermo Fisher Scientific. Restriction endonucleases were obtained from New England Biolabs or from Roche. DNA was purified using PCR- or gel extraction kits from Qiagen. Analytical agarose gel electrophoresis was performed using Sub-Cell cells from Bio-Rad Laboratories. Unless otherwise mentioned, cloning of DNA fragments was performed with the T4 DNA ligase (New England Biolabs). When needed, desphosphorilation of digested plasmid was accomplished with Shrimp Alkaline Phosphatse (Roche). Occasionally, molecular cloning of DNA fragments in plasmids was accomplished by homologous recombination in yeast followed by plasmid purification (see below). Plasmids were amplified and purified from *E. coli* with the Nucleospin plasmid purification kit (Macherey-Nagel). DNA sequencing was performed in the DNA-Sequencing Facility of the Center for Research in Agricultural Genomics (CRAG) or by Macrogen Inc.

6.3.2. Purification of DNA from *S. cerevisiae*

6.3.2.1. Extraction and purification of plasmid DNA

A 5 ml yeast culture in stationary phase was harvested at 2,300 g for 5 min. Cells were suspended in 0.4 ml of lysis buffer (0.2 M Tris-HCl pH 7.5, 0.5 mM NaCl, 1% SDS, 10 mM EDTA) and transferred to a 1.5 ml Eppendorf tube. 150 µl of glass beads and 300 µl of phenol:chloroform:isoamyl alcohol (25:24:1) were added and cells were lysed by vortexing for 2 min. Upon centrifugation at 20,000 g for 5 min, the aqueous phase (upper phase) was transferred into a new 1.5 ml tube and the DNA was further purified by phenol:chloroform extraction. The plasmid DNA was then concentrated by ethanol precipitation and finally resuspended in 50 µl of double distilled water. To obtain pure plasmid DNA, electro-competent *E.coli* cells were transformed with the plasmid recovered from yeast cells. Plasmid DNA was purified from single colonies and analyzed by digestion with restriction enzymes and analytical agarose gel electrophoresis.

6.3.2.2. Extraction and purification of genomic DNA

Approximately 2 x 10^8 yeast cells were harvested (at a culture density of 10^7 cells/ml) and resuspended in 1 ml of 1 M sorbitol. Cells were collected in 1.5 ml Eppendorf tubes, centrifuged at 5,200 g for 2 min, and resuspended in 0.5 ml of Spheroplasting buffer (1 M sorbitol, 50 mMKPO_4 buffer, pH 7.5, 14 mM β-mercaptoethanol, and either 100U/ml zymolyase 20T (Seikagaku) or 250 U/ml lyticase (Sigma-Aldrich)). After incubation for 30 min at 30ºC, spheroplasts were collected at 5,200 g and resuspended in 0.5 ml of 50 mM EDTA pH 8.0, 0.2% SDS. Samples were then incubated for 15 min at 65ºC. 50 µl of 5 M KAc pH 7.5 was added and the tube was incubated on ice for 1h. The precipitate was sedimented at 20.000 xg for 15 min and the supernatant was transferred into a new 1.5 ml Eppendorf tube carefully, in order not to fragment the chromosomes. 1 ml ethanol was added and the genomic DNA precipitate was collected at 20,000 g for 15 s. The supernatant was discarded and the pellet was air-dried and resuspended in 200 µl of TE buffer (10 mMTris pH 7.5, 1 mM EDTA). DNA was then incubated at 37º C for 15 min in the presence of RNAseA (50 µg/ml). For further purification the sample was extracted 3 times with phenol:chloroform:isoamyl alcohol (25:24:1).

Finally, the genomic DNA was precipitated with ethanol and resuspended in 50µl of TE.

6.3.3. Construction of plasmids generated for this study

Plasmids used in this study are listed in Table II. Not previously published plasmids constructed for this study were generated as follows.

Table II. Plasmids

Plasmid	E.coli features	Yeast features	Insert	Reference
YCplac 33	*ori* AMP^R	*CEN4* *URA3*	-	(Gietz & Sugino, 1988)
YCplac111	*ori* AMP^R	*CEN4* *LEU2*	-	(Gietz & Sugino, 1988)
YCplac 22	*ori* AMP^R	*CEN4* *TRP1*	-	(Gietz & Sugino, 1988)
YEplac195	*ori* AMP^R	*2µ* *URA3*	-	(Gietz & Sugino, 1988)
YEplac181	*ori* AMP^R	*2µ* *LEU2*	-	(Gietz & Sugino, 1988)
YEplac112	*ori* AMP^R	*2µ* *TRP1*	-	(Gietz & Sugino, 1988)
pFA6a-3HA-Trp1	*ori* AMP^R	- *TRP1*	*3HA-TRP1*	(Longtine *et al.*, 1998)
pFA6a-3HA-HisMX6	*ori* AMP^R	- *HIS3MX6*	*3HA- HIS3MX6*	(Longtine *et al.*, 1998)
pFA6a-GFP(S65T)-TRP1	*ori* AMP^R	- *TRP1*	*GFP- TRP1*	(Longtine et al., 1998)
YDp-U	*ori* AMP^R	- *URA3*	-	(Berben *et al.*, 1991)
YCp50-*CHC1*	*ori* AMP^R	*CEN4* *URA3*	*CHC1*	S.Lemmon
YEp24-*CHC1*	*ori* AMP^R	*2µ* *URA3*	*CHC1*	S.Lemmon
p50-*CHC1-HA*	*ori* AMP^R	*CEN4* *URA3* *TRP1*	*CHC1-HA*	This study
p50-*chc1-cbsΔ*	*ori* AMP^R	*CEN4* *URA3*	*chc1 cbsΔ*	This study
p50-*chc1-cbsΔ-HA*	*ori* AMP^R	*CEN4* *URA3* *TRP1*	*chc1 cbsΔ-HA*	This study
p195-*chc1-cbsΔ*	*ori* AMP^R	*2µ* *URA3*	*chc1 cbsΔ*	This study
p195-*chc1-cbsΔ-HA*	*ori* AMP^R	*2µ* *URA3* *TRP1*	*chc1 cbsΔ-HA*	This study
p50-*CHC1-GFP*	*ori* AMP^R	*CEN4* *URA3* *TRP1*	*CHC1-GFP*	F.Idrissi
p195-*chc1-cbsΔ-GFP*	*ori* AMP^R	*2µ* *URA3* *TRP1*	*chc1 cbsΔ-GFP*	This study
p111-*CLC1*	*ori* AMP^R	*CEN4* *LEU2*	*CLC1*	This study
P181-*CLC1*	*ori* AMP^R	*2µ* *LEU2*	*CLC1*	This study
p111-*CLC1-HA*	*ori* AMP^R	*CEN4* *LEU2* *HIS3MX6*	*CLC1-HA*	This study
P181-*CLC1-HA*	*ori* AMP^R	*2µ* *LEU2* *HIS3MX6*	*CLC1-HA*	This study
p22-*CLC1-HA*	*ori* AMP^R	*CEN4* *TRP1* *HIS3MX6*	*CLC1-HA*	This study
p112-*CLC1-HA*	*ori* AMP^R	*2µ* *TRP1* *HIS3MX6*	*CLC1-HA*	This study
p111-*clc1-cbsΔ-HA*	*ori* AMP^R	*CEN4* *LEU2* *HIS3MX6*	*clc1 cbsΔ-HA*	This study

pc181-*clc1-cbsΔ-HA*	*ori*	AMP^R	*2µ*	*LEU2 HIS3MX6*	*clc1 cbsΔ-HA*	This study
pGFP-*CLC1*	*ori*	AMP^R	*CEN4*	*TRP1*	*GFP-CLC1*	(Newpher *et al.*, 2005)
pGFP-*CLC1-U*	*ori*	AMP^R	*CEN4*	*URA3*	*GFP-CLC1*	This study
pGFP-*clc1-cbsΔ*	*ori*	AMP^R	*CEN4*	*TRP1*	*GFP-clc1 cbsΔ*	This study
p95-GFP-*clc1 cbsΔ*	*ori*	AMP^R	*2µ*	*URA3 TRP1*	*GFP-clc1 cbsΔ*	This study
pGEX-2T	*ori*	AMP^R	-		GST	Pharmacia
pGEX-5X-3	*ori*	AMP^R	-		GST	Pharmacia
pGST-*CHC1-N*	*ori*	AMP^R	-		GST-*CHC1-N* (aa1-500)	S.Lemmon
pGST-*CHC1-C*	*ori*	AMP^R	-		GST-*CHC1-C* (aa1062-1653)	S.Lemmon
pGST-*CHC1-D*	*ori*	AMP^R	-		GST-*CHC1-D (*aa500-1062)	This study
pGST-*chc1-C-cbsΔ*	*ori*	AMP^R	-		GST-*chc-C cbsΔ* (aa1062-1653)	This study
pGST-*CLC1*	*ori*	AMP^R	-		GST-*CLC1*	S.Lemmon
pGST-*clc1-cbsΔ*	*ori*	AMP^R	-		GST-*clc1 cbsΔ*	This study
pRB1688	*ori*	AMP^R	*CEN6*	*TRP1*	*CMD1*	(Yoshikazu Ohya & Botstein, 1994a)
pRB1646	*ori*	AMP^R	*CEN6*	*TRP1*	*cmd1-226*	(Yoshikazu Ohya & Botstein, 1994a)
pRB1648	*ori*	AMP^R	*CEN6*	*TRP1*	*cmd1-228*	(Yoshikazu Ohya & Botstein, 1994a)
pRB1651	*ori*	AMP^R	*CEN6*	*TRP1*	*cmd1-231*	(Yoshikazu Ohya & Botstein, 1994a)
pRB1659	*ori*	AMP^R	*CEN6*	*TRP1*	*cmd1-239*	(Yoshikazu Ohya & Botstein, 1994a)
pRB1662	*ori*	AMP^R	*CEN6*	*TRP1*	*cmd1-242*	(Yoshikazu Ohya & Botstein, 1994a)
pXY243	*ori*	AMP^R	*2µ*	*LEU2*	-	J.Ortiz
pXY-*CMD1*	*ori*	AMP^R	*2µ*	*LEU2*	*CMD1*	M.I.Geli
pXY-*CMD1-W*	*ori*	AMP^R	*2µ*	*TRP1*	*CMD1*	M.I.Geli
pQE11	*T1*	AMP^R	-		-	Quiagen
pQE11-*CMD1*	*T1*	AMP^R	-		*CMD1*	(M I Geli et al., 1998)
pQE11-*cmd1-226*	*T1*	AMP^R	-		*cmd1-226*	This study
pQE11-*cmd1-228*	*T1*	AMP^R	-		*cmd1-228*	This study
pQE11-*cmd1-231*	*T1*	AMP^R	-		*cmd1-231*	This study
pQE11-*cmd1-239*	*T1*	AMP^R	-		*cmd1-239*	This study
pQE11-*cmd1-242*	*T1*	AMP^R	-		*cmd1-242*	This study

p111-*CLC1*

p111-*CLC1* was constructed by amplifying the *CLC1* gene by PCR using the primers Clc1.EcoRI.-500d and Clc1.BamHI.200u and genomic DNA from a WT strain as template. The fragment was digested with EcoRI and BamHI ligated into the EcoRI/BamHI digested YCplac111.

P181-*CLC1*

p111-*CLC1* was digested with EcoRI and BamHI and ligated into EcoRI/BamHI digested YEplac181 to create P181-*CLC1.*

p111-*clc1-cbsΔ-HA*

p111-*clc-cbsΔ-HA* C-terminal HA truncation was cretated by inserting a DNA fragment coding for 3-HA downstream of the amino acid 212 codon of *CLC1* by homologous recombination in yeast. The HA-fragment was amplified by PCR with primers Clc1.604d.F2and Clc1.637u.R1 and pFA6a-3HA-His3MX6 as template. The amplified fragment was then co-transformed in yeast with p111-*CLC1* and transformants were selected on SDC-Leu-His. Plasmids were recovered and successful recombination tested by restriction analysis.

p50-*chc1-cbsΔ*

The overlap extension PCR technique was used to create construct p50-*chc1 cbsΔ*. In the first step, two PCR fragments (A and B) containing the cbsΔ deletion (amino acids 1491-1539) were obtained using YCp50-*CHC1* as template and the primers Chc1.3819d and Chc1.4453u (to obtain the fragment A) and Chc1**.**4618d and Chc1.term.5061u (to obtain the fragment B). The two DNA products were then used as template in a second round of PCR with the flanking primers Chc1.3819d and Chc1.term.5061u to generate the mutated *chc1-cbsΔ* fragment. The obtained DNA fragment was co-transformed in yeast with the SacI/BmgBI digested YCp50-*CHC1* plasmid to substitute the corresponding WT *CHC1* DNA fragment by the amplified mutant DNA fragment by homologous recombination. Transformants selected on SDC-Ura. Plasmids were recovered and successful substitution of the fragment was tested by restriction analysis. The mutation was confirmed by sequencing.

p195-*chc-cbsΔ*

The DNA fragment containing the ORF of *chc1-cbsΔ* was amplified by PCR using p50-*chc1-cbsΔ* as template and primers Chc1-600.SalId and yHC.200.XmaIu . This fragment was digested with SalI and XmaI. p50-*chc1-cbsΔ* was digested with SalI and XmaI and the SalI/Xm*aI* digested PCR fragment was ligated into it.

p50-*CHC1-HA*, p50-*chc1-cbsΔ-HA* , p195-*chc1-cbsΔ-HA* and p111-*CLC1-HA*

A DNA fragment coding for 3-HA was inserted downstream of *CHC1*, *chc1-cbsΔ* and *CLC1* by homologous recombination in yeast. The HA-fragment was amplified by PCR with either primers Chc1.d.F2 and Chc1.u.R1 (p50-*CHC1-HA*, p50-*chc1-cbsΔ-HA* and p195-*chc1-cbsΔ-HA*) or Clc1.d.F2 and Clc1.u.R1. (p111-*CLC1-HA*) and pFA6a-3HA-Trp1 (p50-*CHC1-HA*, p50-*chc1-cbsΔ-HA* and p195-*chc1-cbsΔ-HA*) or pFA6a-3HA-His3MX6 (p111-*CLC1-HA*) as template. The amplified fragment was then co-transformed in yeast with either p50-*CHC1*, p50-*chc1-cbsΔ,* p195-*chc1-cbsΔ* or p111-*CLC1-HA* and transformants were selected on SDC-Ura-Trp or SDC-Leu-His. Plasmids were recovered and successful recombination tested by restriction analysis.

p181-*CLC1-HA*, p181-*clc1-cbsΔ-HA*, p22-*CLC1-HA* and p112-*CLC1-HA*

p111-*CLC1-HA* or p111-*clc1-cbsΔ-HA* were digested with EcoRI and ligated into EcoRI digested and desphosphorilated YEplac181, YCplac22 and YEplac112 to create p181-*CLC1-HA,* p181-*clc1-cbsΔ-HA*, p22-*CLC1-HA* and p112-*CLC1-HA,* respectively.

p195-*chc1-cbsΔ-GFP*

A DNA fragment coding for GFP was inserted downstream of *CHC1* by recombination in yeast. The GFP-fragment was amplified by PCR with primers Chc1.d.F2 and Chc1.u.R1, and pFA6a-GFP(S65T)-Trp1 as template. The amplified fragment was then co-transformed in yeast with p195-*chc1-cbsΔ* and transformants were selected on SDC-Ura-Trp. Plasmid was recovered and successful recombination was tested by restriction analysis.

pGFP-*CLC1-U*

pGFP-*CLC1-U* was constructed by substituting the *TRP1* marker of the *CLC1* plasmid by *URA3,* by using homologous recombination in yeast. The *URA3* gene was amplified by PCR using the YDp-U plasmid as a template and primers Trp1D.d and Trp1D.u. The amplified fragment was then co-transformed in yeast with the pGFP-*CLC1* plasmid and transformants were selected on SDC-Ura. Plasmids were recovered and successful substitution of the marker was tested by restriction analysis.

pGFP-*clc1-cbsΔ*

A C-terminal truncation was created from pGFP-*CLC1-U* by inserting a DNA fragment coding for a STOP codon downstream the amino acid 212 codon of *CLC1* by homologous recombination in yeast. The DNA fragment was amplified by PCR with primers Clc1.637u.R1 and Clc1.d.F3 and pFA6a-3HA-Trp1 as template. The amplified fragment was then co-transformed in yeast with pGFP-*CLC1-U* and transformants were selected on SDC-Ura-Trp. Plasmids were recovered and successful recombination tested by restriction analysis.

p95-GFP-*clc1-cbsΔ*

A DNA fragment containing the ORF of GFP-*clc1-cbsΔ* was amplified by PCR using pGFP-*clc1-cbsΔ* as template and primers Clc1.EcoRI.-500D and BamHI.200U. This fragment was digested with EcoRI. YEplac195 was digested with EcoRI and subsequently desphosphorilated. The digested PCR fragment was ligated into it.

pGST-*CHC1-D*, pGST-*chc1-C-cbsΔ* and pGST-*clc1-cbsΔ*

pGST-*CHC1-D* was created by amplifying a DNA fragment containing the distal domain of *CHC1* (aa 550-1062) by PCR using p50-*CHC1* as template and primers Chc1.BamHI.1501d and Chc1.3183.Stop.EcoRIu. This fragment was digested with BamHI and EcoRI and ligated into the BamHI/EcoRI digested pGEX-2T.

pGST-*chc1-C-cbsΔ* was created by amplifying the C-terminal domain (aa 1062-1653) of *chc1-cbsΔ* by PCR using the primers Chc1.del.XmaI.3183d and Chc1.del.Stop.XhoIu and p50-*chc1-cbsΔ* as template. This fragment was digested with XmaI and XhoI and ligated into the XmaI/XhoI digested pGEX-5X-3**.**

pGST-*clc1-cbsΔ* was created by amplifying a DNA fragment containing the complete *clc1-cbsΔ* truncation by PCR using p111-*CLC1,* and primers Clc1.BamHI.3d and Clc1.633.Stop.EcoRIu. This fragment was digested with BamHI and EcoRI and ligated into the BamHI/EcoRI digested pGEX-2T.

pQE11-*cmd1-226,* pQE11-*cmd1-228,* pQE11-*cmd1-231,* pQE11-*cmd1-239 and* pQE11-*cmd1-242*

DNA fragments containing the complete *cmd1-226, cmd1-228, cmd1-231, cmd1-239* and *cmd1-242* mutant ORFs were amplified by PCR using pRB1646, pRB1648, pRB1651, pRB1659 and pRB1662 as templates, respectively and primers Cmd1.BamHI.3d and Cmd1.PstI.STOP.u. These fragments were digested with BamHI and PstI and ligated into the BamHI/PstI digested pQE11.

6.3.4 Primers

Primers used in this study are listed in Table III.

Table III. Primers

The sequences of the primers are written from the 5' to the 3' end. Primers amplifying the coding strand are named 5' primers, primers amplifying the complementary strand are 3' primers. Restriction sites are underlined.

Name	Sequence	Restriction site	Direction
Chc1.d.F2	GCTGATGAACAGCGCGATGAACGT TCAACC CACAGG ATTTCGGATCCCCGGGT AATTAA		5'
Chc1.u.R1	ACACGATGGGGTACAGCAAACGAATTATTT TATCCA CGTCGAATTCGAGCTCGT TTAAAC		3'
Clc1.d.F2	TCT TTTGAGATTGAAAGGTAACGCGA GGC TCC CGGTGCTCGGATCCCCGGGTTAATTAA		5'
Clc1.u.R1	TCTTCC TTAGTTCATTATGGT TCT TATTAT TCATCATCA TGAATTCGAGCTCGT TTAAAC		3'
Gga2.d.F2	CCAAGCTGAAGAAACTGCTGTTTTTACGTTA CCTAATGTA**C**GGATCCCCGGGTTAATTAA		5'
Gga2.u.RI	ACATAGAGAAGAGAAAGGATTGATAAGAAA CGCCAGAGG**AGAATTCGAGCTCGTTTAAAC**		
Apl2.d.F2	GGGCGGCAATATAGTGTCACAGGATCTCCTC GATTTATTCCGGATCCCCGGGTTAATTAA		3'
Apl2.u.R1	ATGGTATAATACTTAAGTTCACTACAACGGA CGTTTATAGGAATTCGAGCTCGTTTAAAC		5'
Kex2.d.F2	AGAATTACAGCCTGATGTTCCTCCATCTTCCG GACGATCGCGGATCCCCGGGTTAATTAA		3'
Kex22.u.R1	AATGCTATTTTGTAATTTGAAGCTTTCTGTAC ATATCGAAGAATTCGAGCTCGTTTAAAC		5'

Snf7.d.F2	ATGAAAAAGCATTAAGAGAACTACAAGCAG AAATGGGGCTTCGGATCCCCGGGTTAATTAA		3’
Snf7.u.R1	ACCTTTTTTTTTTCTTTCATCTAAACCGCATAG AACACGTGAATTCGAGCTCGTTTAAAC		5’
Gga2.1527.d	CTCC AACTTAGTGT TCTTATTAGC AGTCCCTAAG TC		5’
Gga2.1991.u	CGGAACACTTCCTCCATTTCAACTTTCCTTTT GG		3’
Apl2.1889.d	CT AGCAAGGCTA ACGATGATGT GCTATTGGAT TTTG		5’
Apl2.2439.u	CGTGCCTCCTGTTTTATCAAACAGATGAG		3’
Kex2.2161.d	GACTCTGAGT ACGATTCTAC TTTGGACAAT GG		5’
Kex2.2663.u	TATTCAGCTGTGGTCTTAAATATGCATTAATT GGACCC		3’
Snf7.458.d	CTG GGGCAAACGA GGTGGATGAA GATGAGCTGG		5’
Snf7.995.u	CGTTATTTGGGTTTTAGTCAATTAAAAGC		3’
Clc1.EcoRI.-500D	AGGGAATTCTGACACTGGAAAATCAGTACCA	EcoRI	5’
Clc1.BamHI.200U	AGGGGATCCATGTGATGTGTTTTTTAGAAGA GAAG	BamHI	3’
Chc1.3819.d	GC TGGCTCAAAT TTGTGGGTTGAAC		5’
Chc1.4453.u	GTCATAAGAATCAACAGCGTCTTGCAAAGC		3’
Chc1.4618.d	GCTTTGCA AGACGCTGTT GATTCTTATG AC TGG AAGGACGCTA TTGAGACGGC		5’
Chc1.term.5061.u	CCCCTCAGATAATCAAAGATGC		5’
Clc1.604d.F2	AACCAAG ATGATGCCGA TATCATTGGG GGT CG GAT CCC CGG GTT AAT TAA		5’
Clc1.637u.R1	CAAAAGAATTTCTTTAAGCTTAGACCTGTC GA ATT CGA GCT CGT TTA AAC		3’
Clc1.d.F3	AACCAAG ATGATGCCGA TATCATTGGG GGT TGA GGC GCG CCA CTT CTA AA		3’
Trp1D.d	GTATACGTGATTAAGCACACAAAGGCAGCT TGGAGTGAATTCCCGGGGATCCGGTGATG		5’
Trp1D.u	GTTAGTGGCCTAGGCAGCTGGACGTTCCA ATAATGACTCATCATAAATAAATTCATAAC AAACA		3’
Chc1.BamHI.1501d	AACCAACCGGATCCCAGTTTGAAA AAATTATTCC TTACTGCC	BamHI	5’
Chc1.3183.Stop.EcoRIu	AACCAACCGAATTCCTAAATTTCATCGGCG TCGTAGTTATCTAA	EcoRI	3’
Chc1.del.XmaI.3183d	AACCAACCCCCGGGGGGCTCCAT TATGTATTGA ACATGATTTG	XmaI	5’

Chc1.del.Stop.XhoIu	AACCAACCCTCGAGTTAAAATCCTGTGGGTTGAACG	XhoI	3’
Clc1.BamHI.3d	AACCAACCGGATCCTCAGAGAAATTCCCTCCTTTGGAAG	BamHI	5’
Clc1.633.Stop.EcoRIu	AACCAACCGAATTCCTAACCCCCAATGATATCGGCATCAT	EcoRI	3’
Cmd1.BamHI.3d	AACCAACCGGATCCTTTCCTCCAATCTTACCGAAGAAC	BamHI	3’
Cmd1.PstI.STOP.u	AACCAACCCTGCAGCTATTTAGATAACAAAGCAGCG	PstI	5’

6.4. Biochemistry techniques

6.4.1. SDS-PAGE, immunoblots, and antibodies

SDS-PAGE was performed as described (Laemmli, 1970) using a Minigel system (Bio-Rad Laboratories). High and low range SDS-PAGE molecular weight standards (Bio-Rad Laboratories) were used for determination of apparent molecular weights. Coomassie Brilliant Blue or Colloidal Brilliant Blue G staining (Sigma) was used for detection of total protein on acrylamide gels. Protein concentration was determined with a Bio-Rad Protein assay (Bio-Rad).

Immunoblots were performed as described (M I Geli et al., 1998). Nitrocellulose membranes (Schleicher and Schuell) were stained with Ponceau Red for detection of total protein. 3% not fat lyophilized milk with 0.1% (v/v) Nonidet P-40 in PBS buffer (137 mMNaCl, 2.7 mMKCl, 10 mM Na_2HPO_4, 2 mM KH_2PO_4) was used as blocking solution. For detection of peroxidase-conjugated antibodies, an enhanced chemoluminiscence (ECL) detection kit (Amersham Biosciences) or a Super Signal West Femto Chemiluminiscent Substrate (Thermo Fisher Scientific) was used.

The primary and secondary antibodies used for detection of proteins are listed in Table IV.

Table IV. Antibodies

Antigen	Source	Dilution	Reference
HA	Mouse monoclonal antibody (clone HA-7), peroxidase-conjugated	1:1000	Sigma
Cmd1	Rabbit serum	1:1000	(M I Geli et al., 1998)
Chc1	Mouse serum	1:150	(Lemmon *et al*.,1988)
GST	Goat polyclonal antibody	1:2000	Amersham
GFP	Mouse polyclonal antibody	1:5000	Roche
Rabbit IgG	Goat antibody, peroxidase-conjugated	1:8000	Sigma
Mouse IgG	Goat antibody, peroxidase-conjugated	1:4000	Sigma
Goat IgG	Rabbit antibody, peroxidase-conjugated	1:10000	Sigma

6.4.2. Protein extraction from yeast

Quick yeast protein extract

Approximately 2-4 x 10^8 cells were harvested at 1,900g (at a culture density of 1-2 x 10^7 cells/ml), transferred to a 1.5 ml Eppendorf tube, and washed twice with 1 ml of IP buffer (50 mM Tris pH 7.5, 150 mM NaCl, 5 mM EDTA). Harvested cells were frozen at -20ºC. After thawing, the pellet was suspended in 100 µl of ice-cold IP buffer containing protease inhibitors (0.5 mM PMSF, 1 µg/ml aprotinin, 1 µg/ml antipain, 1 µg/ml leupeptin, 1µg/ml pepstatin) and glass beads lysed for 15 min at 4ºC. The lysate was resuspended in 100 µl of IP2T buffer (IP buffer + 2% Triton) with protease inhibitors, and transferred to another tube. Unbroken cells and debris were eliminated by centrifugation at 700 g for 10 min at 4ºC. Total protein concentration was determined before boiling the cells extracts in Laemmli sample buffer (final concentration 1% SDS, 100 mM DTT, 10% glycerol, 60 mM Tris-HCl pH 6.8, Bromophenol blue) to be analyzed by SDS-PAGE in gels with the desired acrilamyde (Sigma) concentration or in NuPAGE Bis-Tris 4-12 % gradient gel (Biorad).

6.4.3. Protein purification

6.4.3.1. Purification of recombinant GST-fusion proteins from *E. coli* by affinity chromatography

Recombinant glutathione-S-transferase-tagged proteins (GST-fusion proteins) were purified from BL21 *E.coli* cells according to (Geli *et al.*, 2000). Briefly, 1/100 of an overnight *E.coli* culture was inoculated into minimal media (see section 6.1.1) containing 50 mg/l ampicillin. The culture was grown at 37°C to an OD_{600} of 0.4. Cells were shifted to 24°C and induced at an OD_{600} of 0.7-0.8 with 0.1 mM isopropyl-β-D-thiogalactopyranoside (IPTG) for 2 hrs. Cells were harvested and frozen at –20°C.

For protein purification, cells were thawed in PBST buffer (137 mM NaCl, 2.7 mM KCl, 10 mM Na_2HPO_4, 2 mM KH_2PO_4, 0.5% Tween-20; 30 ml buffer for each liter of bacteria culture) and lysed by sonication (10 pulses of x 30 seconds at 30 second intervals and amplitude of 40%) in the presence of protease inhibitors (1 tablet complete Protease Inhibitor Cocktail Tablets (Roche)/50 ml of buffer). Cell debris were pelleted by centrifugation at 12,000 rpm.

For pull down assays, 20µl of glutathione-Sepharose beads (Amersham Biosciences) equilibrated in PBST buffer were added to the protein extracts obtained from a culture of 100 ml of *E.coli* transformed with pGST, pGST-*CHC1-D*, pGST-*CHC1-N*, pGST-*CLC1* or pGST-*clc1-cbsΔ* or a culture of 250 ml of cells transformed with pGST-*CHC1-C* or pGST-*chc1-cbsΔ* and incubated for 1 h shaking at 4°C. Beads were recovered by using Econo Columns (Bio-Rad Laboratories), washed 3 times with 10 ml of PBST, 2 times with 10 ml of PBS, and equilibrated and adjusted to 50% in IM-B buffer (10 mM Imidazol pH 7.5, 5 mM $CaCl_2$ or 5 mM EDTA, 1% BSA), which was used for the pull down of purified components.

6.4.3.2. Purification of recombinant 6xHis-fusion proteins from *E.coli* by affinity chromatography

Recombinant 6xHis-tagged Cmd1 constructs were purified from BL21 *E.coli* cells as described in 6.4.3.1, using then a Ni-NTA superflow resin (Qiagen) following the protocol for batch purification of 6xHis-tagged proteins from *E. coli* under denaturing conditions specified by the company. Briefly, cells were thawed and

resuspended in buffer B (100mM NaH_2PO_4; 10mM TrisCl; 8M Urea; pH 8.0; 5 ml buffer per gram wet weigh) and lysed by steering the cells at room temperature for 1 hour in the presence of protease inhibitors (1 tablet Complete Protease Inhibitor Cocktail Tablets (Roche)/50 ml of buffer). Cell debris was pelleted by centrifugation at 12,000 rpm. Then, 1 ml of the 50% Ni-NTA slurry was added to the lysate and was mixed by shaking at room temperature for 1 hour. The resin was washed twice with buffer C (100mM NaH_2PO_4; 10mM TrisCl; 8M Urea; pH 6.3) and the recombinant Cmd1 proteins were eluted 4 times with buffer D (100mM NaH_2PO_4; 10mM TrisCl; 8M Urea; pH 5.9)and 4 times with buffer E (100mM NaH_2PO_4; 10mM TrisCl; 8M Urea; pH 4.5). The different fractions were analysed by SDS-PAGE.

Purified tagged proteins were used for pull down assays (see section 6.4.4.1.)

6.4.4. Analysis of protein-protein interactions

6.4.4.1. Pull down assays

For the pull down assay with purified components, 20 µl of GST-Chc1-C, GST-Chc1-C-cbsΔ, GST-Chc1-D, GST-Chc1-N, GST-Clc1, GST-Clc1-cbsΔ, or the equivalent amount of GST-coated glutathione-Sepharose beads (containing approximately 50ng of proteins/µl beads) diluted to 50% in IM-B buffer (10 mM Imidazol pH 7.5, 5 mM $CaCl_2$ or 5 mM EDTA, 1% BSA) (see section 6.4.3.1) was incubated with 1 µg/µl of eluted 6xHis-Cmd1 (see section 6.4.3.2) in a total volume of 1 ml of IM-B buffer (10 mM Imidazol pH 7.5, 5 mM $CaCl_2$ or 5 mM EDTA, 1% BSA) containing protease inhibitors (0.5 mM PMSF, 1 µg/ml aprotinin, 1 µg/ml antipain, 1 µg/ml leupeptin, 1µg/ml pepstatin) in siliconized 1.5 ml Eppendorf tubes for 1h at 4ºC. Beads were collected, washed with IM-B and IM (10 mM Imidazol pH 7.5, 5 mM $CaCl_2$ or 5 mM EDTA) and finally eluted in 40 µl of Laemmli sample buffer(1% SDS, 100 mM DTT, 10% glycerol, 60 mM Tris-HCl pH 6.8, Bromophenol blue).

Quantifications of the band intensity of the 6xHis-tagged proteins pulled down by the GST-fused proteins were performed with ImageJ. The average band intensity of the 6xHis tagged protein was normalized with respect to the band intensity of the corresponding GST-fused protein. The band intensity of the 6xHis tagged protein pulled down by the GST control was subtracted from the result. Final results were normalized to the maximum value. At least 3 independent

experiments were performed per each sample. Average percentage, standard error of the mean (SEM) and p-values for the two-tailed Student's t-test were calculated with Microsoft Excel.

6.4.4.2. Immunoprecipitation of proteins from yeast extracts

For inmunoprecipitations of HA-tagged proteins from yeast, agarose conjugated to a mouse anti-HA antibody (Sigma) was used. Approximately 4 x 10^9 yeast cells expressing HA-tagged protein of interest and grown at the desired temperature were harvested at 1,900 g at a culture density of 1.5 x 10^7 cells/ml, washed twice with IP buffer (50 mM Tris pH 7.5, 150 mM NaCl, 5 mM EDTA), and frozen at -20ºC. After thawing, cells were resuspended in 300 µl of ice-cold IM buffer (10 mM Imidazol pH 7.5) containing protease inhibitors (0.5 mM PMSF, 1 µg/ml aprotinin, 1 µg/ml antipain, 1 µg/ml leupeptin, 1 µg/ml pepstatin) and glass bead-lysed (10 x 1 min) on ice. Triton-X100 was adjusted to 1% and the extract was then centrifuged twice at 700 g to eliminate unbroken cells and cell debris. After measuring and adjusting the protein concentration, the total protein extract was resuspended in 1 ml of IM-T (IM buffer containing protease inhibitors, 1% Triton-X100) containing either $ClCa^{2+}$ 5mM or EDTA 5mM, transferred into a siliconized tube, and incubated with 20µl of 50% anti-HA agarose equilibrated in IM buffer, for 1h in a turning wheel at 4ºC. The agarose beads were collected on Mobicol columns bearing 35 µm pore filters (MoBiTec), washed 5 times with IM-T, and 5 times with IM buffer. Proteins were then eluted from the anti-HA agarose by adding 20 µl of Laemmli sample buffer (1% SDS, 100 mM DTT, 10% glycerol, 60 mMTris-HCl pH 6.8, Bromophenol blue). Elutions were stored at -20ºC until analysis by SDS-PAGE and immunoblot.

For co-immunoprecipitations experiments of Cmd1, the same procedure as the one explained above was followed, except for the fact that the total protein extract was incubated with a polyclonal serum against Cmd1 or preimmune serum, previously bound to protein A sepharose (Amersham Biosciencies) (10 µl of an antibody against Cmd1 (α-Cmd1) for 20 µl sepharose beads).

Quantifications of the band intensity of the proteins co-inmunoprecipitated with the HA-tagged proteins or with Cmd1, were performed with ImageJ. The average band intensity of the co-inmunoprecipitated protein of interest was normalized

with respect to the band intensity of the corresponding inmunoprecipitated HA-tagged protein or Cmd1. The band intensity of the protein inmunoprecipitated by the pre-inmune serum bound to sepharose control was subtracted from the result. Final results were normalized to the corresponding input band size and then to the maximum value or a WT strain. Average percentage, standard error of the mean (SEM) and p-values for the two-tailed Student's t-test were calculated with Microsoft Excel.

6.4.5. Analysis of native protein conformation by native PAGE gels

150 ml of a yeast culture in logarithmic phase grown at a density of 1,5 x 10^7 cells/ml (OD_{600} 0.6) at the desired temperature, from the indicated strains expressing HA-tagged proteins, were harvested by centrifugation at 1,900 g for 5 min at 4 ºC , washed once with 5 ml of lysis buffer LB (25mM Tris, pH 8.5, 5 mM EDTA), and frozen at -80ºC. After thawing, cells were resuspended in 50µl of ice-cold LB containing protease inhibitors (0.5 mM PMSF, 1 µg/ml aprotinin, 1 µg/ml antipain, 1 µg/ml leupeptin, 1 µg/ml pepstatin) and glass bead-lysed (10 x 1 min) on ice. The lysate was resuspended in 200 µl of LB bearing protease inhibitors and transferred to another tube. The sample was then cleared by centrifugation at 700 g for 10 min at 4ºC and the pellet was washed with the same volume of breakage buffer BB (10 mM Tris, pH 7.5, 0.2 mM EDTA, 0.2 mM DTT) containing protease inhibitors and spinned again at 700 g for 10 min at 4ºC. The same volume of the LB (first supernatant) and BB (second supernatant) were mixed and spinned again for 10 min at 700 g at 4C. The supernatant was then transferred to a new tube, clarified twice at 13,000 g for 30 min at 4C, transferred to an 1.5 ml ultracentrifuge tube (Beckman) for the TLA55 rotor of the table top ultracentrifuge Beckman Coulter Optima MAX-XP and clarified twice at 100,000 g for 1 hour. The supernatant was then recovered, the volume was measured and Novex native PAGE Sample Buffer x 4 (Invitrogen) was added to a final x1 concentration. Elutions were stored at -20ºC until analysis by Native PAGE Novex 3-12% gels (Invitrogen) and immunoblot. 10 to 40 µg of proteins were loaded per lane. A sample was loaded separated from the rest, and denatured in conventional SDS-PAGE sample buffer to have the reference where the monomer of the protein of interest runned.

Running and transfer were performed as described by the manufacturer. Briefly, samples were run at 150 V for 30 min using the dark blue cathode buffer (for 200 ml:

10 ml of native PAGE Running buffer x 20, 10 ml of native PAGE cathode additive x 20, deionized water to 200 ml), exchange for the light blue cathode buffer (for 200 ml: 10 ml of native PAGE Running buffer x 20, 1 ml of native PAGE cathode additive x 20, deionized water to 200 ml) and run for extra 60 min at 150 V. Transfer was done to PVDF membranes (Millipore Immobilon) after activating the membrane for 30 seconds in methano,l for 14 hours at 4ºC at 0.6 A using the NuPAGE transfer buffer. Immunoblots were done as usual.

6.5. *In vivo* protein transport assays

6.5.1. Halo assay

A defect in bioactive α-factor production was tested using a plate assay. The assay is based on the observation that *MAT***a** cells bearing double mutations in the *BAR1*/*SST1* and the *SST2* genes cannot recover from the cell cycle arrest induced by the α-factor pheromone (Chan & Otte, 1982).

A lawn of a yeast strain hyper-sensitive to α-factor (*MAT***a** *ssa1 ssa2,* strain RH123) was plated on YPD. To identify yeast defective in bioactive α-factor production, the *Mat***α** strains to be tested from mid-log phase cultures were diluted to 10^7cells/ml in the adequate fresh media and spotted in the YPD plate bearing a lawn of the hyper-sensitive yeast strain. After the liquid was evaporated, plates were incubated for two days at 30ºC. WT yeast cells secreted a bioactive α-factor, which arrested growth of the lawn of mutant *MAT***a** cells, producing a halo around the yeast spot. Strains that secrete an inactive precursor form of α-factor will not be competent to arrest the growth ant thus, will not form a halo.

The halo size for each sample was measured using ImageJ. The average halo size generated by each sample was normalized with respect to the halo size generated by a WT strain. At least 3 independent experiments were performed per each sample. Average percentage, standard error of the mean (SEM) and p-values for the two-tailed Student's t-test were calculated with Microsoft Excel.

6.5.2. Lucifer Yellow uptake assay

Fluid-phase endocytosis was observed microscopically after treating cells with Lucifer yellow CH (LY, Sigma). LY uptake assay was performed as described by (a L. Munn & Riezman, 1994). Briefly, 1 ml of cells grown to early log phase

(approximately $1x10^7$ cells) in the adequate fresh medium was collected by centrifugation and resuspended in 90 µl of fresh medium containing 5 µl of 80 mg/ml LY. Cells were incubated at the desirable temperature for 1 hour with shaking and then washed three times with ice cold washing buffer (50mM sodium phosphate buffer, pH 7.5, containing 10 mM NaN_3 and 10 mM NaF).

Cells were visualized by microscopy in the washing buffer at room temperature (RT), on poly-lysine coated slides using an AF7000 fluorescence microscope (Leica) equipped with a CFP/YFP filter (excitation 436/12, 500/20; BP 467/37,545/45) and a 63x 1.3NA Oil DIC Plan-Apochromat objective. Images were taken with a Hammamatsu Orca CCD digital camera. All images were collected with identical sensitivity and exposure times of 462ms. LasAF files were converted to multi-tiff for imaging processing. The percentage of cells that internalized LY and delivered it to the vacuole were quantified with ImageJ. At least 3 independent experiments were performed per each sample. Average percentage, standard error of the mean (SEM) and p-values for the two-tailed Student's t-test were calculated with Microsoft Excel.

6.5.3. FM4-64 or FM2-10 staining

FM4-64 or FM2-10 labelling to examine endocytic and vacuolar membranes was performed as previously described (Vida & Emr, 1995). Briefly, 1 ml of cells expressing the desired GFP- or mCherry-tagged protein grown to early log phase (approximately $1x10^7$ cells) in the adequate fresh medium at the desired temperature was collected by centrifugation and resuspended in 90 µl YPD or YPD containing 10 mM NaF and 10 mM NaN_3 and incubated for 5 minutes at RT. Cells were then centrifugated and resuspended in 25µl YPD, with or without 10 mM NaF and 10 mM NaN_3, and containing 16 µM FM4-64 (Molecular Probes) or FM2-10 (Biotium). Cells were incubated at the desired temperature for 45 minutes with shaking and then washed three times with ice cold washing buffer (50mM sodium phosphate buffer, pH 7.5, containing 10 mM NaN_3 and 10 mM NaF). Cells were visualized by microscopy in the washing buffer at RT, on poly-lysine coated slides using an AF7000 fluorescence microscope (Leica) equipped with a G/R filter (excitation 470/40, 572/35; BP521/40, BP632/62) and a 63x 1.3NA Oil DIC Plan-Apochromat objective. Images for FM4-64 and FM2-10 were taken with a Hammamatsu Orca CCD digital camera. All images were collected with identical

sensitivity and exposure times 563 ms, 488 ms, for FM4-64 and FM2-10 respectively. LasAF files were converted to multi-tiff for imaging processing.

6.6. Live cell fluorescence imaging of yeast cells

6.6.1. Analysis of co-localization

Cells encoding GFP- and mCherry-tagged proteins were grown to a cell density of 0.75 x 10^7 cells/ml in the appropriate SDC media at the desired temperature. The SDC media used for imaging was filtered or autoclaved at 116ºC to avoid quenching. Cells were harvested, diluted in 25-50 µl SCD and subsequently immobilized in 0.8% low-melt agarose (Bio-Rad) prepared in SDC-M medium (SDC media, 20 mM $KiPO_4$, pH 6.5). Cells were observed at the desired temperature using an AF7000 fluorescence microscope (Leica) equipped with a G/R filter (excitation 470/40, 572/35; BP521/40, BP632/62) and a 63x 1.4NA Oil DIC Plan-Apochromat objective. Images were taken with a Hammamatsu Orca CCD digital camera. All images were collected with identical sensitivity and exposure times of 774 ms (Chc1-GFP, GFP-Clc1 and GFP-Clc1-cbsΔ), 200 ms (Chc1-cbsΔ-GFP) and 970 ms (mCherry-tagged proteins). LasAF files were converted to multi-tiff for imaging processing. Fluorescence images for GFP and mCherry were merged using ImageJ.

Co-localization of GFP- or mCherry-tagged proteins with FM4-64 or FM2-10 (see section 6.5.3) was observed at the desired temperature using an AF7000 fluorescence microscope (Leica) equipped with a G/R filter (excitation 470/40, 572/35; BP521/40, BP632/62) and a 63x 1.4NA Oil DIC Plan-Apochromat objective. Images were taken with a Hammamatsu Orca CCD digital camera. All images were collected with identical sensitivity and exposure times of 563 ms (FM4-64), 488 ms (FM2-10), 921 ms (Chc1-GFP, GFP-Clc1 and GFP-Clc1-cbsΔ), 200 ms (Chc1-cbsΔ-GFP) and 490 ms (mCherry-tagged proteins). LasAF files were converted to multi-tiff for imaging processing. Fluorescence images for FM4-64 or FM2-10 and GFP- or mCherry-tagged proteins were merged using ImageJ.

6.6.2. DAPI staining of the nucleus

DAPI staining for nucleus visualizing was performed as follows. Cells were grown to a cell density of 0.75 x 10^7 cells/ml in the appropriate SDC media. DAPI (Sigma) was added to the culture to a final concentration of 2.5 µg/ml. Cells were grown again

for 30 minutes and then harvested, diluted in 25-50 µl SCD and subsequently visualized by microscopy at RT, on poly-lysine coated slides using an AF7000 fluorescence microscope (Leica) equipped with an ATL filter (excitation 360/40; LP425) and a 63x 1.3NA Oil DIC Plan-Apochromat objective. Images were taken with a Hammamatsu Orca CCD digital camera. All images were collected with identical sensitivity and exposure times 678 ms. GFP-tagged proteins for analysis or co-localization with DAPI were observed with a G/R filter (excitation 470/40, 572/35; BP521/40, BP632/62) and all images were collected with identical sensitivity and exposure times of 774 ms (Chc1-GFP, GFP-Clc1 and GFP-Clc1-cbsΔ) and 200 ms (Chc1-cbsΔ-GFP). LasAF files were converted to multi-tiff for imaging processing. Fluorescence images for DAPI and GFP were merged using ImageJ.

7. BIBLIOGRAPHY

- Abe, K., & Puertollano, R. (2011). Role of TRP channels in the regulation of the endosomal pathway. *Physiology*, 26(1), 14–22.
- Aghamohammadzadeh, S., & Ayscough, K. R. (2009). Differential requirements for actin during yeast and mammalian endocytosis. *Nature cell biology*, 11(8), 1039–42.
- Aghamohammadzadeh, S., & Ayscough, K. R. (2010). The yeast actin cytoskeleton and its function in endocytosis. *Fungal biology reviews*, 24(1-2), 37–46.
- Aguilar, P. S., Fröhlich, F., Rehman, M., Shales, M., Olivera-couto, A., Braberg, H., Shamir, R., et al. (2011). A plasma-membrane E-MAP reveals links of the eisosome with sphingolipid metabolism and endosomal trafficking. *Nature structural & molecular biology*, 17(7), 901–908.
- Aguilar, Rubén C, Longhi, S. A., Shaw, J. D., Yeh, L.-Y., Kim, S., Schön, A., Freire, E., *et al*. (2006). Epsin N-terminal homology domains perform an essential function regulating Cdc42 through binding Cdc42 GTPase-activating proteins. *Proceedings of the National Academy of Sciences of the United States of America*, 103(11), 4116–21.
- Aguilar, Rubén Claudio, Watson, H. A., & Wendland, B. (2003). The yeast Epsin Ent1 is recruited to membranes through multiple independent interactions. *The Journal of biological chemistry*, 278(12), 10737–43.
- Anderson, R. G. W., Goldestein, J. L., & Brown, M. S. (1977). A mutation that impairs the ability of lipoprotein receptors to localise in coated pits on the cell surface of human fibroblasts. *Nature*, 270(5639), 695–699.
- Andersson, A., Forsin, S., Thulin, E., & Vogel, H. J. (1983). Cadmium- 1 13 Nuclear Magnetic Resonance Studies of Proteolytic Fragments of Calmodulin: Assignment of Strong and Weak Cation Binding Sites. *Biochemistry*, 22(10), 2309–2313.
- Antonescu, C. N., Aguet, F., Danuser, G., & Schmid, S. L. (2011). Phosphatidylinositol-(4,5)-bisphosphate regulates clathrin-coated pit initiation, stabilization, and size. *Molecular biology of the cell*, 22(14), 2588–600.
- Apodaca, G., Enrich, C., & Mostovs, K. E. (1994). The Calmodulin Antagonist , W-13 , Alters Transcytosis , Recycling , and the Morphology of the Endocytic Pathway in Madin-Darby canine kidney cells. *The Journal of biological chemistry*, 269(29), 19005–19013.
- Arighi, C. N., Hartnell, L. M., Aguilar, R. C., Haft, C. R., & Bonifacino, J. S. (2004). Role of the mammalian retromer in sorting of the cation-independent mannose 6-phosphate receptor. *The Journal of cell biology*, 165(1), 123–33.
- Asao, H., Sasaki, Y., Arita, T., Tanaka, N., Endo, K., Kasai, H., Takeshita, T., *et al.* (1997). Hrs Is Associated with STAM, a Signal-transducing Adaptor Molecule: ITS SUPPRESSIVE EFFECT ON CYTOKINE-INDUCED CELL GROWTH. *The Journal of biological chemistry*, 272(52), 32785–32791.
- Audhya, A., Foti, M., & Emr, S. D. (2000). Distinct Roles for the Yeast Phosphatidylinositol 4- Kinases , Stt4p and Pik1p , in Secretion , Cell Growth , and Organelle Membrane Dynamics. *Molecular biology of the cell*, 11(8), 2673–2689.

- Austin, C., Hinners, I., & Tooze, S. A. (2000). Direct and GTP-dependent interaction of ADP-ribosylation factor 1 with clathrin adaptor protein AP-1 on immature secretory granules. *The Journal of biological chemistry*, 275(29), 21862–9.
- Ayscough, K. R., Eby, J. J., Lila, T., Dewar, H., Kozminski, K. G., & Drubin, D. G. (1999). Sla1p is a functionally modular component of the yeast cortical actin cytoskeleton required for correct localization of both Rho1p-GTPase and Sla2p, a protein with talin homology. *Molecular biology of the cell*, 10(4), 1061–75.
- Babst, M., Katzmann, D. J., Estepa-Sabal, E. J., Meerloo, T., & Emr, S. D. (2002). Escrt-III: an endosome-associated heterooligomeric protein complex required for mvb sorting. *Developmental cell*, 3(2), 271–82.
- Babst, M., Katzmann, D. J., Snyder, W. B., Wendland, B., & Emr, S. D. (2002). Endosome-Associated Complex, ESCRT-II, Recruits Transport Machinery for Protein Sorting at the Multivesicular Body. *Developmental cell*, 3(8), 283–289.
- Babu, S., Sack, J. S., Greenhough, T., Bugg, C. E., Means, A. R., & Cook, W. J. (1985). Three-dimensional structure of calmodulin. *Nature*, 315(5), 37–40.
- Babu, Y. S., Bugg, C. E., & Cook, W. J. (1988). Structure of calmodulin refined at 2.2 A resolution. *Journal of molecular biology*, 204(1), 191–204.
- Bache, K. G., Stuffers, S., Malerød, L., Slagsvold, T., Raiborg, C., Lechardeur, D., Lukacs, G. L., *et al.* (2006). The ESCRT-III Subunit hVps24 Is Required for Degradation but Not Silencing of the Epidermal Growth Factor Receptor. *Molecular biology of the cell*, 17(6), 2513–2523.
- Bachs, O., Agell, N., & Carafoli, E. (1994). Calmodulin and calmodulin-binding proteins in the nucleus. *Cell calcium*, 16(4), 289–96.
- Baggett, J. J., & Wendland, B. (2001). Clathrin function in yeast endocytosis. *Traffic*, 2(5), 297–302.
- Balcer, H. I., Goodman, A. L., Rodal, A. A., Smith, E., Kugler, J., Heuser, J. E., & Goode, B. L. (2003). Coordinated Regulation of Actin Filament Turnover by a High-Molecular-Weight Srv2/CAP Complex, Cofilin, Profilin, and Aip1. *Current biology*, 13(24), 2159–2169.
- Balderhaar, H. J. K., Arlt, H., Ostrowicz, C., Bröcker, C., Sündermann, F., Brandt, R., Babst, M., *et al.* (2010). The Rab GTPase Ypt7 is linked to retromer-mediated receptor recycling and fusion at the yeast late endosome. *Journal of cell science*, 123(Pt 23), 4085–94.
- Balderhaar, H. J. K., & Ungermann, C. (2013). CORVET and HOPS tethering complexes - coordinators of endosome and lysosome fusion. *Journal of cell science*, 126(6), 1307–16.
- Bar-zvis, D., & Branton, D. (1986). Clathrin-coated Vesicles Contain Two Protein Kinase Activities. *The Journal of biological chemistry*, 261(21), 9614–9621.
- Barbato, G., Ikura, M., Kay, L. E., Pastor, R. W., & Ad, B. (1992). Backbone dynamics of calmodulin studied by 15 N relaxation using inverse detected two-dimensional NMR spectroscopy: The central helix is flexible. *Biochemistry*, 31(23), 5269–5278.

- Bardwell, L., Cook, J. G., Inouye, C. J., & Thorner, J. (1994). Signal propagation and regulation in the mating pheromone response pathway of the yeast Saccharomyces cerevisiae. *Developmental biology*, 166(2), 363–379.
- Barlowe, C., Or, L., Yeung, T., Salama, N., & Rexach, M. F. (1994). COPII : A Membrane Coat Formed by Set Proteins That Drive Vesicle Budding from the Endoplasmic Reticulum. *Cell*, 77(6), 895–907.
- Bazinet, C., Katzen, A. L., Mahowaldo, O. A. P., & Lemmont, S. K. (1993). The Drosophila Clathrin heavy chain gene: Clathrin function is essential in multicellular organisms. *Genetics*, 134(4), 1521–1525.
- Ben-Aroya, S., Pan, X., Boeke, J. D., & Hieter, P. (2010). Making temperature-sensitive mutants. *Methods in enziymology*, 6879(10), 181–204.
- Benedetti, H., Raths, S., Crausaz, F., & Riezman, H. (1994). The END3 Gene Encodes a Protein that Is Required for the Internalization Step of Endocytosis and for Actin Cytoskeleton Organization in Yeast. *Molecular biology of the cell*, 5(9), 1023–1037.
- Berben, G., Dumont, J., Gilliquet, V., Bolle, P., & Hilger, F. (1991). The YDp plasmids: a uniform set of vectors bearing versatile gene disruption cassettes for Saccharomyces cerevisiae. *Yeast*, 7(5), 475–7.
- Berchtold, M.W., Egli, R., Rhyner, J. A., Hameister, H., & Strehler, E. E. (1993). Localization of the human bona fide calmodulin genes CALM1, CALM2, and CALM3 to chromosomes 14q.24.q3, 2p21.1, and 19q13.2-q33. *Genomics*, 16(2), 461–465.
- Berchtold, Martin W, & Villalobo, A. (2014). The many faces of calmodulin in cell proliferation, programmed cell death, autophagy, and cancer. *Biochimica et biophysica acta*, 1843(2), 398–435.
- Bilodeau, P. S., Winistorfer, S. C., Kearney, W. R., Robertson, A. D., & Piper, R. C. (2003). Vps27-Hse1 and ESCRT-I complexes cooperate to increase efficiency of sorting ubiquitinated proteins at the endosome. *The Journal of cell biology*, 163(2), 237–43.
- Bishop, N. E. (2003). Dynamics of endosomal sorting. *International review of cytology*, 232, 1–57.
- Black, D. J., & Persechini, A. (2011). In Calmodulin−IQ Domain Complexes, the Ca2+-Free and Ca2+-Bound. *Biochemistry*, 50(46), 10061–10068.
- Black, M. W., & Pelham, H. R. (2000). A selective transport route from Golgi to late endosomes that requires the yeast GGA proteins. *The Journal of cell biology*, 151(3), 587–600.
- Blank, G. S., & Brodsky, F. M. (1986). Site-specific disruption of clathrin assembly produces novel structures. *The EMBO journal*, 5(9), 2087–95.
- Bobola, N., Jansen, R., Shin, T. H., & Nasmyth, K. (1996). Asymmetric Accumulation of Ash1p in Postanaphase Nuclei Depends on a Myosin and Restricts Yeast Mating-Type Switching to Mother Cells. *Cell*, 84(5), 699–709.
- Boettner, D. R., Chi, R. J., & Lemmon, S. K. (2011). Lessons from yeast for clathrin-mediated endocytosis. *Nature cell biology*, 14(1), 2–10.

- Boettner, D. R., Friesen, H., Andrews, B., & Lemmon, S. K. (2011). Clathrin light chain directs endocytosis by influencing the binding of the yeast Hip1R homologue, Sla2, to F-actin. *Molecular biology of the cell*, 22(19), 3699–714.
- Boettner, D., Wendland, B., Lemmon, S. K., & Goode, B. L. (2009). The F-BAR domain protein Syp1 negatively regulates WASp-Arp2/3 complex activity during endocytic patch formation. *Current biology*, 19(23), 1979–1987.
- Boman, A L. (2001). GGA proteins: new players in the sorting game. *Journal of cell science*, 114(Pt 19), 3413–8.
- Boman, A. L, Salo, P. D., Hauglund, M. J., Strand, N. L., Rensink, S. J., & Zhdankina, O. (2002). ADP-Ribosylation Factor (ARF) Interaction Is Not Sufficient for Yeast GGA Protein Function or Localization. *Molecular biology of the cell*, 13(9), 3078–3095.
- Bonifacino, J. S., & Rojas, R. (2006). Retrograde transport from endosomes to the trans-Golgi network. *Nature reviews. Molecular cell biology*, 7(8), 568–79.
- Bonilla, M., & Cunningham, K. W. (2002). Calcium release and influx in yeast: TRPC and VGCC rule another kingdom. *Science's STKE : signal transduction knowledge environment*, 2002(127), pe17.
- Booth, D. G., Hood, F. E., Prior, I. A., & Royle, S. J. (2011). A TACC3/ch-TOG/clathrin complex stabilises kinetochore fibres by inter-microtubule bridging. *The EMBO journal*, 30(5), 906–19.
- Boucrot, E., Saffarian, S., Massol, R., Kirchhausen, T., & Ehrlich, M. (2009). Role of lipids and actin in the formation of clathrin-coated pits. *Experimental cell research*, 312(20), 4036–4048.
- Boulant, S., Kural, C., Zeeh, J.-C., Ubelmann, F., & Kirchhausen, T. (2011). Actin dynamics counteract membrane tension during clathrin- mediated endocytosis. *Nature cell biology*, 13(9), 1124–1131.
- Bowers, K., & Stevens, T. H. (2005). Protein transport from the late Golgi to the vacuole in the yeast Saccharomyces cerevisiae. *Biochimica et biophysica acta*, 1744(3), 438–54.
- Boyne, J. R., Yosuf, H. M., Bieganowski, P., Brenner, C., & Price, C. (2000). Yeast myosin light chain , Mlc1p , interacts with both IQGAP and Class II myosin to effect cytokinesis. *Journal of cell science*, 113(24), 4533–4543.
- Brandizzi, F., & Barlowe, C. (2013). Organization of the ER–Golgi interface for membrane traffic control. *Nature reviews. Molecular Cell biology*, 14(6), 382–392.
- Breuder, T., Hemenwayt, C. S., Mowa, N. R. A. O., Cardenas, M. E., & Ii, J. H. (1994). Calcineurin is essential in cyclosporin A- and FK506-sensitive yeast strains. *Proceedings of the National Academy of Sciences of the United States of America*, 91(6), 5372–5376.
- Brockerhoff, S. E., Stevens, R. C., & Davis, T. N. (1994). The unconventional myosin, Myo2p, is a calmodulin target at sites of cell growth in Saccharomyces cerevisiae. *The Journal of cell biology*, 124(3), 315–23.
- Brockerhoff, Susan E., & Davis, T. N. (1992). Calmodulin Concentrates at Regions of Cell Growth in Saccharomyces cerevisiae. *The Journal of cell biology*, 118(3), 619–629.

- Brodsky, F. M., Acton, S. L., Nathke, I., Chemistry, P., & Ponnambalam, S. (1991). Clathrin light chains: arrays of protein motifs that regulate coated-vesicle dynamics. *Science*, 16(6),208-213.
- Brodsky, F. M. (1988). Living with clathrin: its role in Intracellular Membrane Traffic. *Science*, 242(18), 1396–1402.
- Brodsky, F. M. (2012). Diversity of Clathrin Function: New Tricks for an Old Protein. *Annual review of cell and developmental biology*, 28, 309-336.
- Brodsky, F. M. (1990). The Calcium-binding Site of Clathrin Light Chains. *The Journal of biological chemistry*, 265(30), 18621–18627.
- Brown, M. S., & Goldstein, J. L. (1977). Role of the Coated of Receptor-Bound Human Fibroblasts Endocytic Vesicle in the Uptake Low Density Lipoprotein in. *Cell*, 10(3), 351–364.
- Brown, S. E., Martin, S. R., & Bayley, P. M. (1997). Kinetic Control of the Dissociation Pathway of Calmodulin-Peptide Complexes. *The Journal of biological chemistry*, 272(6), 3389–3397.
- Brown, W. J., & Farquhar, M. G. (1984). Accumulation of coated vesicles. *Proceedings of the Japan Academy*, 81(8), 5135–5139.
- Burd, C., & Cullen, P. J. (2014). Retromer: a master conductor of endosome sorting. *Cold Spring Harbor perspectives in biology*, 6(2), 1–13.
- Burgoyne, R. D. (1984). Mechanisms of secretion from adrenal chromaffin cells. *Biochimica et biophysica acta*, 779(2), 201–216.
- Burgoyne, R. D., & Clague, M. J. (2003). Calcium and calmodulin in membrane fusion. *Biochimica et biophysica Acta*, 1641(2-3), 137–143.
- Burgoyne, R. D., & Morgan, A. (1995). Ca 2+ and secretory-vesicle. *Trends in neurosciences*, 18(4), 191–196.
- Burgoyne, R. D., & Morgan, A. (1998). Calcium sensors exocytosis. *Cell calcium*, 24(5-6), 367–376.
- Burston, H. E., Maldonado-Báez, L., Davey, M., Montpetit, B., Schluter, C., Wendland, B., & Conibear, E. (2009). Regulators of yeast endocytosis identified by systematic quantitative analysis. *The Journal of cell biology*, 185(6), 1097–110.
- Carafoli, E. (1988). The Intracellular Homeostasis of Calcium : An Overview. *Annals of the New York Academy of Sciences*, 551, 147–157.
- Carafoli, E., Santella, L., Branca, D., & Brini, M. (2001). Generation , Control , and Processing of Cellular Calcium Signals. *Critical reviews in biochemistry and molecular biology*, 36(2), 107–260.
- Carlton, Jeremy G, & Martin-Serrano, J. (2009). The ESCRT machinery: new functions in viral and cellular biology. *Biochemical Society transactions*, 37(Pt 1), 195–9.
- Carlton, Jez G, & Martin-Serrano, J. (2007). Parallels between cytokinesis and retroviral budding: a role for the ESCRT machinery. *Science*, 316(5833), 1908–12.

- Carreno, S., Engqvist-Goldstein, A. E., Zhang, C. X., McDonald, K. L., & Drubin, D. G. (2004). Actin dynamics coupled to clathrin-coated vesicle formation at the trans-Golgi network. *The Journal of cell biology*, 165(6), 781–8.
- Carroll, S. Y., Stimpson, H. E. M., Weinberg, J., Toret, C. P., Sun, Y., & Drubin, D. G. (2012). Analysis of yeast endocytic site formation and maturation through a regulatory transition point. *Molecular biology of the cell*, 23(4), 657–68.
- Carroll, S. Y., Stirling, P. C., Stimpson, H. E. M., Giesselmann, E., Schmitt, M. J., & Drubin, D. G. (2009). A yeast killer toxin screen provides insights into a/b toxin entry, trafficking, and killing mechanisms. *Developmental cell*, 17(4), 552–60.
- Catlett, N. L., Duex, J. E., Tang, F., & Weisman, L. S. (2000). Two distinct regions in a yeast myosin-V tail domain are required for the movement of different cargoes. *The Journal of cell biology*, 150(3), 513–26.
- Chan, R. K., & Otte, C. A. (1982). Physiological Characterization of Saccharomyces cerevisiae Mutants Supersensitive to Gl Arrest by a Factor and ac Factor Pheromones. *Molecular and cellular biology*, 2(1), 21-29.
- Chang, F. S., Han, G.-S., Carman, G. M., & Blumer, K. J. (2005). A WASp-binding type II phosphatidylinositol 4-kinase required for actin polymerization-driven endosome motility. *The Journal of cell biology*, 171(1), 133–42.
- Chang, H. C., Hull, M., & Mellman, I. (2004). The J-domain protein Rme-8 interacts with Hsc70 to control clathrin-dependent endocytosis in Drosophila. *The Journal of cell biology*, 164(7), 1055–64.
- Chen, C. Y., & Brodsky, F. M. (2005). Huntingtin-interacting protein 1 (Hip1) and Hip1-related protein (Hip1R) bind the conserved sequence of clathrin light chains and thereby influence clathrin assembly in vitro and actin distribution in vivo. *The Journal of biological chemistry*, 280(7), 6109–17.
- Chen, C. Y., Reese, M. L., Hwang, P. K., Ota, N., Agard, D., & Brodsky, F. M. (2002). Clathrin light and heavy chain interface: alpha-helix binding superhelix loops via critical tryptophans. *The EMBO journal*, 21(22), 6072–82.
- Chen, D., Jian, Y., Liu, X., Zhang, Y., Liang, J., Qi, X., Du, H., et al. (2013). Clathrin and AP2 are required for phagocytic receptor-mediated apoptotic cell clearance in Caenorhabditis elegans. *PLoS genetics*, 9(5), 1–18.
- Chen, J. L., Ahluwalia, J. P., & Stamnes, M. (2002). Selective effects of calcium chelators on anterograde and retrograde protein transport in the cell. *The Journal of biological chemistry*, 277(38), 35682–7.
- Cheng, Y., Boll, W., Kirchhausen, T., Harrison, S. C., & Walz, T. (2007). Cryo-electron tomography of clathrin-coated vesicles: structural implications for coat assembly. *Journal of molecular biology*, 365(3), 892–9.
- Cheung, W. Y. (1970). Cyclic 3’,5'-nucleotide phosphodiesterase. Demonstration of an activator. *Biochemical and biophysical research communications*, 38(3), 533–538.

- Chi, R. J., Liu, J., West, M., Wang, J., Odorizzi, G., & Burd, C. G. (2014). Fission of SNX-BAR-coated endosomal retrograde transport carriers is promoted by the dynamin-related protein Vps1. *The Journal of cell biology*, 204(5), 793–806.
- Chidambaram, S., Müllers, N., Wiederhold, K., Haucke, V., & von Mollard, G. F. (2004). Specific interaction between SNAREs and epsin N-terminal homology (ENTH) domains of epsin-related proteins in trans-Golgi network to endosome transport. *The Journal of biological chemistry*, 279(6), 4175–9.
- Chin, D., & Means, A. R. (2000). Calmodulin: a prototypical calcium sensor. *Trends in cell biology*, 10(8), 322–8.
- Chin, L. S., Raynor, M. C., Wei, X., Chen, H. Q., & Li, L. (2001). Hrs interacts with sorting nexin 1 and regulates degradation of epidermal growth factor receptor. *The Journal of biological chemistry*, 276(10), 7069–78.
- Choudhury, R., Diao, A., Zhang, F., Eisenberg, E., Saint-pol, A., Williams, C., Konstantakopoulos, A., *et al.* (2005). Lowe Syndrome Protein OCRL1 Interacts with Clathrin and Regulates Protein Trafficking between Endosomes and the Trans-Golgi Network . *Molecular biology of the cell*, 16(8), 3467–3479.
- Chu, D. S., Pishvaee, B., & Payne, G. S. (1996). The light chain subunit is required for clathrin function in Saccharomyces cerevisiae. *The Journal of biological chemistry*, 271(51), 33123–30.
- Cocucci, E., Aguet, F., Boulant, S., & Kirchhausen, T. (2012). The first five seconds in the life of a clathrin-coated pit. *Cell*, 150(3), 495–507.
- Colombo, M. I., Beron, W., & Stahl, P. D. (1997). Calmodulin regulates endosome fusion. *The Journal of biological chemistry*, 272(12), 7707–12.
- Conibear, E. (2010). Converging views of endocytosis in yeast and mammals. *Current opinion in cell biology*, 22(4), 513-518.
- Cooper, A. A., & Stevens, T. H. (1996). Vpsl0p Cycles between the Late-Golgi and Prevacuolar Compartments in Its Function as the Sorting Receptor for Multiple Yeast Vacuolar Hydrolases. *The Journal of cell biology*, 133(3), 529–541.
- Cope, M. J., Yang, S., Shang, C., & Drubin, D. G. (1999). Novel protein kinases Ark1p and Prk1p associate with and regulate the cortical actin cytoskeleton in budding yeast. *The Journal of cell biology*, 144(6), 1203–18.
- Costaguta, G., Stefan, C. J., Bensen, E. S., Emr, S. D., & Payne, G. S. (2001). Yeast Gga coat proteins function with clathrin in Golgi to endosome transport. *Molecular biology of the cell*, 12(6), 1885–96.
- Coticchia, C. M., Revankar, C. M., Deb, T. B., Dickson, R. B., & Johnson, M. D. (2013). Calmodulin modulates Akt activity in human breast cancer cell lines. *Breast cancer research and treatment*, 115(3), 545–560.
- Cowles, C. R., Odorizzi, G., Payne, G. S., & Emr, S. D. (1997). The AP-3 Adaptor Complex Is Essential for Cargo-Selective Transport to the Yeast Vacuole. *Cell*, 91(10), 109–118.

- Crowther, R. A., Finch, J. T., & Pearse, B. M. (1976). On the structure of coated vesicles. *Journal of molecular biology*, 103(4), 785–98.
- Crowther, R. A., & Pearse, B. M. (1981). Assembly and packing of clathrin into coats. *The Journal of cell biology*, 91(3 Pt 1), 790–7.
- Crump, C. M., Xiang, Y., Thomas, L., Gu, F., Austin, C., Tooze, S. A., & Thomas, G. (2001). PACS-1 binding to adaptors is required for acidic cluster motif-mediated protein traffic. *The EMBO journal*, 20(9), 2191–2201.
- Cunningham, K. W. (2011). Acidic calcium stores of Saccharomyces cerevisiae. *Cell calcium*, 50(2), 129–138.
- Cunningham, K. W., & Fink, G. R. (1994). Calcineurin-dependent Growth Control in Saccharomyces cerevisiae Mutants Lacking PMC1 , a Homolog of Plasma Membrane Ca 2 + ATPases. *The Journal of cell biology*, 124(3), 351–363.
- Cyert, M. S. (2001). Genetic analysis of calmodulin and its targets in Saccharomyces cerevisiae. *Annual review of genetics*, 35, 647–72.
- Cyertt, M. S., & Thorner, J. (1992). Regulatory Subunit (CNB1 Gene Product) of Yeast Ca2 + / Calmodulin-Dependent Phosphoprotein Phosphatases Is Required for Adaptation to Pheromone. *Molecular and cellular biology*, 12(8), 3460–3469.
- Daboussi, L., Costaguta, G., & Payne, G. S. (2012). Phosphoinositide-mediated clathrin adaptor progression at the trans-Golgi network. *Nature cell biology*, 14(3), 239–48.
- David, C., McPherson, P. S., Mundigl, O., & de Camilli, P. (1996). A role of amphiphysin in synaptic vesicle endocytosis suggested by its binding to dynamin in nerve terminals. *Proceedings of the National Academy of Sciences of the United States of America*, 93(1), 331–5.
- Davis, T N. (1992). A temperature-sensitive calmodulin mutant loses viability during mitosis. *The Journal of cell biology*, 118(3), 607–17.
- Davis, T N, & Thorner, J. (1989). Vertebrate and yeast calmodulin, despite significant sequence divergence, are functionally interchangeable. *Proceedings of the National Academy of Sciences of the United States of America*, 86(20), 7909–13.
- Davis, Trisha N, Urdea, M. S., Masiarz, F. F. L., & Thorner, J. (1986). Isolation of the Yeast Calmodulin Gene : calmodulin Is an Essential Protein. *Cell*, 423–431.
- De, M., Abazeed, M. E., & Fuller, R. S. (2013). Direct binding of the Kex2p cytosolic tail to the VHS domain of yeast Gga2p facilitates TGN to prevacuolar compartment transport and is regulated by phosphorylation. *Molecular biology of the cell*, 24(4), 495–509.
- De Matteis, M. A., & Godi, A. (2004). PI-loting membrane traffic. *Nature cell biology*, 6(6), 487–92.
- Deisseroth, K., Heist, E. K., & Tsien, R. W. (1998). Translocation of calmodulin to the nucleus supports CREB phosphorylation in hippocampal neurons. *Nature*, 392(6672), 198–202.

- Deloche, O., & Schekman, R. W. (2002). Vps10p Cycles between the TGN and the Late Endosome via the Plasma Membrane in Clathrin Mutants. *Molecular biology of the cell*, 13(December), 4296–4307.
- DeLuca-Flaherty, C., McKay, D. B., Parham, P., & Hill, B. L. (1990). Uncoating protein (hsc70) binds a conformationally labile domain of clathrin light chain LCa to stimulate ATP hydrolysis. *Cell*, 62(5), 875–87.
- Demmel, L., Gravert, M., Ercan, E., Habermann, B., Mu, T., Kukhtina, V., Haucke, V., *et al.* (2008). The Clathrin Adaptor Gga2p Is a Phosphatidylinositol 4-phosphate Effector at the Golgi Exit. *Molecular biology of the cell*, 19(May), 1991–2002.
- Deng, Y., Guo, Y., Watson, H., Au, W. C., Shakoury-Elizeh, M., Basrai, M. A, Bonifacino, J. S., *et al.* (2009). Gga2 mediates sequential ubiquitin-independent and ubiquitin-dependent steps in the trafficking of ARN1 from the trans-Golgi network to the vacuole. *The Journal of biological chemistry*, 284(35), 23830–41.
- Derivery, E., Sousa, C., Gautier, J. J., Lombard, B., Loew, D., & Gautreau, A. (2009). The Arp2/3 activator WASH controls the fission of endosomes through a large multiprotein complex. *Developmental cell*, 17(5), 712–23.
- Di Giovanni, J., Iborra, C., Maulet, Y., Lévêque, C., El Far, O., & Seagar, M. (2010). Calcium-dependent regulation of SNARE-mediated membrane fusion by calmodulin. *The Journal of biological chemistry*, 285(31), 23665–75.
- Dick, I. E., Tadross, M. R., Liang, H., Tay, L. H., Yang, W., & Yue, D. T. (2008). A modular switch for spatial Ca2+ selectivity in the calmodulin regulation of CaV channels. *Nature*, 451(7180), 830–4.
- Dikic, I. (2002). CIN85/CMS family of adaptor molecules. *FEBS letters*, 529(1), 110–5.
- Dodge, G. R., Kovalszky, I., Saitta, B., Mcbride, W., Yi, F., Stokes, G., Renato, V., *et al*. (1991). Human Clathrin Heavy Chain (CLTC): Partial Molecular Cloning , Expression , and Mapping of the Gene to Human Chromosome 17qll -qter revised. *Genetics*, 178(11), 174–178.
- Doherty, G. J., & McMahon, H. T. (2009). Mechanisms of endocytosis. *Annual review of biochemistry*, 78, 857–902.
- Dohlman, H. G., Song, J., Ma, D., Courchesne, W. E., & Thorner, J. (1996). Sst2 , a negative regulator of pheromone signaling in the yeast Saccharomyces cerevisiae : expression , localization , and genetic interaction and physical association with Gpa1 (the G-protein alpha subunit). *Molecular biology of the cell*, 16(9), 5194–5209.
- Doyotte, A., Russell, M. R. G., Hopkins, C. R., & Woodman, P. G. (2005). Depletion of TSG101 forms a mammalian “Class E” compartment: a multicisternal early endosome with multiple sorting defects. *Journal of cell science*, 118(Pt 14), 3003–17.
- Duncan, M. C., Cope, M. J., Goode, B. L., Wendland, B., & Drubin, D. G. (2001). Yeast Eps15-like endocytic protein, Pan1p, activates the Arp2/3 complex. *Nature cell biology*, 3(7), 687–90.

- Duncan, M. C., Costaguta, G., & Payne, G. S. (2003). Yeast epsin-related proteins required for Golgi-endosome traffic define a gamma-adaptin ear-binding motif. *Nature cell biology*, 5(1), 77–81.
- Duncan, M. C., & Payne, G. S. (2005). Protein choreography. *Nature*, 438(12), 571–573.
- Ebashi, S., & Kodama, A. (1965). A new protein factor promoting aggregation of tropomyosin. *Journal of biochemistry*, 58(1), 107–108.
- Edeling, M. A., Smith, C., & Owen, D. (2006). Life of a clathrin coat: insights from clathrin and AP structures. *Nature reviews. Molecular Cell biology*, 7(1), 32–44.
- Ehrlich, M., Boll, W., Oijen, A. Van, Hariharan, R., Chandran, K., Nibert, M. L., & Kirchhausen, T. (2004). Endocytosis by Random Initiation and Stabilization of Clathrin-Coated Pits. *Cell*, 118(5), 591–605.
- Elliott, S., Knop, M., Schlenstedt, G., & Schiebel, E. (1999). Spc29p is a component of the Spc110p subcomplex and is essential for spindle pole body duplication. *Proceedings of the National Academy of Sciences of the United States of America*, 96(11), 6205–10.
- Epp, J. A., & Chant, J. (1997). An IQGAP-related protein controls actin-ring formation and cytokinesis in yeast. *Current biology*, 7(12), 921–9.
- Esk, C., Chen, C.-Y., Johannes, L., & Brodsky, F. M. (2010). The clathrin heavy chain isoform CHC22 functions in a novel endosomal sorting step. *The Journal of cell biology*, 188(1), 131–44.
- Eugster, A., Pe, E., Michel, F., Winsor, B., Letourneur, F., & Friant, S. (2004). Ent5p Is Required with Ent3p and Vps27p for Ubiquitin-dependent Protein Sorting into the Multivesicular Body. *Molecular biology of the cell*, 15(7), 3031–3041.
- Ferguson, S. M., Raimondi, A., Paradise, S., Mesaki, K., Ferguson, A., Destaing, O., Takasaki, J., *et al.* (2010). Coordinated actions of actin and BAR proteins upstream of dynamin at endocytic clathrin-coated pits. *Developmental cell*, 17(6), 811–822.
- Fink, G. R., Buckley, C. M., Dorman, T. E., Levitre, J., & Davidow, L. S. (1989). The Yeast Secretory Pathway Is Perturbed by Mutations in PlWR7 , a Member of a Ca2 + ATPase Family. *Cell*, 58(7), 133–145.
- Finken-Eigen, M., Müller, S., & Köhrer, K. (1997). Cloning and characterization of a dominant-negative vps1 allele of the yeast Saccharomyces cerevisiae . *Biological Chemistry*, 378(10), 1997.
- Flory, M. R., Moser, M. J., Monnat, R. J., & Davis, T. N. (2000). Identification of a human centrosomal calmodulin-binding protein that shares homology with pericentrin. *Proceedings of the National Academy of Sciences of the United States of America*, 97(11), 5919–23.
- Ford, M. G., Pearse, B. M., Higgins, M. K., Vallis, Y., Owen, D. J., Gibson, A., Hopkins, C. R., *et al.* (2001). Simultaneous binding of PtdIns(4,5)P2 and clathrin by AP180 in the nucleation of clathrin lattices on membranes. *Science*, 291(5506), 1051–5.
- Forsburg, S. L. (2001). The art and design of genetic screens: yeast. *Nature reviews. Genetics*, 2(9), 659–68.

- Fotin, A., Cheng, Y., Sliz, P., Grigorieff, N., Harrison, S. C., Kirchhausen, T., & Walz, T. (2004). Molecular model for a complete clathrin lattice from electron cryomicroscopy. *Nature*, 432(7017), 573–9.
- Fotin, A., Kirchhausen, T., Grigorieff, N., Harrison, S. C., Walz, T., & Cheng, Y. (2006). Structure determination of clathrin coats to subnanometer resolution by single particle cryo-electron microscopy. *Journal of structural biology*, 156(3), 453–60.
- Freeman, C. L., Hesketh, G., & Seaman, M. N. J. (2014). RME-8 coordinates the activity of the WASH complex with the function of the retromer SNX dimer to control endosomal tubulation. *Journal of cell science*, 127(Pt 9), 2053–70.
- Friant, S., Pe, E., Eugster, A., Michel, F., Lefkir, Y., Nourrisson, D., & Lyon-gerland, I. F. R. B. (2003). Ent3p Is a PtdIns (3,5) P2 Effector Required for Protein Sorting to the Multivesicular Body. *Developmental cell*, 5(9), 499–511.
- Friend, D. S., & Farquhar, M. G. (1967). Functions of coated vesicles during protein absortion in the rat vas deferens. *The Journal of Cell Biology*, (10), 357–376.
- Frost, A., Unger, V. M., & De Camilli, P. (2009). The BAR domain superfamily: membrane-molding macromolecules. *Cell*, 137(2), 191–6.
- Fuller, R. S., Brake, A. J., & Thornert, J. (1989). Intracellular Targeting and Structural Conservation of a Prohormone-Processing Endoprotease. *Science*, 8(17), 0–4.
- Fuller, R. S., Brakes, A., & Thorner, J. (1989). Yeast prohormone processing enzyme (KEX2 gene product) is a Ca2+-depencdent serine protease. *Proceedings of the National Academy of Sciences of the United States of America*, 86(3), 1434–1438.
- Gagny, B., Wiederkehr, a, Dumoulin, P., Winsor, B., Riezman, H., & Haguenauer-Tsapis, R. (2000). A novel EH domain protein of Saccharomyces cerevisiae, Ede1p, involved in endocytosis. *Journal of cell science*, 113(Pt 1), 3309–19.
- Gall, W. E., Higginbotham, M. a, Chen, C., Ingram, M. F., Cyr, D. M., & Graham, T. R. (2000). The auxilin-like phosphoprotein Swa2p is required for clathrin function in yeast. *Current biology*, 10(21), 1349–58.
- Galletta, B. J., Chuang, D. Y., & Cooper, J. A. (2008). Distinct roles for Arp2/3 regulators in actin assembly and endocytosis. *PLoS biology*, 6(1), e1.
- Galletta, B. J., & Cooper, J. A. (2009). Actin and endocytosis: mechanisms and phylogeny. *Current opinion in cell biology*, 21(1), 20–7.
- Gallop, J. L., Jao, C. C., Kent, H. M., Butler, P. J. G., Evans, P. R., Langen, R., & McMahon, H. T. (2006). Mechanism of endophilin N-BAR domain-mediated membrane curvature. *The EMBO journal*, 25(12), 2898–910.
- Gandhi, M., Archard, V., Blanchoin, L., & Goode, B. L. (2010). Coronin switches roles in actin disassembly depending on the nucleotide state of actin. *Molecular cell*, 34(3), 364–374.
- Geier, B. M., Wiech, H., & Schiebel, E. (1996). Binding of Centrins and Yeast Calmodulin to Synthetic Peptides Corresponding to Binding Sites in the Spindle Pole Body

Components Kar1p and Spc110p. *The Journal of biological chemistry*, 271(45), 28366–28374.

- Geiser, J. R., Sundberg, H. A, Chang, B. H., Muller, E. G., & Davis, T. N. (1993). The essential mitotic target of calmodulin is the 110-kilodalton component of the spindle pole body in Saccharomyces cerevisiae. *Molecular and cellular biology*, 13(12), 7913–24.
- Geiser, J. R., van Tuinen, D., Brockerhoff, S. E., Neff, M. M., & Davis, T. N. (1991). Can calmodulin function without binding calcium? *Cell*, 65(6), 949–59.
- Geli, M. I., Lombardi, R., Schmelzl, B., & Riezman, H. (2000). An intact SH3 domain is required for myosin I-induced actin polymerization. *The EMBO journal*, 19(16), 4281–91.
- Geli, M. I., & Riezman, H. (1998). Endocytic internalization in yeast and animal cells: similar and different. *Journal of cell science*, *111(Pt 8)*, 1031–7.
- Geli, M. I., Wesp, A., & Riezman, H. (1998). Distinct functions of calmodulin are required for the uptake step of receptor-mediated endocytosis in yeast: the type I myosin Myo5p is one of the calmodulin targets. *The EMBO journal*, 17(3), 635–47.
- Geli, M. I., & Riezman, H. (1996). Role of Type I Myosins in Receptor-Mediated Endocytosis in Yeast. *Science*, 272(5261), 533–535.
- Gheorghe, D. M., Aghamohammadzadeh, S., Smaczynska-de Rooij, I. I., Allwood, E. G., Winder, S. J., & Ayscough, K. R. (2008). Interactions between the yeast SM22 homologue Scp1 and actin demonstrate the importance of actin bundling in endocytosis. *The Journal of biological chemistry*, 283(22), 15037–46.
- Gietz, R. D., & Sugino, A. (1988). New yeast Escherichia coli shuttle vectors constructed with in vitro mutagenized yeast genes lacking six-base pair restriction sites. *Gene*, 74(2), 527–534.
- Gillies, A., Taylor, R., & Gestwicki, J. E. (2013). Synthetic lethal interactions in yeast reveal functional roles of J protein co-chaperones. *Molecular bioSystems*, 8(11), 2901–2908.
- Girao, H., Geli, M. I., & Idrissi, F.-Z. (2008). Actin in the endocytic pathway: from yeast to mammals. *FEBS letters*, 582(14), 2112–9.
- Girard, M., Poupon, V., Blondeau, F., & McPherson, P. S. (2005). The DnaJ-domain protein RME-8 functions in endosomal trafficking. *The Journal of biological chemistry*, 280(48), 40135–43.
- Gomez, T. S., & Billadeau, D. D. (2010). A FAM21-containing WASH complex regulates retromer-dependent sorting. *Developmental cell*, 17(5), 699–711.
- Goode, B. L., Rodal, A. A., Barnes, G., & Drubin, D. G. (2001). Activation of the Arp2/3 complex by the actin filament binding protein Abp1p. *The Journal of cell biology*, 153(3), 627–34.
- Grant, B. D., & Donaldson, J. G. (2011). Pathways and mechanisms of endocytic recycling. *Nature reviews. Molecular Cell biology*, 10(9), 597–608.

- Greener, T., Zhao, X., Nojima, H., Eisenberg, E., & Greene, L. E. (2000). Role of Cyclin G-associated Kinase in Uncoating Clathrin-coated Vesicles from Non-neuronal Cells. *The Journal of biological chemistry*, 275(2), 1365–1370.
- Griffiths, G., Hoflack, B., Simons, K., Mellman, I., & Kornfeldt, S. (1988). The Mannose 6-Phosphate Receptor and the Biogenesis of Lysosomes. *Cell*, 52(2), 329–341.
- Grötsch, H., Giblin, J. P., Idrissi, F.-Z., Fernández-Golbano, I.-M., Collette, J. R., Newpher, T. M., Robles, V., *et al*. (2010). Calmodulin dissociation regulates Myo5 recruitment and function at endocytic sites. *The EMBO journal*, 29(17), 2899–914.
- Gu, F., Crump, C. M., & Thomas, G. (2006). Trans-Golgi network sorting. *Cellular and molecular life sciences*, 58(8), 1067–1084.
- Ha, S., Torabinejad, J., Dewald, D. B., Wenk, M. R., Lucast, L., Camilli, P. De, Newitt, R. A., *et al.* (2003). The Synaptojanin-like Protein Inp53 / Sjl3 Functions with Clathrin in a Yeast TGN-to-Endosome Pathway Distinct from the GGA Protein-dependent Pathway. *Molecular biology of the cell*, 14(April), 1319–1333.
- Haar, E., Musacchio, A., Harrison, S. C., & Kirchhausen, T. (1998). Atomic structure of clathrin: a beta propeller terminal domain joins an alpha zigzag linker. *Cell*, 95(4), 563–73.
- Haarer, B. K., Petzold, A., Lillie, S. H., & Brown, S. S. (1994). Identification of MYO4 , a second class V myosin gene in yeast. *Journal of cell science*, 107(4), 1055–1064.
- Hanley, R. M., Putkey, J. A., George, E. Y., Ono, T., Putkey, J. A., & Means, R. (1990). Chimeric calmodulin-cardiac troponin C proteins differentially activate calmodulin target enzymes. *The Journal of biological chemistry*, 265(16), 9228–9235.
- Hay, J. C. (2007). Calcium: a fundamental regulator of intracellular membrane fusion? *EMBO reports*, 8(3), 236–40.
- Helfant, A. H. (2002). Composition of the spindle pole body of Saccharomyces cerevisiae and the proteins involved in its duplication. *Current genetics*, 40(5), 291–310.
- Henne, W. M., Boucrot, E., Meinecke, M., Evergren, E., Vallis, Y., Mittal, R., & Mcmahon, H. T. (2010). FCHo Proteins are Nucleators of Clathrin-Mediated Endocytosis. *Science*, 328(5983), 1281–1284.
- Herman, P. K., Stack, J. H., & Emr, S. D. (1992). An essential role for a protein and lipid kinase complex in secretory protein sorting. *Trends in cell biology*, 2(12), 363–368.
- Hettema, E. H., Lewis, M. J., Black, M. W., & Pelham, H. R. B. (2003). Retromer and the sorting nexins Snx4 / 41 / 42 mediate distinct retrieval pathways from yeast endosomes. *The EMBO journal*, 22(3), 548–557.
- Hilfiker, S., Pieribone, V. a, Czernik, a J., Kao, H. T., Augustine, G. J., & Greengard, P. (1999). Synapsins as regulators of neurotransmitter release. *Philosophical transactions of the Royal Society of London. Series B, Biological sciences*, 354(1381), 269–79.
- Hill, K. L., Catlett, N. L., & Weisman, L. S. (1996). Actin and myosin function in directed vacuole movement during cell division in Saccharomyces cerevisiae. *The Journal of cell biology*, 135(6), 1535–1549.

- Hinrichsen, L., Harborth, J., Andrees, L., Weber, K., & Ungewickell, E. J. (2003). Effect of clathrin heavy chain- and alpha-adaptin-specific small inhibitory RNAs on endocytic accessory proteins and receptor trafficking in HeLa cells. *The Journal of biological chemistry*, 278(46), 45160–70.
- Hinrichsen, L., Meyerholz, A., Groos, S., & Ungewickell, E. J. (2006). Bending a membrane: how clathrin affects budding. *Proceedings of the National Academy of Sciences of the United States of America*, 103(23), 8715–20.
- Hinrichsen, R. D. (1993). Calcium and calmodulin in the control of cellular behavior and motility. *Biochimica et biophysica acta*, 1155(3), 277–93.
- Hirst, J., Lui, W. W., Bright, N. A., Totty, N., Seaman, M. N., & Robinson, M. S. (2000). A family of proteins with gamma-adaptin and VHS domains that facilitate trafficking between the trans-Golgi network and the vacuole/lysosome. *The Journal of cell biology*, 149(1), 67–80.
- Hirst, J., Lindsay, M. R., & Robinson, M. S. (2001). GGAs : Roles of the Different Domains and Comparison with AP-1 and Clathrin. *Molecular biology of the cell*, 12(11), 3573–3588.
- Hirst, J., Miller, S. E., Taylor, M. J., Mollard, G. F. Von, & Robinson, M. S. (2004). EpsinR Is an Adaptor for the SNARE Protein Vti1b. *Molecular biology of the cell*, 15(12), 5593–5602.
- Hirst, J., Motley, A., Harasaki, K., Chew, S. Y. P., & Robinson, M. S. (2003). EpsinR : an ENTH Domain-containing Protein that Interacts with AP-1. *Molecular biology of the cell*, 14(2), 625–641.
- Hoeflich, K. P., & Ikura, M. (2002). Calmodulin in Action : Diversity in Target Recognition and Activation Mechanisms. *Cell*, 108(3), 739–742.
- Holyoak, C. D., Thompson, S., Ortiz Calderon, C., Hatzixanthis, K., Bauer, B., Kuchler, K., Piper, P. W., *et al.* (2000). Loss of Cmk1 Ca(2+)-calmodulin-dependent protein kinase in yeast results in constitutive weak organic acid resistance, associated with a post-transcriptional activation of the Pdr12 ATP-binding cassette transporter. *Molecular microbiology*, 37(3), 595–605.
- Hood, F. E., Williams, S. J., Burgess, S. G., Richards, M. W., Roth, D., Straube, A., Pfuhl, M., *et al.* (2013). Coordination of adjacent domains mediates TACC3-ch-TOG-clathrin assembly and mitotic spindle binding. *The Journal of cell biology*, 202(3), 463–78.
- Hoppins, S., Collins, S. R., Cassidy-Stone, A., Hummel, E., Devay, R. M., Lackner, L. L., Westermann, B., *et al.* (2011). A mitochondrial-focused genetic interaction map reveals a scaffold-like complex required for inner membrane organization in mitochondria. *The Journal of cell biology*, 195(2), 323–40.
- Howard, J. P., Hutton, J. L., Olson, J. M., & Payne, G. S. (2002). Sla1p serves as the targeting signal recognition factor for NPFX(1,2)D-mediated endocytosis. *The Journal of cell biology*, 157(2), 315–26.

- Huang, F., Khvorova, A., Marshall, W., & Sorkin, A. (2004). Analysis of clathrin-mediated endocytosis of epidermal growth factor receptor by RNA interference. *The Journal of biological chemistry*, 279(16), 16657–61.
- Huang, K. M., D'Hondt, K., Riezman, H., & Lemmon, S. K. (1999). Clathrin functions in the absence of heterotetrameric adaptors and AP180-related proteins in yeast. *The EMBO journal*, 18(14), 3897–908.
- Huang, K. M., Gullberg, L., Nelson, K. K., Stefan, C. J., Blumer, K., & Lemmon, S. K. (1997). Novel functions of clathrin light chains: clathrin heavy chain trimerization is defective in light chain-deficient yeast. *Journal of cell science*, *110(Pt 7)*, 899–910.
- Huotari, J., & Helenius, A. (2011). Endosome maturation. *The EMBO journal*, 30(17), 3481–500.
- Hurley, J. H. (2010). The ESCRT complexes. *Critical reviews in biochemistry and molecular biology*, 45(6), 463–487.
- Idrissi, F.-Z., Blasco, A., Espinal, A., & Geli, M. I. (2012). Ultrastructural dynamics of proteins involved in endocytic budding. *Proceedings of the National Academy of Sciences of the United States of America*, 109(39), E2587–94.
- Idrissi, F.-Z., & Geli, M. I. (2014). Zooming in on the molecular mechanisms of endocytic budding by time-resolved electron microscopy. *Cellular and molecular life sciences*, 71(4), 641–57.
- Idrissi, F.-Z., Grötsch, H., Fernández-Golbano, I. M., Presciatto-Baschong, C., Riezman, H., & Geli, M.-I. (2008). Distinct acto/myosin-I structures associate with endocytic profiles at the plasma membrane. *The Journal of cell biology*, 180(6), 1219–32.
- Iida, H., Ohya, Y., Anraku, Y., Treatment, I., Division, A., Proliferation, C., Biology, B., *et al*. (1995). Calmodulin-dependent protein kinase II and calmodulin are required for induced thermotolerance in Saccharomyces cerevisiae. *Current genetics*, 27(2), 190–193.
- Ikura, M., Clore, G. M., Gronenborn, a M., Zhu, G., Klee, C. B., & Bax, A. (1992). Solution structure of a calmodulin-target peptide complex by multidimensional NMR. *Science*, 256(5057), 632–8.
- Ito, H., Fukuda, Y., & Murata, K. (1983). Transformation of intact yeast cells treated with alkali Transformation of Intact Yeast Cells Treated with Alkali Cations. *Journal of Bacteriology*, 153(1), 166–168.
- Jackson, L. P., Kelly, B. T., McCoy, A. J., Gaffry, T., James, L. C., Collins, B. M., Höning, S., *et al.* (2010). A large-scale conformational change couples membrane recruitment to cargo binding in the AP2 clathrin adaptor complex. *Cell*, 141(7), 1220–9.
- Jansen, R., Dowzer, C., Michaelis, C., Galova, M., & Nasmyth, K. (1996). Mother Cell – Specific HO Expression in Budding Yeast Depends on the Unconventional Myosin Myo4p and Other Cytoplasmic Proteins. *Cell*, 84(3), 687–697.
- Johnston, G. C., Prendergast, J. A., & Singer, R. A. (1991). The Saccharomyces cerevisiae MYO2 Gene Encodes an Essential Myosin for Vectorial Transport of Vesicles. *The Journal of cell biology*, 113(3), 539–551.

- Jonsdottir, G. A., & Li, R. (2004). Dynamics of Yeast Myosin I : Evidence for a Possible Role in Scission of Endocytic Vesicles. *Current biology*, 14(17), 1604–1609.
- Julius, D., Blair, L., Brakes, A., Sprague, G., & Thornert, J. (1983). Yeast α factor is processed from a larger precursor polypeptide The essential role of a membrane-bound dipeptidyl aminopeptidase.pdf. *Cell*, 32(3), 839–852.
- Julius, D., Schekman, R., & Thorner, J. (1984). Glycosylation and Processing of Prepro-a-Factor through the Yeast Secretory Pathway. *Cell*, 36(2), 309–318.
- Kadota, K., & Kadota, T. (1973). Isolation of coated vesicles, plain synaptic vesicles, and flocculent material from a crude synaptosome fraction of guinea pig whole brain. *The Journal of cell biology*, 58(1), 135–51.
- Kakiuchi, S., Yamazaki, R., & Nakajima, H. (1970). Properties of a heat-stable phosphodiesterase activating factor isolated from brain extract. *Proceedings of the Japan Academy*, 46(6), 587–592.
- Kaksonen, M., Sun, Y., & Drubin, D. G. (2003). A Pathway for Association of Receptors , Adaptors , and Actin during Endocytic Internalization. *Cell*, 115, 475–487.
- Kaksonen, M., Toret, C. P., & Drubin, D. G. (2005). A modular design for the clathrin- and actin-mediated endocytosis machinery. *Cell*, 123(2), 305–20.
- Kanaseki, T., & Kadota, K. (1969). The “vesicle in a basket”. A morphological study of the coated vesicle isolated from the nerve endings of the guinea pig brain, with special reference to the mechanism of membrane movements. *The Journal of cell biology*, 42(1), 202–20.
- Katzmann, D. J., Babst, M., & Emr, S. D. (2001). Ubiquitin-Dependent Sorting into the Multivesicular Body Pathway Requires the Function of a Conserved Endosomal Protein Sorting Complex , ESCRT-I. *Cell*, 106(7), 145–155.
- Katzmann, D. J., Stefan, C. J., Babst, M., & Emr, S. D. (2003). Vps27 recruits ESCRT machinery to endosomes during MVB sorting. *The Journal of cell biology*, 162(3), 413–23.
- Keen, J. H., Willingham, M. C., & Pastan, I. H. (1979). Clathrin-Coated Vesicles : Isolation , and Factor-Dependent Reassociation Baskets Dissociation of Clathrin. *Cell*, 16(2), 303–312.
- Kelly, B. T., & Owen, D. J. (2011). Endocytic sorting of transmembrane protein cargo. *Current opinion in cell biology*, 23(4), 404–12.
- Kihara, A., Noda, T., Ishihara, N., & Ohsumi, Y. (2001). Two distinct Vps34 phosphatidylinositol 3-kinase complexes function in autophagy and carboxypeptidase Y sorting in Saccharomyces cerevisiae. *The Journal of cell biology*, 152(3), 519–30.
- Kilmartin, J. V, & Goh, P. Y. (1996). Spc110p: assembly properties and role in the connection of nuclear microtubules to the yeast spindle pole body. *The EMBO journal*, 15(17), 4592–602.

- Kim, K., Galletta, B. J., Schmidt, K. O., Chang, F. S., Blumer, K. J., & Cooper, J. A. (2006). Actin-based Motility during Endocytosis in Budding Yeast. *Molecular biology of the cell*, 17(3), 1354 –1363.
- Kirchhausen, T, & Harrison, S. C. (1981). Protein organization in clathrin trimers. *Cell*, 23(3), 755–61.
- Kirchhausen, T., Harrison, S. C., Chow, E. P., Mattaliano, R. J., Ramachandran, K. L., Smart, J., & Brosius, J. (1987). Clathrin heavy chain: molecular cloning and complete primary structure. *Proceedings of the National Academy of Sciences of the United States of America*, 84(24), 8805–9.
- Kirchhausen, T, Harrison, S. C., Parham, P., & Brodsky, F. M. (1983). Location and distribution of the light chains in clathrin trimers. *Proceedings of the National Academy of Sciences of the United States of America*, 80(9), 2481–5.
- Kirchhausen, T., Scarmato, P., Harrison, S. C., Monroe, J. J., Chow, E. P., Mattaliano, R. J., Ramachandran, K. L., et al. (1987). Clathrin light chains LCA and LCB are similar, polymorphic, and share repeated heptad motifs. *Science*, 236(4799), 320–4.
- Kirchhausen, T. (2002). Clathrin Adaptors Really Adapt. *Cell*, 109(4), 413–416.
- Kirchhausen, T., Owen, D., & Harrison, S. C. (2014). Molecular Structure, Function, and Dynamics of Clathrin-Mediated Membrane Traffic. *Cold Spring Harbor perspectives in biology*, 6(5), 1–26.
- Kirchhausen, T. (2000). Clathrin. *Annual review of biochemistry*, 69, 699–727.
- Kishimoto, T., Sun, Y., Buser, C., Liu, J., Michelot, A., & Drubin, D. G. (2011). Determinants of endocytic membrane geometry, stability, and scission. *Proceedings of the National Academy of Sciences of the United States of America*, 108(44), E979–88.
- Klee, C. B., Ren, H., & Wang, X. (1998). Regulation of the Calmodulin-stimulated Protein Phosphatase, Calcineurin. *The Journal of biological chemistry*, 273(22), 13367–13370.
- Knuehl, C., Chen, C.-Y., Manalo, V., Hwang, P. K., Ota, N., & Brodsky, F. M. (2006). Novel binding sites on clathrin and adaptors regulate distinct aspects of coat assembly. *Traffic*, 7(12), 1688–700.
- Krantz, K. C., Puchalla, J., Thapa, R., Kobayashi, C., Bisher, M., Viehweg, J., Carr, C. M., *et al.* (2013). Clathrin coat disassembly by the yeast Hsc70/Ssa1p and auxilin/Swa2p proteins observed by single-particle burst analysis spectroscopy. *The Journal of biological chemistry*, 288(37), 26721–30.
- Krendel, M., Osterweil, E. K., & Mooseker, M. S. (2008). Myosin 1E interacts with synaptojanin-1 and dynamin and is involved in endocytosi. *FEBS letters*, 581(4), 644–650.
- Kretsinger, R. H., Rudnick, S. E., & Weissman, L. J. (1986). Crystal Structure of Calmodulin. *Journal of inorganic chemistry*, 28(2-3), 289–302.
- Kuboniwa, H., Tjandra, N., Grzesiek, S., Ren, H., Klee, C., & A, B. (1995). Solution structure of calcium-free calmodulin. *Nature structural & molecular biology*, 2(9), 768–776.

- Kukulski, W., Schorb, M., Kaksonen, M., & Briggs, J. A. G. (2012). Plasma membrane reshaping during endocytosis is revealed by time-resolved electron tomography. *Cell*, 150(3), 508–20.
- Kukulski, W., Schorb, M., Welsch, S., Picco, A., Kaksonen, M., & Briggs, J. a G. (2011). Correlated fluorescence and 3D electron microscopy with high sensitivity and spatial precision. *The Journal of cell biology*, 192(1), 111–9.
- Kursula, P. (2014). The many structural faces of calmodulin: a multitasking molecular jackknife. *Amino acids*, 46(10), 2295-304.
- Kübler, E., & Riezman, H. (1993). Actin and fimbrin are required for the internalization step of endocytosis in yeast. *The EMBO journal*, 12(7), 2855–62.
- Kübler, E., Schimmöller, F., & Riezman, H. (1994). Calcium-independent calmodulin requirement for endocytosis in yeast. *The EMBO journal*, 13(23), 5539–46.
- Laemmli, U. K. (1970). Cleavage of structural proteins during the assembly of the head of bacteriophage T4. *Nature*, 227(5259), 680–685.
- Lauvrak, S. U., Torgersen, M. L., & Sandvig, K. (2004). Efficient endosome-to-Golgi transport of Shiga toxin is dependent on dynamin and clathrin. *Journal of cell science*, 117(Pt 11), 2321–31.
- Lechler, T., Jonsdottir, G. A., Klee, S. K., Pellman, D., & Li, R. (2001). A two-tiered mechanism by which Cdc42 controls the localization and activation of an Arp2/3-activating motor complex in yeast. *The Journal of cell biology*, 155(2), 261–70.
- Lee, D.-W., Wu, X., Eisenberg, E., & Greene, L. E. (2006). Recruitment dynamics of GAK and auxilin to clathrin-coated pits during endocytosis. *Journal of cell science*, 119(Pt 17), 3502–12.
- Lee, S. Y., & Klevit, R. E. (2000). The Whole Is Not the Simple Sum of Its Parts in Calmodulin from S . cereVisiae. *Biochemistry*, 39, 4225–4230.
- Lemansky, P., Hasilik, A., von Figura, K., Helmy, S., Fishman, J., Fine, R. E., Kedersha, N. L., *et al.* (1987). Lysosomal Enzyme Precursors in Coated Vesicles Derived from the Exocytic and Endocytic Pathways. *The Journal of cell biology*, 104(6), 1743–1748.
- Lemmon, S. K., & Traub, L. M. (2000). Sorting in the endosomal system in yeast and animal cells. *Current opinion in cell biology*, 12(4), 457–66.
- Lemmon, S. K., Freund, C., Conley, K., & Jones, E. W. (1990). Genetic instability of clathrin-deficient strains of Saccharomyces cerevisiae. *Genetics*, 124, 27–38.
- Lemmon, S. K., & Jones, E. W. (1987). Clathrin Requirement for Normal Growth of Yeast. *Science*, 238(4826), 504–509.
- Lemmon, S. K., Lemmon, V. P., & Jones, E. W. (1988). Characterization of Yeast Clathrin and Anticlathrin Heavy-Chain Monoclonal Anti bodies. *Journal of cellular biochemistry*, 36(4), 329–340.
- Lemmon, S. K., & Traub, L. M. (2012). Getting in Touch with the Clathrin Terminal Domain. *Traffic*, 13(4), 511–519.

- Lieto-trivedi, A., & Coluccio, L. M. (2008). Calcium , Nucleotide , and Actin Affect the Interaction of Mammalian Myo1c with its light chain Calmodulin. *Biochemistry*, 47, 10218–10226.
- Lim, H. H., Zhang, T., & Surana, U. (2009). Regulation of centrosome separation in yeast and vertebrates: common threads. *Trends in cell biology*, 19(7), 325–33.
- Lin, M.-C., Galletta, B. J., Sept, D., & Cooper, J. a. (2010). Overlapping and distinct functions for cofilin, coronin and Aip1 in actin dynamics in vivo. *Journal of cell science*, 123(Pt 8), 1329–42.
- Linden, C. D., Dedman, J. R., Chafouleas, J. G., Means, a R., & Roth, T. F. (1981). Interactions of calmodulin with coated vesicles from brain. *Proceedings of the National Academy of Sciences of the United States of America*, 78(1), 308–12.
- Linse, S., Helmersson, A., & Forsen, S. (1991). Calcium Binding to Calmodulin and Its Globular Domains. *The Journal of biological chemistry*, 266(13), 8050–8054.
- Lisanti, M. P., Shapiro, L. S., Moskowitz, N., Hua, E. L., Puszkin, S., & Schook, W. (1982). Isolation and preliminary characterization of clathrin-associated proteins. *European journal of biochemistry*, 125(2), 463–70.
- Liu, J., Sun, Y., Drubin, D. G., & Oster, G. F. (2009). The mechanochemistry of endocytosis. *PLoS biology*, 7(9), 2–16.
- Liu, J.. (1993). FK506 and ciclosporin: molecular probes for studying intracellular signal transduction. *Trends in pharmacology*, 14(5), 182–8.
- Liu, S. H., Towler, M. C., Chen, E., Chen, C. Y., Song, W., Apodaca, G., & Brodsky, F. M. (2001). A novel clathrin homolog that co-distributes with cytoskeletal components functions in the trans-Golgi network. *The EMBO journal*, 20(1-2), 272–84.
- Liu, S., Wong, M. L., & Craik, S. (1995). Regulation of Clathrin Assembly and Trimerization Defined Using Recombinant Triskelion Hubs. *Cell*, 83, 257–267.
- Liu, T.-T., Gomez, T. S., Sackey, B. K., Billadeau, D. D., & Burd, C. G. (2012). Rab GTPase regulation of retromer-mediated cargo export during endosome maturation. *Molecular biology of the cell*, 23(13), 2505–15.
- Liu, X., Heidelberger, R., & Janz, R. (2014). Phosphorylation of syntaxin 3B by CaMKII regulates the formation of t-SNARE complexes. *Molecular and cellular neurosciences*, 60, 53–62.
- Lladó, A., Tebar, F., Calvo, M., Moreto, J., Sorkin, A., & Enrich, C. (2004). Protein KinaseC -Calmodulin Crosstalk Regulates Epidermal Growth Factor Receptor Exit from Early endosomes. *Molecular biology of the cell*, 15(11), 4877–4891.
- Lladó, A., Timpson, P., Vilà de Muga, S., Moretó, J., Pol, A., Grewal, T., Daly, R. J., *et al.* (2008). Protein kinase Cdelta and calmodulin regulate epidermal growth factor receptor recycling from early endosomes through Arp2/3 complex and cortactin. *Molecular biology of the cell*, 19(1), 17–29.
- Loerke, D., Mettlen, M., Schmid, S. L., & Danuser, G. (2011). Measuring the hierarchy of molecular events during clathrin-mediated endocytosis. *Traffic*, 12(7), 815–25.

- Loisel, T. P., Boujemaa, R., Pantaloni, D., & Carlier, M. F. (1999). Reconstitution of actin-based motility of Listeria and Shigella using pure proteins. *Nature*, 401(6753), 613–6.
- Long, R. M. (1997). Mating Type Switching in Yeast Controlled by Asymmetric Localization of ASH1 mRNA. *Science*, 277(5324), 383–387.
- Longtine, M. S., McKenzie, A., Demarini, D. J., Shah, N. G., Wach, A., Brachat, A., Philippsen, P., *et al.* (1998). Additional modules for versatile and economical PCR-based gene deletion and modification in Saccharomyces cerevisiae. *Yeast*, 14(10), 953–61.
- Lu, K. P., & Means, A. R. (1993). Regulation of the cell cycle by calcium and calmodulin. *Endocrine reviews*, 14(1), 40–58.
- Luan, Y., Matsuura, I., Yazawa, M., Nakamura, T., Yagi, K., & Chemistry, A. (1987). Yeast Calmodulin : Structural and Functional Differences Compared. *Journal of biochemistry*, 102(6), 1531–1537.
- Luby-Phelps, K., Hori, M., Phelps, J. M., & Won, D. (1995). Ca2+-regulated Dynamic Compartmentalization of Calmodulin in Living Smooth Muscle Cells. *The Journal of biological chemistry*, 270(37), 21532–21538. d
- Luzio, J. P., Bright, N. A., & Pryor, P. R. (2007). The role of calcium and other ions in sorting and delivery in the late endocytic pathway. *Biochemical Society transactions*, 35(Pt 5), 1088–91.
- Maldonado-Báez, L., Dores, M. R., Perkins, E. M., Drivas, T. G., Hicke, L., & Wendland, B. (2008). Interaction between Epsin / Yap180 Adaptors and the Scaffolds Ede1 / Pan1 Is Required for Endocytosis. *Molecular biology of the cell*, 19(July), 2936–2948.
- Malerød, L., Stuffers, S., Brech, A., & Stenmark, H. (2007). Vps22/EAP30 in ESCRT-II mediates endosomal sorting of growth factor and chemokine receptors destined for lysosomal degradation. *Traffic*, 8(11), 1617–29.
- Mallard, F., Antony, C., Tenza, D., Salamero, J., Goud, B., & Johannes, L. (1998). Direct pathway from early/recycling endosomes to the Golgi apparatus revealed through the study of shiga toxin B-fragment transport. *The Journal of cell biology*, 143(4), 973–990.
- Mao, Y., Nickitenko, A., Duan, X., Lloyd, T. E., Wu, M. N., Bellen, H., & Quiocho, F. A.. (2000). Crystal structure of the VHS and FYVE tandem domains of Hrs, a protein involved in membrane trafficking and signal transduction. *Cell*, 100(4), 447–56.
- Marcusson, E. G., Horazdovsky, B. F., & Cereghino, J. L. (1994). The Sorting Receptor for Yeast Vacuolar Carboxypeptidase Y Is Encoded by the VFW0 Gene. *Cell*, 77(5), 579–586.
- Matheos, D. P., Kingsbury, T. J., Ahsan, U. S., & Cunningham, K. W. (1997). Tcn1p/Crz1p, a calcineurin-dependent transcription factor that differentially regulates gene expression in Saccharomyces cerevisiae. *Genes & Development*, 11(24), 3445–3458.
- Matsuo, K., Nishimura, T., Hayakawa, A., Ono, Y., & Takahashi, M. (2010). Involvement of a centrosomal protein kendrin in the maintenance of centrosome cohesion by modulating Nek2A kinase activity. *Biochemical and biophysical research communications*, 398(2), 217–23.

- Mazur, P., Morin, N., Baginsky, W., El-sherbeini, M., Clemas, J. A., Nielsen, J. B., & Foor, F. (1995). Differential Expression and Function of Two Homologous Subunits of Yeast 1 , 3- - D -Glucan Synthase. *Molecular and cellular biology*, 15(10), 5671–5681.
- McGough, I. J., & Cullen, P. J. (2011). Recent advances in retromer biology. *Traffic*, 12(8), 963–71.
- McGough, I. J., & Cullen, P. J. (2013). Clathrin is not required for SNX-BAR-retromer-mediated carrier formation. *Journal of cell science*, 126(Pt 1), 45–52.
- McLaughlin, S., & Murray, D. (2005). Plasma membrane phosphoinositide organization by protein electrostatics. *Nature*, 438(7068), 605–11.
- McMahon, H. T., & Boucrot, E. (2011). Molecular mechanism and physiological functions of clathrin-mediated endocytosis. *Nature reviews. Molecular Cell biology*, 12(8), 517–533.
- McPherson, P. S., García, E. P., Slepnev, V. I., Sossin, W. S., Bauerfeind, R., Nemoto, Y., & De Camilli, P. (1996). A presynaptic inositol-5-phosphatase. *Letters to Nature*, 379(6563), 353–357.
- Meador, W. E., Means, A. R., & Quiocho, F. A. (1992). Target Enzyme Recognition by Calmodulin : 2 . 4 A Structure of a Calmodulin-Peptide Complex. *Science*, 257(5074), 1251–55.
- Means, A. R. (2000). Regulatory cascades involving calmodulin-dependent protein kinases. *Molecular endocrinology*, 14(1), 4–13.
- Mendizabal, I., Rios, G., Mulet, J. M., Serrano, R., & de Larrinoa, I. F. (1998). Yeast putative transcription factors involved in salt tolerance. *FEBS letters*, 425(2), 323–8.
- Mendozas, I., Rubioli, F., Rodriguez-navarroli, A., & Pardosn, J. M. (1994). The Protein Phosphatase Calcineurin Is Essential for NaCl Tolerance of Saccharomyces cerevisiae. *The Journal of biological chemistry*, 269(12), 8792–8796.
- Merisko, E. M., Welch, J. K., Chen, T. Y., & Chen, M. (1988). Alpha-actinin and calmodulin interact with distinct sites on the arms of the clathrin trimer. *The Journal of biological chemistry*, 263(30), 15705–12.
- Merrifield, C. J., & Kaksonen, M. (2014). Endocytic Accessory Factors and Regulation of Clathrin-Mediated Endocytosis *Cold Spring Harb Perspect Biol*, 6(11), pii: a016733.
- Messa, M., Fernández-Busnadiego, R., Sun, E. W., Chen, H., Czapla, H., Wrasman, K., Wu, Y., *et al.* (2014). Epsin deficiency impairs endocytosis by stalling the actin-dependent invagination of endocytic clathrin-coated pits. *eLife*, 3, e03311.
- Meyer, C., Zizioli, D., Lausmann, S., Eskelinen, E. L., Hamann, J., Saftig, P., von Figura, K., et al. (2000). mu1A-adaptin-deficient mice: lethality, loss of AP-1 binding and rerouting of mannose 6-phosphate receptors. *The EMBO journal*, 19(10), 2193–203.
- Miele, A. E., Watson, P. J., Evans, P. R., Traub, L. M., & Owen, D. J. (2004). Two distinct interaction motifs in amphiphysin bind two independent sites on the clathrin terminal domain beta-propeller. *Nature structural & molecular biology*, 11(3), 242–8.

- Miliaras, N. B., Park, J.-H., & Wendland, B. (2004). The function of the endocytic scaffold protein Pan1p depends on multiple domains. *Traffic*, 5(12), 963–78.
- Mills, I. G., Urbé, S., & Clague, M. J. (2001). Relationships between EEA1 binding partners and their role in endosome fusion. *Journal of cell science*, 114(Pt 10), 1959–65.
- Minowa, O., Yazawa, M., Sobue, K., Ito, K., & Yagi, K. (1988). Calmodulin Fragments Can Not Activate Target Enzymes. *Journal of biochemistry*, 103(3), 531–536.
- Mishra, R., Smaczynska-de Rooij, I. I., Goldberg, M. W., & Ayscough, K. R. (2011). Expression of Vps1 I649K a self-assembly defective yeast dynamin, leads to formation of extended endocytic invaginations. *Communicative & integrative biology*, 4(1), 115–7.
- Misra, S., & Hurley, J. H. (1999). Crystal Structure of a Phosphatidylinositol the FYVE Domain of Vps27p. *Cell*, 97(5), 657–666.
- Mizunuma, M., Hirata, D., Miyaoka, R., & Miyakawa, T. (2001). GSK-3 kinase Mck1 and calcineurin coordinately mediate Hsl1 down-regulation by Ca2+ in budding yeast. *The EMBO journal*, 20(5), 1074–85.
- Mizunuma, M., Hirata, D., Miyahara, K., Tsuchiya, E., & Miyakawa, T. (1998). Role of calcineurin and Mpk1 in regulating the onset of mitosis in budding yeast. *Letters to Nature*, 392(3), 303–306.
- Molinete, M., Dupuis, S., Brodsky, F. M., & Halban, P. A. (2001). Role of clathrin in the regulated secretory pathway of pancreatic β-cells. *Journal of cell science*, 114(16), 3059–66.
- Mooibroek, M. J., Michiel, D. F., & Wang, J. H. (1987). Clathrin light chains are calcium-binding proteins. *The Journal of biological chemistry*, 262(1), 25–8.
- Moon, A. L., Janmey, P. A., Louie, A., & Drubin, D. G. (1993). Cofilin Is an Essential Component of the Yeast Cortical Cytoskeleton. *The Journal of cell biology*, 120(2), 421–435.
- Moser, M. J., Flory, M. R., & Davis, T. N. (1997). Calmodulin localizes to the spindle pole body of Schizosaccharomyces pombe and performs an essential function in chromosome segregation. *Journal of cell science*, 110(Pt 5), 1805–12.
- Moser, M. J., Geiser, J. R., & Davis, T. N. (1996). Ca 2ε -Calmodulin Promotes Survival of Pheromone-Induced Growth Arrest by Activation of Calcineurin and Ca 2ε -Calmodulin-Dependent Protein Kinase. *Molecular and cellular biology*, 16(9), 4824–4831.
- Mueller, S. C., & Branton, D. (1984). Identification of coated vesicles in Saccharomyces cerevisiae. *The Journal of cell biology*, 98(1), 341–6.
- Muller, E. G. D., Snydsman, B. E., Novik, I., Hailey, D. W., Gestaut, D. R., Niemann, C. A., Toole, E. T. O., et al. (2005). The Organization of the Core Proteins of the Yeast Spindle Pole Body. *Molecular biology of the cell*, 16(7), 3341–3352.
- Mullins, C., & Bonifacino, J. S. (2001). Structural Requirements for Function of Yeast GGAs in Vacuolar Protein Sorting , α -Factor Maturation , and Interactions with Clathrin. *Molecular and cellular biology*, 21(23), 7981–7994.

- Munn, A. L., & Riezman, H. (1994). Endocytosis is required for the growth of vacuolar H(+)-ATPase-defective yeast: identification of six new END genes. *The Journal of cell biology*, 127(2), 373–86.
- Munn, A. L., Silveira, L., & Elgort, M. (1991). Viability of Clathrin Heavy-Chain-Deficient Saccharomyces cerevisiae Is Compromised by Mutations at Numerous Loci : Implications for the Suppression Hypothesis. *Molecular and cellular biology*, 11(8), 3868–3878.
- Myers, M. D., & Payne. (2013). Clathrin, adaptors and disease: insights from the yeast Saccharomyces cerevisiae. *Frontiers in bioscience*, 18, 862–891.
- Nakamura, T., Liu, Y., Hiratal, D., Nambal, H., Harada, S., Hirokawa, T., & Miyakawa, T. (1993). FK506-sensitive regulation of intracellular ions in yeast is an important determinant for adaptation to high salt stress conditions. *The EMBO journal*, 12(11), 4063–4071.
- Nannapaneni, S., Wang, D., Jain, S., Schroeder, B., Highfill, C., Reustle, L., Pittsley, D., *et al.* (2010). The yeast dynamin-like protein Vps1:vps1 mutations perturb the internalization and the motility of endocytic vesicles and endosomes via disorganization of the actin cytoskeleton. *European journal of cell biology*, 89(7), 499–508.
- Newpher, T. M., Idrissi, F., Geli, M. I., & Lemmon, S. K. (2006). Novel Function of Clathrin Light Chain in Promoting Endocytic Vesicle Formation. *Molecular biology of the cell*, 17(10), 4343– 4352.
- Newpher, T. M., & Lemmon, S. K. (2006). Clathrin is important for normal actin dynamics and progression of Sla2p-containing patches during endocytosis in yeast. *Traffic*, 7(5), 574–88.
- Newpher, T. M., Smith, R. P., Lemmon, V., & Lemmon, S. K. (2005). In vivo dynamics of clathrin and its adaptor-dependent recruitment to the actin-based endocytic machinery in yeast. *Developmental cell*, 9(1), 87–98.
- Niswonger, M. L., & O´Halloran, T. J. (1997). A novel role for clathrin in cytokinesis. *Proceedings of the National Academy of Sciences of the United States of America*, 94(8), 8575–8578.
- Nothwehr, S. E., Conibear, E., & Stevens, T. H. (1995). Golgi and Vacuolar Membrane Proteins Reach the Vacuole in vpsl Mutant Yeast Cells via the Plasma Membrane. *The Journal of Cell Biology*, 129(1), 35–46.
- Näthke, I., Hill, B. L., Parham, P., & Brodsky, F. M. (1990). The calcium-binding site of clathrin light chains. *The Journal of biological chemistry*, 265(30), 18621–7.
- Näthke, I. S., Heuser, J., Lupas, a, Stock, J., Turck, C. W., & Brodsky, F. M. (1992). Folding and trimerization of clathrin subunits at the triskelion hub. *Cell*, 68(5), 899–910.
- Ohno, H. (2006). Physiological roles of clathrin adaptor AP complexes: lessons from mutant animals. *Journal of biochemistry*, 139(6), 943–8.
- Ohya, Y., Uno, I., Ishikawa, T., & Anraku, Y. (1987). Purification and biochemical properties of calmodulin from Saccharomyces cerevisiae. *European journal of biochemistry*, 168(1), 13–9.

- Ohya, Y., & Botstein, D. (1994a). Diverse essential functions revealed by complementing yeast calmodulin mutants. *Science*, 263(5149), 963–6.
- Ohya, Y., & Botstein, D. (1994b). Structure-Based Systematic Isolation of Conditional-Lethal Mutations. *Genetics*, 138(4), 1041–1054.
- Ohya, Y., Kawasaki, H., & Suzukis, K. (1991). Two Yeast Genes Encoding Calmodulin-dependent Protein Kinases. *The Journal of biological chemistry*, 266(19), 12784–12794.
- Okamoto, C. T., McKinney, J., & Jeng, Y. Y. (2000). Clathrin in mitotic spindles. *American journal of physiology. Cell physiology*, 279(2), 369–74.
- Orci, L., Stamnes, M., Ravazzola, M., Perrelet, A., So, T. H., Rothman, J. E., & Geneva, C.-. (1997). Bidirectional Transport by Distinct Populations of COPI-Coated Vesicles. *Cell*, 90(7), 335–349.
- Osman, M. A., & Cerione, R. A. (1998). Iqg1p, a yeast homologue of the mammalian IQGAPs, mediates cdc42p effects on the actin cytoskeleton. *The Journal of cell biology*, 142(2), 443–55.
- Owen, D. J. (2004). Linking endocytic cargo to clathrin : structural and functional insights into coated vesicle formation. *Biochemical Society transactions*, 32(Pt 1), 1–14.
- Owen, D. J., Collins, B. M., & Evans, P. R. (2004). Adaptors for clathrin coats: structure and function. *Annual review of cell and developmental biology*, 20, 153–91.
- O'Day, D. H. (2003). CaMBOT: profiling and characterizing calmodulin-binding proteins. *Cellular signalling*, 15(4), 347–54.
- O'Day, D. H., & Myre, M. A. (2004). Calmodulin-binding domains in Alzheimer's disease proteins: extending the calcium hypothesis. *Biochemical and biophysical research communications*, 320(4), 1051–4.
- O'Halloran, T. J., & Anderson, R. G. (1992). Characterization of the clathrin heavy chain from Dictyostelium discoideum. *DNA and cell biology*, 11(4), 321–30.
- Pashkova, N., Gakhar, L., Winistorfer, S. C., Sunshine, A. B., Rich, M., Dunham, M. J., Yu, L., *et al.* (2013). The yeast Alix homolog Bro1 functions as a ubiquitin receptor for protein sorting into multivesicular endosomes. *Developmental cell*, 25(5), 520–33.
- Pathmanathan, S., Hamilton, E., Atcheson, E., & Timson, D. J. (2011). The interaction of IQGAPs with calmodulin-like proteins. *Biochemical Society transactions*, 39(2), 694–9.
- Payne, G. S., Baker, D., van Tuinen, E., & Schekman, R. (1988). Protein transport to the vacuole and receptor-mediated endocytosis by clathrin heavy chain-deficient yeast. *The Journal of cell biology*, 106(5), 1453–61.
- Payne, G. S., Hasson, T. B., Hasson, M. S., & Schekman, R. (1987). Genetic and Biochemical Characterization of Clathrin-Deficient Saccharomyces cerevisiae. *Molecular and cellular biology*, 7(11), 3888-98.
- Payne, G. S., & Schekman, R. (1985). A test of clathrin function in protein secretion and cell growth. *Science*, 230(4729), 1009–14.

- Payne, G. S., & Schekman, R. (1989). Clathrin: a Role in the Intracellular Retention of a Golgi Membrane Protein. *Science*, 245, 1358–1365.
- Pearse, B. M. (1975). Coated vesicles from pig brain: purification and biochemical characterization. *Journal of molecular biology*, 97(1), 93–8.
- Pearse, B. M., & Crowther, R. A. (1987). Structure and assembly of coated vesicles. *Annual review of biophysics and biophysical chemistry*, 16(6), 49–68.
- Pearse, B. M. (1982). Coated vesicles from human placenta carry ferritin, transferrin, and immunoglobulin G. *Proceedings of the National Academy of Sciences of the United States of America*, 79(1), 451–455.
- Pearse, B. M. (1988). Receptors compete fos adaptors found in plasma membrane coated pits. *The EMBO journal*, 7(11), 3331–3336.
- Pelham, H. R. B. (2002). Insights from yeast endosomes. *Current opinion in cell biology*, 14(4), 454–62.
- Perrais, D., & Merrifield, C. J. (2005). Dynamics of endocytic vesicle creation. *Developmental cell*, 9(5), 581–92.
- Persechini, A., Kretsinger, R. H., & Davis, T. N. (1991). Calmodulins with deletions in the central helix functionally replace the native protein in yeast cells. *Proceedings of the National Academy of Sciences of the United States of America*, 88(2), 449–52.
- Peters, C., Bayer, M. J., Bühler, S., Andersen, J. S., Mann, M., & Mayer, A. (2001). Trans-complex formation by proteolipid channels in the terminal phase of membrane fusion. *Nature*, 409(6820), 581–8.
- Peters, C. (1999). Control of the Terminal Step of Intracellular Membrane Fusion by Protein Phosphatase 1 . *Science*, 285(5430), 1084–1087.
- Peters, C., & Mayer, A. (1998). Ca2+/calmodulin signals the comletion of docking and triggers a late step of vacuole fusion. *Nature*, 396(6711), 575–580.
- Pfeffer, S. R. (2011). Entry at the trans-face of the Golgi. *Cold Spring Harbor perspectives in biology*, 3(3), 1–11.
- Phan, H. L., Finlay, J. A, Chu, D. S., Tan, P. K., Kirchhausen, T., & Payne, G. S. (1994). The Saccharomyces cerevisiae APS1 gene encodes a homolog of the small subunit of the mammalian clathrin AP-1 complex: evidence for functional interaction with clathrin at the Golgi complex. *The EMBO journal*, 13(7), 1706–17.
- Piao, H. L., Machado, I. M. P., & Payne, G. S. (2007). NPFXD-mediated Endocytosis Is Required for Polarity and Function of a Yeast Cell Wall Stress Sensor. *Molecular biology of the cell*, 18(1), 57–65.
- Pishvaee, B., Costaguta, G., Yeung, B. G., Ryazantsev, S., Greener, T., Greene, L. E., Eisenberg, E., *et al.* (2000). A yeast DNA J protein required for uncoating of clathrin-coated vesicles in vivo. *Nature cell biology*, 2(12), 958–63.
- Pishvaee, B., Munn, A., & Payne, G. S. (1997). A novel structural model for regulation of clathrin function. *The EMBO journal*, 16(9), 2227–39.

- Pley, U. M. (1995). The Interaction of Calmodulin with Clathrin-coated vesicles, triskelions, and light chains. *The Journal of biological chemistry*, 270(5), 2395–2402.
- Popoff, V., Mardones, G. A, Bai, S.-K., Chambon, V., Tenza, D., Burgos, P. V, Shi, A., *et al*. (2009). Analysis of articulation between clathrin and retromer in retrograde sorting on early endosomes. *Traffic*, 10(12), 1868–80.
- Popoff, V., Mardones, G. A, Tenza, D., Rojas, R., Lamaze, C., Bonifacino, J. S., Raposo, G., *et al*. (2007). The retromer complex and clathrin define an early endosomal retrograde exit site. *Journal of cell science*, 120(Pt 12), 2022–31.
- Prosser, D. C., Drivas, T. G., Maldonado-Báez, L., & Wendland, B. (2011). Existence of a novel clathrin-independent endocytic pathway in yeast that depends on Rho1 and formin. *The Journal of cell biology*, 195(4), 657–71.
- Pryor, P. R., Mullock, B. M., Bright, N. A., Gray, S. R., & Luzio, J. P. (2000). The role of intraorganellar Ca(2+) in late endosome-lysosome heterotypic fusion and in the reformation of lysosomes from hybrid organelles. *The Journal of cell biology*, 149(5), 1053–62.
- Puertollano, R. (2006). Endocytic Trafficking and Human Diseases. *Endosomes*, *Chapter 10*, 119–131.
- Qualmann, B., & Kessels, M. (2002). Endocytosis and the cytoskeleton . *International review of cytology*, 220, 93-144.
- Racioppi, L., & Means, A. R. (2012). Calcium/calmodulin-dependent protein kinase kinase 2: roles in signaling and pathophysiology. *The Journal of biological chemistry*, 287(38), 31658–65.
- Radding, W., Williams, J. P., McKenna, M. a, Tummala, R., Hunter, E., Tytler, E. M., & McDonald, J. M. (2000). Calmodulin and HIV type 1: interactions with Gag and Gag products. *AIDS research and human retroviruses*, 16(15), 1519–25.
- Radulescu, A. E., & Shields, D. (2012). Clathrin is required for postmitotic Golgi reassembly. *FASEB journal*, 26(1), 129–36.
- Radulescu, A. E., Siddhanta, A., & Shields, D. (2007). A Role for Clathrin in Reassembly of the Golgi Apparatus. *Molecular biology of the cell*, 18(1), 94–105.
- Raiborg, C., Bache, K. G., Mehlum, A., Stang, E., & Stenmark, H. (2001). Hrs recruits clathrin to early endosomes. *The EMBO journal*, 20(17), 5008–21.
- Raiborg, C., Bache, K. G., Gillooly, D. J., Madshus, I. H., Stang, E., & Stenmark, H. (2002). Hrs sorts ubiquitinated proteins into clathrin-coated microdomains of early endosomes. *Nature cell biology*, 4(5), 394–8.
- Raiborg, C., Wesche, J., Malerød, L., & Stenmark, H. (2006). Flat clathrin coats on endosomes mediate degradative protein sorting by scaffolding Hrs in dynamic microdomains. *Journal of cell science*, 119(Pt 12), 2414–24.
- Raig, S. U. W. C. (1997). The Γ¬LWEQ module : a conserved sequence that signifies F-actin. *Proceedings of the National Academy of Sciences of the United States of America*, 94(5), 5679–5684.

- Rapoport, I., Boll, W., Yu, A., Bo, T., & Kirchhausen, T. (2008). A Motif in the Clathrin Heavy Chain Required for the Hsc70 / Auxilin Uncoating Reaction. *Molecular biology of the cell*, 19(1), 405–413.
- Raths, S., Rohrer, J., Crausaz, F., & Riezman, H. (1993). end3 and end4 : Two Mutants Defective in Receptor-mediated and Fluid-phase Endocytosis in Saccharomyces cer isiae. *The Journal of Cell Biology*, 120(1), 55–65.
- Raymond, C., Howald-Stevenson, I., Vater, C. A., & Stevens, T. H. (1992). Morphological classification of the yeast vacuolar protein-sorting mutants: evidence for a prevacuolar compartment in class E vps mutants. *Molecular biology of the cell*, 23(14), 1389–1402.
- Razi, M., & Futter, C. E. (2006). Distinct Roles for Tsg101 and Hrs in Multivesicular Body Formation and Inward Vesiculation. *Molecular biology of the cell*, 17(8), 3469–3483.
- Reck-peterson, S. L., Provance, D. W., Mooseker, M. S., & Mercer, J. A. (2000). Class V myosins. *Biochimica et biophysica acta*, 1496(1), 36–51.
- Redding, K., Seeger, M., Payne, G. S., & Fuller, R. S. (1996). The effects of clathrin inactivation on localization of Kex2 protease are independent of the TGN localization signal in the cytosolic tail of Kex2p. *Molecular biology of the cell*, 7(11), 1667–77.
- Reider, A., Barker, S. L., Mishra, S. K., Im, Y. J., Maldonado-Báez, L., Hurley, J. H., Traub, L. M., *et al.* (2009). Syp1 is a conserved endocytic adaptor that contains domains involved in cargo selection and membrane tubulation. *The EMBO journal*, 28(20), 3103–16.
- Richter, C., West, M., & Odorizzi, G. (2007). Dual mechanisms specify Doa4-mediated deubiquitination at multivesicular bodies. *The EMBO journal*, 26(10), 2454–64.
- Ricotta, D., Conner, S. D., Schmid, S. L., von Figura, K., & Honing, S. (2002). Phosphorylation of the AP2 mu subunit by AAK1 mediates high affinity binding to membrane protein sorting signals. *The Journal of cell biology*, 156(5), 791–5.
- Robinson, J. S., Klionsky, D. J., Banta, L. M., & Emr, S. D. (1988). Protein Sorting in Saccharomyces cerevisiae : Isolation of Mutants Defective in the Delivery and Processing of Multiple Vacuolar Hydrolases. *Molecular and cellular biology*, 8(11), 4936–4948.
- Robison, A. J. (2014). Emerging role of CaMKII in neuropsychiatric disease. *Trends in neurosciences*, pii: S0166-2236(14)00106-4.
- Rodal, A. A., Manning, A. L., Goode, B. L., & Drubin, D. G. (2003). Negative Regulation of Yeast WASp by Two SH3 Domain-Containing Proteins. *Current biology*, 13(12), 1000–1008.
- Roth, T. F., & Potter, K. R. (1964). Yolk protein uptake in the oocyte of the mosquito Aedes Aegypti.L. *The Journal of cell biology*, 20, 313–332.
- Rothman, J., & Stevens, T. H. (1986). Protein Sorting in Yeast : Mutants Defective in Vacuole Biogenesis Mislocalize Vacuolar Proteins into the Late Secretory Pathway. *Cell*, 47(12), 1041–1051.

- Rotty, J. D., Wu, C., & Bear, J. E. (2013). New insights into the regulation and cellular functions of the ARP2/3 complex. *Nature reviews. Molecular cell biology*, 14(1), 7–12.
- Royle, S. J. (2006). The cellular functions of clathrin. *Cellular and molecular life sciences*, 63(16), 1823–32.
- Royle, S. J. (2012). The role of clathrin in mitotic spindle organisation. *Journal of cell science*, 125(Pt 1), 19–28.
- Royle, S. J., Bright, N. A., & Lagnado, L. (2005). Clathrin is required for the function of the mitotic spindle. *Nature*, 434(7037), 1152–1157.
- Rusnak, F., & Mertz, P. (2000). Calcineurin : Form and Function. *Physiological Reviews*, 80(4), 1483–1522.
- Russell, M. R. G., Shideler, T., Nickerson, D. P., West, M., & Odorizzi, G. (2012). Class E compartments form in response to ESCRT dysfunction in yeast due to hyperactivity of the Vps21 Rab GTPase. *Journal of cell science*, 125(Pt 21), 5208–20.
- Sachse, M., Urbe, S., Oorschot, V., Strous, G. J., & Klumperman, J. (2002). Bilayered Clathrin Coats on Endosomal Vacuoles Are Involved in Protein Sorting toward Lysosomes. *Molecular biology of the cell*, 13(4), 1313–1328.
- Saffarian, S., Cocucci, E., & Kirchhausen, T. (2009). Distinct dynamics of endocytic clathrin-coated pits and coated plaques. *PLoS biology*, 7(9), 1–18.
- Saint-Pol, A., Yélamos, B., Amessou, M., Mills, I. G., Dugast, M., Tenza, D., Schu, P., *et al.* (2004). Clathrin adaptor epsinR is required for retrograde sorting on early endosomal membranes. *Developmental cell*, 6(4), 525–38.
- Sakaba, T., & Neher, E. (2001). Calmodulin Mediates Rapid Recruitment of Fast-Releasing Synaptic Vesicles at a Calyx-Type Synapse. *Neuron*, 32(6), 1119–1131.
- Saksena, S., Sun, J., Chu, T., & Emr, S. D. (2007). ESCRTing proteins in the endocytic pathway. *Trends in biochemical sciences*, 32(12), 561–73.
- Salama, N. R., Yeung, T., & Schekman, R. W. (1993). The Secl 3p complex and reconstitution of vesicle budding from the ER with purified cytosolic proteins. *The EMBO journal*, 12(11), 4073–4082.
- Salisbury, J. L., Condeelis, J. S., & Satir, P. (1980a). Evidence for the involvement of calmodulin in endocytosis. *Annals of the New York Academy of Sciences*, 356, 429–32.
- Salisbury, J. L., Condeelis, J. S., & Satir, P. (1980b). Role of coated vesicles, microfilaments, and calmodulin in receptor-mediated endocytosis by cultured B lymphoblastoid cells. *The Journal of cell biology*, 87(1), 132–41.
- Sambrook, J., & Russel, D. W. (2001). Molecular cloning : a laboratory manual, 3rd edn. *Cold Spring Harbor Laboratory Press*, 1.
- Scarmato, P., & Kirchhausen, T. (1990). Analysis of clathrin light chain-heavy chain interactions using truncated mutants of rat liver light chain LCB3. *The Journal of biological chemistry*, 265(7), 3661–8.

- Schaerer-Brodbeck, C., & Riezman, H. (2000a). Functional interactions between the p35 subunit of the Arp2/3 complex and calmodulin in yeast. *Molecular biology of the cell*, 11(4), 1113–27.
- Schaerer-Brodbeck, C., & Riezman, H. (2000b). Saccharomyces cerevisiae Arc35p works through two genetically separable calmodulin functions to regulate the actin and tubulin cytoskeletons. *Journal of cell science*, *113(Pt 3)*, 521–32.
- Schott, D. H., Collins, R. N., & Bretscher, A. (2002). Secretory vesicle transport velocity in living cells depends on the myosin-V lever arm length. *The Journal of cell biology*, 156(1), 35–9.
- Seaman, M. N. J. (2012). The retromer complex - endosomal protein recycling and beyond. *Journal of cell science*, 125(Pt 20), 4693–702.
- Seaman, M. N. J., Gautreau, A., & Billadeau, D. D. (2013). Retromer-mediated endosomal protein sorting: all WASHed up! *Trends in cell biology*, 23(11), 522–8.
- Seaman, M. N. J., Marcusson, E. G., Cereghino, J. L., & Emr, S. D. (1997a). Endosome to Golgi Retrieval of the Vacuolar Protein Sorting Receptor, Vps10p, Requires the Function of the VPS29 , VPS30 , and VPS35 Gene Products. *The Journal of cell biology*, 137(1), 79–92.
- Seaman, M. N., McCaffery, J. M., & Emr, S. D. (1998). A membrane coat complex essential for endosome-to-Golgi retrograde transport in yeast. *The Journal of cell biology*, 142(3), 665–81.
- Seeger, M., & Payne, G. S. (1992). A role for clathrin in the sorting of vacuolar proteins in the Golgi complex of yeast. *The EMBO journal*, 11(8), 2811–8.
- Seeger, M., & Payne, G. S. (1992). Selective and Immediate Effects of Clathrin Heavy Chain Mutations on Golgi Membrane Protein Retention in Saccharomyces cerevisiae. *The Journal of cell biology*, 118(3), 531–540.
- Seibel, N. M., Eljouni, J., Nalaskowski, M. M., & Wolfgang, H. (2007). Nuclear localization of enhanced green fluorescent homomultimers. *Analytical biochemistry*, 368(1), 95–99.
- Sekiya-Kawasaki, M., Botstein, D., & Ohya, Y. (1998). Identification of functional connections between calmodulin and the yeast actin cytoskeleton. *Genetics*, 150(1), 43–58.
- Sekiya-Kawasaki, M., Groen, A. C., Cope, M. J. T. V, Kaksonen, M., Watson, H. a, Zhang, C., Shokat, K. M., *et al.* (2003). Dynamic phosphoregulation of the cortical actin cytoskeleton and endocytic machinery revealed by real-time chemical genetic analysis. *The Journal of cell biology*, 162(5), 765–72. d
- Shannon, K. B., & Li, R. (2000). A myosin light chain mediates the localization of the budding yeast IQGAP-like protein during contractile ring formation. *Current biology*, 10(12), 727–30.
- Shannon, K. B., & Li, R. (1999). The Multiple Roles of Cyk1p in the Assembly and Function of the Actomyosin Ring in Budding Yeast. *Molecular biology of the cell*, 10(2), 283–296.

- Shaw, J. D., Cummings, K. B., Huyer, G., Michaelis, S., & Wendland, B. (2001). Yeast as a model system for studying endocytosis. *Experimental cell research*, 271(1), 1–9.
- Sherman, F. (2002). Getting Started with Yeast. *Methods in enziymology*, 350, 3–41.
- Shi, A., Sun, L., Banerjee, R., Tobin, M., Zhang, Y., & Grant, B. D. (2009). Regulation of endosomal clathrin and retromer-mediated endosome to Golgi retrograde transport by the J-domain protein RME-8. *The EMBO journal*, 28(21), 3290–302.
- Shih, S. C., Katzmann, D. J., Schnell, J. D., Sutanto, M., Emr, S. D., & Hicke, L. (2002). Epsins and Vps27p/Hrs contain ubiquitin-binding domains that function in receptor endocytosis. *Nature cell biology*, 4(5), 389–93.
- Silady, R. A., Ehrhardt, D. W., Jackson, K., Faulkner, C., Oparka, K., & Somerville, C. R. (2008). The GRV2/RME-8 protein of Arabidopsis functions in the late endocytic pathway and is required for vacuolar membrane flow. *The Plant journal : for cell and molecular biology*, 53(1), 29–41.
- Silveira, L. A., Wong, D. H., Masiarz, F. R., & Schekman, R. (1990). Yeast Clathrin Has a Distinctive Light Chain That Is Important for Cell Growth. *The Journal of cell biology*, 111(4), 1437–1449.
- Singer-krüger, B., Nemoto, Y., Daniell, L., Ferro-novick, S., & Camilli, P. De. (1998). Synaptojanin family members are implicated in endocytic membrane traffic in yeast. *Journal of cell science*, 111(Pt 22), 3347–3356.
- Sirotkin, H., Morrow, B., DasGupta, R., Goldberg, R., Patanjali, S. R., Shi, G., Cannizzaro, L., *et al.* (1996). Isolation of a new clathrin heavy chain gene with muscle-specific expression from the region commonly deleted in velo-cardio-facial syndrome. *Human molecular genetics*, 5(5), 617–24.
- Sites, P., Hill, B. L., Drickamers, K., Brodskyll, F. M., & Parham, P. (1988). Identification of the phosphorylation sites of clathrin light chain LCb. *The Journal of biological chemistry*, 263(12), 5499–5501.
- Skruzny, M., Brach, T., Ciuffa, R., Rybina, S., Wachsmuth, M., & Kaksonen, M. (2012). Molecular basis for coupling the plasma membrane to the actin cytoskeleton during clathrin-mediated endocytosis. *Proceedings of the National Academy of Sciences of the United States of America*, 109(38), E2533–42.
- Slagsvold, T., Pattni, K., Malerød, L., & Stenmark, H. (2006). Endosomal and non-endosomal functions of ESCRT proteins. *Trends in cell biology*, 16(6), 317–26.
- Smaczynska-de Rooij, I. I., Allwood, E. G., Aghamohammadzadeh, S., Hettema, E. H., Goldberg, M. W., & Ayscough, K. R. (2010). A role for the dynamin-like protein Vps1 during endocytosis in yeast. *Journal of cell science*, 123(Pt 20), 3496–506.
- Smaczynska-de Rooij, I. I., Allwood, E. G., Mishra, R., Booth, W. I., Aghamohammadzadeh, S., Goldberg, M. W., & Ayscough, K. R. (2012). Yeast dynamin Vps1 and amphiphysin Rvs167 function together during endocytosis. *Traffic*, 13(2), 317–28.
- Smith, C. M., & Chircop, M. (2012). Clathrin-Mediated Endocytic Proteins are Involved in Regulating Mitotic Progression and Completion. *Traffic*, 13(12), 1628–1641.

- Spang, A., Grein, K., & Schiebel, E. (1996). The spacer protein Spc110p targets calmodulin to the central plaque of the yeast spindle pole body. *Journal of cell science*, *109 (Pt 9)*, 2229–37. R
- Stack, J. H., Herman, P. K., Schu, P. V, & Emr, S. D. (1993). A membrane-associated complex containing the Vpsl 5 protein kinase and the Vps34 Pi 3-kinase is essential for protein sorting to the yeast lysosome-like vacuole. *The EMBO journal*, 12(5), 2195–2204.
- Starovasnik, M. A., Davis, T. N., & Klevit, R. E. (1993). Similarities and differences between yeast and vertebrate calmodulin: an examination of the calcium-binding and structural properties of calmodulin from the yeast Saccharomyces cerevisiae. *Biochemistry*, 32(13), 3261–70.
- Stathopoulos, A. M., & Cyert, M. S. (1997). Calcineurin acts through the CRZ1/TCN1-encoded transcription factor to regulate gene expression in yeast. *Genes & Development*, 11(24), 3432–3444.
- Stefan, C. J., Audhya, A., & Emr, S. D. (2002). The Yeast Synaptojanin-like Proteins Control the Cellular Distribution of Phosphatidylinositol (4 , 5) -Bisphosphate. *Molecular biology of the cell*, 13(2), 542–557.
- Stefan, C. J., Padilla, S. M., Audhya, A., & Emr, S. D. (2005). The Phosphoinositide Phosphatase Sjl2 Is Recruited to Cortical Actin Patches in the Control of Vesicle Formation and Fission during Endocytosis. *Molecular and cellular biology*, 25(8), 2910–2923.
- Stepp, J. D., Huang, K., & Lemmon, S. K. (1997). The Yeast Adaptor Protein Complex, AP-3, Is Essential for the Efficient Delivery of Alkaline Phosphatase by the Alternate Pathway to the Vacuole. *The Journal of cell biology*, 139(7), 1761–1774.
- Stevens, R. C., & Davis, T. N. (1998). Mlc1p Is a Light Chain for the Unconventional Myosin Myo2p in Saccharomyces cerevisiae. *Journal of Cell Biology*, 142(3), 711–722.
- Stimpson, H. E. M., Toret, C. P., Cheng, A. T., Pauly, B. S., & Drubin, D. G. (2009). Early-Arriving Syp1p and Ede1p Function in Endocytic Site Placement and Formation in Budding Yeast. *Molecular biology of the cell*, 20(22), 4640–4651.
- Stirling, D. A., Welch, K. A., & Stark, M. J. (1994). Interaction with calmodulin is required for the function of Spc110p, an essential component of the yeast spindle pole body. *The EMBO journal*, 13(18), 4329–42.
- Stoorvogel, W., Oorschot, V., & Geuze, H. J. (1996). A Novel Class of Clathrin-coated Vesicles Budding from Endosomes. *The Journal of cell biology*, 132(1), 21–33.
- Stradalova, V., Blazikova, M., Grossmann, G., Opekarová, M., Tanner, W., & Malinsky, J. (2012). Distribution of cortical endoplasmic reticulum determines positioning of endocytic events in yeast plasma membrane. *PloS one*, 7(4), 1–11.
- Strynadka, N. C. J., & James, M. N. G. (1990). Model for the Interaction of Amphiphilic Helices With Troponin C and Calmodulin. *Proteins*, 7(3), 234–248.

- Sun, G. H., Hirata, A., Ohya, Y., & Anraku, Y. (1992). Mutations in yeast calmodulin cause defects in spindle pole body functions and nuclear integrity. *The Journal of cell biology*, 119(6), 1625–39.
- Sun, Y., Carroll, S., Kaksonen, M., Toshima, J. Y., & Drubin, D. G. (2007). PtdIns(4,5)P2 turnover is required for multiple stages during clathrin- and actin-dependent endocytic internalization. *The Journal of cell biology*, 177(2), 355–67.
- Sun, Y., Kaksonen, M., Madden, D. T., Schekman, R., & Drubin, D. G. (2005). Interaction of Sla2p's ANTH domain with PtdIns(4,5)P2 is important for actin-dependent endocytic internalization. *Molecular biology of the cell*, 16(2), 717–30.
- Sun, Y., Martin, A. C., & Drubin, D. G. (2006). Endocytic internalization in budding yeast requires coordinated actin nucleation and myosin motor activity. *Developmental cell*, 11(1), 33–46.
- Sundberg, H. A., Goetsch, L., Byers, B., & Davis, T. N. (1996). Role of Calmodulin and Spc 110p Interaction in the Proper Assembly of Spindle Pole Body Components. *The Journal of cell biology*, 133(1), 111–124.
- Suzuki, R., Toshima, J. Y., & Toshima, J. (2012). Regulation of clathrin coat assembly by Eps15 homology domain-mediated interactions during endocytosis. *Molecular biology of the cell*, 23(4), 687–700.
- Svitkina, T. M., & Borisy, G. G. (1999). Arp2/3 Complex and Actin Depolymerizing Factor/Cofilin in Dendritic Organization and Treadmilling of Actin Filament Array in Lamellipodia. *The Journal of cell biology*, 145(5), 1009–1026.
- Swindells, M. B., & Ikura, M. (1996). Pre-formation of the semi-open conformation by the apo-calmodulin C-terminal domain and implications binding IQ-motifs. *Nature structural & molecular biology*, 3(6), 501–504.
- Takizawa, P. A., Sil, A., Swedlow, J. R., Herskowitz, I., & Vale, R. D. (1997). Actin-dependent localization of an RNA encoding a cell-fate determinant in yeast. *Letters to Nature*, 389(9), 90–93.
- Tebar, F., Villalonga, P., Sorkina, T., Agell, N., Sorkin, A., & Enrich, C. (2002). Calmodulin Regulates Intracellular Trafficking of Epidermal Growth Factor Receptor and the MAPK Signaling Pathway. *Molecular biology of the cell*, 13(6), 2057–2068.
- Temkin, P., Lauffer, B., Jager, S., Cimermancic, P., Krogan, N. J., & von Zastrow, M. (2011). SNX27 mediates retromer tubule entry and endosome-to-plasma membrane trafficking of signalling receptors. *Nature cell biology*, 13(6), 715–721.
- Thieman, J. R., Mishra, S. K., Ling, K., Doray, B., Anderson, R. A., & Traub, L. M. (2009). Clathrin regulates the association of PIPKIgamma661 with the AP-2 adaptor beta2 appendage. *The Journal of biological chemistry*, 284(20), 13924–39.
- Anderson, T., Drakenberg, T., Fokskn, S., & Thulin, E. (1982). Characterization of the Ca2 Binding Sites of Calmodulin from Bovine Testis Using 43Ca and ' 13Cd NMR. *European journal of biochemistry*, 126(3), 501–505.
- Tidow, H., & Nissen, P. (2013). Structural diversity of calmodulin binding to its target sites. *The FEBS journal*, 280(21), 5551–65.

- Toret, C. P., Lee, L., Sekiya-Kawasaki, M., & Drubin, D. G. (2008). Multiple pathways regulate endocytic coat disassembly in Saccharomyces cerevisiae for optimal downstream trafficking. *Traffic*, 9(5), 848–59.
- Toshima, J., Toshima, J. Y., Duncan, M. C., Cope, M. J. T. V, Sun, Y., Martin, A. C., Anderson, S., *et al.* (2007). Negative Regulation of Yeast Eps15-like Arp2 / 3 Complex Activator , Pan1p , by the Hip1R-related Protein , Sla2p , during Endocytosis. *Molecular biology of the cell*, 18(2), 658–668.
- Towler, M. C., Gleeson, P. A., Hoshino, S., Rahkila, P., Manalo, V., Ohkoshi, N., Ordahl, C., *et al.* (2004). Clathrin Isoform CHC22 , a Component of Neuromuscular and Myotendinous Junctions, Binds Sorting Nexin 5 and Has Increased Expression during Myogenesis and Muscle Regeneration. *Molecular biology of the cell*, 15(7), 3181–3195.
- Traub, L. M. (2005). Common principles in clathrin-mediated sorting at the Golgi and the plasma membrane. *Biochimica et biophysica acta*, 1744(3), 415–37.
- Traub, L. M. (2009). Clathrin couture: fashioning distinctive membrane coats at the cell surface. *PLoS biology*, 7(9), 1–5.
- Umeda, A., Meyerholz, A., & Ungewickell, E. (2000). Identification of the universal cofactor (auxilin 2) in clathrin coat dissociation. *European journal of cell biology*, 79(5), 336–42.
- Ungewickell, E., & Ungewickell, H. (1991). Bovine brain clathrin light chains impede heavy chain assembly in vitro. *The Journal of biological chemistry*, 266(19), 12710–4.
- Ungewickell, E., & Hinrichsen, L. (2007). Endocytosis: clathrin-mediated membrane budding. *Current opinion in cell biology*, 19(4), 417–25.
- Ungewickell, E., Ungewickell, H., & Holstein, S. E. H. (1997). Functional Interaction of the Auxilin J Domain with the Nucleotide- and Substrate-binding Modules of Hsc70. *The Journal of biological chemistry*, 272(31), 19594–19600.
- Ungewickell, E., & Branton, D. (1981). Assembly units of clatrhin coats. *Nature*, 289(5796), 420–422.
- Ungewickell, E., Ungewickell, H., Holstein, S. E. H., Lindner, R., Prasad, K., Barouch, W., Martin, B., *et al*. (1995). Role of auxilin in uncoating clathrin-coated vesicles. *Nature*, 378(6557), 632–635.
- Valdivia, R. H., Baggott, D., Chuang, J. S., & Schekman, R. W. (2002). The yeast clathrin adaptor protein complex 1 is required for the efficient retention of a subset of late Golgi membrane proteins. *Developmental cell*, 2(3), 283–94.
- van de Graaf, S. F. J., Rescher, U., Hoenderop, J. G. J., Verkaart, S., Bindels, R. J. M., & Gerke, V. (2008). TRPV5 is internalized via clathrin-dependent endocytosis to enter a Ca2+-controlled recycling pathway. *The Journal of biological chemistry*, 283(7), 4077–86.
- van der Bliek, A. M., & Meyerowitz, E. M. (1991). Dynamin-like protein encoded by the Drosophila shibire gene associated with vesicular traffic. *Letters to Nature*, 351(6325), 411–414.

- van Weering, J. R. T., Verkade, P., & Cullen, P. J. (2010). SNX – BAR proteins in phosphoinositide-mediated , tubular-based endosomal sorting. *Seminars in Cell and Developmental Biology*, 21(4), 371–380.
- Verstreken, P., Koh, T.-W., Schulze, K. L., Zhai, R. G., Hiesinger, P. R., Zhou, Y., Mehta, S. Q., *et al.* (2003). Synaptojanin is recruited by endophilin to promote synaptic vesicle uncoating. *Neuron*, 40(4), 733–48.
- Vida, T. A., & Emr, S. D. (1995). A new vital stain for visualizing vacuolar membrane dynamics and endocytosis in yeast. *The Journal of cell biology*, 128(5), 779–92.
- Vida, T. A., Huyer, G., & Emr, S. D. (1993). Yeast vacuolar proenzymes are sorted in the late Golgi complex and transported to the vacuole via a prevacuolar endosome-like compartment. *The Journal of cell biology*, 121(6), 1245–56.
- Wakeham, D. E., Abi-Rached, L., Towler, M. C., Wilbur, J. D., Parham, P., & Brodsky, F. M. (2005). Clathrin heavy and light chain isoforms originated by independent mechanisms of gene duplication during chordate evolution. *Proceedings of the National Academy of Sciences of the United States of America*, 102(20), 7209–14.
- Wall, M. E., Clarage, J. B., & Phillips, G. N. (1997). Motions of calmodulin characterized using both Bragg and diffuse X-ray scattering. *Structure*, 5(12), 1599–1612.
- Walsh, M. P. (1994). Calmodulin and the regulation of smooth muscle contraction. *Molecular and cellular biochemistry*, 135(1), 21–41.
- Walsh, P., Bursać, D., Law, Y. C., Cyr, D., & Lithgow, T. (2004). The J-protein family: modulating protein assembly, disassembly and translocation. *EMBO reports*, 5(6), 567–71.
- Walther, T. C., Brickner, J. H., Aguilar, P. S., Bernales, S., Pantoja, C., & Walter, P. (2006). Eisosomes mark static sites of endocytosis. *Nature*, 439(7079), 998–1003.
- Wang, D., Epstein, D., Khalaf, O., Srinivasan, S., Williamson, W. R., Fayyazuddin, A., Quiocho, F. A., *et al.* (2014). Ca2+-Calmodulin regulates SNARE assembly and spontaneous neurotransmitter release via v-ATPase subunit V0a1. *The Journal of cell biology*, 205(1), 21–31.
- Wang, Y. J., Wang, J., Sun, H. Q., Martinez, M., Sun, Y. X., Macia, E., Kirchhausen, T., *et al.* (2003). Phosphatidylinositol 4 phosphate regulates targeting of clathrin adaptor AP-1 complexes to the Golgi. *Cell*, 114(3), 299–310.
- Wayman, G. A., Lee, Y., Tokumitsu, H., Silva, A., & Thomas, R. (2009). Calmodulin-Kinases: Modulators of Neuronal Development and Plasticity. *Neuron*, 59(6), 914–931.
- Weinberg, J., & Drubin, D. G. (2011). Clathrin-mediated endocytosis in budding yeast. *Trends in cell biology*, 22(1), 1–13.
- Weissbachs, L., Settlemans, J., Kaladys, F., Snijderss, A. J., Murthybll, A. E., Yans, Y., & Bernards, A. (1994). Identification of a Human RasGAP-related Protein Containing Calmodulin-binding Motifs. *The Journal of biological chemistry*, 269(32), 20517–20521.

- Werner-washburne, M., Stone, D. E., & Craig, E. A. (1987). Complex Interactions among Members of an Essential Subfamily of hsp7O Genes in Saccharomyces cerevisiae. *Molecular and cellular biology*, 7(7), 2568–2577.
- Wilbur, J. D., Chen, C.-Y., Manalo, V., Hwang, P. K., Fletterick, R. J., & Brodsky, F. M. (2008). Actin binding by Hip1 (huntingtin-interacting protein 1) and Hip1R (Hip1-related protein) is regulated by clathrin light chain. *The Journal of biological chemistry*, 283(47), 32870–9.
- Wilbur, J. D., Hwang, P. K., Ybe, J. A., Lane, M., Sellers, B. D., Jacobson, M. P., Fletterick, R. J., *et al.* (2010). Conformation switching of clathrin light chain regulates clathrin lattice assembly. *Developmental cell*, 18(5), 841–848.
- Wilcox, C. A., Redding, K., Wright, R., & Fuller, R. S. (1992). Mutation of a tyrosine localization signal in the cytosolic tail of yeast Kex2 protease disrupts Golgi retention and results in default transport to the vacuole. *Molecular biology of the cell*, 3(12), 1353–71.
- Willox, A. K., & Royle, S. J. (2012). Functional a nalysis of interaction sites on the N-terminal domain of clathrin heavy chain. *Traffic*, (4), 1–13.
- Wilsbach, K., & Paynel, G. S. (1993). Vps1p, a member of the dynamin GTPase family , necessary for Golgi membrane protein retention in Saccharomyces cerevisiae. *The EMBO journal*, 12(8), 3049–3059.
- Winter, D., Podtelejnikov, A. V., Mann, M., & Li, R. (1997). The complex containing actin-related proteins Arp2 and Arp3 is required for the motility and integrity of yeast actin patches. *Current biology*, 7(7), 519–29.
- Withee, J. L., Mulholland, J., Jeng, R., & Cyert, M. S. (1997). An essential role of the yeast pheromone-induced Ca2+ signal is to activate calcineurin. *Molecular biology of the cell*, 8(2), 263–77.
- Wu, X.-S., McNeil, B. D., Xu, J., Fan, J., Xue, L., Melicoff, E., Adachi, R., *et al.* (2009). Ca(2+) and calmodulin initiate all forms of endocytosis during depolarization at a nerve terminal. *Nature neuroscience*, 12(8), 1003–10.
- Xia, Y., Tsai, A.-L., Berka, V., & Zweier, J. L. (1998). Superoxide Generation from Endothelial Nitric-oxide Synthase: A Ca2+/CALMODULIN-DEPENDENT AND TETRAHYDROBIOPTERIN REGULATORY PROCESS. *The Journal of biological chemistry*, 273(40), 25804–25808.
- Xiao, J., Kim, L. S., & Graham, T. R. (2006). Dissection of Swa2p / Auxilin Domain Requirements for Cochaperoning Hsp70 Clathrin-uncoating Activity In Vivo. *Molecular biology of the cell*, 17(7), 3281–3290.
- Xing, Y., Böcking, T., Wolf, M., Grigorieff, N., Kirchhausen, T., & Harrison, S. C. (2010). Structure of clathrin coat with bound Hsc70 and auxilin: mechanism of Hsc70-facilitated disassembly. *The EMBO journal*, 29(3), 655–65.
- Yagi, K., Yazawa, M., Kakiuchi, S., & Ohshima, M. (1978). Identification of an activator protein for myosin light chain kinase as the Ca2+ dependent modulator protein. *The Journal of biological chemistry*, 253(5), 1338–1340.

- Yap, K. L., Kim, J., Truong, K., Sherman, M., Yuan, T., & Ikura, M. (2000). Calmodulin target database. *Journal of structural and functional genomics*, 1(1), 8–14.
- Yarar, D., Waterman-Storer, C. M., & Schmid, S. L. (2005). A dynamic actin cytoskeleton functions at multiple stages of clathrin-mediated endocytosis. *Molecular biology of the cell*, 16(2), 964–75.
- Yazawa, M., Nakashima, K., & Yagi, K. (1999). A strange calmodulin of yeast. *Molecular and cellular biochemistry*, 190(1-2), 47–54.
- Ybe, J. A., Greene, B., Liu, S. H., Pley, U., Parham, P., & Brodsky, F. M. (1998). Clathrin self-assembly is regulated by three light-chain residues controlling the formation of critical salt bridges. *The EMBO journal*, 17(5), 1297–303.
- Ybe, J. A., Brodsky, F. M., Hofmann, K., Lin, K., Liu, S., Chen, L., Earnestk, T. N., *et al.* (1999). Clathrin self-assembly is mediated by a tandemly repeated superhelix. *Nature*, 399(6734), 371–375.
- Ybe, J. A., Ruppel, N., Mishra, S., & Vanhaaften, E. (2003). Contribution of Cysteines to Clathrin Trimerization Domain Stability and Mapping of Light Chain Binding. *Traffic*, 4(12), 850–856.
- Ybe, J. A., Perez-Miller, S., Niu, Q., Coates, D. a, Drazer, M. W., & Clegg, M. E. (2007). Light chain C-terminal region reinforces the stability of clathrin heavy chain trimers. *Traffic*, 8(8), 1101–10.
- Ye, Q., Li, X., Wong, A., Wei, Q., & Jia, Z. (2006). Structure of Calmodulin Bound to a Calcineurin Peptide : A New Way of Making. *Biochemistry*, 45, 738–745.
- Ye, Q., Wang, H., Zheng, J., Wei, Q., & Jia, Z. (2008). The complex structure of calmodulin bound to a calcineurin peptide. *Proteins*, 73(1), 19–27.
- Yeung, B. G., Phan, H. L., & Payne, G. S. (1999). Adaptor complex-independent clathrin function in yeast. *Molecular biology of the cell*, 10(11), 3643–59.
- Yim, Y.-I., Sun, T., Wu, L.-G., Raimondi, A., De Camilli, P., Eisenberg, E., & Greene, L. E. (2010). Endocytosis and clathrin-uncoating defects at synapses of auxilin knockout mice. *Proceedings of the National Academy of Sciences of the United States of America*, 107(9), 4412–7.
- Yoshino, H., Izumi, Y., Sakai, K., Takezawa, H., Matsuura, I., Maekawa, H., & Yazawa, M. (1996). Solution X-ray scattering data show structural differences between yeast and vertebrate calmodulin: implications for structure/function. *Biochemistry*, 35(7), 2388–93.
- Young, A., Stoilova-McPhie, S., Rothnie, A., Vallis, Y., Harvey-Smith, P., Ranson, N., Kent, H., *et al.* (2013). Hsc70-induced Changes in Clathrin-Auxilin Cage Structure Suggest a Role for Clathrin Light Chains in Cage Disassembly. *Traffic*, 14(9), 987–996.
- Young, L., Jernigan, R. L., & Covell, D. G. (1994). A role for surface hydrophobicity in protein-protein recognition. *Protein science*, 3(5), 717–729.

- Zeng, G., Yu, X., & Cai, M. (2001). Regulation of yeast actin cytoskeleton-regulatory complex Pan1p/Sla1p/End3p by serine/threonine kinase Prk1p. *Molecular biology of the cell*, 12(12), 3759–72.
- Zhang, M., Abrams, C., Wang, L., Gizzi, A., He, L., Lin, R., Chen, Y., *et al.* (2012). Structural basis for calmodulin as a dynamic calcium sensor. *Structure*, 20(5), 911–923.
- Zhang, M., Takana, T., & Ikura, M. (1995). Calcium-induced conformational transition revealed by the solution structure of apo calmodulin. *Nature structural & molecular biology*, 2(9), 758–767.
- Zhang, Y., Grant, B., & Hirsh, D. (2001). RME-8, a conserved J-domain protein, is required for endocytosis in Caenorhabditis elegans. *Molecular biology of the cell*, 12(7), 2011–21.
- Zhao, Y., & Keen, J. H. (2008). Gyrating clathrin: highly dynamic clathrin structures involved in rapid receptor recycling. *Traffic*, 9(12), 2253–64.

8. APPENDIX I: Supplementary figures

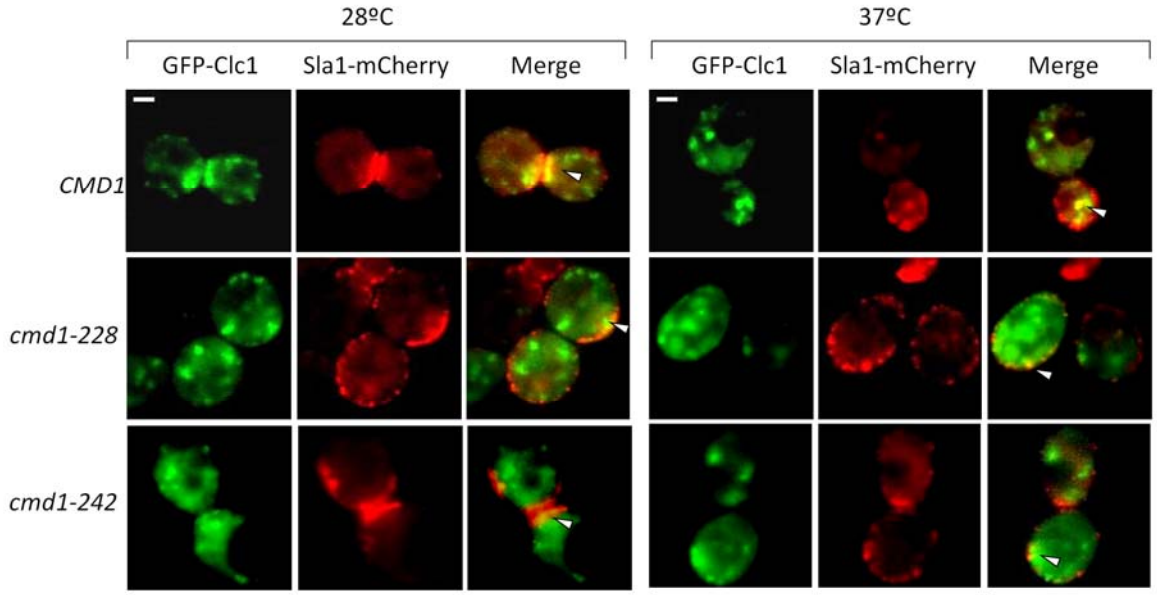

Figure 46. The endocytic marker Sla1 co-localizes with Clc1 in WT *CMD1* and *cmd1-228* and *cmd1-242* mutants to a similar extent. (A) Representative fluorescence micrographs from a *cmd1Δ SLA1-mCherry* strain grown at 28ºC or at 37ºC expressing either Cmd1 or the Cmd1-228 or Cmd1-242 mutants (SCMIG1077, SCMIG1283 and SCMIG1284, respectively) and GFP-Clc1 (pGFP-*CLC1-U*), all expressed from centromeric plasmids under the control of their own promotor. Fluorescence images for GFP (left) and mCherry (middle) were taken and merged (right). Patches of Clc1 associated with Sla1 are seen as yellow in the merge. At least 300 cells were imaged. Scale bar: 2 µm.

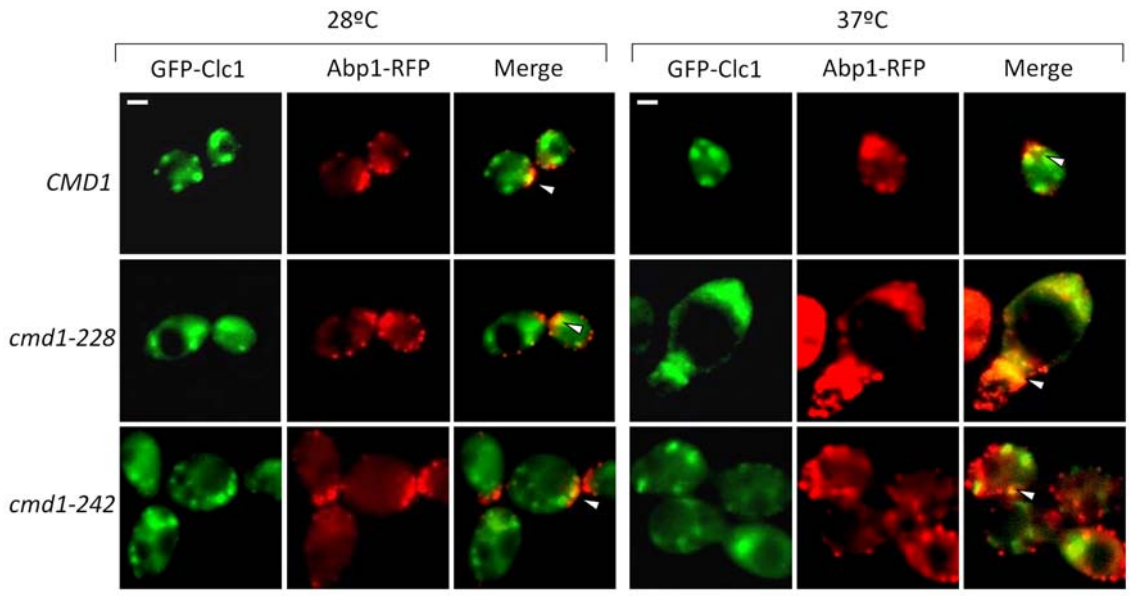

Figure 47. The endocytic marker Abp1 co-localizes with Clc1 in WT *CMD1* and *cmd1-228* and *cmd1-242* mutants to a similar extent. Representative fluorescence micrographs from a *cmd1Δ ABP1-RFP* strain grown at 28ºC or at 37ºC expressing either Cmd1 or the Cmd1-228 or Cmd1-242 mutants (SCMIG1063, SCMIG1281 and SCMIG1282, respectively) and GFP-Clc1 (pGFP-*CLC1-U*), all expressed from centromeric plasmids under the control of their own promotor. Fluorescence images for GFP (left) and mCherry (middle) were taken and merged (right). Patches of Clc1 associated with Abp1 are seen as yellow in the merge. At least 300 cells were imaged. Scale bar: 2 µm.

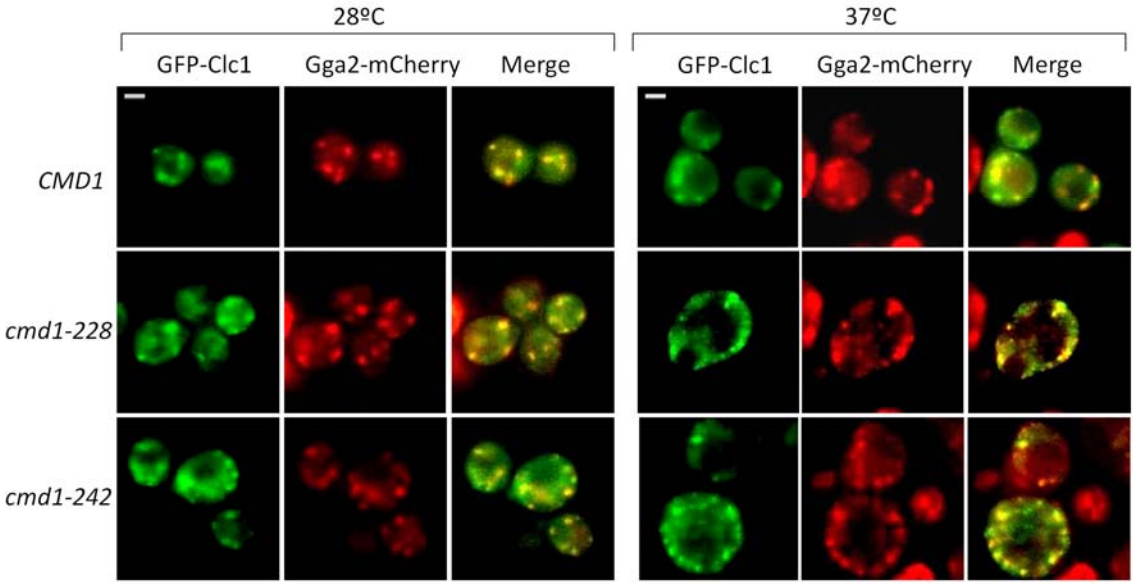

Figure 48. The endocytic marker Gga2 co-localizes with Clc1 in WT *CMD1* and *cmd1-228* and *cmd1-242* mutants to a similar extent. Representative fluorescence micrographs from a *cmd1Δ GGA2-mCherry* strain grown at 28ºC or at 37ºC, expressing either Cmd1 or the Cmd1-228 or Cmd1-242 mutants (SCMIG1286, SCMIG1287 and SCMIG1288, respectively) and the GFP-Clc1 (pGFP-*CLC1-U*) expressed all from a centromeric plasmid under the control of their own promotor. Fluorescence images for GFP (left) and mCherry (middle) were taken and merged (right). Patches of Clc1 associated with Gga1 are seen as yellow in the merge. At least 300 cells were imaged. Scale bar: 2 µm.

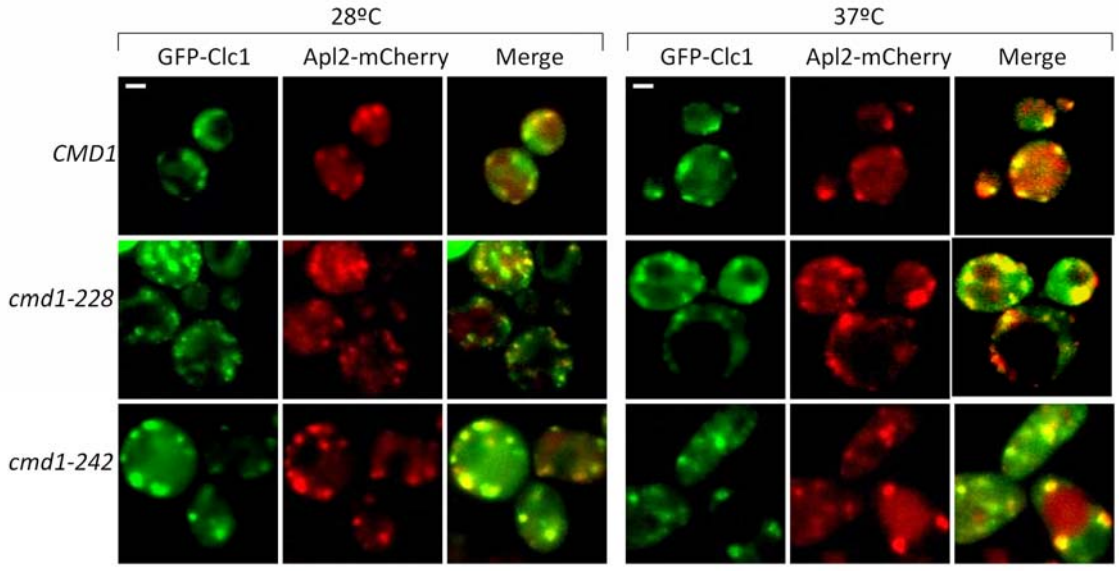

Figure 49. The TGN marker Apl2 co-localizes to a higher extent and on bigger punctae structures with Clc1 in the *cmd1-228* and *cmd1-242* mutants than in WT *CMD1* cells. Representative fluorescence micrographs from a *cmd1Δ APL2-mCherry* strain grown at 28ºC or 37ºC, expressing either Cmd1, the Cmd1-228 or Cmd1-242 mutants (SCMIG1290, SCMIG1291 and SCMIG1292, respectively) and the GFP-Clc1 (pGFP-*CLC1-U*), expressed all from centromeric plasmids under the control of their own promotor. Fluorescence images for GFP (left) and mCherry (middle) were taken and merged (right). Patches of Clc1 associated with Apl2 are seen as yellow in the merge. At least 300 cells were imaged. Scale bar: 2 µm.

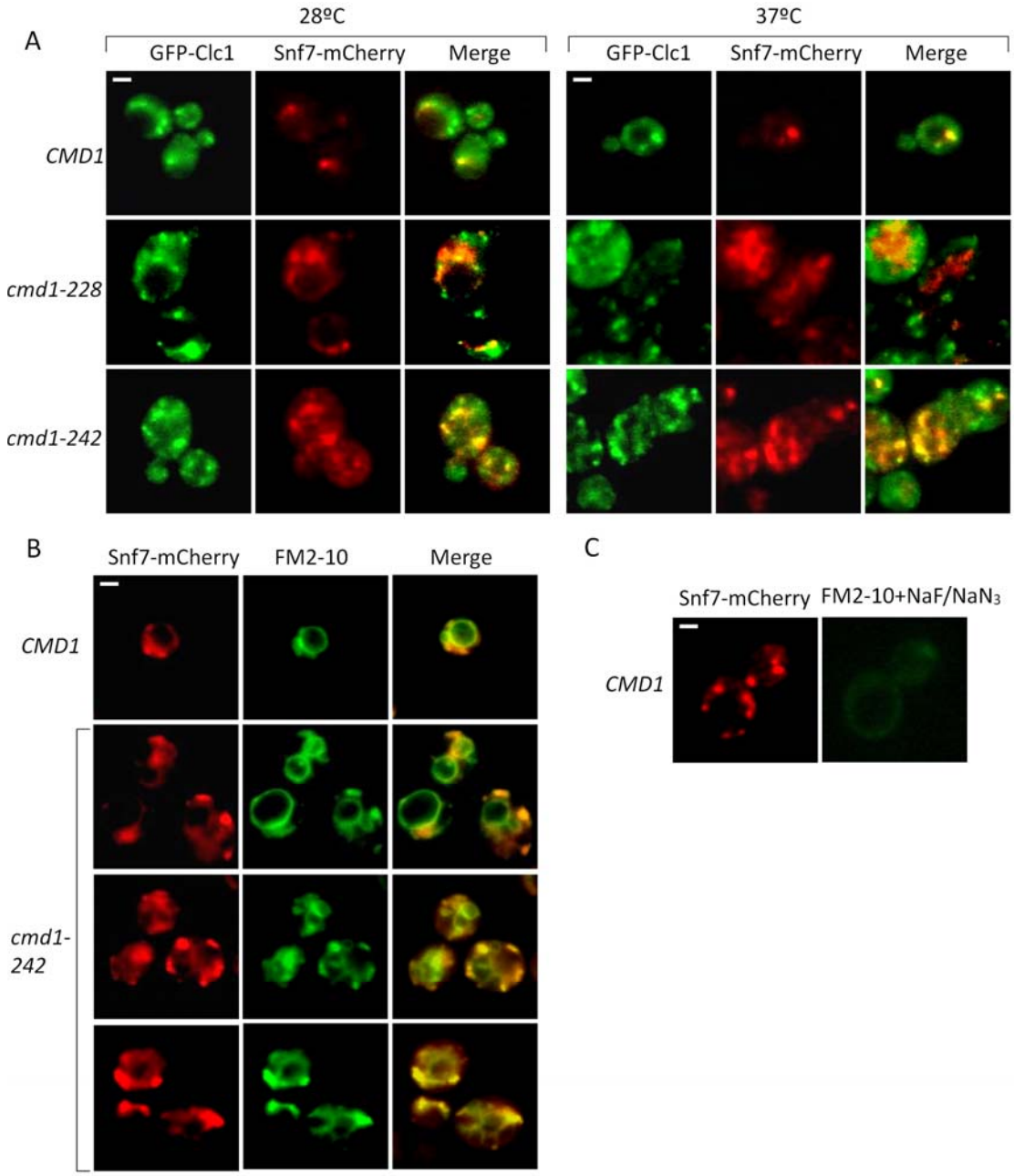

Figure 50. The prevacular compartment marker Snf7 co-localizes with GFP-Clc1 on enlarged structures in the *cmd1-228* and *cmd1-242* mutants. (A) Representative fluorescence images of a *cmd1Δ SNF7-mCherry* strain grown at 28ºC or 37ºC expressing either Cmd1 or the Cmd1-228 or Cmd1-242 mutants (SCMIG1298, SCMIG1299 and SCMIG1300, respectively) and GFP-Clc1 (pGFP-*CLC1-U*), expressed all from centromeric plasmids under the control of their own promotor. Fluorescence images for GFP (left) and mCherry (middle) were taken and merged (right). Patches of Clc1 associated with Snf7 are seen as yellow in the merge. (B) Fluorescence micrographs of *cmd1Δ SNF7-mCherry* cells expressing either the WT Cmd1 or the Cmd1-242 mutant from centromeric plasmids under the control of their own promotor (SCMIG1298 and SCMIG1300, respectively) and incubated with the styril dye FM2-10 for 45 minutes at 37ºC. Fluorescence images for mCherry (left) and FM2-10 (middle) were taken and merged (right). Patches of Snf7 associated with FM2-10 -dyed membranous structures are seen as yellow in the merge. (C) Control for the internalized FM2-10. *cmd1Δ SNF7-mCherry* cells expressing the WT Cmd1 (SCMIG1298) were treated with FM2-10 and 10 mM NaF/NaN_3 to avoid internalization. At least 300 cells were imaged. Scale bar: 2 µm.

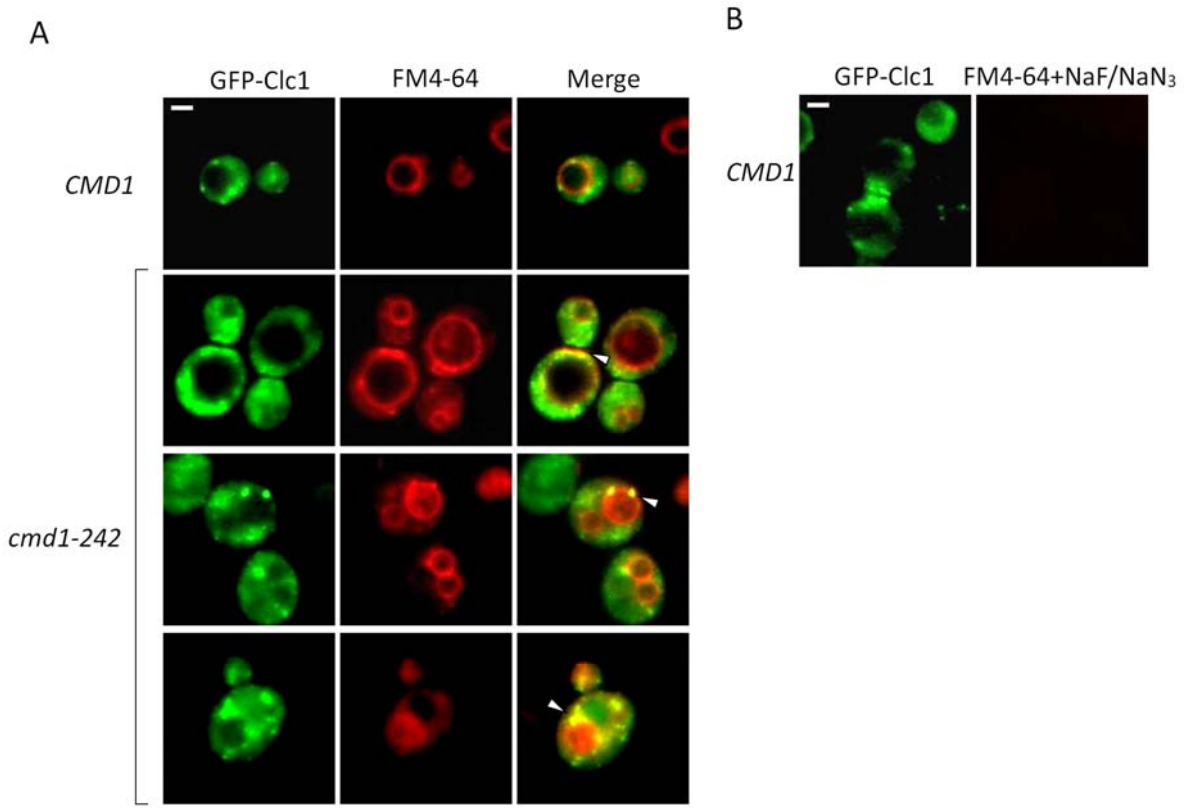

Figure 51. The Clc1-decorated enlarged compartment in the *cmd1-242* mutant at 37ºC is at least partially of endocytic origen. (A) Representative fluorescence micrographs of a *cmd1Δ* strain grown at 37ºC expressing GFP- Clc1 (pGFP-*CLC1-U*) and either Cmd1 or the Cmd1-242 mutant (SCMIG1261 and SCMIG1266, respectively) all from centromeric plasmids under the control of their own promotor, treated with the styril dye FM4-64 for 45 minutes at 37ºC. Fluorescence images for GFP (left) and FM4-64 (middle) were taken and merged (right). Patches of Clc1 associated with FM4-64-dyed membranous structures are seen as yellow in the merge. (B) Control for the internalized FM4-64. *cmd1Δ* cells expressing the WT Cmd1 (SCMIG1261) and the GFP-Clc1 expressed from a centromeric plasmid under the control of its ownpromotor (pGFP-*CLC1-U*) were treated with FM4-64 and 10 mM NaF/NaN_3 to avoid internalization. At least 300 cells were imaged .Scale bar: 2 µm.

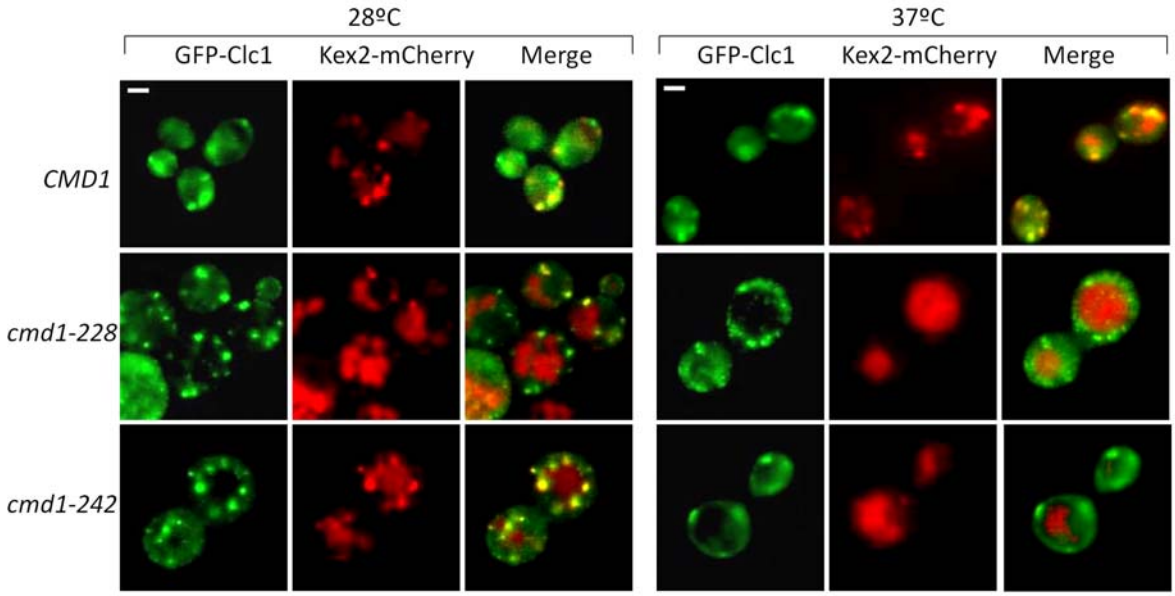

Figure 52. The TGN α-factor processing enzyme Kex2 mislocalizes from the TGN and accumulates in vacuolar structures in *cmd1-228* and *cmd1-242* mutants. Representative fluorescence micrographs from a *cmd1Δ KEX2-mCherry* strain grown at 28ºC or 37ºC expressing either Cmd1, or the Cmd1-228 or Cmd1-242 mutants (SCMIG1294, SCMIG1295 and SCMIG1296, respectively) and the GFP-Clc1 (pGFP-*CLC1-U*) all expressed from centromeric plasmids under the control of their own promotor. Fluorescence images for GFP (left) and mCherry (middle) were taken and merged (right). Patches of Clc1 associated with Kex2 are seen as yellow in the merge. At least 300 cells were imaged. Scale bar: 2 µm.

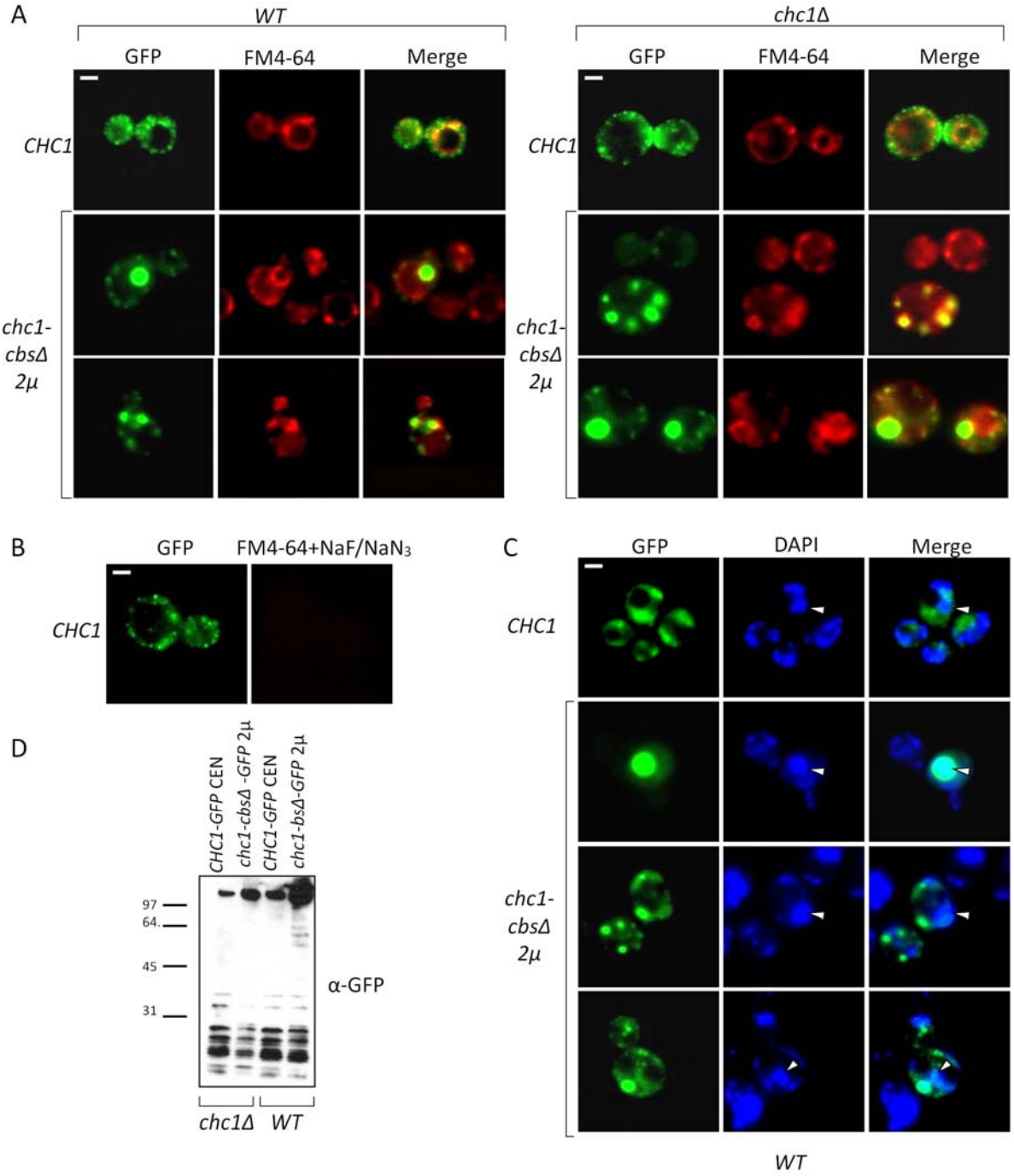

Figure 53. The Chc1-cbsΔ mutant expressed from a multicopy plasmid is delocalized and occasionally accumulates on endosomal structures. (A) Representative fluorescence micrographs of *WT* (BY4742) (left panels) or *chc1Δ* (SL114) (right panels) strains grown at 28ºC expressing either the Chc1-GFP (*CHC1*) or the Chc1-cbsΔ-GFP mutant (*chc1-cbsΔ* 2μ) from centromeric and multicopy plasmids, respectively, under the control of their own promotors (p50-*CHC1-GFP* and p195-*chc1-cbsΔ-GFP*, respectively). Cells were incubated with the styril dye FM4-64 for 45 minutes at 28ºC. Fluorescence images for GFP (left) and FM4-64 (middle) were taken and merged (right). Patches of Chc1 or Chc1-cbsΔ associated with FM4-64-dyed membranous structures are seen as yellow in the merge. (B) Control for the internalized FM4-64. *WT* cells (BY4742) expressing Chc1-GFP (*CHC1-GFP*; p50-*CHC1-GFP*) were incubated with FM4-64, and 10 mM NaF/NaN_3 to avoid internalization. (C) Representative fluorescence micrographs of a *WT* strain (BY4742) expressing either the Chc1-GFP (*CHC1*) or the Chc1-cbsΔ-GFP mutant (*chc1-cbsΔ* 2μ) from centromeric and multicopy plasmid,

respectively, under the control of their own promotors (p50-*CHC1-GFP* and p195-*chc1-cbsΔ-GFP*, respectively) (right images) and incubated with DAPI for nucleus visualization (middle images). Patches of Chc1 or Chc1-cbsΔ accumulated at the DAPI-dyed nucleus are seen as light blue in the merge. The nucleus is indicated by a small white arrow. Scale bar: 2 µm. (D) Immunoblot of total protein extracts to analyze the expression and degradation of Chc1-GFP (*CHC1*-GFP CEN) or Chc1-cbsΔ-GFP (*chc1-cbsΔ*-GFP 2µ) expressed from a centromeric and a multicopy plasmid, respectively under the control of their own promotors (p50-*CHC1-GFP* and p195-*chc1-cbsΔ-GFP*, respectively) in *WT* (BY47421) or *chc1Δ* (SL114) cells. An antibody against GFP (α-GFP), combined with an appropriate secondary antibody, was used to detect GFP-tagged proteins.

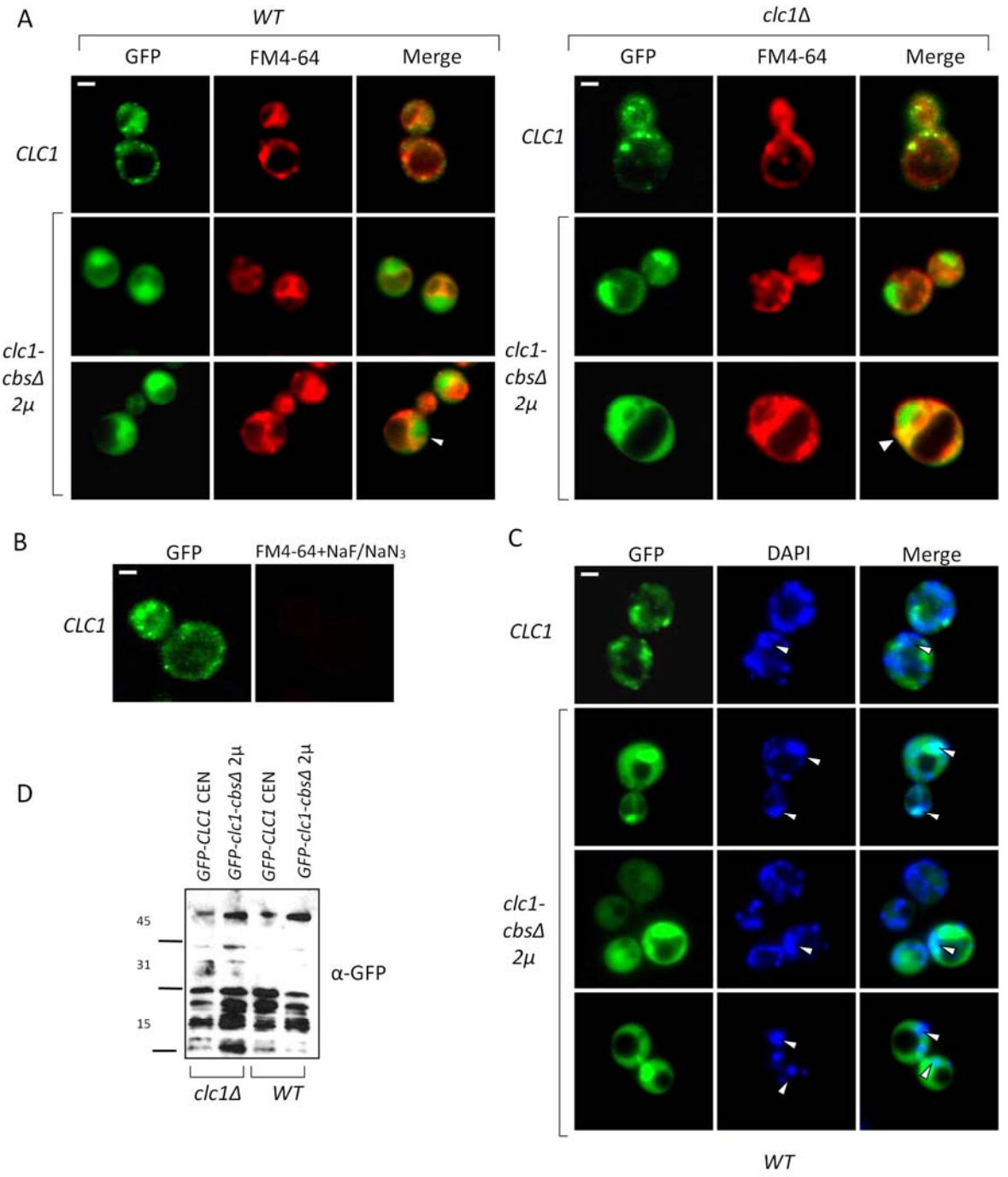

Figure 54. The Clc1-cbsΔ mutant expressed from a multicopy plasmid is delocalized and occasionally accumulates on endosomal structures. (A) Representative fluorescence micrographs of *WT* (BY4742) (left panels) or *clc1Δ* (SL1620) (right panels) strains grown at 28ºC expressing either the GFP-Clc1 (*CLC1*) or the GFP-Clc1-cbsΔ mutant (*clc1-cbsΔ* 2μ) from centromeric and multicopy plasmids, respectively, under the control of their own promotors (pGFP-*CLC1-U* and pGFP-*clc1-cbsΔ,* respectively). Cells were treated with the styril dye FM4-64 for 45 minutes at 28ºC. Fluorescence images for GFP (left) and FM4-64 (middle) were taken and merged (right). Patches of Clc1 or Clc1-cbsΔ associated with FM4-64-dyed membranous structures are seen as yellow in the merge. (B) Control for the internalized FM4-64. *WT* cells (BY4742) expressing GFP-Clc1 (*CLC1;* pGFP-*CLC1-U*) were treated with FM4-64, and 10 mM NaF/NaN_3 to avoid internalization. (C) Representative fluorescence micrographs of a *WT* strain (BY4742) expressing either the GFP-Clc1 (*CLC1*) or the GFP-Clc1-cbsΔ mutant (*clc1-cbsΔ* 2μ) from a centromeric and a multicopy plasmid, respectively, under the control of their own promotor (pGFP-*CLC1-U* and pGFP-*clc1-cbsΔ,* respectively) (right images) and

incubated with DAPI for nucleus visualization (middle images). Patches of Chc1 or Chc1-cbsΔ accumulated at the DAPI-dyed nucleus are seen as light blue in the merge. The nucleus is indicated by a small white arrow. Scale bar: 2 µm. (D) Immunoblot of total protein extracts to analyze the expression and degradation of GFP-Clc1 (GFP-*CLC1* CEN) or GFP-Clc1-cbsΔ (GFP-*clc1-cbsΔ* 2µ) expressed from a centromeric and a multicopy plasmid, respectively, under the control of their own promotors (pGFP-*CLC1-U* and pGFP-*clc1-cbsΔ,* respectively) in *WT* (BY4742) or *clc1Δ* (SL1620) cells. An antibody against GFP (α-GFP) combined with an appropriate secondary antibody, was used to detect GFP-tagged proteins.

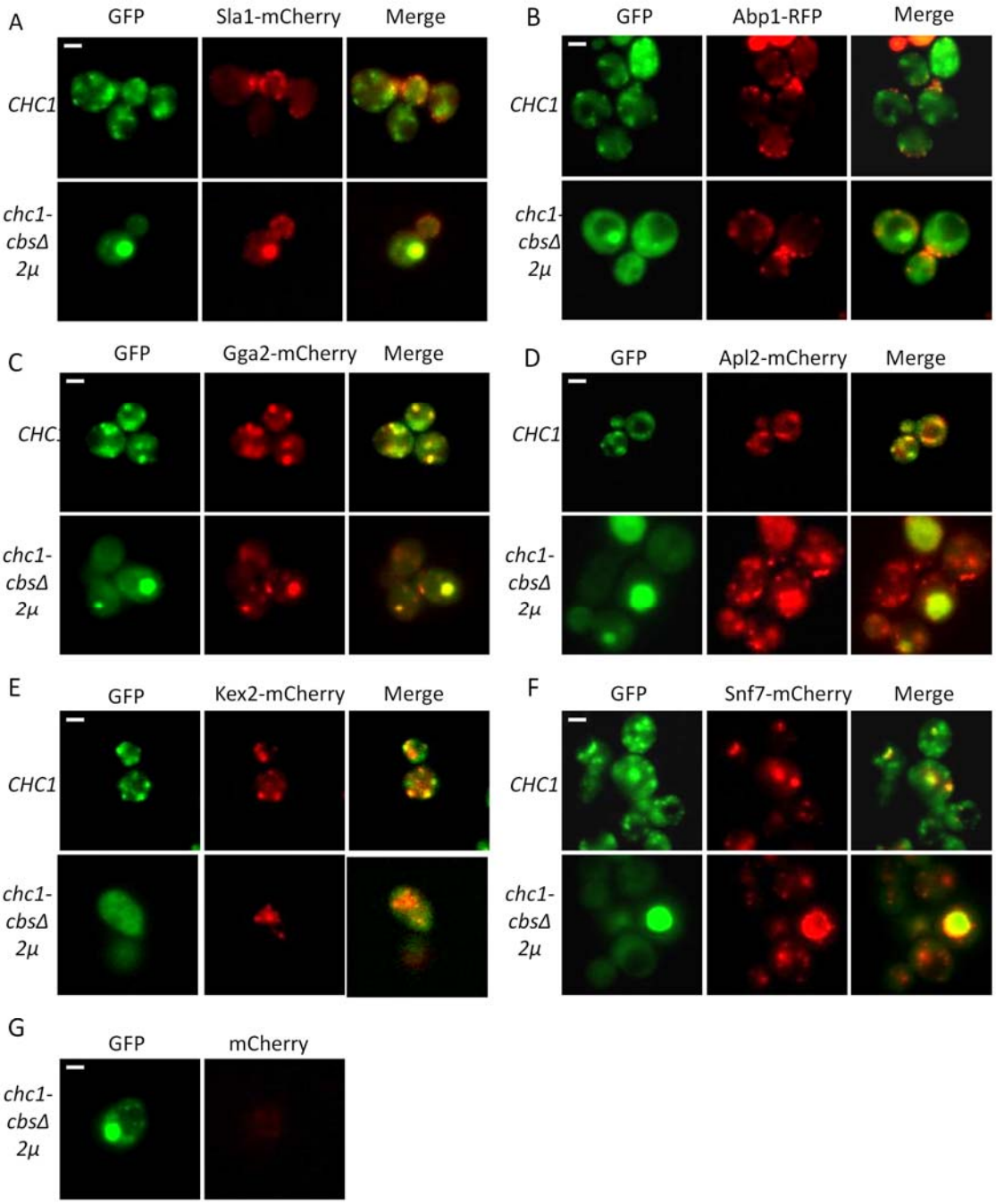

Figure 55. The Chc1-cbsΔ mutant expressed from a multicopy plasmid accumulates on endosomal structures where it co-localizes with Sla1, Gga1, Apl2 and Snf7. Representative fluorescence micrographs from cells expressing either Sla1-mCherry (SCMIG1141)(A), Abp1-RFP *(*SL5156*)* (B)*,* Gga1-mCherry (SCMIG1301) (C), Apl2-mCherry *(SCMIG1302)*(D)*,* Kex2-*mCherry* (SCMIG1303) (E) or Snf7-mCherry (SCMIG1304) (F) strains grown at 28ºC and expressing either the Chc1-GFP (*CHC1*) or the Chc1-cbsΔ-GFP mutant (*chc1-cbsΔ* 2μ) from centromeric and multicopy plasmid, respectively, under the control of their own promotors (p50-*CHC1-GFP* and p195-*chc1-cbsΔ-GFP*, respectively). Fluorescence images for GFP (left) and mCherry (middle) were taken and merged (right). Patches of Chc1 or Chc1-cbsΔ associated with each of the mCherry-tagged markers are seen as yellow in the merge. (G) Fluorescence images from a *WT* strain (BY4742) expressing only Chc1-cbsΔ-GFP (*chc1-cbsΔ* 2μ) from a multicopy plasmid under the control of its own promotor (p195-*chc1-cbsΔ-GFP)* (left) image with the filters for mCherry (right) as control for cross-excitation. Scale bar: 2 μm

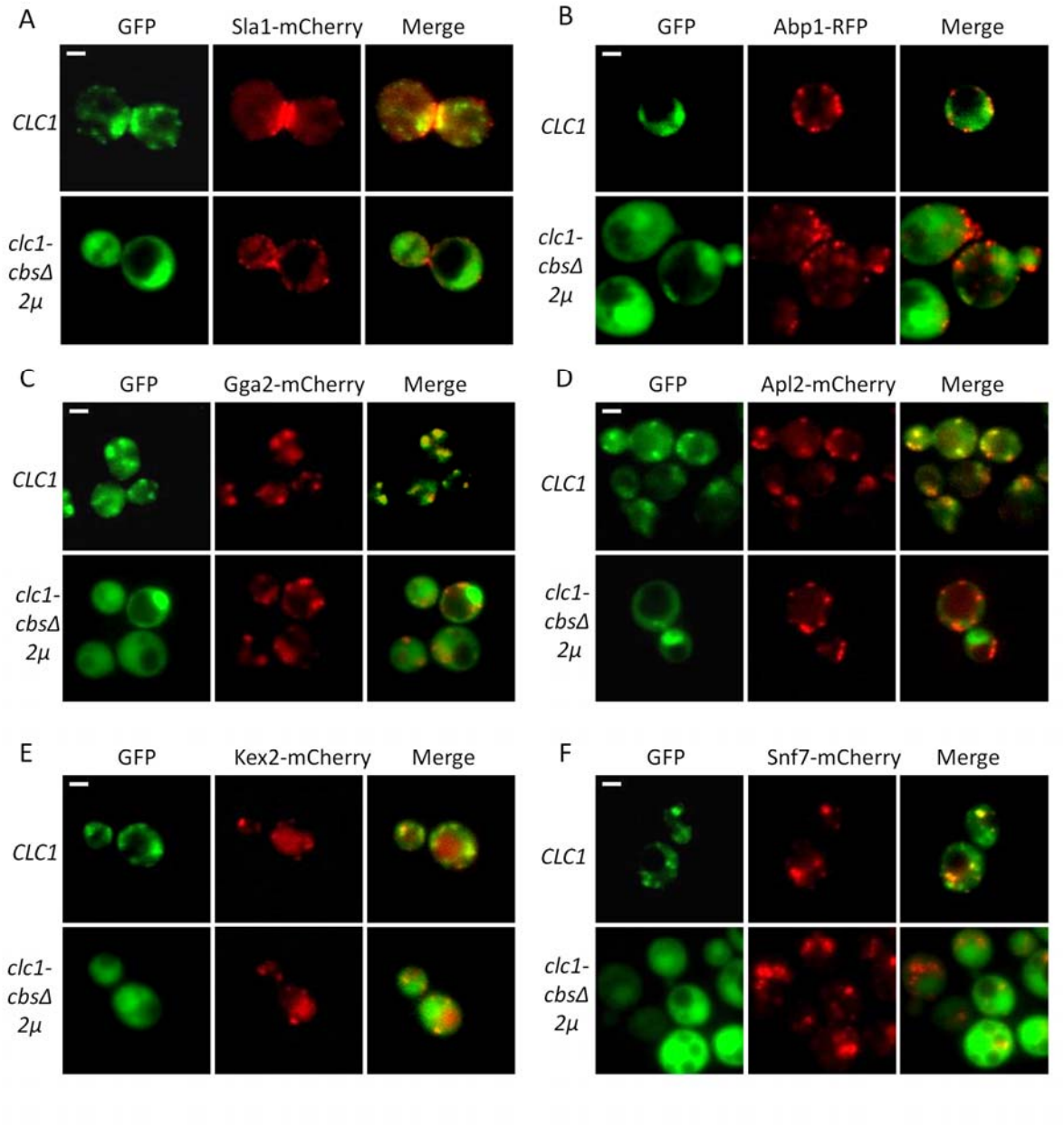

Figure 56. The Clc1-cbsΔ mutant expressed from a multicopy plasmid does not co-localize with the endocytic or TGN-endosomal markers. Representative fluorescence micrographs from cells expressing Sla1-mCherry (SCMIG1141)(A), Abp1-TFP (SL5156) (B), Gga1-mCherry (SCMIG1301) (C), Apl2-mCherry (SCMIG1302)(D), Kex2-mCherry (SCMIG1303) (E) and Snf7-mCherry (SCMIG1304) (F) strains grown at 28ºC and expressing either GFP-Clc1 (*CLC1*) or the GFP-Clc1-cbsΔ mutant (*clc1-cbsΔ* 2μ) from a centromeric and a multicopy plasmid, respectively, under the control of their own promotors (GFP-*CLC1-U* and GFP-*clc1-cbsΔ*, respectively). Fluorescence images for GFP (left) and mCherry (middle) were taken and merged (right). Patches of Clc1 or Clc1-cbsΔ associated with each of the mCherry-tagged markers are seen as yellow in the merge. Scale bar: 2 μm.

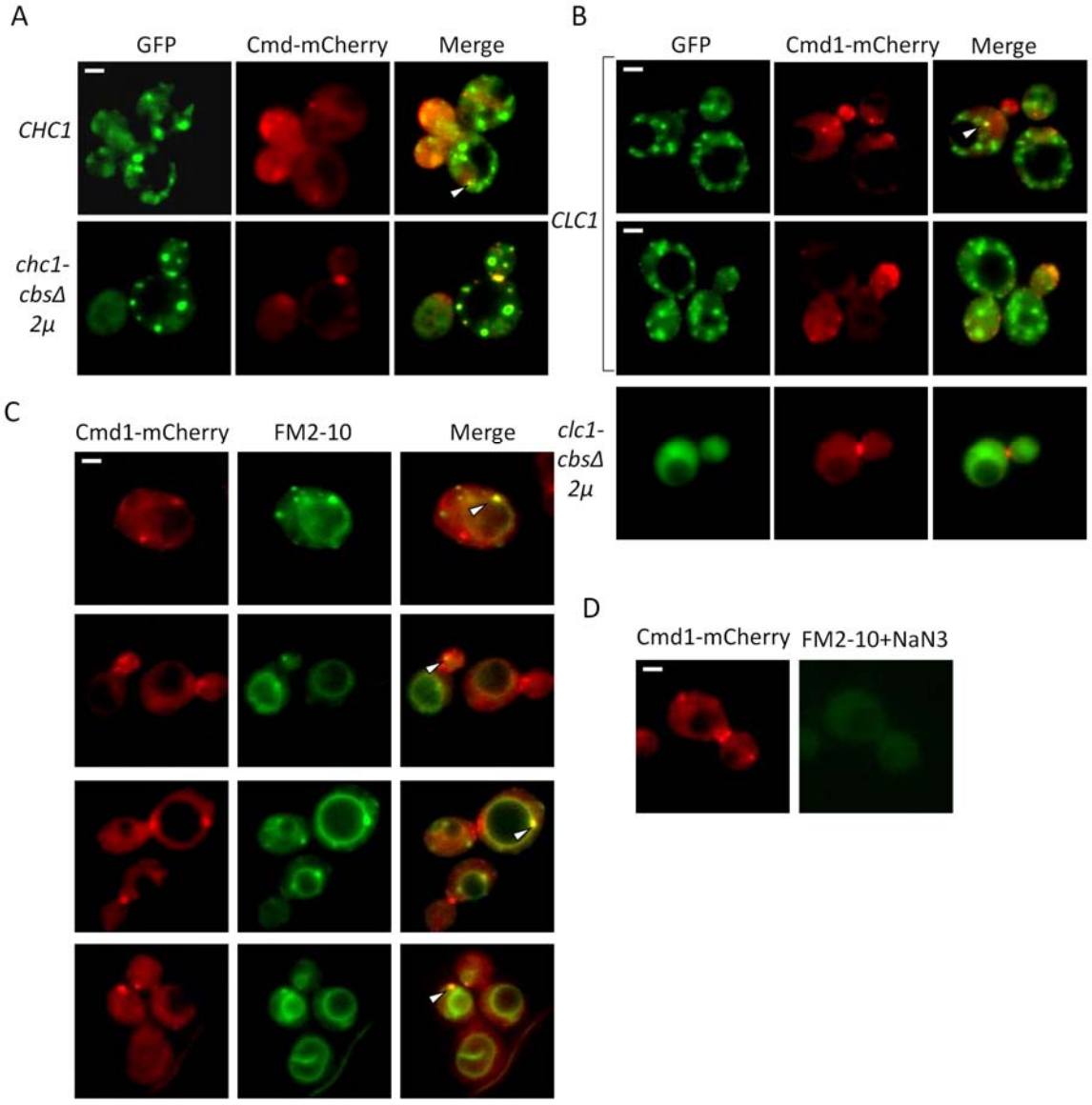

Figure 57. Cmd1 partially co-localizes with Chc1 and Clc1 in a WT strain at the cell poles, at cytokinesis ring, and on a few internal patches of endocytic origin. (A, B) Representative fluorescence micrographs of a *WT CMD1-mCherry* strain (SCMI1080) grown at 28ºC expressing either Chc1-GFP (*CHC1*) (A) or GFP-Clc1 (*CLC1*) (B) from centromeric plasmids (p50-*CHC1-GFP* or pGFP-*CLC1-U,* respectively), or the Chc1-cbsΔ-GFP (*chc1-cbsΔ* 2μ) (A) or GFP-Clc1-cbsΔ (*clc1-cbsΔ* 2μ) (B) mutants from multicopy plasmids (p195-*chc1-cbsΔ* or pGFP-*clc1-cbsΔ*, respectively), all under the control of their own promotors. Fluorescence images for GFP (left) and mCherry (middle) signals were taken and merged (right). Patches of Chc1 or Clc1 associated with Cmd1 are seen as yellow in the merge (white arrows indicate internal patches). (C) Representative fluorescence micrographs of *WT CMD1-mCherry* cells (SCMIG1080) incubated with the styril dye FM2-10 for 45 minutes at 28ºC. Images for mCherry (left) and FM2-10 (middle) were taken and merged (right). Patches of Cmd1 associated with FM2-10-dyed membranous structures are seen as yellow in the merge (indicated by white arrows). (D) Control for the internalized FM2-10. *WT CMD1-mCherry* cells (SCMIG1080) were treated with FM2-10 and 10 mM NaF/NaN_3 to avoid internalization. Scale bar: 2 μm.

9. APPENDIX II: Publications

Contributions to other studies during the thesis period:

- Grötsch, H., Giblin, J. P., Idrissi, F.-Z., Fernández-Golbano, I.-M., Collette, J. R., Newpher, T. M., Robles, V.*, et al.* (2010). Calmodulin dissociation regulates Myo5 recruitment and function at endocytic sites. *The EMBO journal*, 29(17), 2899–914.
- Fernéndez-Golbano, I.M., Idrissi, F.Z., Giblin, J.P., Grosshans, B., Robles, V., Grötsch, H., Borrás, M.M. & Geli, M. I. (2014). A cross-talk between PI(4,5)P_2 and CK2 modulates actin polymerization during endocytic uptake. *Developmental Cell*, 30(6), 746-58.

My thesis is written in

WWW.PHDCOMICS.COM